Universidad de Jaén

TESIS DOCTORAL

•

EFECTO DE FENOLES DEL OLIVO EN PROCESOS DE HIPOXIA Y NEURODEGENERACIÓN

PRESENTADA POR:

Jesús Calahorra García Moreno

DIRIGIDA POR:

Eva Siles Rivas

Ana Cañuelo Navarro

JAÉN, 31 de Julio de 2019

Universidad de Jaén

Área de Bioquímica

Departamento de Biología Experimental

Facultad de Ciencias Experimentales

La Dr. Eva Siles Rivas y la Dr. Ana Cañuelo Navarro, Profesoras Titulares del Área de Bioquímica de la Universidad de Jaén certifican que la Tesis Doctoral titulada: "**Efecto de fenoles del olivo en procesos de hipoxia y neurodegeneración",** que presenta Jesús Calahorra García Moreno para optar al Grado de Doctor con Mención Internacional, ha sido realizada bajo su dirección, reuniendo a su juicio, los requisitos exigidos para esta presentación.

Jaén, 31 de Julio de 2019

Dra. Eva Siles Rivas

Dra. Ana Cañuelo Navarro

Memoria presentada por el graduado

Jesús Calahorra García Moreno

Julio de 2019

Índice

ÍNDICE

Resumen/Abstract

RESUMEN

Los compuestos fenólicos del olivo poseen multitud de propiedades beneficiosas en diversos contextos patológicos. Su potencial antioxidante y antiinflamatorio, junto a otros efectos, han hecho del hidroxitirosol (HT) y el tirosol (TIR), principales fenoles del olivo, objeto de multitud de estudios y ensayos. En esta tesis doctoral se ha evaluado el efecto de estos dos compuestos en patologías en las que la hipoxia juega un papel importante, como el cáncer y el ictus, y en enfermedades amiloides como la enfermedad de Parkinson (EP), todas ellas estrechamente relacionadas con el estrés oxidativo. En los trabajos realizados con células MCF-7 de cáncer de mama sometidas a hipoxia, describimos cómo el HT disminuye el nivel de estrés oxidativo. Aunque a concentraciones elevadas este compuesto modula la respuesta de las rutas PGC-1α/ERRα y PGC-1α/Nrf2, su efecto antioxidante parece estar mediado por una acción directa. En estas mismas células el HT también disminuye los niveles de la subunidad α del factor inducible por hipoxia-1, principal mediador de la respuesta a hipoxia y marcador de mal pronóstico en esta enfermedad, pudiendo actuar a altas concentraciones como agonista de AHR. Por otra parte, mediante el uso de un modelo de oclusión transitoria de la arteria cerebral media en ratones, hemos comprobado que el uso terapéutico de una dieta suplementada con HT mejora el estado físico y cognitivo y afecta positivamente a parámetros clave en la recuperación del ictus isquémico, como el flujo sanguíneo cerebral, la conectividad funcional, la neuroinflamación y la neurogénesis. Finalmente, el análisis del efecto del TIR en modelos de *C. elegans* de la EP pone de manifiesto el potencial neuroprotector de este compuesto frente a la degeneración dopaminérgica y la toxicidad inducidas por la agregación de la α-sinucleína, así como su capacidad antioxidante e inductora de la expresión de chaperonas relacionadas con esta enfermedad. En conclusión, los resultados obtenidos sugieren que tanto el HT como el TIR poseen un gran potencial como moléculas bioactivas con diversos efectos beneficiosos en las patologías analizadas.

ABSTRACT

Hydroxytyrosol (HT) and tyrosol (TYR), the main phenols in the olive tree, have demonstrated an important antioxidant and anti-inflammatory potential. Given the crucial role of oxidative stress in a great number of pathologies, many of them involving hypoxia and protein aggregation, in this doctoral thesis we have evaluated the effect of HT and TYR in cancer and stroke, two hypoxia-related diseases, and in one of the most frequent amyloid diseases, such as Parkinson´s Disease (PD). In the studies performed with MCF-7 breast cancer cells under hypoxic conditions, we described that HT reduced the level of oxidative stress. Although at high concentrations this compound modulated the response of PGC-1α/ERRα and PGC-1α/Nrf2 pathways, its antioxidant effect appears to be mediated by a direct action. In MCF-7 cells, HT also decreased the levels of the hypoxia inducible factor-1 α subunit, the main mediator of hypoxic response and a marker of poor prognosis. However, at high concentrations HT can also act as an AHR agonist. On the other hand, by using a model of transient occlusion of the middle cerebral artery in mice, we have shown that the therapeutic use of a HT-enriched diet improves the physical and cognitive status of the animals together with key parameters for ischemic stroke recovery such as cerebral blood flow, functional connectivity, neuroinflammation and neurogenesis. Finally, the analysis of the effect of TYR in *C. elegans* models of PD demonstrated the neuroprotective potential of this compound against dopaminergic degeneration and toxicity induced by the aggregation of α-synuclein. The mechanism underlying this effect seemed to be also related to its antioxidant capacity and to the induction of specific chaperones involved PD. In conclusion, the results obtained in this doctoral thesis point to HT and TYR as promising bioactive compounds with beneficial effects in these pathologies.

Introducción

1. ACEITE DE OLIVA Y SALUD

El aumento de la esperanza de vida registrado en las últimas décadas en los países desarrollados conlleva una mayor incidencia de diferentes patologías asociadas a la edad y al estilo de vida. Entre estas patologías destacan las patologías cardio- y cerebrovasculares, cáncer, diabetes y enfermedades neurodegenerativas. En este sentido, multitud de estudios epidemiológicos y observacionales apoyan que regímenes alimentarios como el mediterráneo y el asiático, están asociados con una menor incidencia de estas patologías (Figura 1). La dieta mediterránea (DM) se caracteriza por un alto consumo de alimentos de origen vegetal, principalmente frutas y verduras, legumbres, cereales no procesados y nueces, así como por el consumo moderado de pescado, carne de ave, productos lácteos y huevos. Sin embargo el componente fundamental y nexo común entre las diversas culturas mediterráneas es el empleo del aceite de oliva como principal fuente de grasa[1]. De hecho, como se especificará más adelante, la alta proporción de ácidos grasos monoinsaturados (AGMI) y fitonutrientes (en particular vitaminas y fenoles naturales) del aceite de oliva, se han relacionado con la inducción de múltiples vías de señalización involucradas con la homeostasis proteica, la reparación del ADN y con la regulación del metabolismo y de las defensas antioxidantes[2].

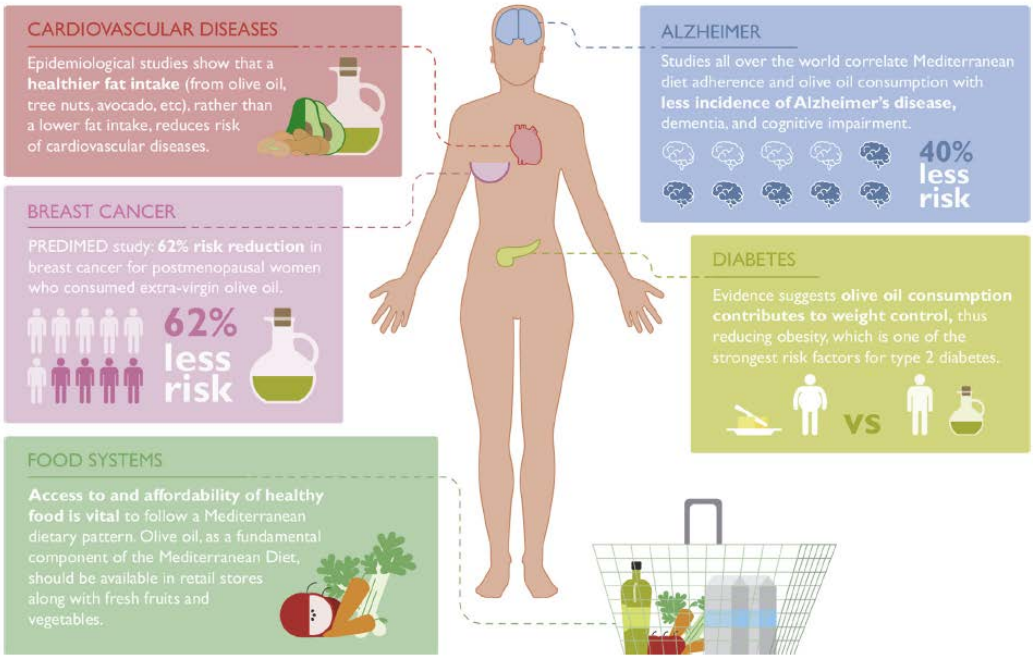

Figura 1. Propiedades saludables del aceite de oliva[2].

Profundizando un poco más en los estudios realizados hasta la fecha, la evidencia científica de la relación entre DM y salud es notoria. En este sentido, se han realizado hasta 7 metaanalisis que demuestran la relación inversa entre adherencia a DM y riesgo de padecer enfermedades cardiovasculares (ECVs)[3]. Si bien la mayoría de los estudios son observacionales, el ensayo clínico nutricional, multicéntrico y aleatorizado PREDIMED (Prevención con Dieta Mediterránea) desarrollado a lo largo de 5 años con 7447 participantes aporta datos muy concluyentes al respecto. Los principales hallazgos del ensayo demuestran que la incidencia de ECV se reduce en un 30% y un 28% cuando se la dieta complementa con aceite de oliva virgen extra (AOVE) o nueces, respectivamente, en comparación con la dieta control[4]. Así, enfermedades cerebrovasculares como el ictus isquémico, también presentan una menor incidencia en consumidores de DM[5]. Por otro lado, en 2015, como parte del estudio PREDIMED se publicaron los resultados sobre la incidencia de cáncer de mama entre 4152 mujeres postmenopáusicas con una edad comprendida entre 60-80 años. Los resultados obtenidos demostraron que la intervención nutricional de 1 litro/semana de AOVE

a lo largo de 5 años disminuyó de forma significativa, en un 62%, el riesgo de padecer cáncer de mama en comparación con el grupo control[6]. Además, estos resultados concuerdan con los de un metaanalisis anterior al estudio PREDIMED en el que también se observó que el consumo de aceite de oliva, no exclusivamente AOVE, estaba inversamente relacionado con la incidencia de cáncer de mama[7]. Por último, los desórdenes cognitivos son un grupo de síndromes que pueden ser clasificados como demencia, deterioro cognitivo leve o deterioro cognitivo asociado a la edad. Estos desórdenes son ocasionados por diferentes patologías neurodegenerativas, y en especial por Alzheimer y Parkinson, las dos más comunes. Estudios observacionales, como el estudio FINGER[8], relacionan una alta adherencia a la DM con un menor riesgo de padecer desórdenes cognitivos y enfermedades neurodegenerativas[9]. El ensayo PREDIMED también pone de manifiesto que la DM complementada con AOVE o nueces se asocia con un menor deterior cognitivo asociado a la edad[10]. En el caso concreto del Parkinson, un estudio observacional sobre 257 enfermos y 200 participantes control apuntaba a que una alta adherencia a la DM estaba asociada con menor probabilidad de padecer esta patología, mientras que una baja adherencia se asociaba con edades más tempranas de aparición de la misma[11].

1.1 Composición del aceite de oliva

El contenido de los diferentes componentes del aceite de oliva varía de forma significativa dependiendo de diversos factores, entre los que cabe destacar su procedencia y su forma de extracción. El empleo de procedimientos de extracción exclusivamente mecánicos, a temperaturas inferiores a 30ºC, y sin solventes químicos dotan al aceite de la denominación "virgen". Análisis posteriores de parámetros relacionados con la acidez y diferentes propiedades organolépticas, permiten a un aceite virgen alcanzar la denominación "extra"[12], siendo precisamente estos en los que se pueden encontrar la máxima concentración de sus numerosos componentes minoritarios, que se pierden prácticamente en su totalidad en los aceites refinados.

Desde un punto de vista químico, los compuestos presentes en el AOVE se pueden dividir en una fracción mayoritaria o saponificable, que corresponde al 98-99% del peso total del aceite, y una fracción minoritaria que supone el 1-2% del peso restante (Figura 2)[13]. Una de las principales propiedades del aceite de oliva es su alta proporción en AGMI, presentes en la fracción mayoritaria. Entre ellos, el ácido oleico es el más abundante (≃72.77%) en proporción a otros ácidos grasos presentes tales como el palmítico (≃12.09%), esteárico (≃3.01%), linoleico (≃9.47%) y α-linolénico (≃0.6%)[14]. Por otro lado, la fracción minoritaria, formada por más de 230 compuestos, se puede clasificar en dos tipos: fracción insaponificable, definida como la fracción extraída mediante solventes después de la saponificación; y la fracción fenólica[15]. Dentro de la fracción fenólica, se incluyen fenoles lipofílicos, tales como tocoferoles o tocotrienoles, y fenoles hidrofílicos. En la fracción fenólica hidrofílica se pueden distinguir 5 clases: 1) alcoholes fenólicos en los que se incluyen compuestos fenólicos simples como el hidroxitirosol (HT), tirosol (TIR) y sus formas glucosiladas; 2) ácidos fenólicos entre los que destacan el ácido gálico, el vanílico y el cafeico; 3) secoiridoides, caracterizados por la presencia de ácido elenólico o sus derivados en su estructura; 4) lignanos, cuya estructura se basa en la condensación de aldehídos aromáticos y 5) flavonoides, caracterizados por contener dos anillos de benceno unidos por una cadena lineal de tres carbonos y que pueden dividirse en flavonas y flavonoles[16].

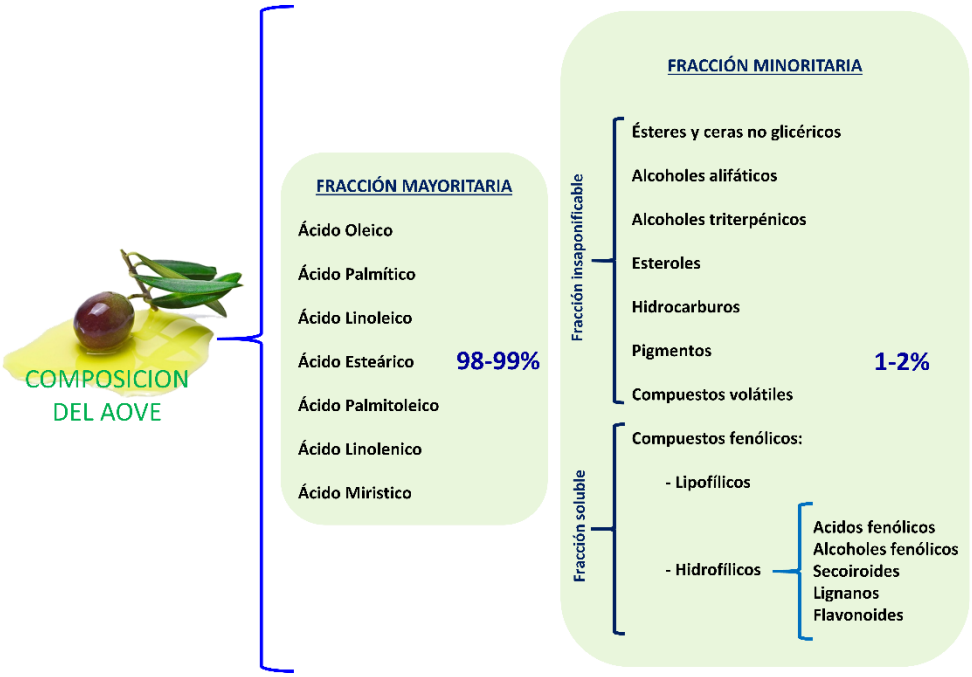

Figura 2. Composición del aceite de oliva virgen extra[16].

Históricamente las propiedades beneficiosas del consumo de aceite de oliva se han atribuido a su fracción saponificable y más concretamente a su alto contenido en AGMI. Sin embargo, otros aceites de origen vegetal también ricos en AGMI (por ejemplo de girasol, lino o soja), no son tan beneficiosos para la salud como el AOVE[17,18]. La diferencia entre estos aceites radica en los compuestos minoritarios del AOVE que no se encuentran presentes en otros aceites obtenidos a partir de semillas. De entre todos estos compuestos, los compuestos fenólicos han demostrado ampliamente ejercer diversos efectos beneficiosos en numerosas patologías[19]. Por todo ello, el interés suscitado por este tipo de compuestos y por su papel sobre la salud ha crecido de forma continua a lo largo de las últimas décadas.

1.2 Compuestos fenólicos del olivo

Los compuestos fenólicos, presentes tanto en el AOVE como en las hojas del olivo, poseen un fuerte carácter bioactivo atribuido principalmente sus propiedades antioxidantes. De forma natural, estos metabolitos secundarios, químicamente caracterizados por la presencia de uno o más anillos aromáticos y con uno o más radicales hidroxilos, son producidos por el olivo como fitoalexinas para combatir infecciones bacterianas y como respuesta a diferentes tipos de estrés ambiental. Su concentración final en el AOVE dependerá de diversos factores, como la variedad de olivo y el estado de maduración del fruto, factores ambientales (altitud, riego), condiciones y método de extracción, así como las medidas y tiempo de almacenaje[12]. Dentro de este grupo, la oleuropeína (OL) junto con el ligstrósido, ambos glucósidos del grupo de los secoiridoides, son los compuestos fenólicos más abundantes tanto en hoja y semilla como en pulpa y piel en la aceituna inmadura. Durante la maduración la OL, éster del ácido elenólico con el HT (hidroxitirosol ó 3,4-dihidroxifeniletanol), y el ligstrósido, éster del ácido elenólico con el TIR (tirosol ó 4-hidroxifeniletanol), son hidroxilados dando lugar a HT y TIR libres. El HT, el TIR, la OL y el ligstrósido y sus derivados representan aproximadamente el 90% de los compuestos fenólicos totales en el AOVE[20,21].

1.2.1 Hidroxitirosol y tirosol

El HT es un fenol anfipático con un peso molecular de 154.16 g/mol. Su estructura consta de un anillo de feniletanol con dos grupos hidroxilo en posiciones 3 y 4 (Figura 3). El HT se puede encontrar en forma libre, como hidroxitirosol-acetato o formando parte de compuestos complejos como la oleacina, verbascósido y OL. Aunque su concentración en el AOVE es muy variable los valores medios oscilan entre 0.5-14.4 mg/Kg, estableciéndose 7.7 mg/Kg como valor medio de HT libre en AOVE, valor resultante del análisis de 48 muestras recogidas en la base de datos phenol-explorer[22]. Las discrepancias en torno a su concentración son debidas a los métodos de análisis empleados para su valoración, así como de los diversos factores mencionados anteriormente. Sin embargo, cabe destacar que estos valores no tienen en cuenta el HT disponible a través de reservorios como la OL y sus derivados.

El TIR con un peso molecular de 138.17 g/mol, tiene una estructura química similar a la del HT, aunque sin presentar el radical hidroxilo en posición 3 (Figura 3). La carencia de ese grupo hidroxilo ha sido relacionada con su menor capacidad antioxidante en comparación con el HT[23]. Su concentración media en AOVE es de 11.3 mg/Kg, siendo así el más abundante[22]. Las propiedades antioxidantes tanto del TIR como del HT, están relacionadas con la donación de hidrógenos y su capacidad para mejorar la estabilidad de radicales libres mediante la formación de puentes de hidrogeno entre los hidrógenos de sus grupos hidroxilo y sus radicales fenoxi[24].

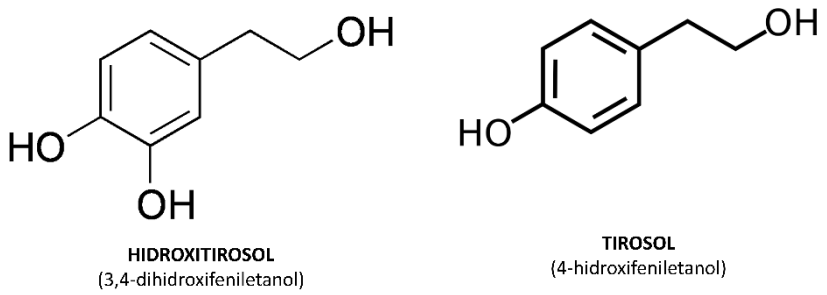

Figura 3. Estructura química del HT y TIR.

Esta ampliamente descrito que los compuestos fenólicos se absorben de forma dosis-dependiente en el intestino. Una vez absorbidos, se hidrolizan (fase I del metabolismo) en los enterocitos y pasan a la fase II, donde son transformados en glucurónidos, sulfatos y productos metilados. Así, el 98% del HT puede detectarse en plasma y orina en forma de glucurónido, y el 2% como forma libre cuando se administra a través del aceite de oliva. La absorción del HT ocurre principalmente por transporte pasivo en el intestino delgado, con una eficiencia que oscila entre el 75% y el 100%. El proceso de absorción depende del vehículo empleado, siendo la forma más efectiva a través del propio aceite[25]. Además, se ha descrito que su absorción está sujeta a factores como la edad, estado hormonal y sexo, manteniéndose por ejemplo durante más tiempo en el cuerpo de ratas hembra que en machos después de su administración oral. Su concentración plasmática máxima se alcanza unos 7 min después de la ingesta, aunque otros autores apuntan a que las concentraciones más altas en plasma son alcanzadas entre 30 min y 1 hora después de su administración oral siendo prácticamente indetectable tras 4 horas[26]. Una vez absorbido, pasa a formar parte de lipoproteínas plasmáticas de alta densidad, actuando como antioxidante y protector. Además, es curioso el hecho de la propia síntesis endógena de HT en humanos. La reducción del 3,4-dihidroxifenil acetaldehído, metabolito originado durante el metabolismo de la dopamina en el cerebro, mediante aldosa/aldehído reductasa da lugar a HT[27].

En 2011, la autoridad europea de seguridad alimentaria (EFSA), publicó un comunicado en el que afirmaba que "los polifenoles del aceite de oliva previenen la oxidación de las LDL", siempre que el aceite contenga no menos de 5 mg de HT y sus derivados (TIR y OL), cantidad alcanzable con el consumo de 20-25 ml de AOVE en el contexto de una dieta equilibrada[28].

2. HIPOXIA

La disminución en el nivel de oxígeno en células, órganos y tejidos juega un papel decisivo en multitud de procesos fisiológicos y patológicos. La hipoxia es beneficiosa en la embriogénesis, la menstruación, la curación de heridas o la diferenciación y mantenimiento de la pluripotencialidad de las células madre[29]. En patologías como las ECVs o la enfermedad renal crónica, la hipoxia moderada también favorece la activación de mecanismos de respuesta al daño que facilitan el restablecimiento de los niveles de O_2 y la recuperación de los tejidos afectados. Sin embargo, en otras patologías como el cáncer la hipoxia favorece la malignidad tumoral al promover el crecimiento y la supervivencia de las células, empeorando el pronóstico de los pacientes. En definitiva, dependiendo de su severidad y de la patología en cuestión, la hipoxia puede resultar enemiga o aliada, además de determinante, al abordar el tratamiento. En los siguientes apartados nos centraremos en el cáncer y el ictus isquémico, dos patologías de gran importancia socioeconómica en las que, como ya se ha mencionado, la hipoxia desempeña un papel central.

2.1 Cáncer

El cáncer agrupa a un conjunto de enfermedades genéticas en las que se combinan la activación de oncogenes y la inactivación de genes supresores de tumores y que se caracterizan no solo por una proliferación celular descontrolada sino también por la capacidad de las células de invadir otros tejidos y diseminarse desde su ubicación original. Aunque algunas mutaciones germinales aumentan el riesgo de sufrir cáncer, la inmensa mayoría de las alteraciones en el ADN de las células tumorales son somáticas.

La incidencia y mortalidad del cáncer a nivel mundial está aumentando de forma progresiva. Las razones son complejas pero se atribuyen principalmente al aumento de la población y de la esperanza de vida, así como a cambios en la prevalencia y distribución de sus principales factores de riesgo, muchas veces asociados al desarrollo socioeconómico[30]. Concretamente en España, según los últimos datos del Instituto Nacional de Estadística, el cáncer constituye la segunda causa de mortalidad (26,7%) detrás de las enfermedades del sistema circulatorio (28,8%) y delante de las del sistema respiratorio (12,2%), ocupando el primer lugar entre los hombres (300,1 fallecidos por cada 100.000) y el segundo entre las mujeres (188,8 fallecidos por cada 100.000). Dentro de la multitud y diversidad de patologías englobadas bajo este término, el de mama es la neoplasia maligna más común entre las mujeres y una de las tres más frecuentes en todo el mundo, junto con el cáncer de pulmón y colon[31]. El 95% de las pacientes con cáncer de mama son mujeres de 40 años o más y su tasa de supervivencia mejora con el diagnóstico precoz lo que explica la importancia de los programas de prevención, detección y estudio de cáncer de mama[32].

En los tumores sólidos, como el cáncer de mama, el crecimiento celular descontrolado da lugar a regiones poco irrigadas en las que la presión parcial de oxígeno (O_2), comprendida entre 40-60 mm Hg (5-13% O_2) en tejidos normales, disminuye hasta alcanzar aproximadamente los 8-10 mm Hg (~1% O_2)[33]. La hipoxia generada en estos microambientes favorece la progresión y malignidad tumoral. De hecho, la práctica totalidad de las características que definen a una célula tumoral, descritas por Hanahan y Weinberg en el año 2000 y revisadas en 2011 (Figura 4), se encuentran relacionadas con la hipoxia[34]. Así, procesos como la

angiogénesis, la reprogramación metabólica, la supervivencia celular, la invasividad o la capacidad metastásica de las células tumorales, no pueden ser estudiados sin tener en cuenta el papel que la hipoxia ejerce sobre ellos. Por tanto, es fácil entender que la hipoxia favorezca la quimio- y radiorresistencia y por ende ejerza un impacto negativo en la respuesta de los pacientes a los tratamientos[35].

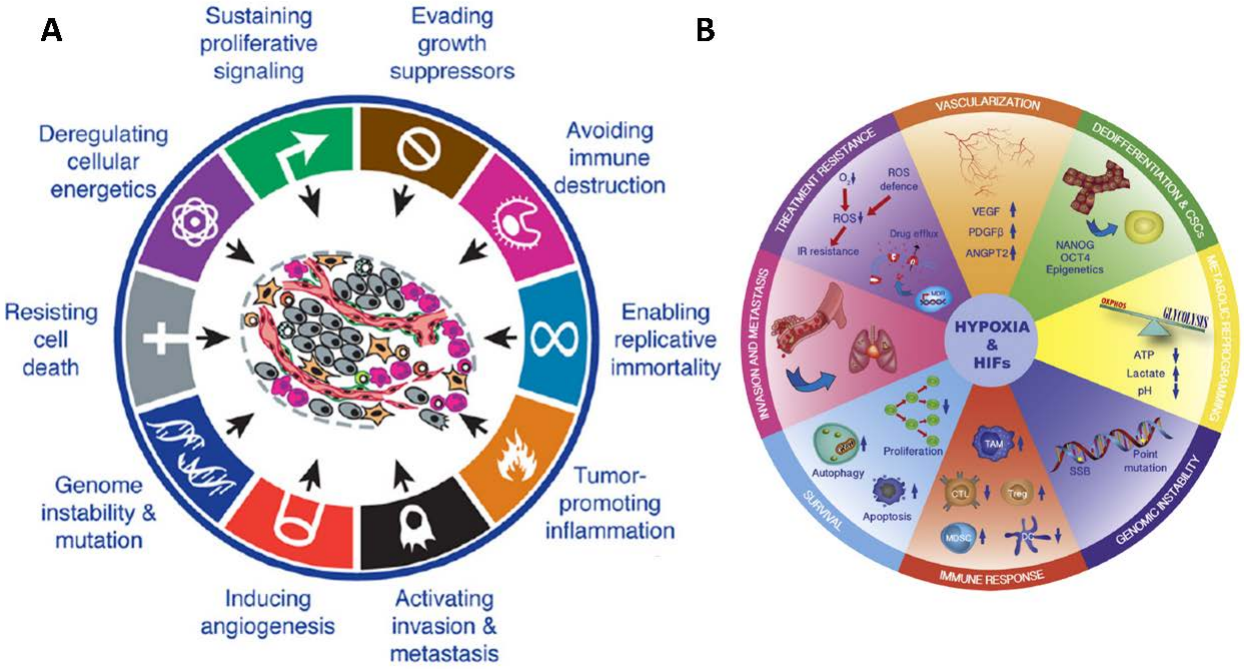

Figura 4. (A) Principales características de las células tumorales[34]. (B) Características de las células tumorales afectadas por la hipoxia[36].

2.1.1 Estrés oxidativo, hipoxia y malignidad tumoral

El estrés oxidativo resulta del desequilibrio entre la producción de especies reactivas de oxígeno (ERO) y la capacidad antioxidante de la célula. Las principales fuentes de ERO son la cadena respiratoria mitocondrial, el citocromo P450 y las enzimas NADPH oxidasa (NOX), xantina oxidasa y lipooxigenasa[37]. En las células tumorales los niveles de ERO son superiores a los de las células sanas. Este hecho se debe a múltiples factores entre los que se podrían citar su mayor actividad metabólica, la modificación de la funcionalidad mitocondrial, la sobre-activación de rutas de transducción de señales inducidas por factores de crecimiento, la infiltración del tumor con células del sistema inmune o a la mayor actividad de oxidasas, ciclooxigenasas, lipoxigenasas o de la timidina fosforilasa[38]. Además, como se ha mencionado, el crecimiento del tumor genera regiones en las que la distancia de las células a los vasos sanguíneos supera el límite de difusión del oxígeno (200 µm), lo que conlleva una situación de hipoxia que favorece aún más la producción de estas especies[39]. El mecanismo por el la hipoxia aumenta la producción de ERO parece estar relacionado con su efecto sobre los complejos I, II y III de la cadena de transporte de electrones e implicaría cambios estructurales que, por ejemplo, aumentan la vida media de la semiquinona y favorecen la salida de superóxido ($O_2^{\cdot-}$) al espacio intermembrana[40]. De hecho, se ha descrito que el uso de inhibidores específicos de cada uno de estos complejos, previene la acumulación de ERO durante la hipoxia[41].

Las consecuencias derivadas del estrés oxidativo dependen en gran medida del nivel que este llegue a alcanzar (Figura 5). Una gran sobreproducción de ERO producida por ejemplo durante la quimio- o radioterapia genera un daño letal en la célula que, al poner en marcha diferentes procesos de muerte celular

como la apoptosis o la necroptosis, resulta positivo para el control tumoral (Figura 5C)[38]. Sin embargo, a concentraciones menores (subletales) las ERO actúan como moléculas de señalización que promueven todas las etapas de desarrollo del cáncer (Figura 5B). De hecho, potencian la mutación y la inestabilidad genómica, pudiendo dar lugar a la activación de proto-oncogenes y la inactivación de genes supresores de tumores que favorecen la transformación de una célula sana en una célula tumoral. Las ERO también favorecen, de forma indirecta, cambios epigenéticos como la hipermetilación del promotor de la E-caderina que potencia la capacidad metastásica de las células tumorales[42]. De igual forma, la oxidación de receptores de factores de crecimiento, quinasas, fosfatasas o factores de transcripción modifica su actividad y puede también favorecer el fenotipo maligno. Entre otros ejemplos, la oxidación de la Cys-118 de Ras inhibe su actividad GTPasa y provoca la activación descontrolada de la vía MAPK/Erk1/2 que, además de retroactivar la producción de ERO vía NOX y promover la proliferación celular, favorece otros procesos como la angiogénesis, la supervivencia celular o la motilidad[43]. La oxidación del centro catalítico de la fosfatasa PTEN, impide la inactivación de la ruta de PI3K/Akt induciendo procesos como la proliferación celular, evasión de la muerte celular, angiogénesis o inactivación de p53[44]. En definitiva, se establece un círculo vicioso en el que un aumento inicial de ERO favorece la transformación tumoral y, a su vez, la activación de determinadas señales oncogénicas en las células transformadas y su entorno potencia la malignidad tumoral y la formación de más ERO.

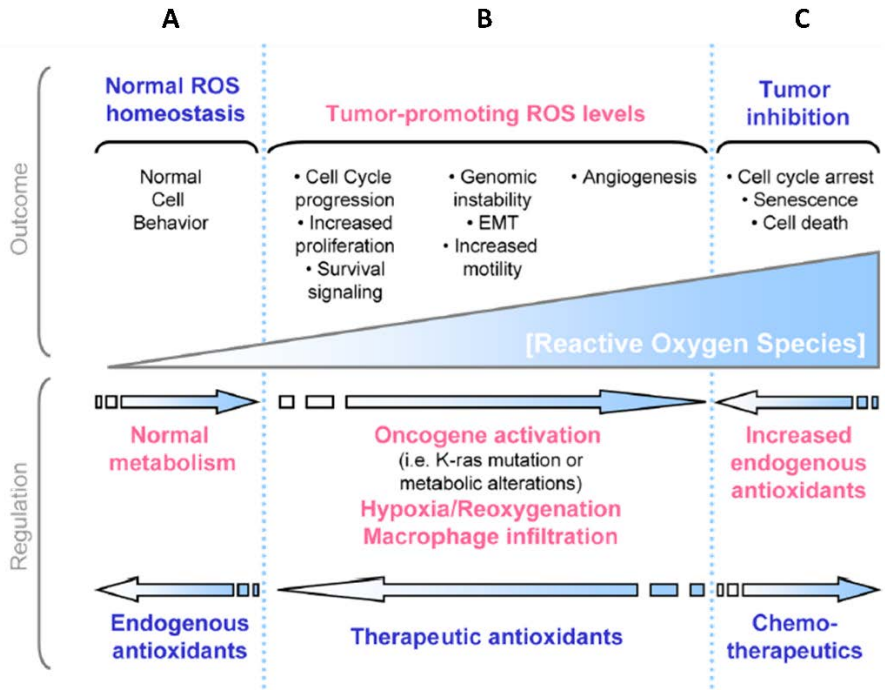

Figura 5. Efecto de las ERO en función de su concentración. (A) En las células normales los niveles de ERO se mantienen estables gracias al equilibrio entre su producción y eliminación. **(B)** La ruptura de ese balance por eventos tumorigénicos como la activación de oncogenes (como K-ras), la hipoxia/reoxigenación y la infiltración de macrófagos, favorece la formación y progresión tumoral. **(C)** La sobreproducción de ERO inducida por la quimio- y radioterapia da lugar a la detención del ciclo celular y a la muerte de las células tumorales[38].

De lo expuesto hasta ahora se deduce que la célula tumoral se ve beneficiada por el estrés oxidativo, siempre y cuando se mantenga en unos niveles controlados que no produzcan un daño excesivo. Para ejercer esa función de control resultan clave diferentes mecanismos de defensa antioxidante como los inducidos por el factor 2 relacionado con el factor nuclear eritroide-2 (Nrf2) (Figura 6). Nrf2 es un factor de transcripción que, una vez en el núcleo, puede unirse a promotores que presentan elementos de respuesta

antioxidante (ARE) induciendo la transcripción de diversos genes relacionados con mecanismos de respuesta antioxidante y de detoxificación. En condiciones basales, Nrf2 se encuentra secuestrado en el citoplasma por su represor Keap-1. Sin embargo, el aumento en los niveles de ERO provoca la oxidación de 3 cisteínas claves de Keap-1 (Cys-151, Cys-273 y Cys-288) originando un cambio conformacional que permite la disociación de Nrf2. Keap1 disociado se ubiquitina para su degradación en el proteasoma, mientras que Nrf2 se transloca al núcleo, donde heterodimeriza con el factor de transcripción MAF para iniciar la transcripción de diversos genes como la superóxido dismutasa (SOD), hemooxigenasa-1 (HO-1), NAD(P)H:quinona oxidorreductasa-1 (NQO1), y glutatión-transferasas (GSTs) que reducen el nivel de estrés oxidativo[45]. La actividad de Nrf2 también puede ser potenciada por coactivadores como PGC-1α, principal regulador de la biogénesis mitocondrial que también interacciona con otros factores de transcripción[46].

El papel de Nrf2 en cáncer es controvertido. Debido a la implicación del estrés oxidativo en la iniciación y progresión del cáncer, la respuesta antioxidante mediada por Nrf2 ha sido objeto de estudio por su papel quimiopreventivo. El carácter protector de Nrf2 en cáncer se ha demostrado en ratones knockout ($Nrf2^{-/-}$). La ausencia de Nrf2 aumentó la susceptibilidad a procesos neoplásicos gástricos y de colon y promovió la metástasis pulmonar y ósea de células de melanoma[47-49]. Estos estudios demuestran la función protectora de la ruta de Nrf2 en cáncer, la cual se deriva de su capacidad para mantener el equilibrio de ERO en la célula. Sin embargo, su hiperactivación en tumores origina un ambiente que puede favorecer la supervivencia de las células cancerígenas protegiéndolas de un daño oxidativo excesivo, como el inducido por la quimio- y radioterapia[50].

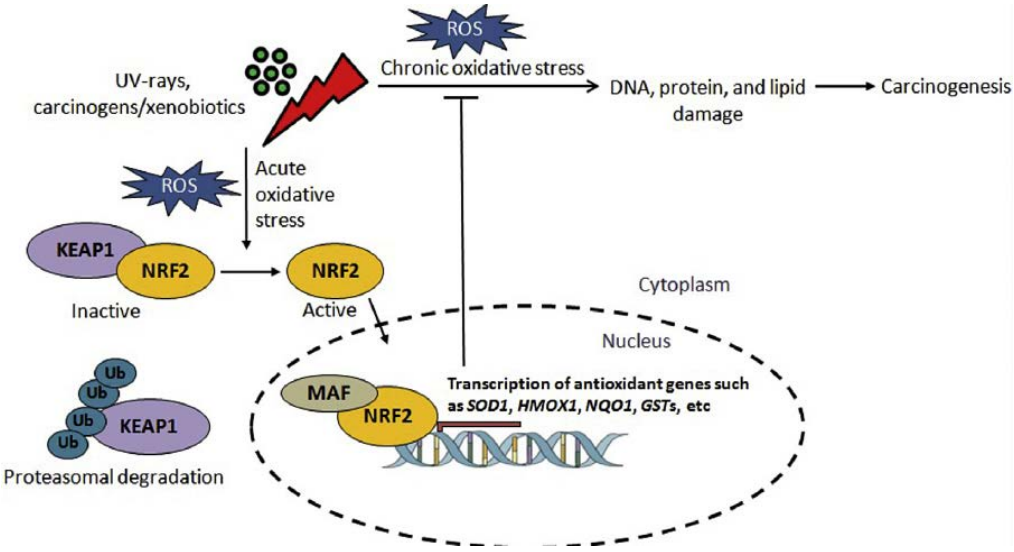

Figura 6. Activación de Nrf2 en respuesta al estrés oxidativo[51].

2.1.2 *Factor inducible por hipoxia: estructura y regulación de HIF-1 y su papel en cáncer*

La respuesta adaptativa a la hipoxia, inicialmente desfavorable para el crecimiento celular, es mediada por los factores inducibles por hipoxia (HIFs). Los HIFs son heterodimeros constituidos por dos subunidades, la subunidad α (HIF-1α, HIF-2α o HIF-3α) sensible al oxígeno y la subunidad β (HIF-β o ARNT), de expresión constitutiva. La existencia de tres variantes de subunidad α conlleva la formación de tres factores de transcripción diferentes, HIF-1, HIF-2 o HIF-3.

Las subunidades HIFs pertenecen a la familia de proteínas *basic helix–loop–hélix* (bHLH)-*PER-ARNT-SIM* (PAS) (Figura 7) en la que se incluyen otras como el receptor de hidrocarburos de arilo (AHR). Los dominios bHLH y PAS son esenciales para la heterodimerización de las subunidades α y β y para la unión a los

elementos de respuesta a hipoxia (*hypoxia response elements*, HRE) de los genes diana[52]. Además, todas las subunidades presentan dominios de transactivación (TAD). En HIF-1α y HIF-2α se diferencian dos dominios de transactivación diferentes, el NH2-terminal (N-TAD) y el COOH-terminal (C-TAD). El dominio C-TAD participa en la interacción con coactivadores como CBP/p300 mientras que el N-TAD, presente solo en las subunidades α, permite su estabilización. De hecho, N-TAD está incluido en un dominio mayor, el dominio de degradación dependiente de oxígeno (*oxygen dependent degradation domain,* ODDD) en el que aparecen dos prolinas (Pro-402/Pro-564) y una lisina (Lys-532) que, como veremos más adelante, son claves en la regulación de la vida media de la subunidad y en la regulación de la actividad transcripcional[53].

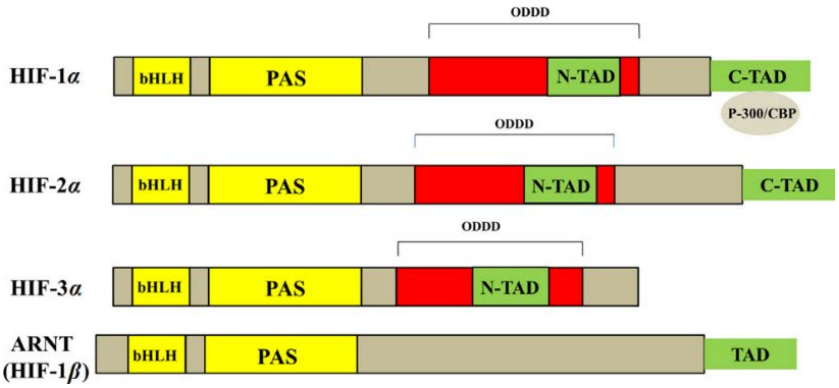

Figura 7. Representación esquemática de la estructura de las principales subunidades HIFs[54].

Dado que HIF-1 es el miembro más conocido de esta familia, y el más ubicuamente expresado, nos centraremos en él. El principal mecanismo de regulación de HIF-1 es la degradación de su subunidad α de forma dependiente de oxígeno[52]. HIF-1α es una proteína muy inestable en condiciones de normoxia, con una $t_{1/2}$ inferior a 5 minutos. Su rápido recambio se debe a la hidroxilación de las Pro-402 y Pro-564 del ODDD (Figura 8A). La hidroxilación de estos residuos está catalizada por unas enzimas llamadas HIF prolil hidroxilasas (PHDs), cuyo dominio catalítico reconoce un motivo LXXLAP del ODDD. Las PHDs pertenecen a la familia de dioxigenasas dependientes de Fe^{+2} y α-cetoglutarato que, con el requerimiento de ascorbato para mantener el estado ferroso del hierro, rompen el oxígeno molecular para hidroxilar sus sustratos a la vez que oxidan y descarboxilan el α-cetoglutarato generando succinato. La hidroxilación de estos residuos permite el reconocimiento por la proteína von Hipel-Lindau (VHL) que, conjuntamente con otras proteínas (elongina B, elongina C, Cul2 y Rbx), actúa como una E3 ubiquitina ligasa mediando la ubiquitinación y degradación de HIF-1α en el proteosoma. La dependencia de O_2 de las PHDs, provoca la inhibición de su actividad en situaciones de hipoxia y, por tanto, la estabilización de la subunidad α que podrá dirigirse al núcleo donde, gracias a su dimerización con HIF-β y a su interacción con el complejo p300/CBP, inducirá la transcripción de genes que presenten HRE (Figura 8B)[55].

Aunque la degradación de HIF-1α en situaciones de hipoxia es la principal forma de regulación del nivel de HIF-1, existen otros mecanismos que en un contexto oncogénico cobran especial importancia. Así, los factores de crecimiento, las citoquinas, las ERO y el NO, entre otros, pueden también favorecer la acumulación de HIF-1α. En este sentido, diversos trabajos han demostrado la participación de las rutas PI3K/Akt, de la proteína quinasa C (PKC) o del factor nuclear de células T activadas (NFAT) en la regulación transcripcional de HIF-1α en respuesta al tratamiento con TNFα/IL-4, TNF-α/IL-1β o angiotensina II o ante un incremento en la producción de ROS (Figura 8C)[56]. La activación de la PI3K también actúa favoreciendo la traducción de HIF-1α a través de la proteína quinasa B (PKB/Akt) y de la diana de rapamicina en células

de mamífero (mTOR) (Figura 8D). Concretamente, la actividad de mTOR inhibe mediante fosforilación, la unión del factor eucariótico de iniciación de la traducción 4E (eIF-4E) a su proteína de unión (4E-BP1), permitiendo así que eIF-4E se una al Cap de los ARNm y aumente su traducción[57]. Además, mTOR también fosforila y activa a la quinasa de la proteína ribosomal S6 (S6K ó P70) que, a su vez fosforila y activa a S6 favoreciendo también la traducción de HIF-1α[58]. La cascada Ras/Raf/MEK/ERK^{MAPK} ejerce un efecto similar al inducir, de forma directa o indirecta, la fosforilación de 4E-BP1 y S6K. Las ERO y el óxido nítrico (NO), especialmente elevado en el ambiente tumoral como consecuencia de la activación de la NO sintasas inducible (iNOS) y endotelial (eNOS), también favorecen la acumulación de HIF-1 por inhibición de las PHDs, incluso en condiciones de normoxia. En el caso de las ERO, el mecanismo que subyace implica la oxidación del Fe^{+2} de su centro activo[59]. El NO puede inhibir la acción de las PHDs al competir con el O_2 por el centro catalítico o por S-nitrosilación de varios de sus residuos. Además, la S-nitrosilación de VHL y del propio HIF-1α impide el reconocimiento mutuo y favorece la acumulación de que HIF-1α aunque este haya sido previamente hidroxilado por las PHDs[58,60].

Los mecanismos descritos hasta ahora actúan aislada o conjuntamente para modificar el nivel de HIF-1α, pero la actividad transcripcional de HIF-1, en la que los TADs desempeñan un papel clave, también está sometida a regulación dependiente de oxígeno. Así, en condiciones de normoxia el factor inhibidor de HIF (FIH), otra dioxigenasa dependiente de O_2 y de α-cetoglutarato, hidroxila un residuo de asparragina en el dominio C-TAD de HIF-1α (Asn-803) impidiendo la unión de los coactivadores CBP/p300 y, por tanto, la actividad transcripcional HIF-1. Al igual que ocurría con las PHDs, las ERO también inhiben la actividad de FIH mediante la oxidación directa del Fe^{+2} de su centro catalítico, favoreciendo así la actividad transcripcional de HIF-1 α[61].

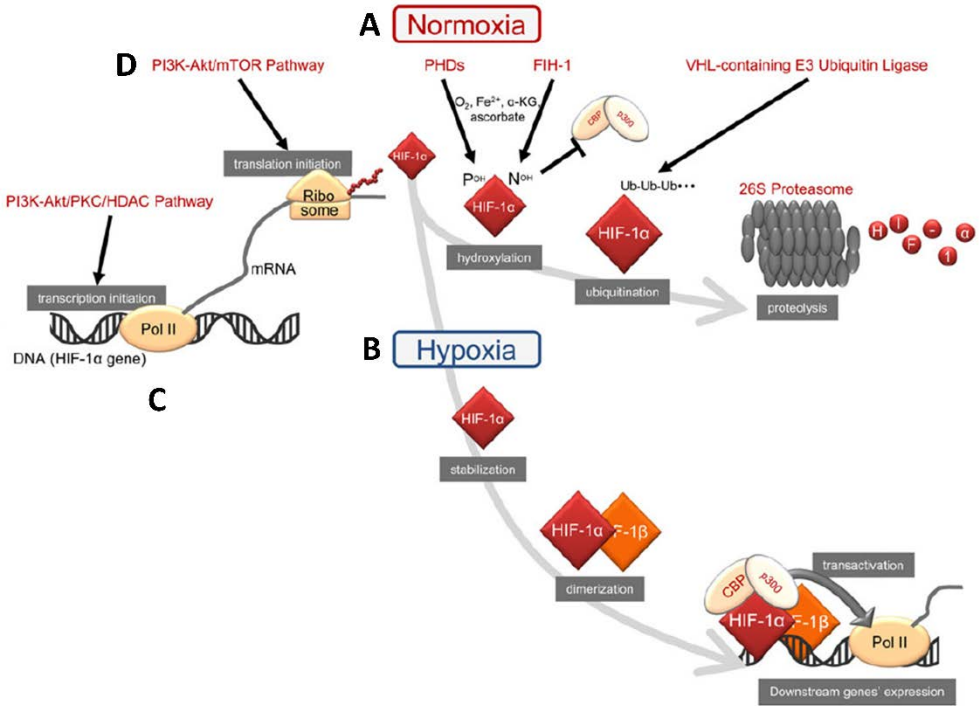

Figura 8. Mecanismos implicados en la activación de HIF-1[62].

El resultado final de la activación de HIF-1 es la expresión de una gran variedad de genes que presentan HRE y que están implicados en todos los procesos relacionados con la malignidad tumoral (Figura 4). Por tanto, la expresión de HIF-1α es un indicador de mal pronóstico y su inhibición una posible estrategia terapéutica

en el tratamiento antitumoral. Entre los procesos regulados por HIF-1 se encuentran la proliferación celular, la muerte celular, la adaptación del metabolismo, la respuesta inmune, la inestabilidad genómica, la angiogénesis, la desdiferenciación y pluripotencialidad así como la invasión y la metástasis. Respecto al primero de ellos, la actividad transcripcional de HIF-1 provoca por ejemplo la detención del ciclo celular mediante la inhibición de Myc. Esta inhibición ocurre por diferentes mecanismos como el desplazamiento de Myc de su unión al ADN bien por la interacción física con HIF-1α o por el solapamiento de sus regiones de unión lo que, de una u otra forma, facilita la derepresión de los inhibidores de las quinasas dependientes de ciclina p21 y p27, que también pueden ser inducidos directamente por HIF-1. Además, la actividad transcripcional de Myc también se inhibe mediante Mxi-1, gen diana de HIF-1, que compite con Myc por su unión a Max para formar el factor de transcripción activo[63]. El efecto de HIF-1 sobre la muerte celular es complejo. Por un lado, HIF-1 podría reducir la apoptosis al inhibir la expresión del gen proapototico Bid[64]. Por otra parte, la inducción de BNIP3 y BNIP3L podría favorecer la apoptosis y la autofagia[65,66]. La inducción de la autofagia en un tumor maligno establecido puede resultar negativa ya que contribuye a la supervivencia celular y a la resistencia al tratamiento. La adaptación metabólica resulta también clave para la supervivencia en situaciones de hipoxia y, de hecho, el efecto Warburg (utilización de la glucólisis aeróbica como fuente de energía en lugar de la fosforilación oxidativa mitocondrial[67]) a pesar de haber sido descrito en la primera mitad del siglo XX es una característica de las células tumorales que ha suscitado gran interés en los últimos años. La actividad transcripcional de HIF-1 facilita esta adaptación mediante la expresión de transportadores de membrana como el transportador de glucosa 1 (Glut-1), enzimas como la fosfofructoquinasa (PFK), lactato deshidrogenasa (LDHA)[68] o la piruvato deshidrogenasa quinasa 1 (PDK1) que inhibe la conversión de piruvato en acetil-CoA[69]. HIF-1 también favorece la inmunosupresión por ejemplo, mediante la inducción de la proteína PD-L1 que inhibe la actividad de los linfocitos T[70] o la inestabilidad genómica al inhibir la expresión de genes relacionados con la reparación del ADN como MSH2, MSH6 y BRCA1[71]. Así, se ha demostrado que después de la exposición a radiación ultravioleta, células tumorales cultivadas en condiciones de hipoxia, presentan un mayor número de mutaciones y una menor tasa de reparación del ADN que células cultivadas en normoxia[72]. La angiogénesis, formación de nuevos vasos a partir de la vasculatura preexistente, resulta también clave para facilitar la llegada de oxígeno y nutrientes al tumor. Uno de los uno de los factores de crecimiento más característicos regulado positivamente por HIF-1, es el factor angiogénico VEGF (factor de crecimiento vascular endotelial)[73] o el péptido vasoactivo adrenomedulina (AM) cuya inhibición produce una reducción significativa en la progresión tumoral[74]. HIF-1 también favorece la sobreexpresión de genes característicos de células pluripotentes como Notch o la telomerasa favoreciendo por tanto el fenotipo de células madre tumorales[75]. Por último, la metástasis es la principal causa de muerte por cáncer. El 29% de las pacientes de cáncer de mama primario presentan altos niveles de la proteína HIF-1α, pero este valor aumenta hasta el 69% en los casos de cáncer de mama que cursan con metástasis. De hecho, HIF-1 favorece la transición epitelio-mesénquima mediante la acción de sus genes diana SNAIL, TWIST y Zeb, al provocar la represión de la E-cadherina, principal encargada de mantener la cohesión celular[76-78]. Por otro lado, HIF-1 también favorece la invasividad de las células tumorales y la degradación de la matriz extracelular mediante la sobreexpresión de catepsina D, metaloproteasas de matriz (MMP2 y MMP9) y la activación de Met[79-81].

2.1.3 *Cáncer y compuestos fenólicos del olivo*

Los estudios acerca de las propiedades antitumorales de los compuestos fenólicos del olivo han aumentado progresivamente en las últimas décadas. Hasta la fecha, se han publicado estudios en multitud de líneas celulares de cáncer, predominando los estudios en cáncer de mama, además de varios trabajos en modelos animales.

En los estudios realizados *in vitro*, destacan los efectos antiproliferativo y proapoptoticos del HT y de la OL[82-84]. La estimulación de la apoptosis observada para estos compuestos fenólicos se ha relacionado con el aumento de cJNK, p53, Bax y *citocromo c*. También se ha descrito que el HT y la OL inhiben la angiogenesis mediante la inhibición de la activación de NFκB y la disminución de la expresión de la ciclooxigenasa-2 (COX-2), de la formación de ERO y de la liberación de MMP9[19]. En líneas celulares de cáncer de mama, el HT provoca detención del ciclo celular al disminuir los niveles de ciclina D1[85]. También inhibe la expresión del receptor 2 del factor de crecimiento epidérmico humano (HER2)[86]. Por último, un estudio reciente, demuestra la capacidad del HT para inhibir procesos metastásicos y reducir las características de célula madre de varias líneas de cáncer de mama triple negativas[87].

El carácter anti-tumoral de estos compuestos también se ha observado en modelo *in vivo*. Un estudio en el que se utilizaron ratones atímicos con xenoinjertos de células HT-29 demostró que el HT inhibía el crecimiento tumoral en un 50%, reduciendo la expresión del marcador tumoral Ki-67 y activando la caspasa-3. Además, estos efectos se asociaron a una reducción en la angiogénesis, efecto debido, a una inhibición de HIF-1α, y su diana VEGF, así como de la prostaglandina-E sintasa microsomal 1 (mPGEs-1)[88]. En otro estudio, el HT fue capaz de inhibir el crecimiento de los xenoinjertos de células TFK-1 de colangiocarcinoma en ratones, disminuyendo también el marcador Ki-67[89]. De manera similar, el HT inhibió el crecimiento del tumor derivado de la inyección subcutánea de células de glioma C6 en ratas Wistar[90]. También se ha estudiado el carácter quimiopreventivo del HT en un modelo de tumor mamario inducido químicamente con DMBA (7,12-dimetil-1,2-benzantraceno) en ratas Sprague-Dawley hembra, demostrando su capacidad para reducir el volumen de los tumores[91]. Por último, su combinación con Placitaxel, quimiterapico utilizado comúnmente en el tratamiento del cáncer de mama, fue capaz de reducir el volumen de los tumores en comparación con el tratamiento solo con placitaxel, mejorando además el estado antioxidante sin comprometer la capacidad antitumoral del quimioterapico[92].

2.2 ICTUS ISQUEMICO

2.2.1 *Generalidades y terapias*

El termino ictus, del latin “golpe”, se utiliza para designar aquella enfermedad cerebrovascular que se presenta de un modo súbito. El ictus es una de las principales causas de muerte y discapacidad. Concretamente, en Europa es responsable de 1,1 millones de muertes/año y en España afecta a unas 130.000 personas/año, de las que el 60% fallece o quedan discapacitadas[93]. El estudio internacional INTERSTROKE, realizado en 32 países con 26919 participantes, identificó hasta 10 factores de riesgo potencialmente modificables y relacionados con el ictus: hipertensión, actividad física, ratio ApoB/ApoA1, dieta, relación cintura-cadera, factores psicosociales, causas cardiacas, tabaquismo, consumo de alcohol y la diabetes mellitus[94].

Existen dos tipos principales de ictus (Figura 9): el ictus hemorrágico producido por la ruptura de un vaso con la consiguiente hemorragia cerebral y el ictus isquémico causado por una disrupción abrupta y sostenida del flujo sanguíneo cerebral (FSC), generalmente debida a trombosis arteriales[95]. Este último, que es el más común (80-85% de los casos), produce infartos generalmente en el territorio irrigado por la arteria cerebral media. La zona infartada tiene un núcleo, tejido con ausencia total o casi de FSC que se daña de forma irreversible, y una zona de penumbra susceptible de recuperación, en las que las neuronas inicialmente retienen su potencial de membrana en reposo, pero no su capacidad de disparar potenciales

de acción[96]. La extensión y gravedad de la lesión cerebral resultante después de la isquemia, depende de factores como el nivel de reducción del FSC, la duración de la isquemia o la existencia de una circulación colateral eficaz. El mantenimiento de una adecuada presión arterial es clave dado que la pérdida de funcionalidad de las células endoteliales y de la musculatura lisa del vaso afectado hace que la presión de perfusión cerebral pase a depender de la presión arterial. Aunque hay varias formas de clasificar la severidad del infarto a nivel clínico, la más aceptada consiste en una combinación de diagnóstico por neuroimagen, que permite analizar la lesión establecida, y la evaluación neurológica[97].

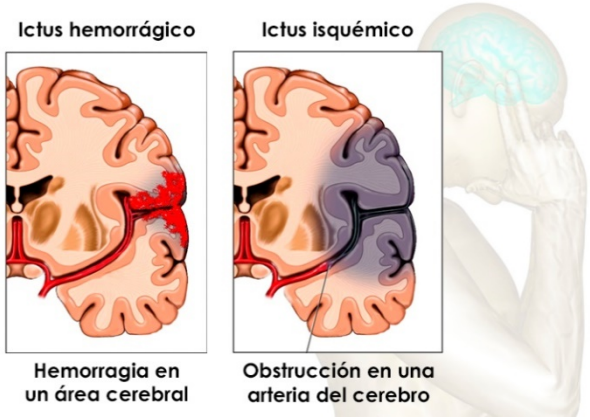

Figura 9. Principales tipos de ictus.

A pesar de la alta incidencia de ictus, aún no hay un tratamiento efectivo disponible para prevenir la lesión en los ictus hemorrágicos. En el caso de los isquémicos, las estrategias actuales incluyen la terapia farmacológica (activador tisular del plasminógeno recombinante, rtPA), métodos mecánicos (disrupción mediante dispositivos stent-retriever y/o extracción mediante succión del trombo) o la combinación de ambas[98]. La diana de todas ellas es la recuperación del tejido de la penumbra. Así, el tratamiento con rtPA actúa en la fase aguda del ictus disolviendo el coágulo y mejorando el FSC. Sin embargo, el 10-40% de los pacientes tratados desarrollan procesos hemorrágicos que aumentan la morbi- mortalidad y, si no es administrado dentro de las primeras horas después del accidente cerebrovascular (3-4,5 h), no evita la neurodegeneración adicional[99]. Recientemente la terapia endovascular, que incluye la trombólisis farmacológica intraarterial y la trombectomía mecánica, ha supuesto un gran logro en el tratamiento del ictus isquémico. De hecho, su efectividad tanto a corto como a largo plazo ha quedado demostrada en diferentes ensayos clínicos, aun aplicándose hasta 8 horas tras el accidente cerebrovascular[100]. Además de estas aproximaciones terapéuticas, en las últimas décadas, se han probado otras estrategias (aspirina, cirugía descompresora, hipotermia, inhibidores frente a mediadores moleculares del daño isquémico) con resultados poco relevantes [101-103]. Cualquier intervención futura, tanto preventiva como terapéutica, debería ir no solo dirigida a la restauración del flujo sanguíneo en la zona infartada sino también a potenciar mecanismos de protección de forma eficaz.

2.2.2 *El daño isquémico*

El metabolismo del cerebro y el mantenimiento de sus funciones están íntimamente ligados a la existencia de un FSC que garantice la adecuada liberación de glucosa y oxígeno. Por tanto, ante una isquemia cerebral se produce una lesión neuronal que será la suma del daño originado por la propia isquemia, más el causado tras la recuperación del FSC (etapa de reperfusión). Se podría decir que en la primera etapa se producen las causas que desencadenan las reacciones que tienen lugar en la segunda, y que implican un aumento del

daño e inflamación propios de esta patología[104]. El conjunto de cambios bioquímicos y secuenciales que acontece tras la depleción de oxígeno y glucosa generada por un ictus es conocido como cascada isquémica. A grandes rasgos, la cascada isquémica engloba la excitotoxicidad mediada por glutamato, la formación en exceso de ERO y especies reactivas de nitrógeno (ERN), la disfunción mitocondrial, la ruptura de la barrera hematoencefálica y la inflamación[105]. El conocimiento de todos estos procesos resulta clave para entender la progresión de la lesión y la destrucción celular asociada al ictus. Por tanto, pasamos a detallarlos de modo somero (Figura 10).

Tras el ictus, la caída del FSC inhibe de forma inmediata la cadena de transporte electrónico y la fosforilación oxidativa desviando el metabolismo de la glucosa hacia la glucólisis anaerobia con la consiguiente formación de lactato. El rendimiento energético de esta forma de catabolismo es mucho menor que le aeróbico lo que, unido a la poca disponibilidad de glucosa y al prácticamente nulo nivel de glucógeno de las neuronas, agrava la depleción energética[106]. Los mecanismos encargados del mantenimiento de la homeostasis iónica (ej. Na^+/K^+ ATPasa, Ca^{++} ATPasas) son dependientes de ATP. Por tanto, la caída en el nivel de ATP provoca un aumento en el nivel de Na^+ que conlleva la despolarización de la membrana de la neurona. A su vez, la despolarización provoca la elevación en los niveles de Ca^{+2} intracelulares por apertura de canales sensibles al voltaje, e induce la liberación desde las terminales presinápticas de glutamato. En la neurona post-sináptica el glutamato interactúa con receptores ionotrópicos ej. NMDA (N-metil-D-aspartato) o AMPA (ácido alfa-amino-3-hidroxi-5-metil-4-isoxazolpropiónico) generando una entrada masiva de calcio, sodio y agua que puede acabar desembocando en la muerte neuronal[107]. Además, el glutamato también puede actuar sobre receptores metabotrópicos acoplados a proteínas G. Los de tipo I, asociados a proteínas Gq, activan la fosfolipasa C produciendo inositol-1,4,5-trisfosfato que, mediante determinados canales de Ca^{+2} del retículo endoplasmático provoca la salida de más Ca^{+2} hacia el citosol. A su vez, el aumento del Ca^{+2} activa la iNOS favoreciendo la formación de NO y diversas enzimas hidrolíticas (proteasas, lipasas, nucleasas). Además, el Ca^{+2} en la mitocondria puede provocar la apertura de poros de transición de permeabilidad mitocondrial lo que potencia, entre otros, la salida de proteínas que favorecerán la apoptosis, la inhibición de la cadena de transporte electrónico y la disrupción de la fosforilación oxidativa (de hecho, se potencia la actividad ATP hidrolasa de la F_0F_1-ATP sintasa). La alteración de la cadena respiratoria durante la fase isquémica conllevará un incremento en la producción de $O_2^{\cdot-}$ mitocondrial cuando se reestablezca, al menos parcialmente, el FSC en la fase de reperfusión (Figura 11) [108]. Además, el aumento de Ca^{+2} también activa la fosfolipasa A_2 que hidroliza fosfolípidos de membrana liberando ácido araquidónico sobre el que actuarán las enzimas ciclo- y lipooxigenasas para formar eicosanoides en un proceso en el que también se puede producir $O_2^{\cdot-}$. Por último, el calcio también activa la enzima NADPH oxidasa contribuyendo a la formación de más $O_2^{\cdot-}$. El $O_2^{\cdot-}$ de diversos orígenes al combinarse con NO, generará una especie altamente dañina, el peroxinitrito ($ONOO^-$) contribuyendo así al daño celular[109]. El cerebro es especialmente sensible al aumento de todas estas especies reactivas debido a su alto consumo basal de oxígeno, a su alta concentración en lípidos, a los altos niveles de hierro que actúan como prooxidantes durante situaciones de estrés y a su limitada capacidad antioxidante. Por tanto, la producción descontrolada de estas especies puede tener graves consecuencias en el funcionamiento del sistema nervioso central y conllevar importantes secuelas en los pacientes.

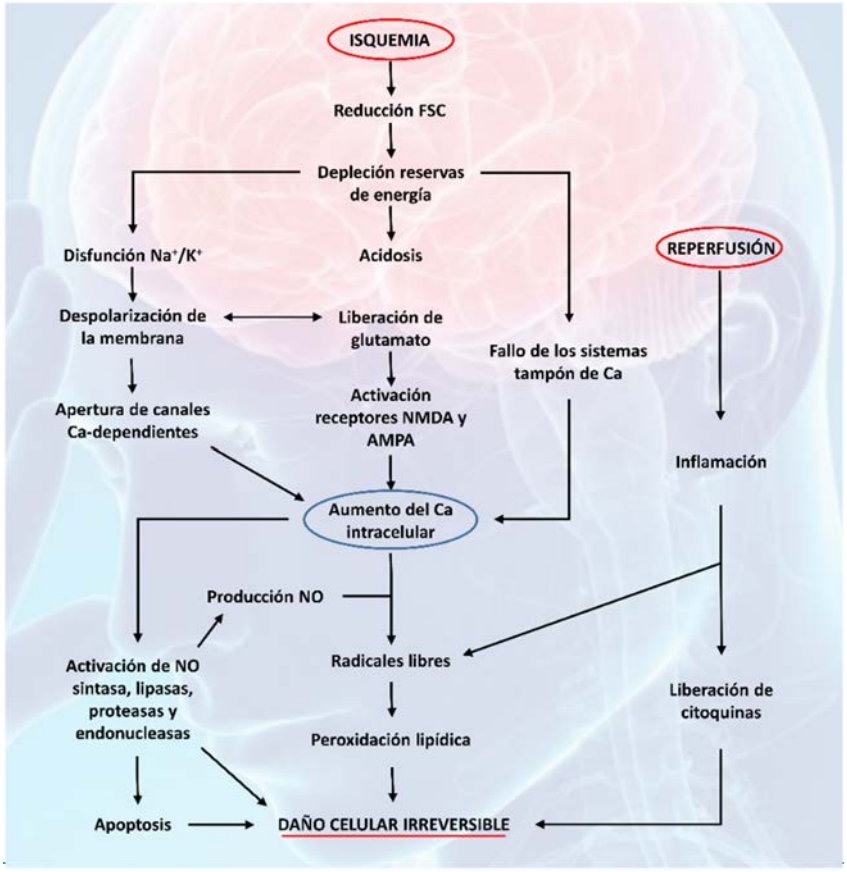

Figura 10. Cascada isquémica.

Una de las consecuencias directas de los cambios bioquímicos descritos en el apartado anterior, es la alteración de la barrera hematoencefálica (BHE)[110]. La BHE está constituida por las células endoteliales de los capilares, por la lámina basal que las rodea, por pericitos vasculares y por los pies terminales de los astrocíticos. Todo ello forma una unidad neurovascular dinámica regulada también por neuronas, microglia y células inmunes. La principal función de la BHE es la de separar la sangre circulante del líquido extracelular del cerebro y permitir el paso selectivo de H_2O, glucosa, aminoácidos, y de algunos gases, así como de moléculas solubles en lípidos por difusión pasiva, además de proteger al cerebro de neurotoxinas. Los mediadores químicos liberados durante el daño isquémico actúan sobre la integridad de la BHE aumentando su permeabilidad. Así, por ejemplo, la liberación de ERO activa metaloproteasas de matriz (MMP), que digieren la lámina basal[111]. Esta acción puede ser tanto directa, a través de la oxidación o nitrosilación de las MMP o indirecta, a través de la acción de factores de transcripción como NF-κB y AP-1, reguladores de la transcripción de las MMP[112]. Además, las uniones estrechas celulares que mantienen unidas las células endoteliales se alteran por la modificación en la concentración de Ca^{+2}. Todo esto unido a la liberación de mediadores proinflamatorios (por ejemplo, moléculas liberadas por la muerte de neuronas) refuerza la ruptura de la barrera y la migración de células sanguíneas al parénquima cerebral donde cooperarán con la microglia, que también se habrá activado por la sobreproducción de ERO, en la inducción de la respuesta inflamatoria. De hecho, la cicatriz glial y la respuesta neuroinflamatoria a la isquemia juegan un papel importante en la alteración del FSC y en la destrucción tisular[113]. Así, la activación de los astrocitos, pero sobre todo de la microglía, representan los primeros eventos del proceso de inflamación. Las células microgliales exhiben una variedad de fenotipos que, a grandes rasgos, se pueden simplificar en dos[114]. El fenotipo M1 que produce mediadores proinflamatorios, como niveles altos de ROS y NO, incrementando el daño asociado al ictus, y el fenotipo M2 que muestra un efecto antiinflamatorio y

reparador. Aunque la dinámica de su polarización es compleja, cuando se mantiene activada de forma prolongada tras un accidente cerebrovascular exhibe un fenotipo M1 que contribuye al daño tisular, de ahí que proteínas como Iba1 (*ionized calcium binding adaptor molecule 1*) expresada específicamente en la línea celular microglía/macrófagos sea utilizada para determinar el grado de recuperación de la zona infartada[115].

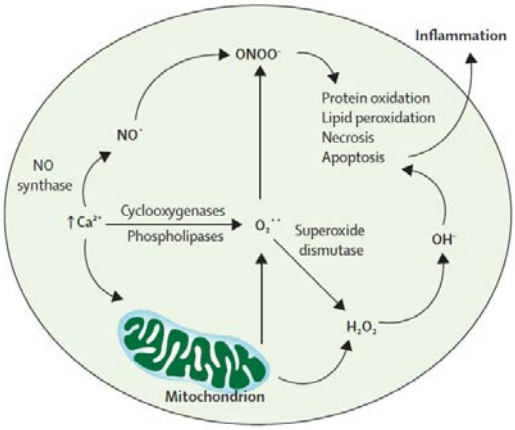

Figura 11. Mediadores del estrés oxidativo y nitrosativo en la isquemia cerebral. El aumento de calcio tras el ictus aumenta la generación de anión $O_2^{\cdot-}$, peróxido de hidrógeno (H_2O_2), radical hidroxilo ($OH^{\cdot}$), NO, y $OONO^-$ especialmente en la zona de la penumbra y de forma más acentuada después de la reperfusión. Los radicales $OH^{\cdot}$ y el $OONO^-$, resultantes de la interacción entre el NO y el anión $O_2^{\cdot-}$, promueven la oxidación y la nitración proteica, la peroxidación de lípidos, el daño mitocondrial y del ADN, así como, la activación o inhibición de vías de señalización que promueven la respuesta inflamatoria, la apoptosis y la necrosis[116].

El deterioro de las neuronas tras el ictus implica la retracción y/o ruptura de axones con pérdida de los correspondientes circuitos neuronales, originando daños funcionales difíciles de recuperar[117]. Además de controlar la producción de radicales libres y disminuir la inflamación, potenciar la neuro- y sinaptogenesis es otra estrategia a considerar para facilitar la recuperación de los pacientes. Después del ictus, las células madre neurales de la zona subventricular de los ventrículos laterales y del giro dentado del hipocampo, principales nichos de neurogénesis, pueden ser activadas, proliferando y produciendo neuroblastos susceptibles de contribuir a la reparación del daño, además de ayudar también en la formación de la cicatriz glial. La cicatriz glial, formada principalmente por astrocitos, glia NG2 y microglia, se define como el borde compacto de tejido que se forma alrededor del núcleo del infarto[118]. Si bien puede ejercer un efecto beneficioso durante la fase aguda del ictus, impide el crecimiento axónico en etapas más tardías, por lo que una gliosis desmesurada durante la etapa de formación de la cicatriz, resulta contraproducente para la neurogénesis. De hecho, tras un ictus, las células madres neurales pueden ser dañadas, inhibiendo la neurogénesis a favor de la gliosis, mediante un mecanismo favorecido por la hipoxia a través de Notch. Así, la protección de estas células madre resultaría clave para aumentar la neurogénesis y disminuir la gliosis. Factores de crecimiento como BDNF favorecen este efecto[119]. Concretamente, BDNF, induce la proliferación y diferenciación de las células madre mediante diferentes mecanismos, como la ruta PI3K/Akt/mTOR o ERK1/2, tras su unión a los receptores relacionados con la tropomiosina con actividad tirosina quinasa. La evaluación de la neurogénesis en adultos se puede llevar a cabo mediante marcadores como la doblecortina (DCX), proteína asociada a microtúbulos que estabiliza el citoesqueleto y que se expresa en precursores neurales y sus descendientes hasta la consecución de neuronas maduras[120]. La regeneración axónica es también un paso indispensable para la reconstrucción de los circuitos neuronales perdidos por efecto del daño isquémico y una consecuencia del proceso de neurogénesis. El crecimiento axónico debe concluir con

el establecimiento de las conexiones sinápticas (sinaptogenesis) y con el desarrollo de nuevos circuitos que restablezcan las funciones neuronales perdidas. Ambos procesos se pueden valorar mediante el uso de diferentes marcadores. PSD95 (*postsynaptic density protein 95*) es una proteína localizada en las regiones postsinapticas, que regula la plasticidad de las sinapsis glutamatérgicas y la formación de espinas dendríticas[121]. Por otro lado, la sinaptofisina (Syn) es una glicoproteína transmembrana localizada en los terminales presinapticos fundamental para la formación y función de las vesículas presinápticas. Se encuentra tanto en las sinapsis excitatorias como en las inhibitorias[122]. Ambas, decrecen por efecto de la isquemia por lo que también son de gran utilidad para determinar el grado de daño isquémico y la evolución de proceso de recuperación[123].

2.2.3 *Compuestos fenólicos e ictus*

Todos los estudios que existen hasta el momento sobre la acción neuroprotectora del HT en una situación de isquemia han sido realizados en utilizando un modelo de isquemia *ex vivo*, que emplea secciones gruesas de cerebro obtenidas con vibratomo. Dichas secciones son incubadas con diferentes concentraciones de HT o extraídas de animales previamente tratados, durante un tiempo variable (generalmente 7 días), con dosis de HT comprendidas entre 1-20mg/kg/día[124-128]. En ambas aproximaciones, los resultados obtenidos indican que el HT ejerce un efecto neuroprotector asociado a: 1) menor liberación de LDH, 2) disminución del nivel de estrés nitrosativo y oxidativo y 3) disminución de la inflamación. El efecto neuroprotector de este compuesto en situaciones de isquemia también ha sido estudiado en ratas diabéticas, llegando a la conclusión de que su acción neuroprotectora no está exclusivamente ligada a su acción antioxidante[126,127]. En el caso del TIR, existe un único estudio en el que se describe cómo el tratamiento intraperitoneal con 3, 10 ó 30 mg/kg de TIR, es capaz de reducir el volumen del infarto y mejorar el estado neurológico de ratas tras un ictus por oclusión transitoria de la arteria cerebral media (tMCAO)[129].

3. ENFERMEDAD DE PARKINSON

El Parkinson (EP) es la segunda enfermedad neurodegenerativa más común después del Alzheimer (EA), afectando al 0.3% de toda la población mundial, y entre al 1- 3% de la población mayor de 65 años[130]. Esta patología tiene lugar de forma esporádica en la mayoría de los casos (90-95%) y está caracterizada por la pérdida específica de hasta el 60% de las neuronas dopaminérgicas de la *sustantia nigra pars compacta* (SN). La pérdida de estas neuronas, resulta en una reducción de hasta un 90% en los niveles de dopamina en el núcleo estriado, causando la disfunción motora propia de esta enfermedad[131]. Su diagnóstico tiene lugar con la aparición de los primeros síntomas motores, pero puede ir precedida por una fase premotora o prodrómica de hasta 20 años. La fase premotora se caracteriza por síntomas no motores específicos como estreñimiento, depresión y perdida olfativa[132]. Durante la progresión, las funciones motoras empeoran, pudiendo ser inicialmente paliadas con terapias sintomáticas. Sin embargo, a medida que avanza la enfermedad, surgen complicaciones relacionadas con el tratamiento a largo plazo, que incluyen fluctuaciones motoras y no motoras, disquinesia y psicosis[133]. En la etapa avanzada de la enfermedad, las características motoras y no motoras resistentes al tratamiento son prominentes e incluyen síntomas motores axiales, como inestabilidad postural, congelación de la marcha, caídas, disfagia, disfunción del habla e incluso asfixia. A nivel celular, además de la pérdida neuronal, la EP se caracteriza por la presencia de cuerpos de inclusión citosólicos denominados Cuerpos de Lewy en la SN y, de forma más extensiva, en otras regiones del cerebro. Los Cuerpos de Lewy están compuestos por diferentes proteínas entre las que

se incluyen la α-sinucleína (α-syn), principal proteína que se agrega en esta enfermedad, además de la presencia de otras proteínas como ubiquitina, p62 y multitud de chaperonas moleculares[134]. La presencia de α-syn agregada también se ha observado en un grupo de enfermedades neurodegenerativas denominadas sinucleopatías que incluyen, además del EP, el Parkinson con demencia y la demencia con Cuerpos de Lewy[135]. En todas estas enfermedades, la mayoría de estudios apoyan un papel causal de la α-syn en la neurotoxicidad asociada a las mismas. Asimismo, existe un paralelismo obvio entre estas sinucelopatías y otras enfermedades como el AD, el Huntington, la ELA, las enfermedades priónicas y la diabetes tipo II, todas ellas consideradas también como enfermedades por mal plegamiento proteico o PMDs (Protein-misfolding diseases)[136]. Los diferentes casos de Parkinson familiar han servido para identificar mutaciones en multitud de genes directamente implicados con la enfermedad. Así, la identificación de mutaciones en el gen de la α-syn (SNCA), fue clave para identificar a esta proteína como componente mayoritario de los Cuerpos de Lewy. Además de SNCA, las formas autosómicas dominantes de EP están asociadas principalmente a mutaciones en LRRK2, y más recientemente a nuevos genes identificados como son VPS35, EIF4G1, DNAJC13 y CHCHD2. Por otro lado, los genes DJ-1, PINK1 y más comúnmente *Parkin*, están asociados con las formas autosómicas recesivas de la enfermedad. A diferencia de los casos autosómicos dominantes, que tienden a tener una edad de inicio similar a la EP esporádica, el parkinsonismo hereditario recesivo se asocia con un inicio muy temprano de la enfermedad (menores de 40 años). A grandes rasgos, y en especial mutaciones en SNCA, afectan a la función mitocondrial, al metabolismo de la dopamina y al sistema ubiquitina-proteasoma[137].

3.1 *Características de la α-syn*

La α-syn es una proteína pequeña (14.460 Da), abundante y altamente conservada que constituye aproximadamente el 1% de las proteínas totales de la fracción soluble citosólica del cerebro. Es una proteína presináptica de 140 aa que muestra una importante versatilidad estructural. En condiciones fisiológicas, se considera una proteína intrínsecamente desordenada o naturalmente desplegada, aunque cuando se asocia con fosfolípidos de membrana puede adoptar una estructura α-helicoidal[138]. Otros autores, sugieren que de forma nativa la α-syn se agrupa formando tetrámeros[139]. Por otro lado, cuando forma agregados fibrilares como los que aparecen en los Cuerpos de Lewy, adquiere una conformación característica formada por estructura secundaria en lámina-β plegada. Su secuencia primaria puede dividirse en 3 regiones (Figura 12)[140]:

1. Región N terminal (1-60 residuos). Extremo anfipático responsable de la unión a fosfolípidos de membrana. Incluye 4 repeticiones imperfectas de 11 residuos con un motivo conservado de unión a lípidos (KTKEGV) y en ella se encuentran las mutaciones asociadas con la EP autosómica dominante.

2. Región central (61-95). Contiene el dominio NAC (Non-Aβ Component of Alzheimer disease plaques), y es altamente hidrofóbica, lo que favorece la agregación patológica de la proteína.

3. Región C terminal (96-14). Altamente acídica y rica en prolina, lo que previene la agregación. Esta región es diana de la mayoría de modificaciones post-traduccionales de la proteína, algunas de ellas, como la fosforilación de la serina S129, está relacionada con un gran aumento en la insolubilidad de la α-syn.

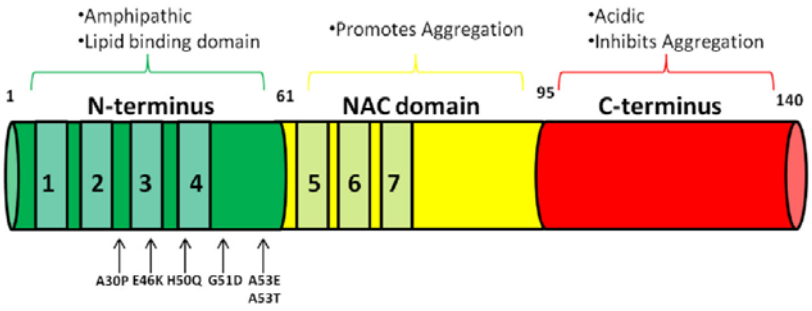

Figura 12. Representación esquemática de la estructura de la α-syn[141].

Aunque la función fisiológica de la α-syn aún no es muy clara, parece evidente su implicación en procesos tales como la transmisión sináptica e inducción de la liberación de neurotransmisores, el tráfico vesicular, la neuroplasticidad o la unión a ácidos grasos[142]. Además, debido a su excepcional plasticidad conformacional, es capaz de interaccionar con múltiples dianas celulares. En el caso de la EP, la propiedad para agregarse de la α-syn se atribuye al dominio central hidrofóbico, mientras que el extremo C-teminal acídico parece prevenir el ensamblaje. Así, en la cascada de agregación patológica, el primer paso sería la formación de un intermediario parcialmente plegado capaz de promover la auto-asociación de la proteína y la formación de varias especies oligoméricas. Con el tiempo, estos oligómeros transitorios interaccionan entre ellos dando lugar a un núcleo amiloidogénico donde se van agregando diferentes proteínas solubles formando protofibrillas y fibras maduras, mientras que otros formarían agregados amorfos e insolubles o bien oligómeros solubles más estables (Figura 13)[143]. *In vitro*, el proceso de agregación de la α-syn sigue un patrón dependiente de la nucleación que se puede dividir en tres etapas: (i) la fase de latencia, cuando los monómeros se ensamblan para formar núcleos de agregación; (ii) la fase de alargamiento, cuando las fibrillas crecen exponencialmente; (iii) la fase estacionaria, cuando el agotamiento de los monómeros conduce a una disminución en la tasa de crecimiento[142]. La fase de latencia se caracteriza por importantes cambios estructurales y representa el paso limitante en la velocidad de agregación. Los oligómeros se convierten en protofibrillas, y estas últimas se asocian para formar fibrillas amiloides maduras. Ciertas condiciones, como altas temperaturas o valores bajos de pH, favorecen este proceso. Las fibrillas de amiloide crecen rápidamente durante la fase de alargamiento mediante la adición de monómeros en los extremos de las fibrillas. Esta etapa es termodinámicamente favorable debido a la compactación de la proteína, disminuyendo la superficie total expuesta. La privación de monómeros culmina en la fase estacionaria, donde la mayoría de α-syn se encuentra formando fibrillas. Sin embargo, en todas las fases, hay un equilibrio dinámico donde coexisten simultáneamente diferentes conformaciones y estados de agregación[144].

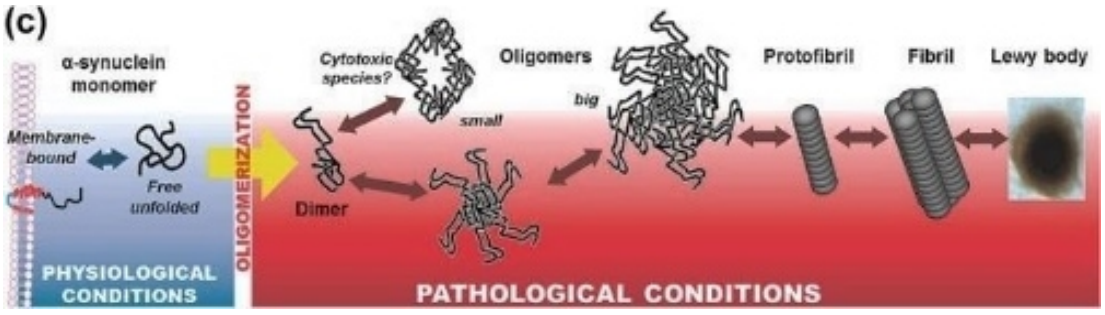

Figura 13. Cascada de polimerización de la α-syn en condiciones patológicas[145].

Algunos de los principales factores que desencadenan y/o modulan la cascada de agregación de la α-syn, son su sobreexpresión por mutiplicación genómica del locus SNCA, mutaciones específicas en SNCA (A30P, A53T y E46K), el estrés oxidativo, la exposición a iones metálicos y la disminución de la eficacia de los sistemas proteolíticos, entre otros factores[146]. Por otro lado, se han identificado distintos factores capaces de inhibir la fibrilación de α-syn tales como modificaciones por oxidación de metionina, nitración de tirosina o catecolaminas, altas concentraciones de alcoholes y de osmolitos, así como numerosos flavonoides[140,147].

Durante décadas, los depósitos amiloides fibrilares de gran tamaño, como los cuerpos de Lewy en la EP o las placas amiloides en el AD, fueron considerados los causantes de estas enfermedades, debido a que su presencia en los cerebros de los pacientes era manifiesta y a que su distribución anatómica coincidía con las áreas de mayor neurodegeneración. No obstante, este concepto se ha cuestionado cada vez con más fuerza en los últimos tiempos ya que una gran cantidad de datos experimentales indican que, en realidad, las principales especies tóxicas son los núcleos de agregación y oligómeros que preceden a la formación de fibras maduras[148]. Así, numerosos estudios demuestran que estos oligómeros intermedios que se generan *in vivo*, no solo en células en cultivo sino también en tejido de modelos animales y de humanos con estas patologías, están directamente asociados con el daño celular y tisular, contribuyendo al mismo[149]. En este sentido, la idea de que las fibras maduras serían depósitos inertes de precursores mucho más tóxicos, sugiere que su formación podría ser un mecanismo de defensa para reducir la presencia de estas especies oligoméricas. Esto explicaría la falta de correlación directa observada entre la cantidad de depósitos amiloides en el cerebro de pacientes de la EP o AD y la severidad de los síntomas clínicos[150]. Los motivos tras la toxicidad diferencial entre oligómeros y fibras amiloides puede ser atribuida a sus estructuras. Por un lado, los oligómeros presentan expuestas superficies hidrófobas ricas en láminas-β que favorecen la agregación, mientras que, en las fibrillas, estas superficies se encuentran internalizadas en la estructura. Además, los oligómeros son más pequeños, lo que facilita su difusión entre células, en comparación con las fibrillas más alargadas y grandes. Por último, la estructura desordenada e inestable natural de los oligómeros, presenta multitud de extremos reactivos lo que favorece la interacción con diferentes dianas celulares. Por lo tanto, prevenir los pasos tempranos de oligomerización y agregación podrían resultar prometedores para detener el proceso degenerativo asociado con el mal plegamiento y acumulación de este tipo de proteínas[151].

El análisis *post mortem* de cerebros humanos ha revelado que la progresión de la neuropatología parkinsoniana sigue una serie de etapas secuenciales. Inicialmente, las lesiones comienzan en el bulbo olfatorio, el núcleo olfativo anterior y el núcleo motor dorsal del nervio vago en lo que se considera la primera etapa[152]. Durante la segunda etapa, la patología se disemina a los núcleos de rafe inferior, las porciones magnocelulares de la formación reticular y el locus coeruleus[153]. En la tercera etapa, la patología alcanza el cerebro medio, afectando fundamentalmente a la SN. La patología se extiende entonces a la corteza durante la cuarta etapa. En las dos últimas etapas, la patología alcanza el neocortex prefrontal y las áreas premotoras, las áreas sensoriales primarias y el campo motor primario[154,155]. Esta progresión sistemática de la patología unida a la capacidad de la α-syn para propagarse desde tejidos enfermos a sanos incluso entre diferentes especies, apoyan la teoría de que la dispersión patológica de la α-syn reúne las características propias de una enfermedad priónica[156,157]. Esta teoría apoya a que una vez formados los agregados α-syn en las neuronas, estos pueden diseminarse a neuronas vecinas y promover la agregación de la α-syn nativa mediante interacciones directas, al igual que ocurre en otras enfermedades priónicas. Entre los mecanismos propuestos para explicar la propagación de la α-syn entre células, se incluye el transporte a través de poros de membrana, la difusión pasiva, la exo- y endocitosis, el transporte mediante exosomas y la posibilidad de transporte mediante proteínas *carrier*, entre otros[140].

3.2 *Papel del estrés oxidativo en la enfermedad de Parkinson*

Un vínculo común entre los procesos neurodegenerativos es su susceptibilidad al daño oxidativo. Como se ha mencionado en el apartado 2 de esta introducción, las células del cerebro, especialmente las neuronas, son muy vulnerables a los efectos perjudiciales de las ERO. Tanto en los casos idiopáticos como genéticos de la EP, el estrés oxidativo es uno de los mecanismos que conducen a la disfunción y muerte neuronal. Se ha descrito cómo la SN de pacientes de EP muestran altos niveles de lípidos, proteínas y ADN oxidados así como bajos niveles de GSH reducido, todo ello debido, a la sobreproducción de ERO asociada a la enfermedad, ocasionada por la disfunción mitocondrial o por el propio metabolismo de la dopamina, ente otros procesos (Figura 14)[158,159]. Así, la inhibición del complejo I mediante el empleo de neurotoxinas como MPTP y rotenona, así como mutaciones en el ADN mitocondrial en modelos animales, dan lugar a diferentes características Parkinsonianas[160]. Por otro lado, se ha descrito, como la sobreexpresión de α-syn es responsable de la disfunción mitocondrial observada a nivel del complejo I de la cadena de transporte de electrones[161]. De este modo se crea un círculo vicioso en el que la alteración mitocondrial da lugar a un aumento de las ERO, cuyo efecto oxidativo favorece la agregación de la α-syn, propiciando a su vez un mayor daño mitocondrial. Además, la actividad de las enzimas tirosina hidroxilasa y monoamina oxidasa, implicadas en la síntesis de dopamina a partir de tirosina, generan grandes cantidades de ERO, lo que hace especialmente sensibles a las neuronas dopaminergicas. El hierro que actúa como cofactor de la tirosina hidroxilasa, puede mediante la reacción de Fenton, generar radicales $O_2^{\cdot-}$ y peróxido de hidrógeno que contribuyen a aumentar el estrés oxidativo en estas neuronas[162]. Además, se ha descrito cómo las neuronas dopaminérgicas en la SN de pacientes de EP acumulan múltiples deleciones en el ADN mitocondrial. De hecho, algunos de los genes identificados para el Parkinson familiar codifican proteínas que se localizan en la mitocondria y están relacionados con las funciones de la misma, como PINK-1, Parkina y DJ-1[163]. Finalmente, la neuroinflamación, causada por la activación crónica de la microglía en respuesta a α-syn agregada y a otras moléculas como la neuromelanina o MMP-3, también constituye una fuente continua de ERO como el anión $O_2^{\cdot-}$ o el NO, exacerbando aún más el daño oxidativo en esta enfermedad[164].

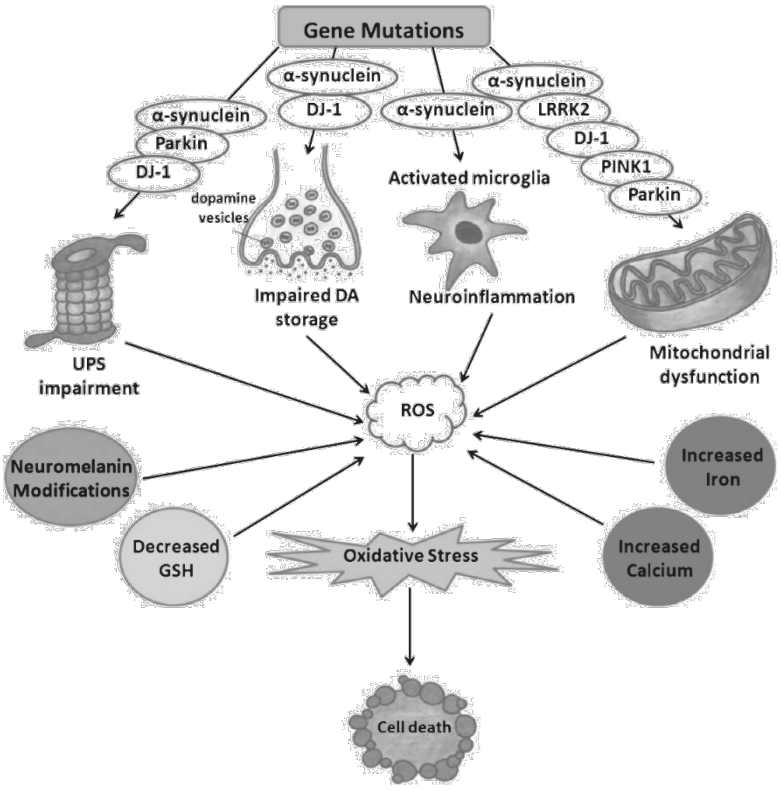

Figura 14. Mecanismos subyacentes al aumento del estrés oxidativo en la EP[158].

3.3 *Papel de las chaperonas moleculares en el Parkinson*

La denominada Red de Proteostasis (PN) se encarga de proteger la funcionalidad del proteoma y previene la acumulación de proteínas mutadas, dañadas o mal plegadas[146]. En el caso de las enfermedades neurodegenerativas, el factor de riesgo más determinante es el envejecimiento; así, existen muchas pruebas que sugieren un vínculo entre envejecimiento, proteotoxicidad mediada por agregación y pérdida de proteostasis, ésta última, de hecho, se ha señalado recientemente como una de las principales características que intervienen en el proceso de envejecimiento[165].

Un componente central de la red de proteostasis son las chaperonas moleculares y co-chaperonas, que previenen el mal plegamiento y redirigen intermediarios no nativos hacia el estado nativo o bien hacia su eliminación por el sistema ubiquitina-proteosoma y autofagia[166]. Las chaperonas moleculares, la mayoría de las cuales pertenecen a la familia de las proteínas de choque térmico (HSPs), son la primera línea de defensa frente al mal plegamiento y la agregación proteica. Estas proteínas ejercen su papel bajo condiciones celulares normales y bajo la influencia del estrés, como por ejemplo el estrés térmico, que aumenta la concentración de proteínas mal plegadas. Las chaperonas se clasifican de acuerdo con su peso molecular: Hsp40, Hsp70, Hsp90, Hsp100 y otras de menor tamaño (menos de 30 kDa), conocidas como sHSPs (small Heat Shock Proteins)[167].

En la EP, la presencia de varias HSPs (Hsp70 y Hsp90) en los cuerpos de Lewy confirma un importante papel de las chaperonas en la enfermedad. Así, numerosos estudios señalan que aumentos en la expresión de Hsp70, Hsp40 o Hsp27 reducen la agregación y/o toxicidad de la α-syn[168]. Además, recientemente se ha descrito que la Hsp70 puede promover la actividad de la ubiquitín ligasa E3 para degradar a la α-syn[169]. Por otro lado, un estudio reciente ha identificado redes de chaperonas cuyos patrones de expresión son inducidos o reprimidos de forma común en el cerebro humano tanto en el envejecimiento como en las principales enfermedades neurodegenerativas[170]. La existencia de esta correlación, subraya el papel central del chaperoma en envejecimiento y en enfermedades como la EP. En este mismo estudio, se comprobó que hay un elevado paralelismo entre la expresión de genes de estas chaperonas en enfermedades neurodegenerativas y sus ortólogos en modelos de estas enfermedades en el nematodo *Caenorhabditis elegans (C. elegans)*. De hecho, la inactivación de muchos de estos genes mediante RNAi en este modelo animal exacerbó la toxicidad asociada a las proteínas amiloides típicas de estas patologías. En base a los numerosos datos experimentales, la inducción de HSPs se postula como una estrategia muy prometedora en el tratamiento de las enfermedades neurodegenerativas[170].

3.4 *Caenorhabditis elegans como modelo de enfermedades neurodegenerativas*

A lo largo de los años, los modelos en mamíferos han dado lugar a grandes avances en el campo de las enfermedades neurodegenerativas, aunque la complejidad de su cerebro, así como las limitaciones experimentales derivadas de su uso (elevado coste económico y temporal), suponen un obstáculo importante en el análisis de muchos de los factores que participan en estas enfermedades *in vivo*. Por otro lado, aunque el uso de líneas celulares humanas neuronales y no neuronales para el estudio de mecanismos moleculares asociados a estos desórdenes y la búsqueda de nuevos tratamientos terapéuticos ha sido de gran utilidad, estos modelos *in vitro* no pueden reproducir las interacciones que tienen lugar entre los distintos tipos celulares, que sólo se puede conseguir mediante el empleo de organismos completos. Teniendo en cuenta estos factores y el hecho de que muchos de los genes ligados a enfermedades humanas funcionan en rutas evolutivamente conservadas que pueden ser fácilmente estudiadas en organismos más

simples, el uso de invertebrados modelo supone un nuevo frente de estudio en el cual se están obteniendo grandes logros y avances.

C. elegans es un nematodo de forma cilíndrica no parasitario que vive en el suelo y que se alimenta principalmente de bacterias. Fue introducido como organismo modelo por primera vez a comienzos de la década de los 60 por Sydney Brenner[171] y, gracias al gran número de ventajas que este organismo ofrece, se convirtió rápidamente en un sistema muy utilizado. Entre las principales ventajas de este organismo modelo se encuentran su simplicidad anatómica, su pequeño tamaño y su corto ciclo de vida (Figura 15). Además, la alta homología encontrada entre su genoma y el de humanos, y el hecho de que las principales rutas de señalización de ambos están sorprendentemente conservadas, se han plasmado en la generación de estirpes transgénicas que recapitulan muchas enfermedades que afectan a humanos, entre ellas las enfermedades neurodegenerativas más importantes. Se estima que alrededor del 42% de los genes asociados a enfermedades humanas tienen un ortólogo en *C. elegans*, incluyendo genes relacionados con la EA, la EP o el cáncer de colón hereditario, entre otras[172]. *C. elegans* presenta un linaje celular invariable, que en el caso del hermafrodita adulto es de 959 células somáticas y de 1031 en el macho. Sorprendentemente, un tercio del total de células, 302 en concreto para el hermafrodita, son neuronas, cuyas sinapsis y conectividades han sido mapeadas al completo, haciendo de este nematodo un organismo modelo muy interesante para estudios relacionados con aspectos moleculares y funcionales del sistema nervioso[173]. La utilidad de *C. elegans* como modelo de enfermedades neurodegenerativas queda patente en el hecho de que numerosas rutas implicadas en estas patologías han sido identificadas gracias al estudio con este nematodo. Como ejemplo, el trabajo con modelos de EP en *C. elegans* ha contribuido a desentrañar cómo la α-syn es capaz de bloquear el tráfico vesicular entre el retículo endoplasmático y el aparato de Golgi, uno de los mecanismos celulares implicados en la toxicidad de este péptido[174]. En este sentido, el hecho de que las rutas implicadas en el procesamiento, empaquetado y transporte de dopamina se han conservado durante la evolución, sugiere que *C. elegans* podría ser un modelo válido para los estudios relacionados con la degeneración de neuronas dopaminérgicas. Concretamente, se han caracterizado estirpes transgénicas de *C. elegans* que sobreexpresan tanto las formas silvestres como mutadas de α-syn, parkina y DJ-1, tres de las proteínas cuya disfunción provoca la EP[175]. Así, la sobreexpresión de α-syn humana provoca deficiencias motoras en estos nematodos, con una clara degeneración de las neuronas dopaminérgicas y la agregación de las proteínas en el citoplasma celular. La existencia de únicamente 8 neuronas dopaminérgicas en *C.elegans* (4 CEP, 2 ADE y 2 PDE) también supone una ventaja, ya que simplifica bastante los estudios de neurodegeneracion.

En los últimos años se viene empleando cada vez más este modelo animal para realizar screenings de alto rendimiento (High-throughput screenings o HTS) en la búsqueda de fármacos o pequeñas moléculas con potencial terapéutico en el tratamiento de enfermedades neurodegenerativas e incluso en el envejecimiento[176,177]. Estas técnicas facilitan la búsqueda de compuestos candidatos y generan información sobre los efectos dosis-respuesta que permiten delimitar la dosis mínima eficaz, así como las dosis tóxicas. A pesar de la resistente cutícula que rodea a estos nematodos, se ha demostrado que una gran cantidad de moléculas pequeñas y fármacos pueden traspasar esta cutícula con una eficiencia relativamente elevada, mientras que otros muchos pueden ser ingeridos junto con la bacteria que sirve de alimento para los nematodos. Por otro lado, también se está utilizando con éxito para identificar genes modificadores de agregación en modelos de Huntington, EA o la EP en este nematodo, empleando en este caso RNAi y analizando su efecto sobre la toxicidad y agregación de las proteínas amiloides en estos modelos. Así, por ejemplo, estudios recientes utilizando estas estirpes de *C. elegans*, han conseguido identificar un conjunto de genes conservados en mamíferos implicados en los procesos de agregación proteica, como MOAG-

4/SERF, sir-2.1/SIRT1 o lagr-1/LASS2 entre otros, capaces de modular positiva o negativamente la agregación de proteínas neurotóxicas en estas patologías[178,179].

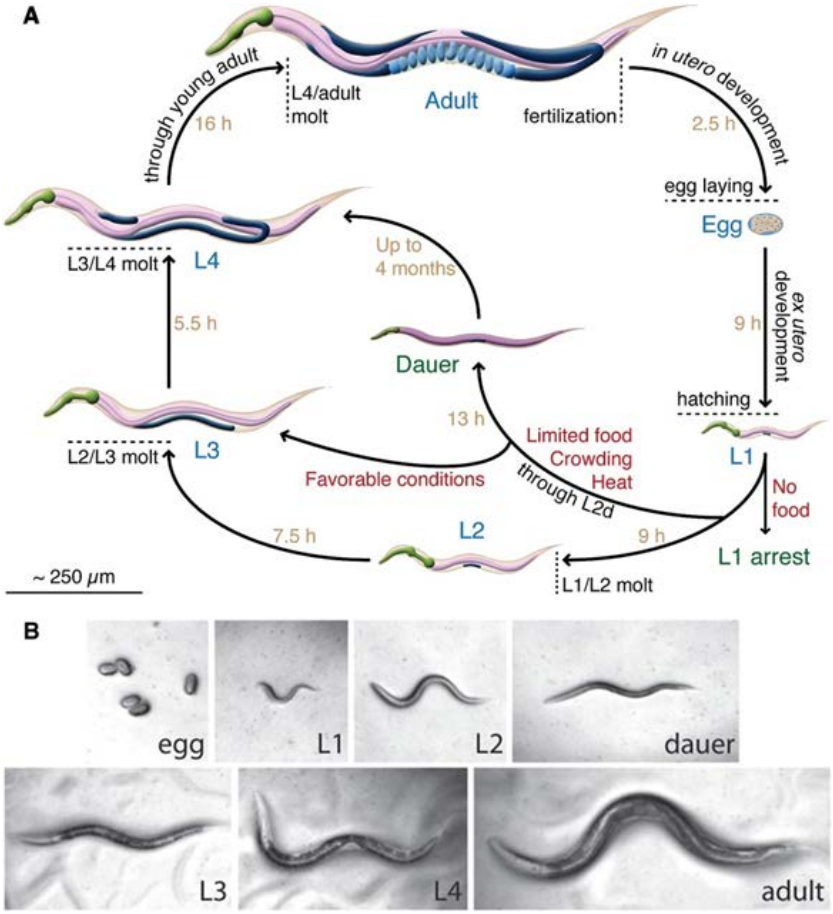

Figura 15. Ciclo de vida de *C. elegans* a 22ºC[180].

3.5 *Compuestos fenólicos del olivo y neurodegeneración*

Al igual que en los apartados anteriores referentes al cáncer y al ictus, el interés sobre el efecto de diversos compuestos fenólicos del olivo frente a diferentes enfermedades neurodegenerativas es creciente y patente en la bibliografía. Así, se ha descrito como estos compuestos interfieren *in vitro* e *in vivo* con la agregación amiloide de péptidos Aβ, la proteína Tau y la α-syn, redireccionando la agregación fibrilar hacia la formación de agregados amorfos no tóxicos[181,182]. En la actualidad, existen dos modelos para explicar el autoensamblaje de proteínas amiloides. De acuerdo con la teoría del "apilamiento π", los residuos aromáticos de las proteínas se ensamblarían a través de interacciones no covalentes π-π, mientras que el segundo modelo, que podría coexistir con el primero, está relacionado con interacciones hidrofóbicas entre estas proteínas[183]. De acuerdo con estos modelos, los polifenoles obstaculizarían la agregación proteica a través de la interacción de sus anillos fenólicos con los residuos aromáticos de las proteínas amiloidogénicas, evitando el apilamiento π, además de mediante la asociación de sus grupos hidroxilos con las regiones hidrofóbicas de estas proteínas[184,185]. Por otro lado, la capacidad antioxidante de estos compuestos es indudablemente otro mecanismo que estaría plausiblemente vinculado a su efecto antiagregación. Así, estudios recientes describen la capacidad de compuestos como el HT, la OL y la OL-aglicona para inhibir la fibrilación de Tau y reducir los depósitos amiloides, además de potenciar otros procesos clave en la EA, como serían la autofagia y la mejora de la función cognitiva[186,187,188]. En lo referente a la EP, estudios *in vitro* describen como la OL y el HT disminuyen el estrés oxidativo mediante la inducción

de diferentes enzimas antioxidantes, así como, su capacidad para inhibir la apoptosis, y ejercer un papel protector frente a multitud de toxinas (DA, 6-OHD y MPP)[189,190]. En relación al TIR, también se ha descrito su carácter protector frente a diferentes neurotoxinas, atenuando la disfunción mitocondrial e induciendo la expresión de enzimas antioxidantes como SOD-1, SOD-2 y DJ-1[191,192]. En definitiva, aunque es patente el potencial de estos compuestos sobre múltiples mecanismos implicados en estas patologías, el uso de modelos *in vitro* en la mayoría de los estudios hasta la fecha, carece de las ventajas del empleo de organismos completos. En este sentido, la utilización de modelos como *C. elegans*, representa una aproximación prometedora para investigar su efecto sobre diversos mecanismos moleculares subyacentes a patologías como la EP. De hecho, estudios realizados en este modelo demuestran, por ejemplo, como la administración de OL a la estirpe CL2600 de *C. elegans* que expresa Aβ3–42 de forma constitutiva, reduce los depósitos de placa y la formación de oligómeros tóxicos en la musculatura del animal, reduciendo la parálisis y aumentando su esperanza de vida[193].

Referencias bibliográficas

1 Trichopoulou, A. & Lagiou, P. Healthy traditional Mediterranean diet: an expression of culture, history, and lifestyle. *Nutrition reviews* **55**, 383-389 (1997).

2 Visioli, F. *et al.* Olive oil and prevention of chronic diseases: Summary of an International conference. *Nutrition, Metabolism and Cardiovascular Diseases* **28**, 649-656, doi:10.1016/j.numecd.2018.04.004 (2018).

3 Salas-Salvadó, J., Becerra-Tomás, N., García-Gavilán, J. F., Bulló, M. & Barrubés, L. Mediterranean diet and cardiovascular disease prevention: What do we know? *Progress in cardiovascular diseases*, doi:10.1016/j.pcad.2018.04.006 (2018).

4 Estruch, R. *et al.* Primary prevention of cardiovascular disease with a Mediterranean diet supplemented with extra-virgin olive oil or nuts. *New England Journal of Medicine* **378**, e34, doi:10.1056/NEJMoa1800389 (2018).

5 Gardener, H. *et al.* Mediterranean-style diet and risk of ischemic stroke, myocardial infarction, and vascular death: the Northern Manhattan Study. *The American journal of clinical nutrition* **94**, 1458-1464, doi:10.3945/ajcn.111.012799 (2011).

6 Toledo, E. *et al.* Mediterranean diet and invasive breast cancer risk among women at high cardiovascular risk in the PREDIMED trial: a randomized clinical trial. *JAMA internal medicine* **175**, 1752-1760, doi:10.1001/jamainternmed.2015.4838 (2015).

7 Psaltopoulou, T., Kosti, R. I., Haidopoulos, D., Dimopoulos, M. & Panagiotakos, D. B. Olive oil intake is inversely related to cancer prevalence: a systematic review and a meta-analysis of 13800 patients and 23340 controls in 19 observational studies. *Lipids in health and disease* **10**, 127, doi:10.1186/1476-511X-10-127 (2011).

8 Ngandu, T. *et al.* A 2 year multidomain intervention of diet, exercise, cognitive training, and vascular risk monitoring versus control to prevent cognitive decline in at-risk elderly people (FINGER): a randomised controlled trial. *The Lancet* **385**, 2255-2263, doi:10.1016/S0140-6736(15)60461-5 (2015).

9 Scarmeas, N., Stern, Y., Tang, M. X., Mayeux, R. & Luchsinger, J. A. Mediterranean diet and risk for Alzheimer's disease. *Annals of Neurology: Official Journal of the American Neurological Association and the Child Neurology Society* **59**, 912-921, doi:10.1002/ana.20854 (2006).

10 Valls-Pedret, C. *et al.* Mediterranean diet and age-related cognitive decline: a randomized clinical trial. *JAMA internal medicine* **175**, 1094-1103, doi:10.1001/jamainternmed.2015.1668 (2015).

11 Alcalay, R. N. *et al.* The association between Mediterranean diet adherence and Parkinson's disease. *Movement Disorders* **27**, 771-774, doi:10.1002/mds.24918 (2012).

12 Cicerale, S., Conlan, X. A., Sinclair, A. J. & Keast, R. S. Chemistry and health of olive oil phenolics. *Critical reviews in food science and nutrition* **49**, 218-236, doi:10.1080/10408390701856223 (2008).

13 Aparicio-Soto, M., Sánchez-Hidalgo, M., Rosillo, M. Á., Castejón, M. L. & Alarcón-de-la-Lastra, C. Extra virgin olive oil: a key functional food for prevention of immune-inflammatory diseases. *Food & function* **7**, 4492-4505, doi:10.1039/c6fo01094f (2016).

14 Gunstone, F. D., Harwood, J. L. & Dijkstra, A. J. *The lipid handbook with CD-ROM.* (CRC press, 2007).

15 Covas, M.-I. *et al.* Minor components of olive oil: evidence to date of health benefits in humans. *Nutrition Reviews* **64**, S20-S30 (2006).

16 Granados-Principal, S., Quiles, J. L., Ramirez-Tortosa, C. L., Sanchez-Rovira, P. & Ramirez-Tortosa, M. C. Hydroxytyrosol: from laboratory investigations to future clinical trials. *Nutrition reviews* **68**, 191-206, doi:10.1111/j.1753-4887.2010.00278.x (2010).

17 Aguilera, C. *et al.* Sunflower oil does not protect against LDL oxidation as virgin olive oil does in patients with peripheral vascular disease. *Clinical nutrition* **23**, 673-681, doi:10.1016/j.clnu.2003.11.005 (2004).

18 Harper, C. R., Edwards, M. C. & Jacobson, T. A. Flaxseed oil supplementation does not affect plasma lipoprotein concentration or particle size in human subjects. *The Journal of nutrition* **136**, 2844-2848, doi:10.1093/jn/136.11.2844 (2006).

19 Rigacci, S. & Stefani, M. Nutraceutical properties of olive oil polyphenols. An itinerary from cultured cells through animal models to humans. *International journal of molecular sciences* **17**, 843, doi:10.3390/ijms17060843 (2016).

20 De la Torre-Carbot, K. *et al.* Characterization and quantification of phenolic compounds in olive oils by solid-phase extraction, HPLC-DAD, and HPLC-MS/MS. *Journal of agricultural and food chemistry* **53**, 4331-4340, doi:10.1021/jf0501948 (2005).

21 Saibandith, B., Spencer, J., Rowland, I. & Commane, D. Olive polyphenols and the metabolic syndrome. *Molecules* **22**, 1082, doi:10.3390/molecules22071082 (2017).

22 Neveu, V. *et al.* Phenol-Explorer: an online comprehensive database on polyphenol contents in foods. *Database* **2010**, doi:10.1093/database/bap024 (2010).

23 Balducci, V., Incerpi, S., Stano, P. & Tofani, D. Antioxidant activity of hydroxytyrosyl esters studied in liposome models. *Biochimica et Biophysica Acta (BBA)-Biomembranes* **1860**, 600-610, doi:10.1016/j.bbamem.2017.11.012 (2018).

24 Visioli, F., Poli, A. & Gall, C. Antioxidant and other biological activities of phenols from olives and olive oil. *Medicinal research reviews* **22**, 65-75, doi:10.1016/j.bbamem.2017.11.012 (2002).

25 Tuck, K. L., Freeman, M. P., Hayball, P. J., Stretch, G. L. & Stupans, I. The in vivo fate of hydroxytyrosol and tyrosol, antioxidant phenolic constituents of olive oil, after intravenous and oral dosing of labeled compounds to rats. *The Journal of nutrition* **131**, 1993-1996, doi:10.1093/jn/131.7.1993 (2001).

26 Domínguez-Perles, R., Auñón, D., Ferreres, F. & Gil-Izquierdo, A. Gender differences in plasma and urine metabolites from Sprague–Dawley rats after oral administration of normal and high doses of hydroxytyrosol, hydroxytyrosol acetate, and DOPAC. *European journal of nutrition* **56**, 215-224, doi:10.1007/s00394-015-1071-2 (2017).

27 Rodríguez-Morató, J. *et al.* Metabolic disposition and biological significance of simple phenols of dietary origin: Hydroxytyrosol and tyrosol. *Drug metabolism reviews* **48**, 218-236, doi:10.1080/03602532.2016.1179754 (2016).

28 EFSA Panel on Dietetic Products, N. & Allergies. Scientific Opinion on the substantiation of health claims related to polyphenols in olive and protection of LDL particles from oxidative damage (ID 1333, 1638, 1639, 1696, 2865), maintenance of normal blood HDL cholesterol concentrations (ID 1639), maintenance of normal blood pressure (ID 3781),"anti-inflammatory properties"(ID 1882),"contributes to the upper respiratory tract health"(ID 3468),"can help to maintain a normal function of gastrointestinal tract"(3779), and "contributes to body defences against external agents"(ID 3467) pursuant to Article 13 (1) of Regulation (EC) No 1924/2006. *EFSA Journal* **9**, 2033, doi:10.2903/j.efsa.2011.2033 (2011).

29 Cavadas, M. A., Cheong, A. & Taylor, C. T. The regulation of transcriptional repression in hypoxia. *Experimental cell research* **356**, 173-181, doi:10.1016/j.yexcr.2017.02.024 (2017).

30 Bray, F. *et al.* Global cancer statistics 2018: GLOBOCAN estimates of incidence and mortality worldwide for 36 cancers in 185 countries. *CA: a cancer journal for clinicians* **68**, 394-424, doi:10.3322/caac.21492 (2018).

31 Ferlay, J. *et al.* Cancer incidence and mortality worldwide: sources, methods and major patterns in GLOBOCAN 2012. *International journal of cancer* **136**, E359-E386, doi:10.1002/ijc.29210 (2015).

32 Alkabban, F. M. & Ferguson, T. Cancer, Breast. *Treasure Island: StatPearls Publishing* (2018).

33 Zimna, A. & Kurpisz, M. Hypoxia-inducible factor-1 in physiological and pathophysiological angiogenesis: applications and therapies. *BioMed research international* **2015**, doi:10.1155/2015/549412 (2015).

34 Hanahan, D. & Weinberg, R. A. Hallmarks of cancer: the next generation. *cell* **144**, 646-674, doi:10.1016/j.cell.2011.02.013 (2011).

35 Doktorova, H., Hrabeta, J., Khalil, M. A. & Eckschlager, T. Hypoxia-induced chemoresistance in cancer cells: The role of not only HIF-1. *Biomedical Papers of the Medical Faculty of Palacky University in Olomouc* **159**, doi:10.5507/bp.2015.025 (2015).

36 Wigerup, C., Påhlman, S. & Bexell, D. Therapeutic targeting of hypoxia and hypoxia-inducible factors in cancer. *Pharmacology & therapeutics* **164**, 152-169 (2016).

37 Li, X. *et al.* Targeting mitochondrial reactive oxygen species as novel therapy for inflammatory diseases and cancers. *Journal of hematology & oncology* **6**, 19, doi:10.1186/1756-8722-6-19 (2013).

38 Liou, G.-Y. & Storz, P. Reactive oxygen species in cancer. *Free radical research* **44**, 479-496, doi:10.3109/10715761003667554 (2010).

39 Tafani, M. *et al.* The interplay of reactive oxygen species, hypoxia, inflammation, and sirtuins in cancer initiation and progression. *Oxidative medicine and cellular longevity* **2016**, doi:10.1155/2016/3907147 (2016).

40 Muller, F. L., Liu, Y. & Van Remmen, H. Complex III releases superoxide to both sides of the inner mitochondrial membrane. *Journal of Biological Chemistry* **279**, 49064-49073, doi:10.1074/jbc.M407715200 (2004).

41 Kondoh, M. *et al.* Hypoxia-induced reactive oxygen species cause chromosomal abnormalities in endothelial cells in the tumor microenvironment. *PloS one* **8**, e80349, doi:10.1371/journal.pone.0080349 (2013).

42 Lim, S.-O. *et al.* Epigenetic changes induced by reactive oxygen species in hepatocellular carcinoma: methylation of the E-cadherin promoter. *Gastroenterology* **135**, 2128-2140. e2128, doi:10.1053/j.gastro.2008.07.027 (2008).

43 Hayes, T. K. & Der, C. J. in *Ras Superfamily Small G Proteins: Biology and Mechanisms 1* 135-156 (Springer, 2014).

44 Jing, Y. *et al.* Cadmium increases HIF-1 and VEGF expression through ROS, ERK, and AKT signaling pathways and induces malignant transformation of human bronchial epithelial cells. *Toxicological sciences* **125**, 10-19, doi:10.1093/toxsci/kfr256 (2011).

45 Lu, M. C., Ji, J. A., Jiang, Z. Y. & You, Q. D. The Keap1–Nrf2–ARE pathway as a potential preventive and therapeutic target: an update. *Medicinal research reviews* **36**, 924-963, doi:10.1002/med.21396 (2016).

46 Li, P. A., Hou, X. & Hao, S. Mitochondrial biogenesis in neurodegeneration. *Journal of neuroscience research* **95**, 2025-2029, doi:10.1002/jnr.24042 (2017).

47 Satoh, H. *et al.* Nrf2-deficiency creates a responsive microenvironment for metastasis to the lung. *Carcinogenesis* **31**, 1833-1843, doi:10.1093/carcin/bgq105 (2010).

48 Ramos-Gomez, M. *et al.* Sensitivity to carcinogenesis is increased and chemoprotective efficacy of enzyme inducers is lost in nrf2 transcription factor-deficient mice. *Proceedings of the National Academy of Sciences* **98**, 3410-3415, doi:10.1073/pnas.051618798 (2001).

49 Menegon, S., Columbano, A. & Giordano, S. The dual roles of NRF2 in cancer. *Trends in molecular medicine* **22**, 578-593, doi:10.1016/j.molmed.2016.05.002 (2016).

50 Panieri, E. & Saso, L. Potential Applications of NRF2 Inhibitors in Cancer Therapy. *Oxidative medicine and cellular longevity* **2019**, doi:10.1155/2019/8592348 (2019).

51 Chikara, S. *et al.* Oxidative stress and dietary phytochemicals: Role in cancer chemoprevention and treatment. *Cancer Letters* **413**, 122-134, doi:10.1016/j.canlet.2017.11.002 (2018).

52 Wang, G. L., Jiang, B.-H., Rue, E. A. & Semenza, G. L. Hypoxia-inducible factor 1 is a basic-helix-loop-helix-PAS heterodimer regulated by cellular O2 tension. *Proceedings of the national academy of sciences* **92**, 5510-5514, doi:10.1073/pnas.92.12.5510 (1995).

53 Lisy, K. & Peet, D. Turn me on: regulating HIF transcriptional activity. *Cell death and differentiation* **15**, 642, doi:10.1038/sj.cdd.4402315 (2008).

54 Masoud, G. N. & Li, W. HIF-1α pathway: role, regulation and intervention for cancer therapy. *Acta Pharmaceutica Sinica B* **5**, 378-389, doi:10.1016/j.apsb.2015.05.007 (2015).

55 Kaelin Jr, W. G. & Ratcliffe, P. J. Oxygen sensing by metazoans: the central role of the HIF hydroxylase pathway. *Molecular cell* **30**, 393-402, doi:10.1016/j.molcel.2008.04.009 (2008).

56 Koshikawa, N., Hayashi, J.-I., Nakagawara, A. & Takenaga, K. Reactive oxygen species-generating mitochondrial DNA mutation up-regulates hypoxia-inducible factor-1α gene transcription via phosphatidylinositol 3-kinase-Akt/protein kinase C/histone deacetylase pathway. *Journal of Biological Chemistry* **284**, 33185-33194, doi:10.1074/jbc.M109.054221 (2009).

57 Laughner, E., Taghavi, P., Chiles, K., Mahon, P. C. & Semenza, G. L. HER2 (neu) signaling increases the rate of hypoxia-inducible factor 1α (HIF-1α) synthesis: novel mechanism for HIF-1-mediated vascular endothelial growth factor expression. *Molecular and cellular biology* **21**, 3995-4004, doi:10.1128/MCB.21.12.3995-4004.2001 (2001).

58 Semenza, G. L. Targeting HIF-1 for cancer therapy. *Nature reviews cancer* **3**, 721, doi:10.1631/jzus.B1400221 (2003).

59 Quintero, M., Brennan, P. A., Thomas, G. J. & Moncada, S. Nitric oxide is a factor in the stabilization of hypoxia-inducible factor-1α in cancer: role of free radical formation. *Cancer research* **66**, 770-774, doi:10.1158/0008-5472.CAN-05-0333 (2006).

60 Ho, J. D., Man, H. J. & Marsden, P. A. Nitric oxide signaling in hypoxia. *Journal of molecular medicine* **90**, 217-231, doi:10.1016/B978-0-12-800254-4.00007-6 (2012).

61 Koivunen, P., Hirsilä, M., Günzler, V., Kivirikko, K. I. & Myllyharju, J. Catalytic properties of the asparaginyl hydroxylase (FIH) in the oxygen sensing pathway are distinct from those of its prolyl 4-hydroxylases. *Journal of Biological Chemistry* **279**, 9899-9904, doi:10.1074/jbc.M312254200 (2004).

62 Harada, H. Hypoxia-inducible factor 1–mediated characteristic features of cancer cells for tumor radioresistance. *Journal of radiation research* **57**, i99-i105, doi:10.1093/jrr/rrw012 (2016).

63 Hubbi, M. E. & Semenza, G. L. Regulation of cell proliferation by hypoxia-inducible factors. *American Journal of Physiology-Cell Physiology* **309**, C775-C782, doi:10.1152/ajpcell.00279.2015 (2015).

64 Erler, J. T. *et al.* Hypoxia-mediated down-regulation of Bid and Bax in tumors occurs via hypoxia-inducible factor 1-dependent and-independent mechanisms and contributes to drug resistance. *Molecular and cellular biology* **24**, 2875-2889, doi:10.1128/MCB.24.7.2875-2889.2004 (2004).

65 Mellor, H. R. & Harris, A. L. The role of the hypoxia-inducible BH3-only proteins BNIP3 and BNIP3L in cancer. *Cancer and Metastasis Reviews* **26**, 553, doi:10.1007/s10555-007-9080-0 (2007).

66 Bellot, G. *et al.* Hypoxia-induced autophagy is mediated through hypoxia-inducible factor induction of BNIP3 and BNIP3L via their BH3 domains. *Molecular and cellular biology* **29**, 2570-2581, doi:10.1128/MCB.00166-09 (2009).

67 Vander Heiden, M. G., Cantley, L. C. & Thompson, C. B. Understanding the Warburg effect: the metabolic requirements of cell proliferation. *science* **324**, 1029-1033, doi:10.1126/science.1160809 (2009).

68 Keith, B., Johnson, R. S. & Simon, M. C. HIF1α and HIF2α: sibling rivalry in hypoxic tumour growth and progression. *Nature Reviews Cancer* **12**, 9, doi:10.1038/nrc3183 (2012).

69 Kim, J.-w., Tchernyshyov, I., Semenza, G. L. & Dang, C. V. HIF-1-mediated expression of pyruvate dehydrogenase kinase: a metabolic switch required for cellular adaptation to hypoxia. *Cell metabolism* **3**, 177-185, doi:10.1016/j.cmet.2006.02.002 (2006).

70 Noman, M. Z. *et al.* PD-L1 is a novel direct target of HIF-1α, and its blockade under hypoxia enhanced MDSC-mediated T cell activation. *Journal of Experimental Medicine* **211**, 781-790, doi:10.1084/jem.20131916 (2014).

71 Lu, Y., Chu, A., Turker, M. S. & Glazer, P. M. Hypoxia-induced epigenetic regulation and silencing of the BRCA1 promoter. *Molecular and cellular biology* **31**, 3339-3350 (2011).

72 Yuan, J., Narayanan, L., Rockwell, S. & Glazer, P. M. Diminished DNA repair and elevated mutagenesis in mammalian cells exposed to hypoxia and low pH. *Cancer research* **60**, 4372-4376 (2000).

73 Caporarello, N. *et al.* Classical VEGF, Notch and Ang signalling in cancer angiogenesis, alternative approaches and future directions. *Molecular medicine reports* **16**, 4393-4402, doi:10.3892/mmr.2017.7179 (2017).

74 Larráyoz, I. M., Martínez-Herrero, S., García-Sanmartín, J., Ochoa-Callejero, L. & Martínez, A. Adrenomedullin and tumour microenvironment. *Journal of translational medicine* **12**, 339, doi:10.1186/s12967-014-0339-2 (2014).

75 Keith, B. & Simon, M. C. Hypoxia-inducible factors, stem cells, and cancer. *Cell* **129**, 465-472, doi:10.1016/j.cell.2007.04.019 (2007).

76 Imai, T. *et al.* Hypoxia attenuates the expression of E-cadherin via up-regulation of SNAIL in ovarian carcinoma cells. *The American journal of pathology* **163**, 1437-1447, doi:10.1016/S0002-9440(10)63501-8 (2003).

77 Zhang, P., Liu, Y., Feng, Y. & Gao, S. SNAIL gene inhibited by hypoxia-inducible factor 1α (HIF-1α) in epithelial ovarian cancer. *International journal of immunopathology and pharmacology* **29**, 364-375, doi:10.1177/0394632016641423 (2016).

78 Yang, M.-H. *et al.* Direct regulation of TWIST by HIF-1α promotes metastasis. *Nature cell biology* **10**, 295, doi:10.1038/ncb1691 (2008).

79 Liu, Z.-j., Semenza, G. L. & Zhang, H.-f. Hypoxia-inducible factor 1 and breast cancer metastasis. *Journal of Zhejiang University-SCIENCE B* **16**, 32-43, doi:10.1631/jzus.B1400221 (2015).

80 Pennacchietti, S. *et al.* Hypoxia promotes invasive growth by transcriptional activation of the met protooncogene. *Cancer cell* **3**, 347-361, doi:10.1016/S1535-6108(03)00085-0 (2003).

81 Gilkes, D. M., Semenza, G. L. & Wirtz, D. Hypoxia and the extracellular matrix: drivers of tumour metastasis. *Nature Reviews Cancer* **14**, 430, doi:10.1038/nrc3726 (2014).

82 Marchetti, C. *et al.* Oleuropein-enriched olive leaf extract affects calcium dynamics and impairs viability of malignant mesothelioma cells. *Evidence-Based Complementary and Alternative Medicine* **2015**, doi:10.1155/2015/908493 (2015).

83 Anter, J. *et al.* A pilot study on the DNA-protective, cytotoxic, and apoptosis-inducing properties of olive-leaf extracts. *Mutation Research/Genetic Toxicology and Environmental Mutagenesis* **723**, 165-170, doi:10.1016/j.mrgentox.2011.05.005 (2011).

84 Han, J., Talorete, T. P., Yamada, P. & Isoda, H. Anti-proliferative and apoptotic effects of oleuropein and hydroxytyrosol on human breast cancer MCF-7 cells. *Cytotechnology* **59**, 45-53, doi:10.1007/s10616-009-9191-2 (2009).

85 Bouallagui, Z., Han, J., Isoda, H. & Sayadi, S. Hydroxytyrosol rich extract from olive leaves modulates cell cycle progression in MCF-7 human breast cancer cells. *Food and chemical toxicology* **49**, 179-184, doi:10.1016/j.fct.2010.10.014 (2011).

86 Menendez, J. A. *et al.* Olive oil's bitter principle reverses acquired autoresistance to trastuzumab (Herceptin™) in HER2-overexpressing breast cancer cells. *BMC cancer* **7**, 80, doi:10.1186/1471-2407-7-80 (2007).

87 Cruz-Lozano, M. *et al.* Hydroxytyrosol inhibits cancer stem cells and the metastatic capacity of triple-negative breast cancer cell lines by the simultaneous targeting of epithelial-to-mesenchymal transition, Wnt/β-catenin and TGFβ signaling pathways. *European journal of nutrition*, 1-13, doi:10.1007/s00394-018-1864-1 (2018).

88 Terzuoli, E. *et al.* Inhibition of hypoxia inducible factor-1α by dihydroxyphenylethanol, a product from olive oil, blocks microsomal prostaglandin-E synthase-1/vascular endothelial growth factor expression and reduces tumor angiogenesis. *Clinical Cancer Research* **16**, 4207-4216, doi:10.1158/1078-0432.CCR-10-0156 (2010).

89 Li, S. *et al.* Hydroxytyrosol inhibits cholangiocarcinoma tumor growth: an in vivo and in vitro study. *Oncology reports* **31**, 145-152, doi:10.3892/or.2013.2853 (2014).

90 Martínez-Martos, J. M. *et al.* Phenolic compounds oleuropein and hydroxytyrosol exert differential effects on glioma development via antioxidant defense systems. *journal of functional foods* **11**, 221-234, doi:10.1016/j.jff.2014.09.006 (2014).

91 Granados-Principal, S. *et al.* Hydroxytyrosol inhibits growth and cell proliferation and promotes high expression of sfrp4 in rat mammary tumours. *Molecular nutrition & food research* **55**, S117-S126, doi:10.1002/mnfr.201000220 (2011).

92 El-azem, N. *et al.* Modulation by hydroxytyrosol of oxidative stress and antitumor activities of paclitaxel in breast cancer. *European journal of nutrition*, 1-9, doi:10.1007/s00394-018-1638-9 (2018).

93 Nichols, M. *et al.* European cardiovascular disease statistics 2012. (2012).

94 O'Donnell, M. J. *et al.* Global and regional effects of potentially modifiable risk factors associated with acute stroke in 32 countries (INTERSTROKE): a case-control study. *The Lancet* **388**, 761-775, doi:10.1016/S0140-6736(16)30506-2 (2016).

95 Meschia, J. F. & Brott, T. Ischaemic stroke. *European journal of neurology* **25**, 35-40, doi:10.1111/ene.13409 (2018).

96 Lo, E. H. A new penumbra: transitioning from injury into repair after stroke. *Nature medicine* **14**, 497, doi:10.1038/nm1735 (2008).

97 Sommer, C. J. Ischemic stroke: experimental models and reality. *Acta neuropathologica* **133**, 245-261, doi:10.1007/s00401-017-1667-0 (2017).

98 Jauch, E. C. *et al.* Guidelines for the early management of patients with acute ischemic stroke: a guideline for healthcare professionals from the American Heart Association/American Stroke Association. *Stroke* **44**, 870-947, doi:10.1161/STR.0b013e318284056a (2013).

99 Choi, J. H. & Pile-Spellman, J. Reperfusion changes after stroke and practical approaches for neuroprotection. *Neuroimaging Clinics* **28**, 663-682, doi:10.1016/j.nic.2018.06.008 (2018).

100 Lee, M. & Ovbiagele, B. Stroke in 2017: Intensive and extensive—advances in stroke management. *Nature Reviews Neurology*, doi:10.1038/nrneurol.2017.187 (2018).

101 Detante, O., Muir, K. & Jolkkonen, J. Cell Therapy in Stroke—Cautious Steps Towards a Clinical Treatment. *Translational stroke research* **9**, 321-332, doi:10.1007/s12975-017-0587-6 (2018).

102 van der Worp, H. B. *et al.* EuroHYP-1: European multicenter, randomized, phase III clinical trial of therapeutic hypothermia plus best medical treatment vs. best medical treatment alone for acute ischemic stroke. *International Journal of Stroke* **9**, 642-645, doi:10.1111/ijs.12294 (2014).

103 Broussalis, E. *et al.* Current therapies in ischemic stroke. Part B. Future candidates in stroke therapy and experimental studies. *Drug discovery today* **17**, 671-684, doi:10.1016/j.drudis.2012.02.011 (2012).

104 Wu, M.-Y. *et al.* Current mechanistic concepts in ischemia and reperfusion injury. *Cellular Physiology and Biochemistry* **46**, 1650-1667, doi:10.1159/000489241 (2018).

105 Dirnagl, U., Iadecola, C. & Moskowitz, M. A. Pathobiology of ischaemic stroke: an integrated view. *Trends in neurosciences* **22**, 391-397, doi:10.1016/S0166-2236(99)01401-0 (1999).

106 Pignataro, G., Simon, R. P. & Xiong, Z.-G. Prolonged activation of ASIC1a and the time window for neuroprotection in cerebral ischaemia. *Brain* **130**, 151-158, doi:10.1093/brain/awl325 (2006).

107 Mergenthaler, P., Dirnagl, U. & Meisel, A. Pathophysiology of stroke: lessons from animal models. *Metabolic brain disease* **19**, 151-167 (2004).

108 Stavrovskaya, I. G. & Kristal, B. S. The powerhouse takes control of the cell: is the mitochondrial permeability transition a viable therapeutic target against neuronal dysfunction and death? *Free Radical Biology and Medicine* **38**, 687-697, doi:10.1016/j.freeradbiomed.2004.11.032 (2005).

109 Allen, C. L. & Bayraktutan, U. Oxidative stress and its role in the pathogenesis of ischaemic stroke. *International journal of stroke* **4**, 461-470, doi:10.1111/j.1747-4949.2009.00387.x (2009).

110 Shirley, R., Ord, E. & Work, L. Oxidative stress and the use of antioxidants in stroke. *Antioxidants* **3**, 472-501, doi:10.3390/antiox3030472 (2014).

111 Grieb, P., Forster, R., Strome, D., Goodwin, C. & Pape, P. O2 exchange between blood and brain tissues studied with 18O2 indicator-dilution technique. *Journal of Applied Physiology* **58**, 1929-1941 (1985).

112 Cortez, D. M. *et al.* Interleukin-17 Stimulates MMP1 Expression in Primary Human Cardiac Fibroblasts Via p38 MAPK and ERK1/2-Dependent C/EBPβ, NF-κB, and AP-1 Activation. *American Journal of Physiology-Heart and Circulatory Physiology*, doi:10.1152/ajpheart.00928.2007 (2007).

113 Gelderblom, M. *et al.* Temporal and spatial dynamics of cerebral immune cell accumulation in stroke. *Stroke* **40**, 1849-1857, doi:10.1161/STROKEAHA.108.534503 (2009).

114 Patel, A. R., Ritzel, R., McCullough, L. D. & Liu, F. Microglia and ischemic stroke: a double-edged sword. *International journal of physiology, pathophysiology and pharmacology* **5**, 73 (2013).

115 Ito, D., Tanaka, K., Suzuki, S., Dembo, T. & Fukuuchi, Y. Enhanced expression of Iba1, ionized calcium-binding adapter molecule 1, after transient focal cerebral ischemia in rat brain. *Stroke* **32**, 1208-1215, doi:10.1161/01.STR.32.5.1208 (2001).

116 Chamorro, Á., Dirnagl, U., Urra, X. & Planas, A. M. Neuroprotection in acute stroke: targeting excitotoxicity, oxidative and nitrosative stress, and inflammation. *The Lancet Neurology* **15**, 869-881, doi:10.1016/S1474-4422(16)00114-9 (2016).

117 Carmichael, S. T., Kathirvelu, B., Schweppe, C. A. & Nie, E. H. Molecular, cellular and functional events in axonal sprouting after stroke. *Experimental neurology* **287**, 384-394, doi:10.1016/j.expneurol.2016.02.007 (2017).

118 Adams, K. L. & Gallo, V. The diversity and disparity of the glial scar. *Nature neuroscience* **21**, 9, doi:10.1038/s41593-017-0033-9 (2018).

119 Koh, S.-H. & Park, H.-H. Neurogenesis in stroke recovery. *Translational stroke research* **8**, 3-13, doi:10.1007/s12975-016-0460-z (2017).

120 Li, J.-H. *et al.* Bioactive components of Chinese herbal medicine enhance endogenous neurogenesis in animal models of ischemic stroke: a systematic analysis. *Medicine* **95**, doi:10.1097/MD.0000000000004904 (2016).

121 Coley, A. A. & Gao, W.-J. PSD95: a synaptic protein implicated in schizophrenia or autism? *Progress in Neuro-Psychopharmacology and Biological Psychiatry* **82**, 187-194, doi:10.1016/j.pnpbp.2017.11.016 (2018).

122 Egbujo, C. N., Sinclair, D. & Hahn, C.-G. Dysregulations of synaptic vesicle trafficking in schizophrenia. *Current psychiatry reports* **18**, 77, doi:10.1007/s11920-016-0710-5 (2016).

123 Liu, P. *et al.* Time-course investigation of blood–brain barrier permeability and tight junction protein changes in a rat model of permanent focal ischemia. *The Journal of Physiological Sciences* **68**, 121-127, doi:10.1007/s12576-016-0516-6 (2018).

124 González-Correa, J. A. *et al.* Neuroprotective effect of hydroxytyrosol and hydroxytyrosol acetate in rat brain slices subjected to hypoxia–reoxygenation. *Neuroscience letters* **446**, 143-146, doi:10.1016/j.neulet.2008.09.022 (2008).

125 Cabrerizo, S. *et al.* Role of the inhibition of oxidative stress and inflammatory mediators in the neuroprotective effects of hydroxytyrosol in rat brain slices subjected to hypoxia reoxygenation. *The Journal of nutritional biochemistry* **24**, 2152-2157, doi:10.1016/j.jnutbio.2013.08.007 (2013).

126 De La Cruz, J. P. *et al.* Differences in the neuroprotective effect of orally administered virgin olive oil (Olea europaea) polyphenols tyrosol and hydroxytyrosol in rats. *Journal of agricultural and food chemistry* **63**, 5957-5963, doi:10.1021/acs.jafc.5b00627 (2015).

127 De La Cruz, J. *et al.* Role of the catechol group in the antioxidant and neuroprotective effects of virgin olive oil components in rat brain. *The Journal of nutritional biochemistry* **26**, 549-555, doi:10.1016/j.jnutbio.2014.12.013 (2015).

128 Reyes, J. J. *et al.* Neuroprotective effect of hydroxytyrosol in experimental diabetes mellitus. *Journal of agricultural and food chemistry* **65**, 4378-4383, doi:10.1021/acs.jafc.6b02945 (2017).

129 Bu, Y. *et al.* Neuroprotective effect of tyrosol on transient focal cerebral ischemia in rats. *Neuroscience letters* **414**, 218-221, doi:10.1016/j.neulet.2006.08.094 (2007).

130 Raza, C. & Anjum, R. Parkinson's disease: Mechanisms, translational models and management strategies. *Life sciences*, doi:10.1016/j.lfs.2019.03.057 (2019).

131 Duce, J. A. *et al.* Post translational changes to α-synuclein control iron and dopamine trafficking; a concept for neuron vulnerability in Parkinson's disease. *Molecular neurodegeneration* **12**, 45, doi:10.1186/s13024-017-0186-8 (2017).

132 Postuma, R. B. *et al.* Identifying prodromal Parkinson's disease: pre-motor disorders in Parkinson's disease. *Movement Disorders* **27**, 617-626, doi:10.1002/mds.24996 (2012).

133 Hely, M. A., Morris, J. G., Reid, W. G. & Trafficante, R. Sydney multicenter study of Parkinson's disease: Non-L-dopa–responsive problems dominate at 15 years. *Movement disorders: official journal of the Movement Disorder Society* **20**, 190-199, doi:10.1002/mds.20324 (2005).

134 Wakabayashi, K. *et al.* The Lewy body in Parkinson's disease and related neurodegenerative disorders. *Molecular neurobiology* **47**, 495-508, doi:10.1007/s12035-012-8280-y (2013).

135 Alafuzoff, I. & Hartikainen, P. in *Handbook of clinical neurology* Vol. 145 339-353 (Elsevier, 2018).

136 Walker, L. C. & LeVine, H. Corruption and spread of pathogenic proteins in neurodegenerative diseases. *Journal of Biological Chemistry* **287**, 33109-33115, doi:10.1074/jbc.R112.399378 (2012).

137 Kalia, L. V. & Lang, A. E. Parkinson disease in 2015: evolving basic, pathological and clinical concepts in PD. *Nature reviews Neurology* **12**, 65, doi:10.1016/S0140-6736(14)61393-3 (2016).

138 Stefanis, L. α-Synuclein in Parkinson's disease. *Cold Spring Harbor perspectives in medicine* **2**, a009399, doi:10.1101/cshperspect.a009399 (2012).

139 Bartels, T., Choi, J. G. & Selkoe, D. J. α-Synuclein occurs physiologically as a helically folded tetramer that resists aggregation. *Nature* **477**, 107, doi:10.1038/nature10324 (2011).

140 Vasili, E., Dominguez-Meijide, A. & Outeiro, T. F. Spreading of α-Synuclein and tau: a systematic comparison of the mechanisms involved. *Frontiers in Molecular Neuroscience* **12**, 107, doi:10.3389/fnmol.2019.00107 (2019).

141 Butler, B., Sambo, D. & Khoshbouei, H. Alpha-synuclein modulates dopamine neurotransmission. *Journal of chemical neuroanatomy* **83**, 41-49, doi:10.1016/j.jchemneu.2016.06.001 (2017).

142 Villar-Piqué, A., Lopes da Fonseca, T. & Outeiro, T. F. Structure, function and toxicity of alpha-synuclein: the Bermuda triangle in synucleinopathies. *Journal of neurochemistry* **139**, 240-255, doi:10.1111/jnc.13249 (2016).

143 Ghosh, D., Mehra, S., Sahay, S., Singh, P. K. & Maji, S. K. α-synuclein aggregation and its modulation. *International journal of biological macromolecules* **100**, 37-54, doi:10.1016/j.ijbiomac.2016.10.021 (2017).

144 Buell, A. K. *et al.* Solution conditions determine the relative importance of nucleation and growth processes in α-synuclein aggregation. *Proceedings of the National Academy of Sciences* **111**, 7671-7676, doi:10.1073/pnas.1315346111 (2014).

145 Treusch, S., Cyr, D. M. & Lindquist, S. Amyloid deposits: protection against toxic protein species? *Cell cycle* **8**, 1668-1674, doi:10.4161/cc.8.11.8503 (2009).

146 Poewe, W. *et al.* Parkinson disease. *Nature reviews Disease primers* **3**, 17013, doi:10.1038/nrdp.2017.13 (2017).

147 Dhouafli, Z. *et al.* Inhibition of protein misfolding and aggregation by natural phenolic compounds. *Cellular and molecular life sciences* **75**, 3521-3538, doi:10.1007/s00018-018-2872-2 (2018).

148 Jones, D. R., Moussaud, S. & McLean, P. Targeting heat shock proteins to modulate α-synuclein toxicity. *Therapeutic advances in neurological disorders* **7**, 33-51, doi:10.1177/1756285613493469 (2014).

149 Bengoa-Vergniory, N., Roberts, R. F., Wade-Martins, R. & Alegre-Abarrategui, J. Alpha-synuclein oligomers: a new hope. *Acta neuropathologica* **134**, 819-838, doi:10.1007/s00401-017-1755-1 (2017).

150 Lansdall, C. J. An effective treatment for Alzheimer's disease must consider both amyloid and tau. *Bioscience Horizons: The International Journal of Student Research* **7**, doi:10.1093/biohorizons/hzu002 (2014).

151 Verma, M., Vats, A. & Taneja, V. Toxic species in amyloid disorders: Oligomers or mature fibrils. *Annals of Indian Academy of Neurology* **18**, 138, doi:10.4103/0972-2327.144284 (2015).

152 Ordonez, D. G., Lee, M. K. & Feany, M. B. α-synuclein induces mitochondrial dysfunction through spectrin and the actin cytoskeleton. *Neuron* **97**, 108-124. e106, doi:10.1016/j.neuron.2017.11.036 (2018).

153 Prots, I. *et al.* α-Synuclein oligomers induce early axonal dysfunction in human iPSC-based models of synucleinopathies. *Proceedings of the National Academy of Sciences* **115**, 7813-7818, doi:10.1073/pnas.1713129115 (2018).

154 Braak, H. *et al.* Staging of brain pathology related to sporadic Parkinson's disease. *Neurobiology of aging* **24**, 197-211, doi:10.1016/S0197-4580(02)00065-9 (2003).

155 Braak, H., Rüb, U., Gai, W. & Del Tredici, K. Idiopathic Parkinson's disease: possible routes by which vulnerable neuronal types may be subject to neuroinvasion by an unknown pathogen. *Journal of neural transmission* **110**, 517-536, doi:10.1007/s00702-002-0808-2 (2003).

156 Olanow, C. W. & Prusiner, S. B. Is Parkinson's disease a prion disorder? *Proceedings of the National Academy of Sciences* **106**, 12571-12572, doi:10.1073/pnas.0906759106 (2009).

157 Bernis, M. E. *et al.* Prion-like propagation of human brain-derived alpha-synuclein in transgenic mice expressing human wild-type alpha-synuclein. *Acta neuropathologica communications* **3**, 75, doi:10.1186/s40478-015-0254-7 (2015).

158 Dias, V., Junn, E. & Mouradian, M. M. The role of oxidative stress in Parkinson's disease. *Journal of Parkinson's disease* **3**, 461-491, doi:10.3233/JPD-130230 (2013).

159 Bose, A. & Beal, M. F. Mitochondrial dysfunction in Parkinson's disease. *Journal of neurochemistry* **139**, 216-231, doi:10.1111/jnc.13731 (2016).

160 Gash, D. M. *et al.* Trichloroethylene: Parkinsonism and complex 1 mitochondrial neurotoxicity. *Annals of neurology* **63**, 184-192, doi:10.1002/ana.21288 (2008).

161 Subramaniam, S. R., Vergnes, L., Franich, N. R., Reue, K. & Chesselet, M.-F. Region specific mitochondrial impairment in mice with widespread overexpression of alpha-synuclein. *Neurobiology of disease* **70**, 204-213, doi:10.1016/j.nbd.2014.06.017 (2014).

162 Zucca, F. A. *et al.* Interactions of iron, dopamine and neuromelanin pathways in brain aging and Parkinson's disease. *Progress in neurobiology* **155**, 96-119, doi:10.1016/j.pneurobio.2015.09.012 (2017).

163 Gasser, T. Update on the genetics of Parkinson's disease. *Movement disorders: official journal of the Movement Disorder Society* **22**, S343-S350, doi:10.1002/mds.21676 (2007).

164 Hwang, O. Role of oxidative stress in Parkinson's disease. *Experimental neurobiology* **22**, 11-17, doi:10.5607/en.2013.22.1.11 (2013).

165 López-Otín, C., Blasco, M. A., Partridge, L., Serrano, M. & Kroemer, G. The hallmarks of aging. *Cell* **153**, 1194-1217, doi:10.1016/j.cell.2013.05.039 (2013).

166 Schmidt, M. & Finley, D. Regulation of proteasome activity in health and disease. *Biochimica et Biophysica Acta (BBA)-Molecular Cell Research* **1843**, 13-25, doi:10.1016/j.bbamcr.2013.08.012 (2014).

167 Chiti, F. & Dobson, C. M. Protein misfolding, amyloid formation, and human disease: a summary of progress over the last decade. *Annual review of biochemistry* **86**, 27-68, doi:10.1146/annurev-biochem-061516-045115 (2017).

168 Sharma, S. K. & Priya, S. Expanding role of molecular chaperones in regulating α-synuclein misfolding; implications in Parkinson's disease. *Cellular and molecular life sciences* **74**, 617-629, doi:10.1007/s00018-016-2340-9 (2017).

169 Maiti, P., Manna, J., Veleri, S. & Frautschy, S. Molecular chaperone dysfunction in neurodegenerative diseases and effects of curcumin. *BioMed research international* **2014**, doi:10.1155/2014/495091 (2014).

170 Brehme, M. *et al.* A chaperome subnetwork safeguards proteostasis in aging and neurodegenerative disease. *Cell reports* **9**, 1135-1150, doi:10.1016/j.celrep.2014.09.042 (2014).

171 Brenner, S. The genetics of Caenorhabditis elegans. *Genetics* **77**, 71-94 (1974).

172 Markaki, M. & Tavernarakis, N. Modeling human diseases in Caenorhabditis elegans. *Biotechnology journal* **5**, 1261-1276, doi:10.1002/biot.201000183 (2010).

173 White, J. G., Southgate, E., Thomson, J. N. & Brenner, S. The structure of the nervous system of the nematode Caenorhabditis elegans. *Philos Trans R Soc Lond B Biol Sci* **314**, 1-340 (1986).

174 Cooper, A. A. *et al.* α-Synuclein blocks ER-Golgi traffic and Rab1 rescues neuron loss in Parkinson's models. *Science* **313**, 324-328, doi:10.1126/science.1129462 (2006).

175 Caldwell, G. A. & Caldwell, K. A. Traversing a wormhole to combat Parkinson's disease. *Disease models & mechanisms* **1**, 32-36, doi:10.1242/dmm.000257 (2008).

176 Lublin, A. & Link, C. Alzheimer's disease drug discovery: in vivo screening using Caenorhabditis elegans as a model for β-amyloid peptide-induced toxicity. *Drug Discovery Today: Technologies* **10**, e115-e119, doi:10.1016/j.ddtec.2012.02.002 (2013).

177 Petrascheck, M., Ye, X. & Buck, L. B. A high-throughput screen for chemicals that increase the lifespan of Caenorhabditis elegans. *Annals of the New York Academy of Sciences* **1170**, 698-701, doi:10.1111/j.1749-6632.2009.04377.x (2009).

178 Burggraaff, R. *et al.* A30 Identification of MOAG-4/SERF as a regulator of age related proteotoxicity. *Journal of Neurology, Neurosurgery & Psychiatry* **81**, A10-A10, doi:10.1016/j.cell.2010.07.020 (2010).

179 Sin, O., Michels, H. & Nollen, E. A. Genetic screens in Caenorhabditis elegans models for neurodegenerative diseases. *Biochimica et Biophysica Acta (BBA)-Molecular Basis of Disease* **1842**, 1951-1959, doi:10.1016/j.bbadis.2014.01.015 (2014).

180 Altun, Z. & Hall, D. WormAtlas. *URL http://www. wormatlas. org* **1384** (2002).

181 Ladiwala, A. R. A., Dordick, J. S. & Tessier, P. M. Aromatic small molecules remodel toxic soluble oligomers of amyloid β through three independent pathways. *Journal of Biological Chemistry* **286**, 3209-3218, doi:10.1074/jbc.M110.173856 (2011).

182 Rigacci, S. *et al.* Aβ (1-42) aggregates into non-toxic amyloid assemblies in the presence of the natural polyphenol oleuropein aglycon. *Current Alzheimer Research* **8**, 841-852, doi:10.2174/156720511798192682 (2011).

183 Cheng, B. *et al*. Inhibiting toxic aggregation of amyloidogenic proteins: a therapeutic strategy for protein misfolding diseases. *Biochimica et Biophysica Acta (BBA)-General Subjects* **1830**, 4860-4871, doi:10.1016/j.bbagen.2013.06.029 (2013).

184 Ahmad, E. *et al.* A mechanistic approach for islet amyloid polypeptide aggregation to develop anti-amyloidogenic agents for type-2 diabetes. *Biochimie* **93**, 793-805, doi:10.1016/j.biochi.2010.12.012 (2011).

185 Wu, C., Lei, H., Wang, Z., Zhang, W. & Duan, Y. Phenol red interacts with the protofibril-like oligomers of an amyloidogenic hexapeptide NFGAIL through both hydrophobic and aromatic contacts. *Biophysical journal* **91**, 3664-3672, doi:10.1529/biophysj.106.081877 (2006).

186 Grossi, C. *et al.* The polyphenol oleuropein aglycone protects TgCRND8 mice against Aß plaque pathology. *PLoS One* **8**, e71702, doi:10.1371/journal.pone.0071702 (2013).

187 Luccarini, I. *et al.* Oleuropein aglycone counteracts Aβ42 toxicity in the rat brain. *Neuroscience letters* **558**, 67-72, doi:10.1016/j.neulet.2013.10.062 (2014).

188 Daccache, A. *et al.* Oleuropein and derivatives from olives as Tau aggregation inhibitors. *Neurochemistry international* **58**, 700-707, doi:10.1016/j.neuint.2011.02.010 (2011).

189 Pasban-Aliabadi, H. *et al.* Inhibition of 6-hydroxydopamine-induced PC12 cell apoptosis by olive (Olea europaea L.) leaf extract is performed by its main component oleuropein. *Rejuvenation research* **16**, 134-142, doi:10.1089/rej.2012.1384 (2013).

190 Yu, G. *et al.* Hydroxytyrosol induces phase II detoxifying enzyme expression and effectively protects dopaminergic cells against dopamine- and 6-hydroxydopamine induced cytotoxicity. *Neurochemistry international* **96**, 113-120, doi:10.1016/j.neuint.2016.03.005 (2016).

191 Vauzour, D., Corona, G. & Spencer, J. P. Caffeic acid, tyrosol and p-coumaric acid are potent inhibitors of 5-S-cysteinyl-dopamine induced neurotoxicity. *Archives of Biochemistry and Biophysics* **501**, 106-111, doi:10.1016/j.abb.2010.03.016 (2010).

192 Dewapriya, P., Himaya, S., Li, Y.-X. & Kim, S.-K. Tyrosol exerts a protective effect against dopaminergic neuronal cell death in in vitro model of Parkinson's disease. *Food chemistry* **141**, 1147-1157, doi:10.1016/j.foodchem.2013.04.004 (2013).

193 Diomede, L., Rigacci, S., Romeo, M., Stefani, M. & Salmona, M. Oleuropein aglycone protects transgenic C. elegans strains expressing Aβ42 by reducing plaque load and motor deficit. *PLoS one* **8**, e58893, doi:10.1371/journal.pone.0058893 (2013).

Hipótesis y Objetivos/ Hypothesis and Aims

HIPÓTESIS

Los compuestos fenólicos del olivo poseen un gran potencial como moléculas bioactivas en diferentes contextos patológicos. Partiendo de su capacidad antioxidante como piedra angular de sus propiedades, multitud de estudios describen cómo estos compuestos pueden modular gran variedad de mecanismos moleculares. Considerando la importancia del estrés oxidativo en patologías en las que la hipoxia juega un papel importante, como el cáncer y el ictus, y en enfermedades amiloides como la EP, se podría esperar que el HT y el TIR, los dos fenoles mayoritarios del AOVE, ejercieran un efecto beneficioso en estas patologías. La seguridad para el consumo humano de estos compuestos potencia aún más el interés de esta investigación.

OBJETIVOS

Para probar nuestra hipótesis, se abordaron una serie de objetivos, detallados a continuación, empleando diferentes modelos que permitieron el estudio de aspectos relevantes de cada enfermedad estudiada. Concretamente se evaluó el efecto de estos compuestos del olivo sobre:

- El estrés oxidativo en células de cáncer de mama MCF-7, comparando su efecto en condiciones de normoxia e hipoxia (Objetivo 1).

- El mecanismo de respuesta a la hipoxia mediado por HIF-1 en esa misma línea celular (Objetivo 2).

- La respuesta a una lesión isquémica inducida mediante un modelo de tMCAo en ratones (Objetivo 3).

- Los mecanismos patológicos asociados con la agregación de α-syn en la EP en modelos de *C. elegans* (Objetivo 4).

HYPOTHESIS

Olive tree phenolic compounds have a great potential as bioactive molecules in a number of pathologies. Although they are widely known for their antioxidant activity, different studies have demonstrated that these molecules can also act on other molecular pathways. HT and TYR are the main phenols in the olive tree and constitute the main simple phenols in EVOO. Given the crucial role of oxidative stress in hypoxia-associated diseases, such as cancer and ictus, and in amyloid diseases, such as PD, we propose that these molecules, enriched in EVOO, exert a protective effect on these pathologies. Moreover, the fact that these compounds are recognized as safe for human intake further increases the interest of this research.

AIMS

To address our hypothesis, we used different experimental models to investigate important features of the analyzed pathologies. In particular, we proposed to evaluate the effect of these olive phenols on:

- The oxidative stress level of hypoxic and normoxic MCF-7 breast cancer cells (Aim 1).
- HIF-1-mediated response to hypoxia in MCF-7 cells (Aim 2).
- The recovery from an ischemic lesion induced by a tMCAo model in mice (Aim 3).
- The pathological mechanisms associated with the aggregation of α-syn in *C. elegans* models of PD (Aim 4).

Artículos

Artículo 1

La hipoxia modula el efecto antioxidante del hidroxitirosol en células MCF-7 de cáncer de mama

Jesús Calahorra, Esther Martínez-Lara, Cristina De Dios, Eva Siles

PLoS One. 2018; 13(9):e0203892

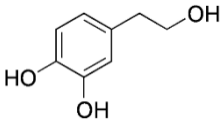

PLOS ONE

RESEARCH ARTICLE

Hypoxia modulates the antioxidant effect of hydroxytyrosol in MCF-7 breast cancer cells

Jesús Calahorra, Esther Martínez-Lara, Cristina De Dios[¤], Eva Siles*

Department of Experimental Biology, University of Jaén, Campus Las Lagunillas s/n, Jaén, Spain

¤ Current address: Department of Cell Death and Proliferation, Biomedical Research Institute of Barcelona—Higher Council for Scientific Research (IIBB-CSIC), Barcelona, Spain
* esiles@ujaen.es

Citation: Calahorra J, Martínez-Lara E, De Dios C, Siles E (2018) Hypoxia modulates the antioxidant effect of hydroxytyrosol in MCF-7 breast cancer cells. PLoS ONE 13(9): e0203892. https://doi.org/10.1371/journal.pone.0203892

Editor: Pankaj K. Singh, University of Nebraska Medical Center, UNITED STATES

Received: June 8, 2018

Accepted: August 29, 2018

Published: September 20, 2018

Data Availability Statement: All relevant data are within the paper and its Supporting Information files.

Funding: The author(s) received no specific funding for this work.

Competing interests: The authors have declared that no competing interests exist.

Abstract

Although cancer is multifactorial, a strong correlation between this pathology and increased oxidative stress has long been stablished. Hypoxia, inherent to solid tumors, increases reactive oxygen species and should be taken into account when analyzing the response of tumor cells to antioxidants. The Mediterranean diet has been related to a lower incidence of cancer, and particularly of breast cancer. Given that hydroxytyrosol (HT) is largely responsible for the antioxidant properties of olive oil, we have performed a comprehensive and comparative study of its effect on the oxidative stress response of the human breast cancer cell line MCF-7 in hypoxia and normoxia. Our results demonstrate that the antioxidant action of HT is particularly effective in a hypoxic environment. Moreover, we have observed that this polyphenol modulates the transcription and translation of members of the PGC-1α/ERRα and PGC-1α/Nrf2 pathways. However, while the transcriptional effects of HT are similar in normoxic and hypoxic conditions, its translational action is less prominent and partially attenuated in hypoxia, and therefore cannot completely explain the antioxidant effect of HT. Consequently, our results underscore that the hypoxic environment of tumor cells should be considered when analyzing the effect of bioactive compounds. Besides, this study also points to the importance of assessing the regulatory role of HT at both mRNA and protein level to get a complete picture of its effects.

Introduction

Cancer is a generic term for a large group of diseases which figure among the leading causes of morbidity and mortality worldwide. In women, the most common cancer is breast cancer, contributing more than 25% of the total number of new cases diagnosed in 2012 [1]. Although cancer is multifactorial, a strong correlation between this pathology and increased oxidative stress has long been stablished. In fact, overproduction of reactive oxygen species (ROS) as a consequence of genetic, metabolic and microenvironment-associated alterations is known to promote both tumor initiation and progression [2].

Oxidative stress is the result of an unbalance between ROS production and detoxification. This species are constantly formed in aerobic organisms, particularly in mitochondria. In this

sense, although cancer cells show high rates of glycolysis, they also retain functional mitochondria, essential for tumorigenesis, in which oxidative phosphorylation occurs [3]. Mitochondrial biogenesis is regulated by PPARγ coactivator-1α (PGC-1α). This protein interacts and coactivates the estrogen-related receptor α (ERRα) and the nuclear respiratory factor 2 (Nrf2) [4]. ERRα is an "orphan" nuclear receptor whose activity is not regulated by ligand binding. This protein induces the transcription of the enzymes of the tricarboxylic acid cycle and oxidative phosphorylation, enabling adaptive metabolic events, such as biomass synthesis, that are crucial in cancer development [5]. Nrf2 acts as a heterodimer with other transcription factors such as Mafs, promoting the expression of target genes with one or more antioxidant response elements (ARE, TCAG/CXXXGC) in their promoter region. Among others, those targets are antioxidant, NADPH generating and glutathione synthesis enzymes, proteins involved in xenobiotic metabolism and efflux, and heat shock proteins [6]. The central function of ERRα and Nrf2 reinforces the importance of finding new molecules that modulates their activity, particularly under pathological situations highly linked to oxidative stress such as cancer.

In solid tumors, the high cell proliferation, the abnormal anatomy of blood vessels and their obstruction or compression imply the appearance of hypoxic areas. As an example, the average O_2 pressure in breast tumors is approximately 80% lower than in normal breast tissue [7]. This hypoxic microenvironment further increases oxidative stress, promoting tumor development and malignancy, and should be taken into account when performing studies about the molecular response of tumor cells.

A number of studies have revealed that in the Mediterranean countries the incidence of breast cancer is lower than in other developed countries, pointing to the dietary practice as possible cause of this effect [8–10]. The Mediterranean diet is characterized by a high intake of fruits, vegetables, whole grains, legumes and healthy fats such as olive oil. Olive oil is mainly composed of fatty acids, particularly oleic acid and linoleic acid. However, in recent years much attention has been paid to the minor components of olive oil. This fraction represents no more than 2% of the olive oil weight and includes flavonoids, lignans or secoiridoids and phenolic compounds such as hydroxytyrosol (3,4-dihydroxyphenylethanol; HT), endowed with antioxidant properties [11]. Although some authors have studied the antioxidant action of this polyphenol in breast cancer [12–14], there is a lack of a comprehensive analysis of its molecular effect in hypoxic conditions. With this background, and considering the importance of hypoxia in tumor microenvironment, the objective of the present study was to comparatively analyze the effect of HT treatment in the oxidative response of hypoxic and normoxic MCF-7 cells, widely used in breast cancer research.

Materials and methods

Chemicals and reagents

HT (purity ≥98%) was obtained from Extrasynthese (Lyon, France). Dulbecco's modified Eagle's medium (DMEM) was from BiochromAG (Berlin, Germany). RNA was isolated using the RNeasyPlus Mini kit (Qiagen, Hilden, Germany) and cDNA was prepared with Maxima First Strand cDNA Synthesis Kit for RT-qPCR (Fermentas Intl., Vilnius, Lithuania). Real-time PCR was performed using SYBR Fast Master Mix (2x) Universal (KAPABiosystems, Massachusetts, USA). Primers were synthesized by Biomedal S.L. (Sevilla, Spain). Nrf2 siRNA (sc-37049), scramble siRNA (scr siRNA) and the transfection reagent were from Santa Cruz Biotechnology (CA, USA). Opti-MEM reduced serum medium was bought from Thermo Fisher Scientific. α-Tubulin antibody, foetal bovine serum (FBS), sulforhodamine B (SRB), trichloroacetic acid (TCA), 2′,7′-dichlorofluorescin diacetate (DCFH-DA), glutathione reductase (GR), reduced glutathione, NADPH, cumene hydroperoxide, and other general reagents were

from Sigma (St. Louis, MO, USA). Heme oxygenase-1 (HO-1) was measured with the enzyme linked immunosorbent assay (ELISA) kit CSB-E08266h from Cusabio (Barksdale, USA). Primary antibodies (PGC-1α, Nrf2, ERRα, SIRT3) were purchased from Santa Cruz Biotechnology, Inc., (CA, USA) except anti-α-tubulin (Sigma, St. Louis, Mo, USA).

Cell culture and treatments

Human breast cancer MCF-7 cells were grown in 10% foetal bovine serum supplemented DMEM at 37˚C in 5% CO_2 and 21% O_2. Cells were pre-treated or not with HT, dissolved in ethanol immediately before use, for 16 h under normoxic conditions (21% O_2), being cultured during the last 4 h either in normoxic or hypoxic conditions (1% O_2). Controls were treated with an equal ethanol concentration.

Cytotoxicity assay

The cytotoxic effect of HT was evaluated using the SRB assay as previously described [15]. Briefly, 4 x 10^4 cells/well were plated in 24-well tissue culture plates (Nunc, Rosbilde, Denmark). The plates were incubated for 24 h to allow the cells to adhere. HT was then added to the corresponding wells at a range of concentrations (0 to 600 μM), each concentration being used in at least four replicate wells. After 16 h of treatment, last 4 h either in normoxic or hypoxic conditions, the medium was removed and the cultures were washed with PBS. Cells were fixed at 4˚C with 10% TCA for 30 min and then washed with tap water to remove TCA. Plates were air dried and stored until use. TCA-fixed cells were stained for 20 min with 0.4% (w/v) SRB dissolved in 1% acetic acid. After staining, SRB was removed and cultures were rinsed with 1% acetic acid to eliminate unbound dye. The cultures were air dried and bound dye was solubilized with 10 mM Tris base (pH 10.5). Optical density was read in a plate reader (ThermoLabSystem Multiscan Ascent) at 492 nm. Cell survival was measured as the percentage of absorbance compared with that obtained in non HT-treated cells.

Measurement of intracellular generation of ROS

Intracellular generation of ROS was analysed using DCFH-DA as a probe [16]. ROS in the cells oxidize DCFH, yielding highly fluorescent 2´,7´-dichlorofluorescein (DCF). Briefly, cells were cultured in 96-well plates (10^4 cells/well) and treated for 16 h with HT (0–200μM), being cultured during the last 4 h either in normoxic or hypoxic conditions. 30 min before the end of the experiment, cells were washed with Krebs buffer (pH 7.3) and incubated with 10 μM DCFH-DA. Once the incubation was finished, cells were washed three times and DCF fluorescence was measured in a plate reader (ThermoLabSystem Multiscan Ascent) at an excitation wavelength of 488 nm and emission wavelength of 535 nm.

Quantitative Real-time PCR (qRT-PCR)

Gene expression of PGC-1α, ERRα, Nrf2, HO-1, GSTA2 (Glutathione S-Transferase Alpha 2), and SIRT3 (Sirtuin-3) were quantitatively assessed by real-time PCR using peptidylprolyli-somerase A (PPIA) as the normalizing gene. Real-time PCR was performed in a MxPro thermal cycler (Stratagene, California, USA) using SYBR Fast Master Mix (2x) Universal. The sequences of primers are shown in Table 1. Experiments were performed in triplicate, and the relative quantities of target genes, corrected with the normalizing gene PPIA, were calculated using the Stratagene MxProTM QPCR Software.

Table 1. Primer details.

primer	forward (5′-3′)	reverse (5′-3′)
PGC-1α	TGCTTTTGCTGCTCTTGAAA	TTACCTGCGCAAGCTTCTCT
ERRα	GCTGCCCTGCTGCAACTA	GCCTCGTGCAGAGCTTCTC
Nrf2	TCAGGCTCAGTCACCTGAAA	TTGGCTTCTGGACTTGGAAC
HO-1	ATGACACCAAGGACCAGAGC	GTGTAAGGACCCATCGGAGA
GSTA2	GAGCCACGGACAAGACTACC	CACTGTGGGCAGGTTACTGA
SIRT3	AACATCGATGGGCTTGAGAG	AGAACACAATGTCGGGCTTC
PPIA	TTCATCTGCACTGCCAAGAC	TCGAGTTGTCCACAGTCAGC

https://doi.org/10.1371/journal.pone.0203892.t001

Western blot

For western blot analysis, equal amounts of denatured total-protein extracts (30 μg) were loaded and separated on a 7.5% (PGC-1α), or 10% (SIRT3, Nrf2 and ERRα) SDS-polyacrylamide gel. Proteins in the gel were transferred to a PVDF membrane and then blocked. Monoclonal antibodies to PGC-1α, Nrf2, ERRα, SIRT3 and to α-tubulin, as a loading control, were used for detection of the respective proteins. Antibody reaction was revealed by means of chemiluminescence detection procedures according to the manufacturer's recommendations (ECL kit, Amersham Corp., Buckinghamshire, UK).

Se-independent glutathione peroxidase activity

Se-independent glutathione peroxidase (GPX) activity, as indicative of GSTA2 activity, was determined in a coupled assay with GR using cumene hydroperoxide as a substrate [17]. To prepare samples, at the end of each incubation period, cells were collected, washed with cold PBS, lysed for 20 min at 4˚C in EBC buffer (20 mM Tris–HCl pH 8; 150 mM NaCl, 1 mM EDTA, 0.5% NP-40) and sonicated. After centrifugation at 14,000 *g* for 15 min at 4˚C, supernatants were collected and protein was quantified [18].

HO-1 determination

HO-1 was measured with a commercial ELISA kit according to manufacturer's instructions. To prepare samples, cells of each experimental condition were collected and lysed in PBS by sonication. After centrifugation at 14,000 *g* for 30 min, supernatants were separated and protein was quantified [18].

Nrf2 siRNA transfection

Nrf2 siRNA and scr siRNA were transfected with transfection reagent according to the protocol of the manufacturer´s. Briefly, MCF-7 cells (16×10^4/well) were plated into 6-well plates, allowed to adhere for 24 h and incubated with fresh Opti-MEM Reduced Serum Medium containing siNrf2 (50 nM) or scr-siRNA (50 nM) for 5 h. The transfection medium was then replaced with fresh DMEM containing 10% FBS for 48 h before further treatment with HT and/or hypoxia. To quantify the efficiency of siNrf2, siNrf2 and scr siRNA transfected MCF-7 cells were lysed and prepared for determining Nrf2 mRNA expression by RT-PCR.

Statistical analysis

Data are expressed as means ± SD of at least three independent experiments. Statistical comparisons between the different experimental groups and their corresponding controls were

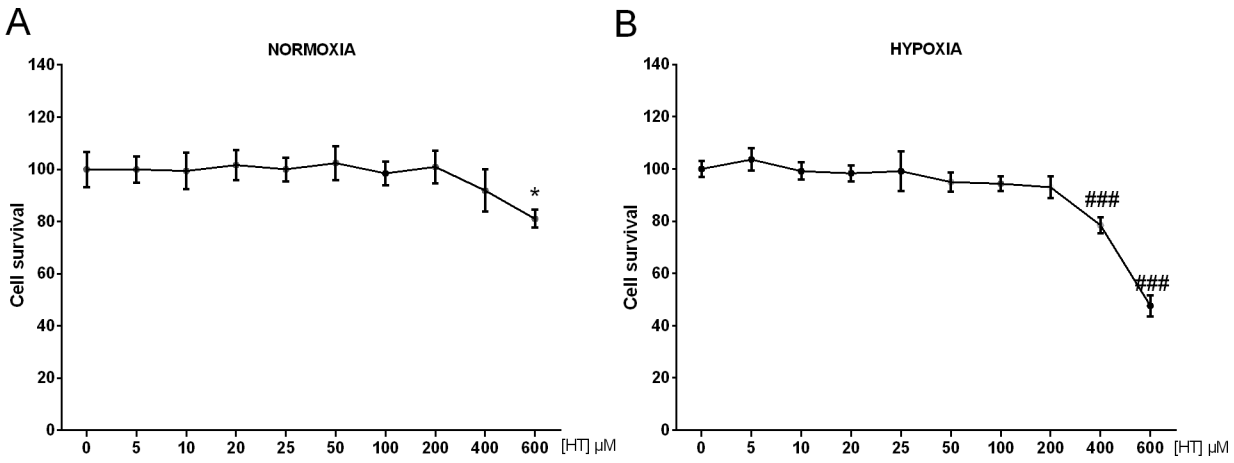

Fig 1. High concentrations of HT are necessary to affect MCF-7 cell proliferation. The cytotoxic effect of HT was evaluated in (A) normoxic cells and (B) hypoxic cells by the SRB assay. Values represent the mean ± SD from three independent experiments. Statistically significant differences with the corresponding non-treated normoxic or hypoxic cells:* $p<0.05$ and ### $p<0.001$, respectively.

https://doi.org/10.1371/journal.pone.0203892.g001

made with Student's t-test, accepting $p<0.05$ as the level of significance, using GraphPad Prism 6 software (GraphPad Software Inc.).

Results

Cytotoxic effect of HT on MCF-7 cells

The cytotoxic effect of HT in MCF-7 cells after 16 h of treatment is shown in Fig 1A. Our results indicated that concentrations as high as 600 μM were necessary to affect cell proliferation. To comparatively analyse the effect of HT in normoxic and hypoxic conditions, we evaluated whether the cytotoxicity of HT could be influenced by a decrease in O_2 pressure. To achieve this goal, MCF-7 cells were incubated under hypoxia during the last 4 h of HT-treatment. This experimental condition has been previously used by our group [19] and is strong enough to achieve an adaptive response to this situation, such as the induction of hypoxia inducible factor-1 (results not shown). As shown in Fig 1B, a 400 μM HT-treatment resulted toxic to MCF-7 cells, suggesting that hypoxia increases HT cytotoxicity although both, 400 and 600 μM, are extremely high concentrations.

HT exerts an antioxidant effect in hypoxic conditions

HT is reportedly described as an antioxidant compound. Thus, we next evaluated the effect of the treatment of MCF-7 cells with sub-cytotoxic concentrations of HT (0.1–200 μM) on the oxidative stress level. In normoxia, none of the concentrations assayed exerted any effect on this parameter (Fig 2A). However, when we analysed those same concentrations in hypoxic conditions (Fig 2B), a significant decrease was achieved by HT 5 μM and persisted until 200 μM.

PGC-1α expression is differentially regulated by HT in hypoxia

Given the impact of HT on the oxidative stress level, we evaluated whether this effect was related to a change in PGC-1α expression (Fig 3). The analysis of the transcriptional level of PGC-1α (Fig 3A) indicated that, although HT exerted no effect on the transcription of this coactivator at low concentrations, it decreased its level at high doses (100 and 200 μM), both in

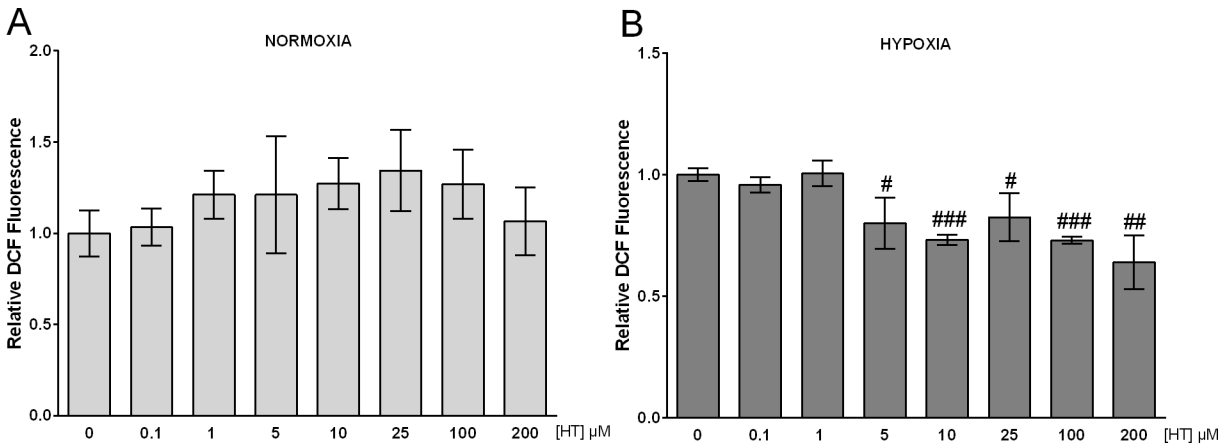

Fig 2. HT decreases the oxidative stress level only in hypoxic conditions. Oxidative stress level measured by DCF fluorescence in (A) normoxic cells and (B) hypoxic cells. Values represent the mean ± SD from three independent experiments. Statistically significant differences with the corresponding non-treated hypoxic cells: $^{\#}$ $p<0.05$, $^{\#\#}$ $p<0.01$ and $^{\#\#\#}$ $p<0.001$.

https://doi.org/10.1371/journal.pone.0203892.g002

normoxic and in hypoxic conditions. This result prompted us to determine whether PGC-1α protein was also down-regulated at 100 and 200μM. As shown in Fig 3B, the transcriptional changes induced by HT did not parallel the expression of PGC-1α at the protein level. In normoxic conditions, the same doses of HT that decreased transcription promoted the upregulation of the PGC-1α protein, while HT seemed to exert no effect in a hypoxic environment. Hence, the transcriptional and translational effects of HT do not seem to follow a similar pattern of response.

ERRα expression is hardly affected by HT independently of the O_2 pressure

The effect of PGC-1α is mediated by coactivation of transcription factors such as ERRα. The differential response of PGC-1α to HT treatment in normoxic and hypoxic conditions led us

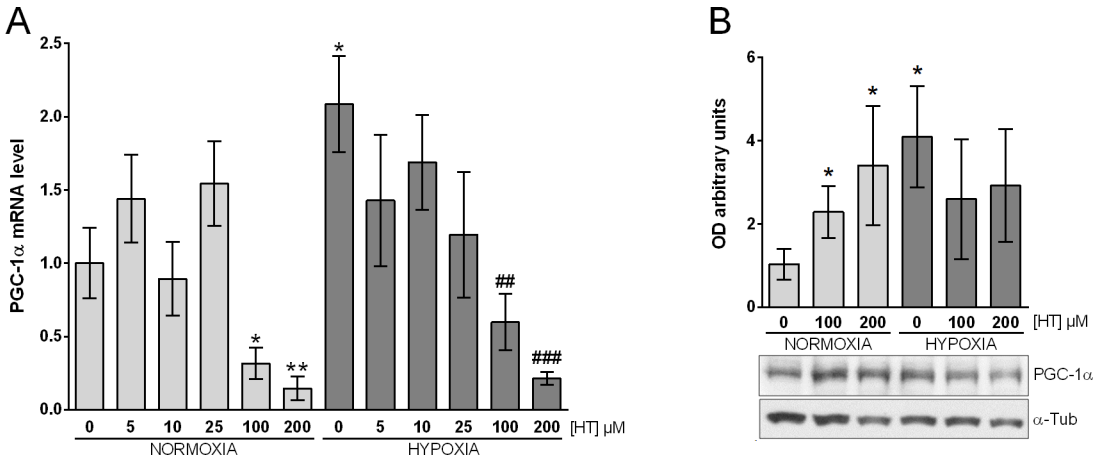

Fig 3. PGC-1α expression is differentially regulated by HT in normoxic and hypoxic conditions. (A) PGC-1α mRNA levels relative to normoxic non HT-treated cells after normalization against PPIA. (B) Densitometric quantifications of PGC-1α protein relative to α-tubulin (α-Tub). A representative immunoblot from a single experiment is shown. Values represent the mean ± SD from three independent experiments. Statistically significant differences with the corresponding non-treated normoxic cells: * $p<0.05$, ** $p<0.01$. Statistically significant differences with the corresponding non-treated hypoxic cells: $^{\#\#}$ $p<0.01$, $^{\#\#\#}$ $p<0.001$.

https://doi.org/10.1371/journal.pone.0203892.g003

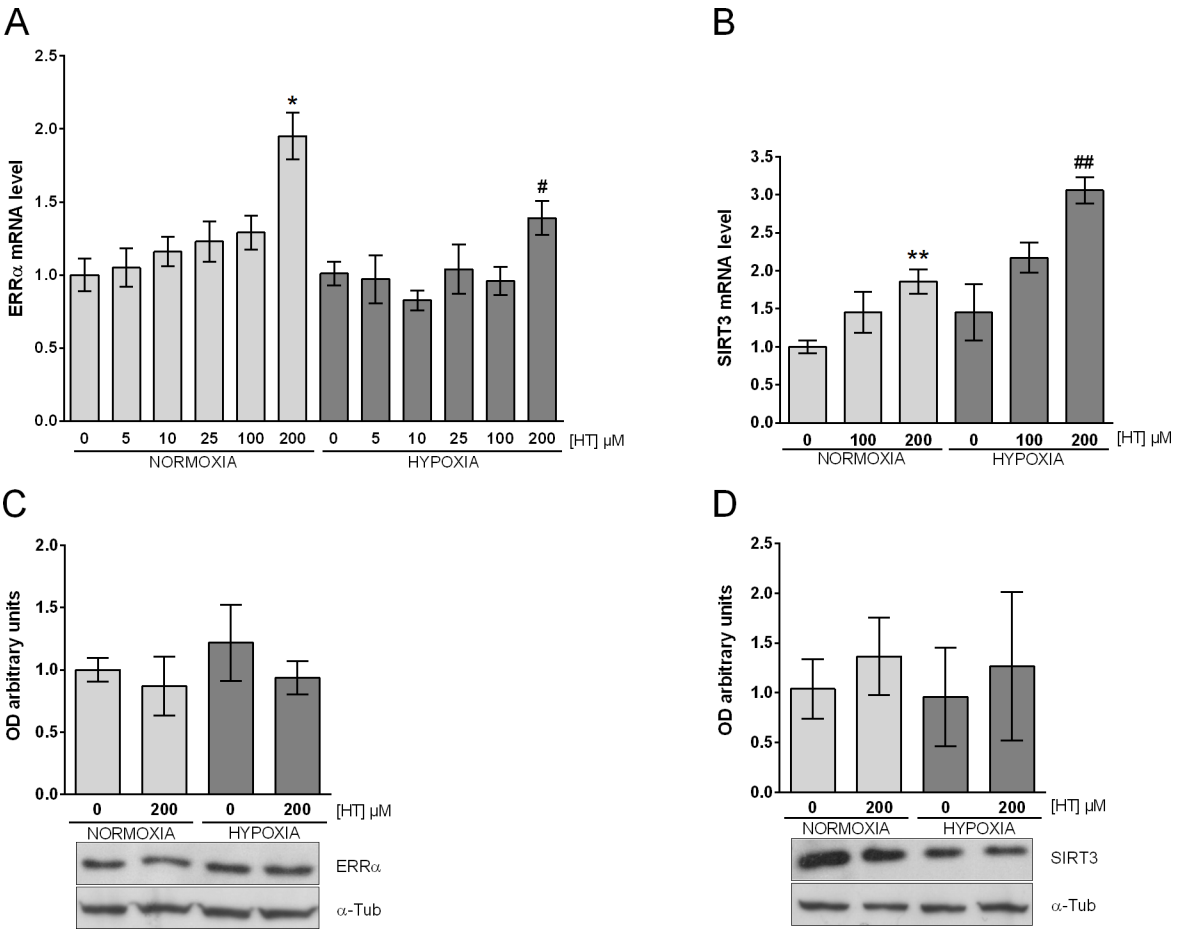

Fig 4. HT exerts a similar effect on the PGC-1α/ERRα pathway in normoxia and hypoxia. (A) ERRα and (B) SIRT3 mRNA levels. The results are expressed as mRNA expression relative to normoxic non HT-treated cells after normalization against PPIA. Densitometric quantifications of (C) ERRα and (D) SIRT3 protein relative to α-tubulin (α-Tub). A representative immunoblot from a single experiment is shown. Values represent the mean ± SD from three independent experiments. Statistically significant differences with the corresponding non-treated normoxic cells: * $p<0.05$, ** $p<0.01$. Statistically significant differences with the corresponding non-treated hypoxic cells: # $p<0.05$, ## $p<0.01$.

https://doi.org/10.1371/journal.pone.0203892.g004

to evaluate the influence of this polyphenol on ERRα levels. Our results (Fig 4A) indicated that, the ERRα mRNA expression was not affected either by hypoxia or by HT-treatment with the exception of the 200 μM HT-dose, which induced ERRα levels independently of the oxygen concentration. However, no changes were observed when we analysed the expression of ERRα at the protein level (Fig 4C). After confirming that HT exerted a different regulation on PGC-1α and ERRα at 100 and 200 μM, we addressed the activity of the PGC-1α/ERRα pathway at both doses by evaluating the expression of one of its target gene, SIRT3. As shown in Fig 4B, SIRT3 mRNA expression was only increased by a 200 μM HT-treatment in normoxia and hypoxia. However, again this increase did not lead to higher protein levels (Fig 4D). Consequently, it may be assumed that although HT transcriptionally regulates the PGC-1α/ERRα pathway, this effect is not finally reflected at the protein level.

HT consistently up-regulates Nrf2 in normoxia and hypoxia

In addition to analysing the expression and activity of the PGC-1α/ERRα pathway, we also evaluated the effect of HT on Nrf2 (Fig 5). As shown in Fig 5A, the transcription of Nrf2

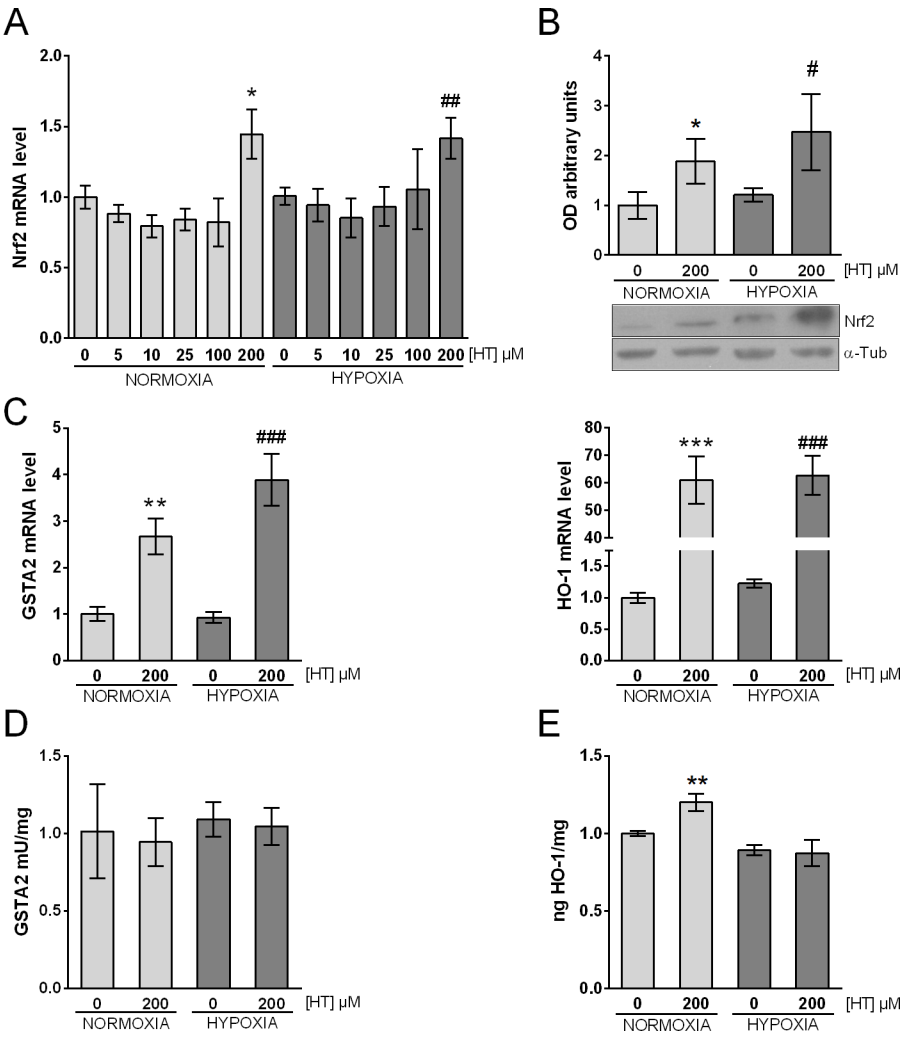

Fig 5. HT up-regulates Nrf2 both in normoxic and hypoxic conditions. (A) Transcriptional levels of Nrf2 in HT-treated (0–200 μM) normoxic and hypoxic cells. Effect of HT 200 μM on: (B) Nrf2 protein expression, (C, D) mRNA levels of the Nrf2 target genes GSTA2 and HO-1, (E) GSTA2 activity, and (F) HO-1 protein level. The mRNA results are expressed as relative to normoxic non HT-treated cells after normalization against PPIA. Densitometric quantification of Nrf2 protein is shown as relative to α-tubulin (α-Tub). A representative immunoblot from a single experiment is shown. Values represent the mean ± SD from three independent experiments. Statistically significant differences with the corresponding non-treated normoxic cells: * $p<0.05$, ** $p<0.01$, *** $p<0.001$. Statistically significant differences with the corresponding non-treated hypoxic cells: $^{\#}$ $p<0.05$, $^{\#\#}$ $p<0.01$, $^{\#\#\#}$ $p<0.001$.

https://doi.org/10.1371/journal.pone.0203892.g005

increased at the highest concentration analysed (200 μM), both in normoxia and hypoxia. In this case, however, the transcriptional upregulation was accompanied by a parallel protein increase (Fig 5B). Having demonstrated the effect of HT 200 μM on Nrf2, we monitored the activity of this transcription factor by quantifying the mRNA expression of GSTA2 and HO-1, two antioxidant proteins induced by Nrf2. As shown in Fig 5C and 5D, GSTA2 and HO-1 mRNA levels were increased at 200 μM, both in normoxia and hypoxia, perfectly paralleling Nrf2 induction. To our knowledge, no GSTA2-antibodies are commercialized. However, GSTA2 exhibits a Se-independent GPX activity that can be evaluated by using cumene hydroperoxide as a substrate [20]. The quantitation of this activity in the different experimental conditions indicated that neither hypoxia nor HT-treatment promoted any change (Fig 5E).

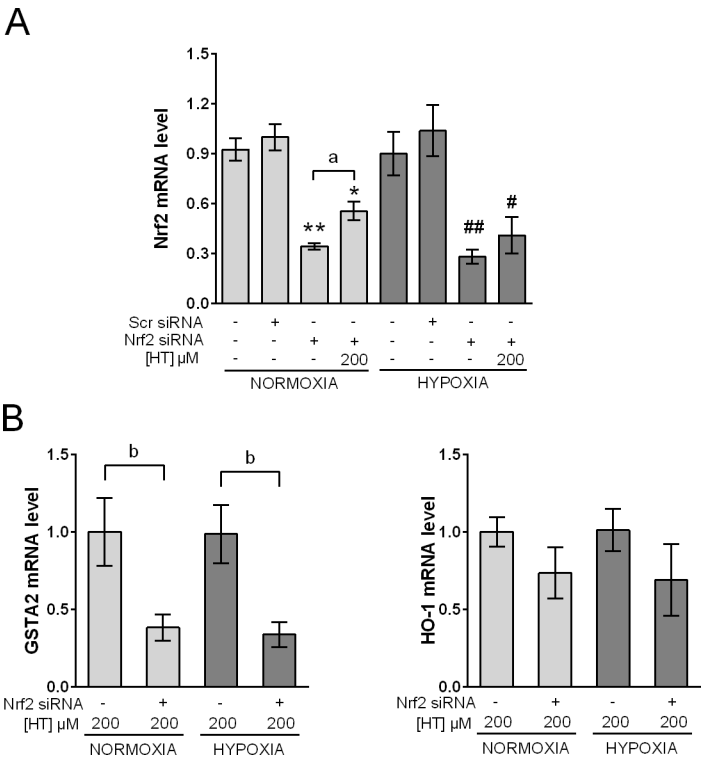

Fig 6. Nrf2 silencing reduces GSTA2 but not HO-1 mRNA levels. (A) Knockdown of Nrf2 with siNrf2 in control and HT-treated (200 μM) normoxic and hypoxic cells. The results are expressed as mRNA level relative to normoxic scr siRNA/non HT-treated cells after normalization against PPIA. (B) Effect of Nrf2-silencing on the transcription level of GSTA2 and HO-1 in normoxic and hypoxic cells after treatment with HT 200 μM. The results are expressed as mRNA levels relative to normoxic HT-treated cells after normalization against PPIA. Values represent the mean ± SD from three independent experiments. Statistically significant differences with the corresponding non-treated normoxic cells: * $p<0.05$, ** $p<0.01$. Statistically significant differences with the corresponding non-treated hypoxic cells: $^{\#}$ $p<0.05$, $^{\#\#}$ $p<0.01$. Statistically significant differences with the corresponding Nrf2-silenced non-HT-treated cells: ^{a} $p<0.05$. Statistically significant differences with the corresponding non-Nrf2-silenced HT-treated cells: ^{b} $p<0.05$.

https://doi.org/10.1371/journal.pone.0203892.g006

However, HT induced the expression of HO-1 (Fig 5F) although this effect was only achieved in normoxic conditions.

HT induces HO-1 independently of Nrf2

To further determine the responsibility of Nrf2 on the increased transcription of GSTA2 and HO-1 in cells treated with 200 μM HT, we determined their mRNA levels after knocking-down Nrf2 by siRNA (Fig 6A). Our results (Fig 6B) indicated that, in these conditions, the expression of GSTA2 was significantly reduced, suggesting that Nrf2 is largely responsible for its transcriptional induction both in normoxia and in hypoxia. Nevertheless, HO-1 mRNA levels were not significantly affected by Nrf2 silencing. Consequently, it may be assumed that the huge response in the transcription of this enzyme to HT is not exclusively linked to Nrf2.

Discussion

The intake of food rich in bioactive components such as polyphenols has been related to a lower incidence of tumors, and particularly to breast cancer [8–10]. In an *in vitro* study with human embryonic kidney renal cells, we previously demonstrated that HT, a phenolic compound considered highly responsible for the beneficial effects of olive oil, modulates the

response to hypoxia [19]. Hypoxia is crucial in tumor microenvironment and in the response to anti-cancer treatments. Although in recent years much effort has been dedicated to understand the molecular mechanisms underlying the effect of HT in cancer cells, and particularly in breast cancer cells, there is a lack of a comprehensive study of the way hypoxia modulates its action. Breast cancer is often modelled using established cell lines. However, breast cancer is a remarkable heterogeneous disease that can be classified into different subtypes with diverse prognosis and response to treatments. MCF-7 cells, one of the most commonly used breast cancer cell line in the world, have been extensively employed to assess the antioxidant effect of HT. Therefore, in the present study we use these cells, representative of luminal A breast cancer, to assess the influence of hypoxia in the antioxidant response to HT.

The effect of HT on the proliferation rate of MCF-7 cells has been previously reported in the literature. Although the data may differ according to the particular experimental conditions, there is strong evidence in support of the concept that high concentrations of HT are necessary to achieve a cytotoxic effect on this cell line. Particularly, Han et al. [21] described that an incubation with 50 μg/ml of HT (~324 μM) induced apoptosis in MCF-7 cells after 12 h of treatment. Warletta et al. [12] was unable to report any effect on the cell proliferation rate when this cell line was treated for 24 h with up to 100 μM of HT. More recently, El-azem et al. [14] described that, when cells were treated for 72 h with HT, 50 μM was the minimum concentration able to achieve a significant but low decrease on cell proliferation. Our results, came to the same conclusion as concentrations as high as 600 μM were necessary to affect cell proliferation when we treated cells with HT for 16 h. However, the main aim of this work is to comparatively analyse the effect of HT in normoxic and hypoxic conditions. Therefore, we evaluated if the cytotoxicity of HT could be influenced by a decrease in the O_2 pressure. In those conditions, a treatment with HT 400 μM results toxic, supporting, for the first time, the proposition that hypoxia increases HT cytotoxicity. Phenolic concentration in extra-virgen olive oil (EVOO) depends on several variables: (i) the olive cultivar and the ripening stage of fruit; (ii) environmental factors; (iii) extraction conditions and systems; and (iv) storage conditions and time [22]. Therefore, the data regarding the particular values of HT in EVOO are very heterogeneous. Some authors point that, at best, the content of HT can reach levels of about 7.5 mg/Kg [23]. However, other studies point to values around 60 mg/Kg [24]. Similar discordances are observed if we focus on the plasma concentration of HT after the ingestion of EVOO. If the degree of absorption proposed by Visioli et al. [25] is considered, up to 49 μM hydroxytyrosol could be found in plasma [26]. Nevertheless, it has been also published [27] that the maximum plasma concentration of free HT after an ingestion of 25 ml of EVOO reaches 4.4 ng/mL (approximately 28 nM). In any case, those concentrations are far from the ones we and others have described as cytotoxic. Hence, although the susceptibility to HT may differ according to the cancer cell line, it seems that the concentration of HT in EVOO is not likely to exert a toxic effect on breast cancer cells either in normoxic or in hypoxic conditions. However, the additive effect of the many other bioactive compounds of olive oil cannot be dismissed.

Cancer cells, due to altered metabolism, inadequate tumor vascular network and macrophage infiltration, are known to have higher level of oxidative stress than non-transformed cells [28, 29]. Moreover, many therapeutic interventions further increase ROS production. Sublethal oxidative stress accelerates tumor progression and raises the risk of metastasis by increasing mutation rate, cell growth and blood supply signalling pathways [30]. The data presented here corroborate the antioxidant activity of HT in hypoxic but not in normoxic conditions. These results resemble the previous findings by Warleta et al. [13], who described that HT did not exert any antioxidant effect in MCF-7 cells cultured in standard conditions, but was antioxidant after inducing a ROS burst with H_2O_2. In tumors we can find two different

types of hypoxia [31]: i) chronic hypoxia, adjacent to necrotic areas, due to a distance between the cells and the vasculature greater than the diffusion distance of oxygen (100–150 μm) [32]; and ii) acute hypoxia, caused by temporary obstruction or variable blood flow in tumor vessels [33]. The latter involves reperfusion periods in which ROS are further increased. Consequently, our results support the notion that in tumors HT may be beneficial to minimize the ROS burst associated to hypoxia. A lower oxidative stress level in breast cancer patients receiving chemotherapy correlates with higher survival rates [34], and it has been recently described that the co-treatment with paclitaxel and HT decreases the oxidative stress without counteracting the effect of chemotherapy [14]. Therefore, the hypoxic environment may have exerted a crucial role in this beneficial effect of HT.

Mitochondria are one of the major sources of ROS production, and clinical studies have reported altered mitochondrial function in human cancers [29]. PGC-1α, a major regulator of mitochondrial function, oxygen consumption and oxidative phosphorylation [35], is known to be induced in hypoxic conditions [36]. The link between HT and PCG-1α expression has been scarcely analysed in the literature and even less in hypoxic conditions. In adipocytes and in excessive exercised-rats, HT supplementation has been reported to increase PGC-1α level and the activity and expression of mitochondrial electron complexes [37, 38]. Similarly, Signorile et al. [39] described that the repression of PCG-1α and mitochondrial oxidative phosphorylation in serum starved fibroblast was reversed by HT-treatment. However, those authors only analysed the effect of HT at the protein level. In the present study we evaluated the transcriptional and translational effects of HT on PGC-1α expression. At the mRNA level, no effect was observed with the lowest concentrations of HT, but strikingly high doses (100 and 200 μM) induced a sharp decrease in PGC-1α transcription in normoxic and hypoxic cells. Therefore, the transcriptional effect of HT PGC-1α does not seem to be modulated by the hypoxic environment. Interestingly, at the protein level results were different. In agreement with previous reports, our data reinforced the positive influence of HT on the expression of the PCG-1α. Nevertheless, this effect was abolished in a hypoxic environment, suggesting that the antioxidant action of HT in this situation should be achieved by other regulatory mechanisms. In this sense, we could hypothesize that an increased activity of the pre-existing PGC-1α protein, rather than an increased expression, may be involved in the antioxidant action of HT under hypoxic conditions.

The effect of PGC-1α is mediated by coactivation of transcription factors such as ERRα. ERRα is an orphan nuclear receptor with a demonstrated role in tumor biology, and particularly in breast cancer. In fact, a relation between elevated ERRα activity and a shorter disease-free survival was described in a genomic analysis of more than 800 breast tumors [5]. It has also been published that the downregulation of ERRα in MCF-7 cells inhibits cell proliferation and decreases the growth of xenografts [5, 40]. Nevertheless, our data indicated that ERRα hardly responds to HT treatment neither in normoxia nor in hypoxia, suggesting that the effects of HT cannot be attributed to changes in the level of this protein. The transcriptional activity of ERRα seems to be independent of ligand binding but is regulated by the expression and activity of its coregulators. SIRT3, a major mitochondrial NAD^+-dependent deacetylase, which has been related to poor prognosis in breast cancer [41], is a target gene of ERRα/PGC-1α. The effect of HT on the expression of SIRT3, at the transcriptional and translational level, perfectly reproduced those of ERRα. Thus, even though this polyphenol does not seem to increase the expression of ERRα protein, the up-regulation of SIRT3 mRNA indicates a higher activity of the PGC-1α/ERRα pathway that again does not involve a change in SIRT3 protein. These inconsistent results may be attributed to the existence of post-transcriptional mechanisms of regulation and have also been reported recently in mice receiving a diet supplemented with HT [42]. In these animals, phosphorylation is one of the biological processes described to

be modulated, and it has been previously published that HT-treatment significantly increases the activity of Akt [43]. Given that the transcriptional activity of ERRα is induced by this kinase [44], it could be speculated that HT may promote the increase in the mRNA of SIRT3 by activating ERRα, rather than by increasing ERRα protein. Non-coding RNAs and RNA-binding proteins are known to exert a crucial role in translation, and the modulatory role of HT on the expression of both of them has already been suggested [42, 45]. Besides, HT also regulates the expression of different translation factors in a cell dependent manner [42]. The effect of HT on all these molecules could hinder the translation of the components of the PGC-1α/ERRα pathway. Further studies evaluating the influence of HT on these regulatory molecules in both normoxic and hypoxic conditions would be necessary in order to unravel the complex transcriptional/translational modulation induced by this polyphenol.

Nrf2, also coactivated by PGC-1α, was initially described as an activator of the cytochrome oxidase subunit IV. However, today it is known to regulate the expression of hundreds of genes with ARE sequences. Although the effect of HT on Nrf2 at the protein level has already been published, the literature regarding a transcriptional regulation of HT on Nrf2 is scarce. Hao et al. [37] analysed the transcription of Nrf2 after 48 h of treatment with HT (0–50 μM) and, strikingly, they observed an enhanced mRNA level only at 1 μM, but the mechanisms involved in this effect remain to be elucidated. The data presented here showed that, in MCF-7 cells, HT induces a transcriptional up-regulation of Nrf2 at 200 μM, which involves a parallel protein increase. Furthermore, in contrast to the results observed in the analysis of PGC-1α, this regulatory role of HT was preserved in hypoxic conditions suggesting that Nrf2 exerts a crucial role in the response to HT. Nrf2 induces the expression of over a hundred protective genes that, among other functions, are involved in ROS scavenging and detoxification of carcinogens. To act as a transcription factor, Nrf2 must translocate to the nucleus where it will bind to the ARE of its target genes, inducing gene transcription. However, under basal conditions, Nrf2 is kept in the cytoplasm and targeted to degradation by its binding to a cysteine residue of the Kelch-like ECH-associated protein 1 (Keap1). In this sense, the induction of Nrf2 by HT has been attributed to: i) the phosphorylation of Nrf2 by kinases such as ERK and Akt [43], and ii) the alkylation of the cysteine residue involved in Nrf2/Keap binding by the ortho-quinone intermediate of HT [46]. These post-translational modifications will allow Keap-1 dissociation from Nrf2, which will then translocate to the nucleus and act as a transcription factor. GSTA2 and HO-1 are some of the antioxidant proteins induced by Nrf2. GSTA2 functions in the detoxification of electrophilic compounds and also exhibits glutathione peroxidase activity. HO-1 is the inducible isoform of HO in mammals, and catalyses the degradation of heme group into carbon monoxide and the antioxidant biliverdin/bilirubin with the parallel release of iron, which will be sequestered by ferritin. In the present study, the increase in Nrf2 protein observed in normoxic and hypoxic cells after treatment with HT 200 μM involved a higher transcription of both target genes, supporting the proposition that HT induces not only the expression, but also the activity of Nrf2. Nevertheless, this increased mRNA levels were not translated in proteins, with the exception of HO-1 whose expression was increased only in normoxia. These findings, together with those of PGC-1α, seem to suggest that the translational effects of HT are at least partially down-regulated in a hypoxic situation, and consequently the antioxidant effect of HT in hypoxic conditions can be hardly attributed to an increased protein expression of antioxidant enzymes.

Most of the studies regarding HT suggest the crucial role of Nrf2 in the effect of this polyphenol and, as shown above, in MCF-7 cells HT promotes the expression of Nrf2 both in normoxia and in hypoxia. However, antioxidant enzymes can also be increased by Nrf2-independent mechanisms. In fact, by silencing Nrf2, we have demonstrated that although GSTA2 is exclusively dependent on Nrf2, other mechanisms seem be involved in the transcription of

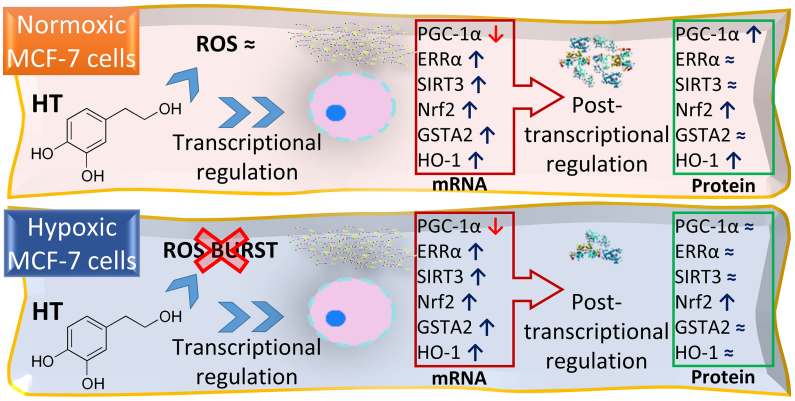

Fig 7. Comparative effect of HT on the oxidative response of MCF-7 cells in normoxic and hypoxic conditions. HT-treatment dampens the hypoxia-associated oxidative stress increase. The transcriptional regulation exerted by this polyphenol on the PGC-1α/ERRα and PGC-1α/Nrf2 pathways is not affected by O_2 tension. However, hypoxia attenuates its translational effect, maybe due to the induction of posttranscriptional mechanisms of regulation by HT.

https://doi.org/10.1371/journal.pone.0203892.g007

HO-1. The Nrf2 independent induction of HO-1 has been previously reported in the literature. In this sense, the natural xanthone gartanin is known to induce HO-1 independently of Nrf2 [47], and nitro-linoleic acid was described to promote HO-1 expression in Nrf2 deficient cells through cAMP, AP-1 and E-box response element interactions [48]. Moreover, in muscle atrophy, HO-1 increase was dependent on forkhead box O1 (FOXO1) but not on Nrf2 [49]. Therefore, our results evidence the existence of Nrf2-independent mechanisms also involved in the effect of HT.

Conclusions

In conclusion, the data presented here and summarized in Fig 7 suggest that the antioxidant action of HT is particularly effective in hypoxic conditions. This polyphenol modulates the transcription and translation of different proteins of the PGC-1α/ERRα and PGC-1α/ Nrf2 pathways, typically involved in the antioxidant response. While the transcriptional effects of HT are similar in normoxic and hypoxic conditions, its translational action is less prominent and partially attenuated in a hypoxic environment. Therefore: i) the direct effect of this polyphenol must be the main responsible for its antioxidant action in hypoxia; ii) the discordance between the mRNA and protein results points to the importance of assessing the regulatory role of HT at both levels to get a complete picture of HT effects, and iii) the hypoxic environment of tumor cells should not be diminished when analyzing the effect of this or other bioactive compounds.

Supporting information

S1 File. Cytotoxic effect of HT in normoxic and hypoxic MCF-7 cells.
(XLSX)

S2 File. Effect of HT on the oxidative stress level in normoxic and hypoxic MCF-7 cells.
(XLSX)

S3 File. Effect of HT treatment on the expression of PGC-1α.
(XLSX)

S4 File. Effect of HT treatment on the expression of ERRα and SIRT3.
(XLSX)

S5 File. Effect of HT treatment on Nrf2 expression and activity.
(XLSX)

S6 File. Effect of Nrf2 silencing on the mRNA levels of GSTA2 and HO-1 in normoxic and hypoxic MCF-7 cells after treatment with HT 200 μM.
(XLSX)

Acknowledgments

Technical and human (Ana Jiménez and Ricardo Oya) support provided by CICT of Universidad de Jaén is gratefully acknowledged.

Author Contributions

Conceptualization: Esther Martínez-Lara, Eva Siles.

Formal analysis: Jesús Calahorra, Eva Siles.

Investigation: Jesús Calahorra, Esther Martínez-Lara, Cristina De Dios, Eva Siles.

Methodology: Jesús Calahorra, Esther Martínez-Lara, Eva Siles.

Supervision: Eva Siles.

Writing – original draft: Eva Siles.

Writing – review & editing: Esther Martínez-Lara, Eva Siles.

References

1. World Cancer Research Fund International: Breast cancer statistics. Available from: (http://www.wcrf.org/int/cancer-facts-figures/data-specific-cancers/breast-cancer-statistics).
2. Panieri E, Santoro MM. ROS homeostasis and metabolism: a dangerous liason in cancer cells. Cell Death Dis. 2016; 7: e2253. https://doi.org/10.1038/cddis.2016.105 PMID: 27277675
3. Ward PS, Thompson CB. Metabolic reprogramming: a cancer hallmark even Warburg did not anticipate. Cancer Cell. 2012; 21: 297–308. https://doi.org/10.1016/j.ccr.2012.02.014 PMID: 22439925
4. Scarpulla RC, Vega RB, Kelly DP. Transcriptional integration of mitochondrial biogenesis. Trends Endocrinol Metab. 2012; 23: 459–466. https://doi.org/10.1016/j.tem.2012.06.006 PMID: 22817841
5. Chang CY, McDonnell DP. Molecular pathways: the metabolic regulator estrogen-related receptor α as a therapeutic target in cancer. Clin Cancer Res. 2012; 18: 6089–6095. https://doi.org/10.1158/1078-0432.CCR-11-3221 PMID: 23019305
6. Lu MC, Ji JA, Jiang ZY, You QD. The Keap1-Nrf2-ARE Pathway As a Potential Preventive and Therapeutic Target: An Update. Med Res Rev. 2016; 36: 924–963. https://doi.org/10.1002/med.21396 PMID: 27192495
7. Vaupel P, Mayer A, Höckel M. Tumor hypoxia and malignant progression. Methods Enzymol. 2004; 381: 335–354. https://doi.org/10.1016/S0076-6879(04)81023-1 PMID: 15063685
8. La Vecchia C, Negri E, Franceschi S, Decarli A, Giacosa A, Lipworth L. Olive oil, other dietary fats, and the risk of breast cancer (Italy). Cancer Causes Control. 1995; 6: 545–550. PMID: 8580304
9. García-Segovia P, Sánchez-Villegas A, Doreste J, Santana F, Serra-Majem L. Olive oil consumption and risk of breast cancer in the Canary Islands: a population-based case-control study. Public Health Nutr. 2006; 9: 163–167. PMID: 16512965
10. Toledo E, Salas-Salvadó J, Donat-Vargas C, Buil-Cosiales P, Estruch R, Ros E, et al. Mediterranean Diet and Invasive Breast Cancer Risk Among Women at High Cardiovascular Risk in the PREDIMED Trial: A Randomized Clinical Trial. JAMA Intern Med. 2015; 175: 1752–1760. https://doi.org/10.1001/jamainternmed.2015.4838 PMID: 26365989
11. Hu T, He XW, Jiang JG, Xu XL. Hydroxytyrosol and its potential therapeutic effects. J Agric Food Chem. 2014; 62: 1449–1455. https://doi.org/10.1021/jf405820v PMID: 24479643

12. Warleta F, Quesada CS, Campos M, Allouche Y, Beltrán G, Gaforio JJ. Hydroxytyrosol protects against oxidative DNA damage in human breast cells. Nutrients. 2011; 3, 839–857. https://doi.org/10.3390/nu3100839 PMID: 22254082

13. Granados-Principal S, El-Azem N, Pamplona R, Ramirez-Tortosa C, Pulido-Moran M, Vera-Ramirez L, et al. Hydroxytyrosol ameliorates oxidative stress and mitochondrial dysfunction in doxorubicin-induced cardiotoxicity in rats with breast cáncer. Biochem Pharmacol. 2014; 90: 25–33. https://doi.org/10.1016/j.bcp.2014.04.001 PMID: 24727461

14. El-Azem N, Pulido-Moran M, Ramirez-Tortosa CL, Quiles JL, Cara FE, Sanchez-Rovira P, et al. Modulation by hydroxytyrosol of oxidative stress and antitumor activities of paclitaxel in breast cancer. Eur J Nutr. 2018 Feb 21. https://doi.org/10.1007/s00394-018-1638-9 PMID: 29468462

15. Valenzuela MT, Núñez MI, Villalobos M, Siles E, Olea N, Pedraza V, et al. Relationship between doxorubicin cell sensitivity, drug-induced DNA double-strand breaks, glutathione content and P-glycoprotein in mammalian tumor cells. Anti-Cancer Drugs. 1995; 6: 749–757. PMID: 8845487

16. Wang H, Joseph JA. Quantifying cellular oxidative stress by dichlorofluorescein assay using microplate reader. Free Radic Biol Med. 1999; 27: 612–616. PMID: 10490282

17. Flohé L, Günzler WA. Assays of glutathione peroxidase. Methods Enzymol. 1984; 105: 114–121. PMID: 6727659

18. Bradford MM. A rapid and sensitive method for the quantification of microgram quantities of protein utilizing the principle of protein-dye binding. Anal Biochem. 1976; 72: 248–254. PMID: 942051

19. Martínez-Lara E, Peña A, Calahorra J, Cañuelo A, Siles E. Hydroxytyrosol decreases the oxidative and nitrosative stress levels and promotes angiogenesis through HIF-1 independent mechanisms in renal hypoxic cells. Food Funct. 2016; 7: 540–548. https://doi.org/10.1039/c5fo00928f PMID: 26608793

20. Ketterer B, Meyer DJ, Clark AG, Soluble glutathione transferase isozymes. In: Sies H., Ketterer B. Eds. Glutathione conjugation: mechanisms and biological significance; London, Academic Press. 1988. pp. 73–135.

21. Han J, Talorete TP, Yamada P, Isoda H. Anti-proliferative and apoptotic effects of oleuropein and hydroxytyrosol on human breast cancer MCF-7 cells. Cytotechnology. 2009; 59: 45–53. https://doi.org/10.1007/s10616-009-9191-2 PMID: 19353300

22. Rigacci S, Stefani M. Nutraceutical Properties of Olive Oil Polyphenols. An Itinerary from Cultured Cells through Animal Models to Humans. Int J Mol Sci. 2016 May 31. 17(6). pii: E843. https://doi.org/10.3390/ijms17060843 PMID: 27258251

23. García-Martínez O, De Luna-Bertos E, Ramos-Torrecillas J, Ruiz C, Milia E, Lorenzo ML., et al. Phenolic Compounds in Extra Virgin Olive Oil Stimulate Human Osteoblastic Cell Proliferation. PLoS One. 2016 Mar 1. 11(3):e0150045. https://doi.org/10.1371/journal.pone.0150045 PMID: 26930190

24. Alarcón Flores MI, Romero-González R, Garrido Frenich A, Martínez Vidal JL. Analysis of phenolic compounds in olive oil by solid-phase extraction and ultra high performance liquid chromatography-tandem mass spectrometry. Food Chem. 2012; 134: 2465–2472. https://doi.org/10.1016/j.foodchem.2012.04.058 PMID: 23442712

25. Visioli F, Galli C, Bornet M, Mattei A, Patelli R, Galli G, et al. Olive oil phenolics are dose-dependently absorbed in humans. FEBS Lett. 2000; 468: 159–160. PMID: 10692578

26. Quiles JL, Farquharson AJ, Simpson DK, Grant I, Wahle KWJ. Olive oil phenolics: effects on DNA oxidation and redox enzyme mRNA in prostate cells. Br J Nutr. 2002; 88: 225–234. https://doi.org/10.1079/BJN2002620 PMID: 12207832

27. Pastor A, Rodríguez-Morató J, Olesti E, Pujadas M, Pérez-Mañá C, Khymenets O, et al. Analysis of free hydroxytyrosol in human plasma following the administration of olive oil. J Chromatogr A. 2016; 1437: 183–190. https://doi.org/10.1016/j.chroma.2016.02.016 PMID: 26877176

28. Szatrowski TP, Nathan CF. Production of large amounts of hydrogen peroxide by human tumor cells. Cancer Res. 1991; 51: 794–798. PMID: 1846317

29. Carew JS, Huang P. Mitochondrial defects in cancer. Mol Cancer. 2002; 1: 9. Available from: http://www.molecular-cancer.com/content/1/1/9 https://doi.org/10.1186/1476-4598-1-9 PMID: 12513701

30. Brown NS, Bicknell R. Hypoxia and oxidative stress in breast cancer. Oxidative stress: its effects on the growth, metastatic potential and response to therapy of breast cancer. Breast Cancer Res. 2001; 3: 323–327. https://doi.org/10.1186/bcr315 PMID: 11597322

31. Brown JM. Tumor hypoxia in cancer therapy. Methods Enzymol. 2007; 435: 297–321. https://doi.org/10.1016/S0076-6879(07)35015-5 PMID: 17998060

32. Thomlinson RH, Gray LH. The histological structure of some human lung cancers and the possible implications for radiotherapy. Brit J Cancer. 1995; 9: 539–549.

33. Brown JM. Evidence for acutely hypoxic cells in mouse tumours, and a possible mechanism of reoxygenation. Br J Radiol. 1979; 52: 650–656. https://doi.org/10.1259/0007-1285-52-620-650 PMID: 486895

34. Vera-Ramirez L, Sanchez-Rovira P, Ramirez-Tortosa MC, Ramirez-Tortosa CL, Granados-Principal S, Lorente JA, et al. Oxidative stress status in metastatic breast cancer patients receiving palliative chemotherapy and its impact on survival rates. Free Radic Res. 2012; 46: 2–10. https://doi.org/10.3109/10715762.2011.635658 PMID: 22035543

35. Fernandez-Marcos PJ. Auwerx J. Regulation of PGC-1alpha, a nodal regulator of mitochondrial biogenesis. Am J Clin Nutr. 2011; 93: 884S–890S. https://doi.org/10.3945/ajcn.110.001917 PMID: 21289221

36. Shoag J, Arany Z. Regulation of hypoxia-inducible genes by PGC-1 alpha. Arterioscler Thromb Vasc Biol. 2010; 30: 662–666. https://doi.org/10.1161/ATVBAHA.108.181636 PMID: 19948845

37. Hao J, Shen W, Yu G, Jia H, Li X, Feng Z, et al. Hydroxytyrosol promotes mitochondrial biogenesis and mitochondrial function in 3T3-L1 adipocytes. J Nutr Biochem. 2010; 21: 634–644. https://doi.org/10.1016/j.jnutbio.2009.03.012 PMID: 19576748

38. Feng Z, Bai L, Yan J, Li Y, Shen W, Wang Y., et al. Mitochondrial dynamic remodeling in strenuous exercise-induced muscle and mitochondrial dysfunction: regulatory effects of hydroxytyrosol. Free Radic Biol Med. 2011; 50: 1437–1446. https://doi.org/10.1016/j.freeradbiomed.2011.03.001 PMID: 21421045

39. Signorile A, Micelli L, De Rasmo D, Santeramo A, Papa F, Ficarella R, et al. Regulation of the biogenesis of OXPHOS complexes in cell transition from replicating to quiescent state: involvement of PKA and effect of hydroxytyrosol. Biochim Biophys Acta. 2014; 1843: 675–684. https://doi.org/10.1016/j.bbamcr.2013.12.017 PMID: 24389246

40. Chisamore MJ, Cunningham ME, Flores O, Wilkinson HA, Chen JD. Characterization of a novel small molecule subtype specific estrogen-related receptor alpha antagonist in MCF-7 breast cancer cells. PLoS One. 2009; 4(5): e5624. https://doi.org/10.1371/journal.pone.0005624 PMID: 19462000

41. Yu FY, Xu Q, Wu DD, Lau AT, Xu YM. The Prognostic and Clinicopathological Roles of Sirtuin-3 in Various Cancers. PLoS One. 2016; 11(8):e0159801. https://doi.org/10.1371/journal.pone.0159801 PMID: 27483432

42. Tomé-Carneiro J, Crespo MC, García-Calvo E, Luque-García JL, Dávalos A, Visioli F. Proteomic evaluation of mouse adipose tissue and liver following hydroxytyrosol supplementation. Food Chem Toxicol. 2017; 107: 329–338. https://doi.org/10.1016/j.fct.2017.07.009 PMID: 28689060

43. Martín MA, Ramos S, Granado-Serrano AB, Rodríguez-Ramiro I, Trujillo M, Bravo L. et al. Hydroxytyrosol induces antioxidant/detoxificant enzymes and Nrf2 translocation via extracellular regulated kinases and phosphatidylinositol-3-kinase/protein kinase B pathways in HepG2 cells. Mol Nutr Food Res. 2010; 54: 956–966. https://doi.org/10.1002/mnfr.200900159 PMID: 20166143

44. Ariazi EA, Kraus RJ, Farrell ML, Jordan VC, Mertz JE. Estrogen-related receptor alpha1 transcriptional activities are regulated in part via the ErbB2/HER2 signaling pathway. Mol Cancer Res. 2007; 5: 71–85. https://doi.org/10.1158/1541-7786.MCR-06-0227 PMID: 17259347

45. Tomé-Carneiro J, Crespo MC, Iglesias-Gutierrez E, Martín R, Gil-Zamorano J, Tomas-Zapico C, et al. Hydroxytyrosol supplementation modulates the expression of miRNAs in rodents and in humans. Nutr Biochem. 2016; 34: 146–155.

46. Peng S, Zhang B, Yao J, Duan D. Dual protection of hydroxytyrosol, an olive oil polyphenol, against oxidative damage in PC12 cells. Food Funct. 2015; 6: 2091–2100. https://doi.org/10.1039/c5fo00097a PMID: 26037629

47. Gao XY, Wang SN, Yang XH, Lan WJ, Chen ZW, Chen JK, et al. Gartanin Protects Neurons against Glutamate-Induced Cell Death in HT22 Cells: Independence of Nrf-2 but Involvement of HO-1 and AMPK. Neurochem Res. 2016; 41: 2267–2277. https://doi.org/10.1007/s11064-016-1941-x PMID: 27161377

48. Wright MM, Kim J, Hock TD, Leitinger N, Freeman BA, Agarwal A. Human haem oxygenase-1 induction by nitro-linoleic acid is mediated by cAMP, AP-1 and E-box response element interactions. Biochem. J. 2009; 422: 353–361. https://doi.org/10.1042/BJ20090339 PMID: 19534727

49. Kang J, Jeong MG, Oh S, Jang EJ, Kim HK, Hwang ES. A FoxO1-dependent, but NRF2-independent induction of heme oxygenase-1 during muscle atrophy. FEBS Letters. 2014; 588: 79–85. https://doi.org/10.1016/j.febslet.2013.11.009 PMID: 24269680

Artículo 2

Efecto del hidroxitirosol, uno de los principales fenoles del aceite de oliva, sobre la respuesta a la hipoxia de HIF-1 en células de cáncer de mama

Jesús Calahorra, Esther Martínez-Lara, José M. Granadino-Roldán, Juan M. Martí, Ana Cañuelo, Santos Blanco, F. Javier Oliver, Eva Siles

Enviado a *Scientifics Reports*

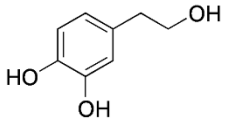

Crosstalk between hydroxytyrosol, a major olive oil phenol, and HIF-1 in breast cancer cells

Jesús Calahorra[1], Esther Martínez-Lara[1], José M. Granadino-Roldán[2], Juan M. Martí[3], Ana Cañuelo[1], Santos Blanco[1], F. Javier Oliver[3], and Eva Siles[*1]

[1] Departamento de Biología Experimental Universidad de Jaén, Campus Las Lagunillas s/n, Jaén, 23071, Spain
[2] Departamento de Química Física y Analítica, Universidad de Jaén, Campus Las Lagunillas s/n, Jaén, 23071, Spain.
[3] Instituto López Neyra de Parasitología y Biomedicina, IPBLN, CSIC PTS-Granada, Armilla, 18016, Spain.
[*]esiles@ujaen.es

Abstract

Olive oil intake has been linked with a lower incidence of breast cancer. Hypoxic microenvironment in solid tumors, such as breast cancer, is known to play a crucial role in cancer progression and in the failure of anticancer treatments. HIF-1 is the main effector in hypoxic response, and given that hydroxytyrosol (HT) is one of the main bioactive compounds in olive oil, in this study we deepen into its modulatory role on HIF-1. Our results demonstrate that HT decreases HIF-1α protein, probably by downregulating oxidative stress and by inhibiting the PI3K/Akt/mTOR pathway. Strikingly, the expression of HIF-1 target genes (lactate deshydrogenasa A, glucose transporter-1, adrenomedullin and vascular endothelial growth factor) do not show a parallel decrease. Particularly, AM and VEGF are up-regulated by high concentrations of HT even in HIF-1α silenced cells, pointing to HIF-1 independent mechanism of regulation. In fact, we show, by in silico modelling and transcriptional analysis, that high doses of HT may act as an agonist of the aryl hydrocarbon receptor favoring the induction of these angiogenic genes. In conclusion, we suggest that the effect of HT in a hypoxic environment is largely affected by its concentration and involves both HIF-1 dependent and independent mechanisms.

Introduction

Breast cancer is the most common cancer diagnosed in women and the second leading cause of death from cancer among them[1]. Approximately 25%–40% of invasive breast cancers exhibit hypoxic regions in which oxygen pressure is diminished[2]. This hypoxic microenvironment favors cancer progression and metastasis and should be taken into account in cancer research.

Hypoxia inducible factor-1 (HIF-1) is the key factor in the adaptive response to hypoxia. The binding of HIF-1 to hypoxic response elements (HREs) regulates the transcription of a plethora of genes involved, among others, in glucose metabolism, cell proliferation, cell survival and angiogenesis[3]. Therefore, HIF-1 overexpression is strongly related with poor prognosis and resistance to chemotherapy and radiotherapy[4,5]. HIF-1 is a heterodimeric transcription factor composed by the oxygen-sensitive α subunit HIF-1α and the constitutive subunit ARNT. HIF-1α transcription, translation and stability are highly regulated in an oxygen-dependent and oxygen-independent manner. At the transcriptional level, HIF-1α expression is regulated by different transcription factors such as Sp1, NF-κB, Erg1 and by HIF-1 itself [6-8]. The translation of HIF-1α mRNA can be upregulated through the PI3K/Akt/mTOR pathway. Particularly, mTOR when activated by Akt, mediates the phosphorylation of p70 S6 kinase (S6K) that induces HIF-1α translation through the ribosomal protein S6[9]. Once translated, and under normoxic conditions, HIF-1α subunit is quickly degraded due to the activity of the prolyl-4-hydroxylases (PHDs) that label HIF-1α enabling its ubiquitination by the pVHL and its degradation in the proteasome. Conversely, the hypoxic conditions inhibit PHDs activity and promote HIF-1α stabilization. Besides this oxygen-dependent regulation of HIF-1α, reactive oxygen species (ROS) and nitric oxide (NO), crucial in tumorigenesis and particularly high in cancer cells[10,11], also contribute to the stabilization of HIF-1α by inhibiting PHDs activity under both hypoxic and normoxic conditions[12-14]. Finally, the transcriptional activity of HIF-1 can be modulated by the factor inhibiting HIF-1 (FIH) which hydroxylates a critical asparagine residue (Asn-803), in an oxygen-dependent manner, blocking coactivator recruitment[15]. HIF-1α is also dependent on the

expression and activity of Poly(ADP-ribose) polymerase-1 (PARP-1)[16,17], a nuclear, zinc-finger, DNA-binding protein activated in response to oxidative and nitrosative stress. This enzyme plays an important role in a number of processes such as DNA repair, chromatin remodeling, transcription, or regulation of the cell cycle, among others[18]. PARP inhibition has been demonstrated to exert beneficial effects hindering prometastasic activities and adaptation of tumor to different microenvironments such as hypoxia environment [19].

Lifestyles factors play a significant role in the risk of suffering breast cancer[20]. The PREDIMED study, a large dietary intervention trial, showed the beneficial effect of a Mediterranean diet supplemented with extra-virgin olive oil (EVOO) in the primary prevention of breast cancer[21]. Olive oil is mainly composed of fatty acids, particularly oleic acid, but its mechanical extraction at temperatures lower than 30ºC also afford a high concentration of different minor components, such as polyphenols. The foremost phenolic alcohol is hydroxytyrosol (HT). Several studies have demonstrated the beneficial properties of this simple compound in a number of models and cancer linked events[22,23], and particularly in breast cancer[24-27]. In fact, we have recently described that hypoxia modulates the antioxidant effect of HT in MCF-7 breast cancer cells[28]. With this background, and considering the importance of hypoxia and HIF-1 in breast cancer progression and response to anticancer treatments, the aim of the present study is to investigate the effect of HT in the expression and transcriptional activity of this protein. Our results indicate that in hypoxic MCF-7 breast cancer cells, HT decreases the expression of HIF-1α, an effect probably linked to its antioxidant action and to the down-regulation of the PI3K/Akt/mTOR pathway. Although very positive to counteract cancer malignancy, these effects are achieved at relatively high concentrations. Moreover, we demonstrate that HT can even act as an AHR agonist.

Results

Nitric oxide levels are not affected by HT during hypoxia.

In a previous study[19], we reported that a sub-cytotoxic treatment of hypoxic MCF-7 cells with HT (5-200 μM, 16h) decreased the oxidative stress level. NO is also crucial in the response to hypoxia. Therefore, we have evaluated the effect of those same concentrations of HT in NO production. Conversely to what previously described for ROS, HT exerted no significant effect on the production of NO (Fig. 1).

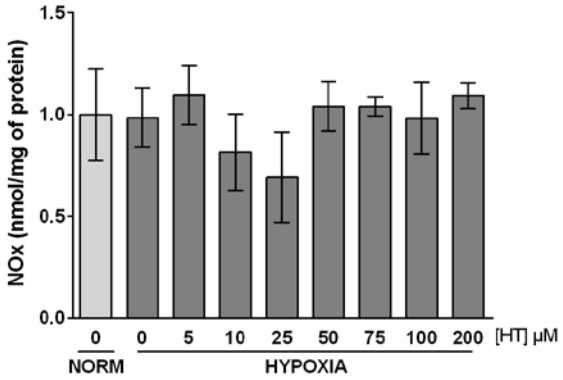

Figure 1. HT exerts no effect on NO levels in hypoxic MCF-7 cells. Values represent the mean ± SD from three independent experiments.

PARP-1 activity is decreased by high doses of HT.

ROS and NO damage DNA and modulate the activity of PARP-1, a protein largely involved in cancer progression that also modulates HIF-1α response. To assess whether the antioxidant effect of HT treatment decreased the expression and activity of this enzyme, we evaluated PARP-1 levels and PARylated proteins by using specific antibodies. As shown in Fig. 2, the expression of PARP-1 was increased in hypoxic conditions but returned to basal levels when cells were treated with concentrations of HT equal to or greater than 75 μM. Similarly, PARylated proteins in hypoxic cells were also decreased by HT but only at 200 μM.

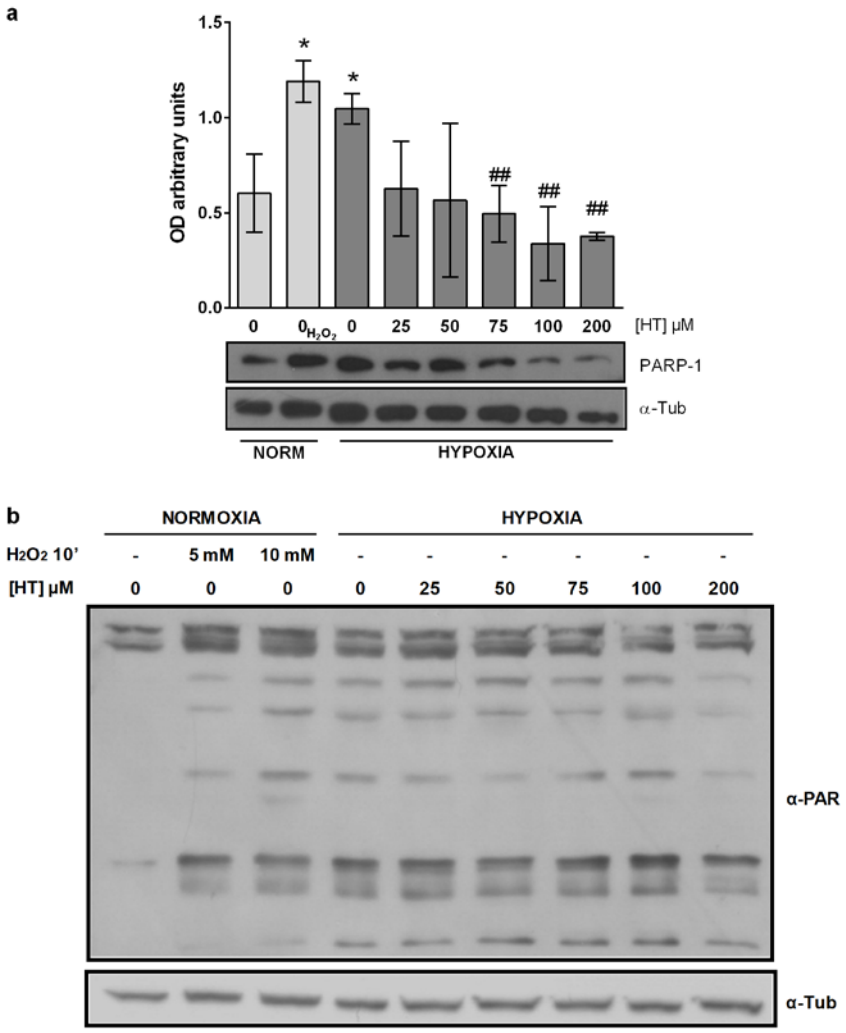

Figure 2. PARP-1 protein level and activity are decreased by HT. (a) Densitometric quantifications of PARP-1, protein level relative to α-tubulin (α-Tub). A representative immunoblot is shown. Values represent the mean ± SD from three independent experiments. Statistically significant differences with the corresponding non-treated normoxic cells: * $p<0.05$. Statistically significant differences with the corresponding non-treated hypoxic cells: $^{##}$ $p<0.01$, $^{###}$ $p<0.001$. (b) α-PAR representative immunoblot.

HT reduces HIF-1α stability in a dose dependent manner, in part, through the mTOR pathway.
Although no changes were detected in NO levels (Fig. 1), the impact of HT treatment on the oxidative stress and the link between ROS and HIF-1α stability, lead us to evaluate the effect of HT in the mRNA and protein level of HIF-1α. No effects were detected on the expression of HIF-1α mRNA, suggesting that HT does not modulate the transcription of this gene (Fig. 3A). However, the western-blot analysis revealed that HT was able to reduce HIF-1α protein levels in a dose dependent manner from 50 µM until 200 µM (Fig. 3B). With the aim of getting mechanistic information underlying this effect, we determined the impact of HT on the protein level of p-mTOR, p-P70 S6 Kinase and p-S6. p-mTOR (Fig. 3C) was decreased by treatment with HT 200 µM and their downstream activated targets, p-P70 and p-S6 (Fig. 3D and 3E), were reduced by HT 100 and 200 µM.

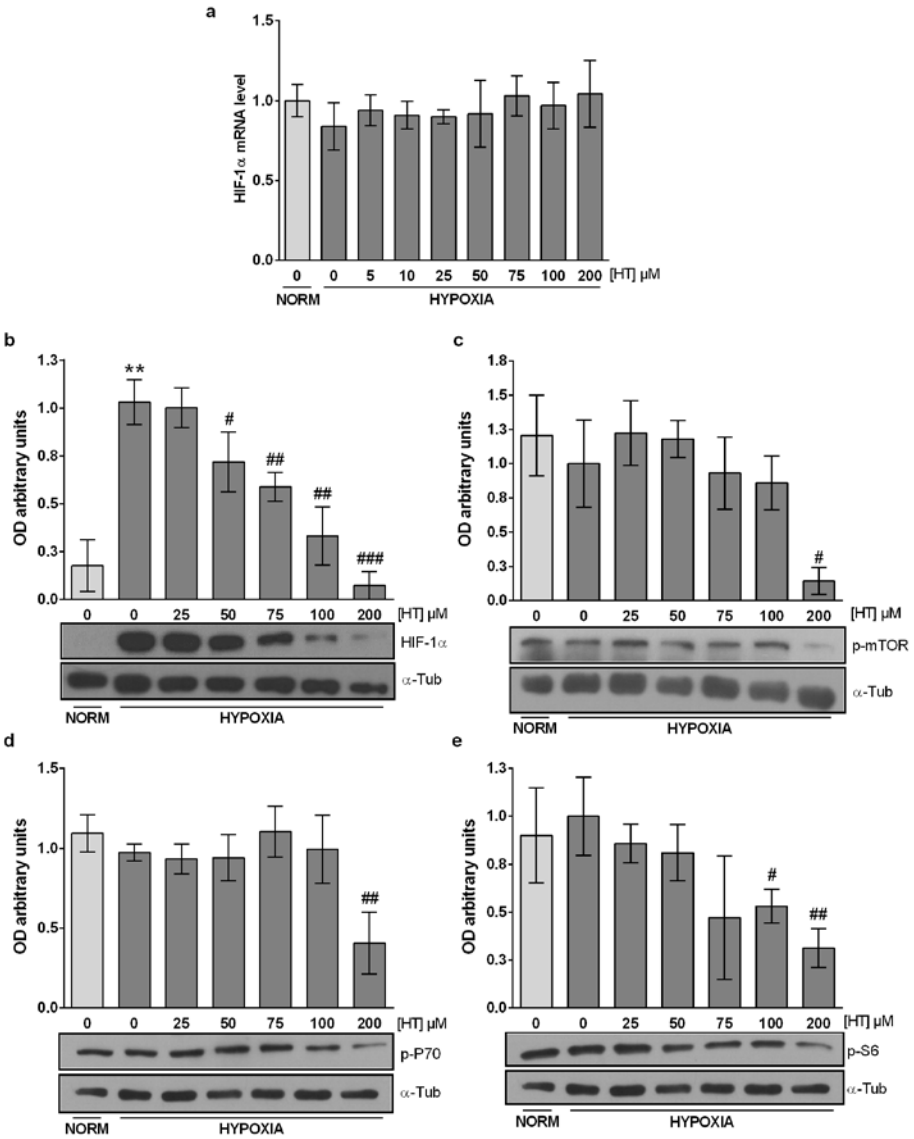

Figure 3. HT down-regulates HIF-1α in a dose dependent manner: m-TOR pathway involvement (a) Effect of HT on HIF-1α mRNA levels relative to hypoxic non HT-treated cells after normalization against PPIA. Densitometric quantifications of HIF-1α (b), p-mTOR (c), p-P70 (d), p-S6 (e) protein level relative to α-tubulin (α-Tub). A representative immunoblot is shown. Values represent the mean ± SD from three independent experiments. Statistically significant differences with the corresponding non-treated normoxic cells: *** $p<0.001$. Statistically significant differences with the corresponding non-treated hypoxic cells: $^{\#}$ $p<0.05$, $^{\#\#}$ $p<0.01$, $^{\#\#\#}$ $p<0.001$.

High concentrations of HT up-regulates HIF-1α targets.

We next evaluated the effect of HT on the transcriptional activity of HIF-1. For that purpose, we analyzed the mRNA levels of the angiogenic targets adrenomedullin (AM) and vascular endothelial growth factor (VEGF), and of the metabolic targets glucose transporter-1 (GLUT-1) and lactate dehydrogenase A (LDHA). As expected, the expression of all these genes was up-regulated under hypoxia (Fig. 4). Surprisingly, and despite HIF-1α protein was down-regulated by HT treatment, the two highest concentration of this polyphenol (100 and 200 μM) promoted the up-regulation of AM, VEGF and GLUT-1. Hence, the transcriptional activity of HIF-1 and the protein levels of HIF-1α do not follow a similar pattern of response when MCF-7 cells are treated with high concentrations of HT.

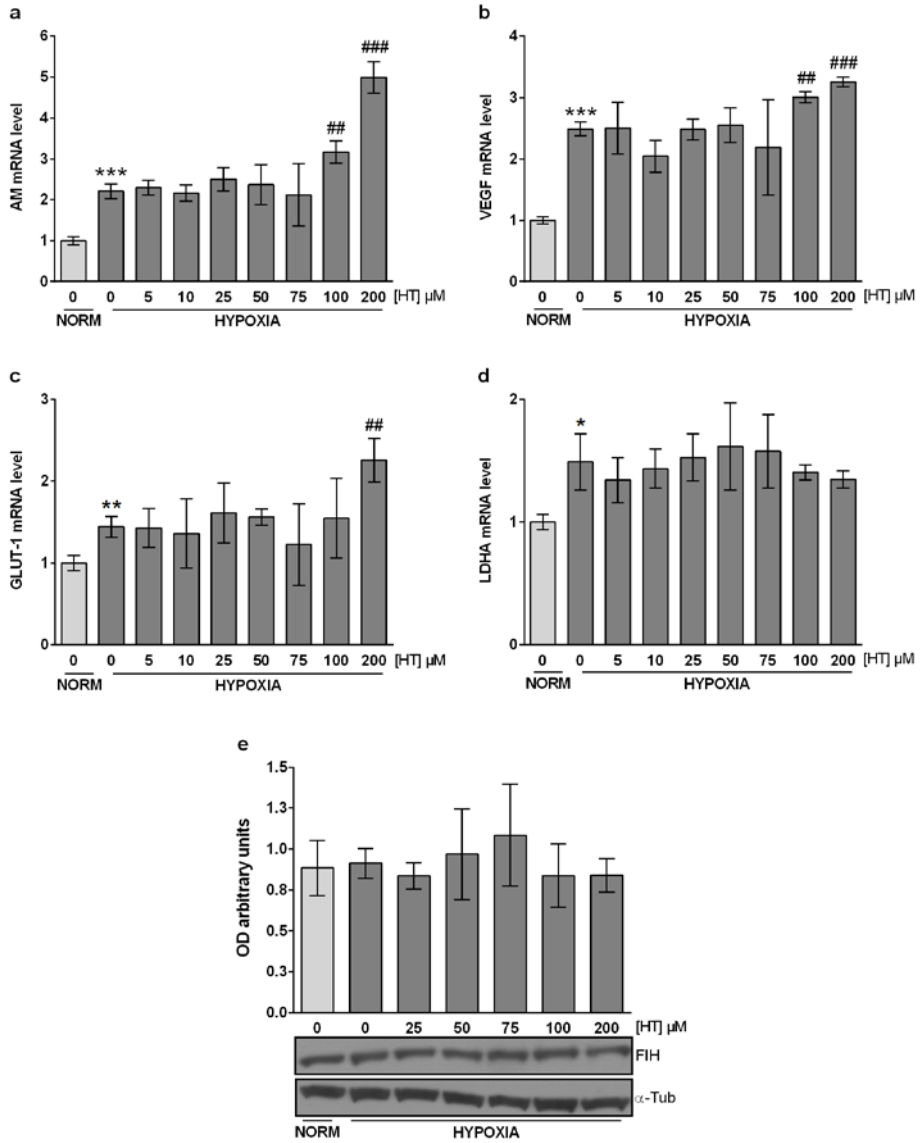

Figure 4. The effect of HT on HIF-1 targets does not parallel HIF-1α expression. AM (a), VEGF (b), GLUT-1 (c) and (d) LDHA mRNA levels. Results are expressed as mRNA expression relative to normoxic non HT-treated cells after normalization against PPIA. (e) The up-regulation of HIF-1α targets by HT is not due to FIH inhibition. Densitometric quantifications of FIH protein level relative to α-tubulin (α-Tub). A representative immunoblot is shown. Values represent the mean ± SD from three independent experiments. Statistically significant differences with the corresponding non-treated normoxic cells: * $p<0.05$, ** $p<0.01$, *** $p<0.001$. Statistically significant differences with the corresponding non-treated hypoxic cells: $^{\#\#}$ $p<0.01$, $^{\#\#\#}$ $p<0.001$.

The up-regulation of HIF-1α targets by HT is not due to FIH inhibition.

The transcriptional activity of HIF-1 is modulated by FIH. The opposite effect of HT in the expression and transcriptional activity of HIF-1 led us to evaluate the influence of this polyphenol on FIH (Fig. 4E). No changes in the expression of this protein were observed.

GLUT-1 but not AM and VEGF overexpression by HT, is HIF-1α dependent.

AM, VEGF and GLUT-1 have been consistently described as HIF-1 target genes. However, the HIF-1 pathway did not seem to explain their overexpression after treatment with HT 100 and 200µM. In order to determine the implication of HIF-1 in such overexpression we analyzed whether the up-regulation of AM, VEGF and GLUT-1 persisted after knocking down HIF-1α (Fig. 5A). As shown in Fig. 5B, the silencing of HIF-1α abrogated the HT-induced overexpression of GLUT-1. However, AM and VEGF genes remained overexpressed in HT-treated cells after silencing HIF-1α (Fig. 5C, D). These results indicate that HT exerts its transcriptional regulation of AM, VEGF through HIF-1-dependent and independent mechanisms.

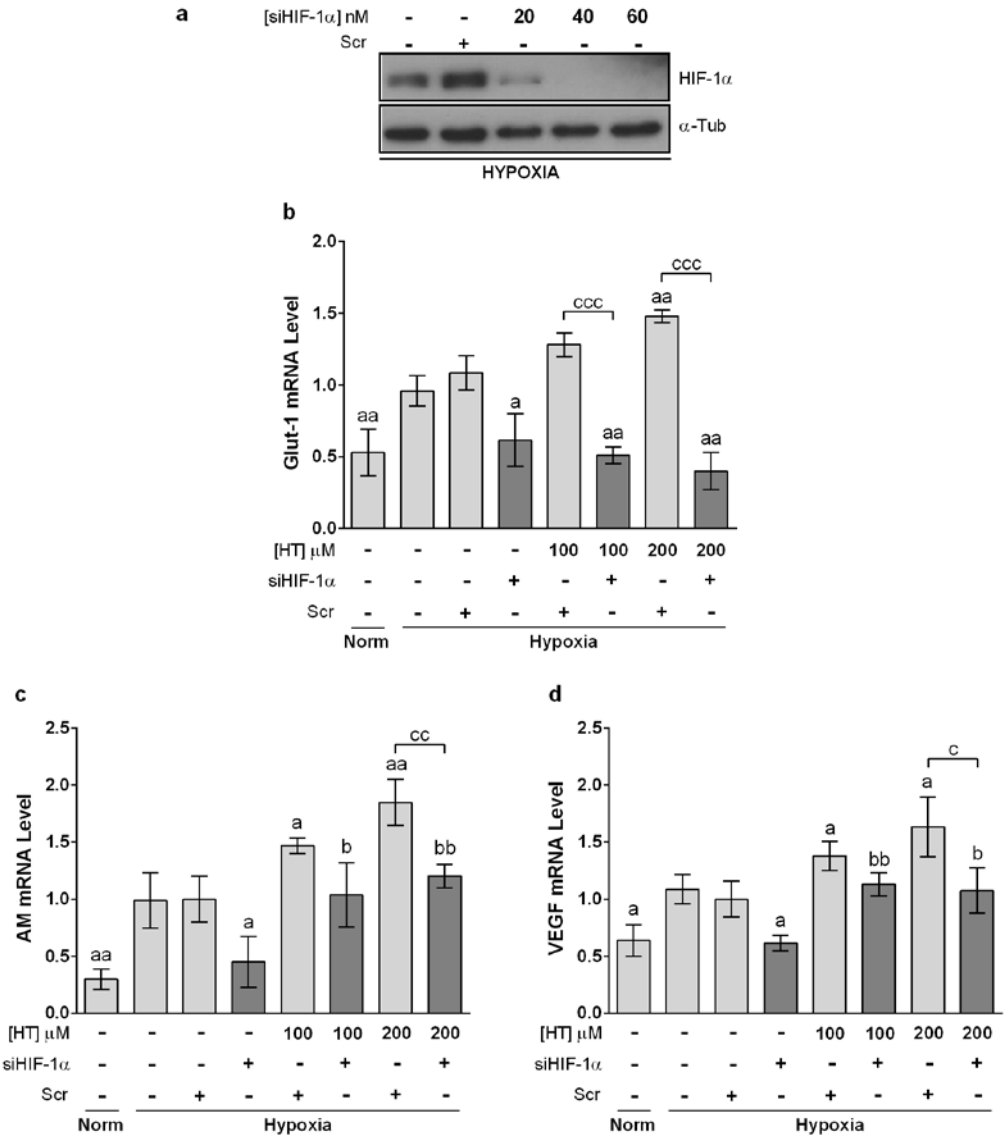

Figure 5. HIF-1α silencing abolishes HT-dependent GLUT-1 upregulation but not AM and VEGF. (a) Representative immunoblot of HIF-1α knockdown with different concentrations of siHIF-1α. Effect of HIF-1α –silencing (siHIF-1α 40nM) on the transcription level of (b) GLUT-1, (c) AM and (d) VEGF in hypoxic cells after treatment with HT 100 and 200 μM. Results are expressed as mRNA levels relative to Scr hypoxic cells after normalization against PPIA. Values represent the mean ± SD from three independent experiments. Statistically significant differences with the corresponding Scr-siRNA transfected hypoxic cells: ^{a} $p<0.05$, ^{aa} $p<0.01$. Statistically significant differences with the corresponding HIF-1α-silenced cells: ^{b} $p<0.05$, ^{bb} $p<0.01$. Statistically significant differences with the corresponding HT treated-non silenced cells: ^{c} $p<0.05$, ^{cc} $p<0.01$, ^{ccc} $p<0.001$.

The effect of HT on the hypoxic response is also mediated by HIF-1-independent pathways.

Apart from HIF-1, HIF-2 is also involved in the up-regulation of certain genes in response to a hypoxic stimulus. Thus, we next addressed the possible involvement of HIF-2 in the transcriptional response to HT. For that purpose, we quantified the expression of the specific HIF-2 target Oct-4 in hypoxic HT-treated cells. As shown in Fig. 6A, HT produced no effect on the mRNA level of this gene, suggesting that HIF-2α is not involved in the up-regulation of AM and VEGF. It has been previously reported that AM and VEGF genes contain xenobiotic response elements (XRE)[29,30] and therefore can be regulated by the aryl hydrocarbon receptor (AHR). CYP1A1 is a sensitive measure of AHR activation and we found that it was intensely overexpressed at high HT doses (Fig. 6B). The AHR repressor (AHRR) is also known to be induced in response to AHR activation[31] and, in agreement with the previous result, its expression was also induced at high HT concentrations (Fig. 6C). These results strongly suggest that at high concentrations, HT acts as an AHR ligand

and may induce AM and VEGF expression through this pathway. AHR and HIF-1 must heterodimerize with ARNT to carry out its transcriptional activity. Therefore, by silencing ARNT the effect of both HIF-1 and AHR would be concomitantly abolished. As shown in Fig. 7B, the effect of HT on CYP1A1 was almost completely abolished in ARNT-silenced hypoxic cells, further corroborating that at high concentrations HT binds and activates the AHR pathway. However, the effect of HT on AM or VEGF although significantly decreased was not completely abrogated (Fig. 7C and 7D), suggesting the involvement of additional mechanisms of regulation, not linked with ARNT.

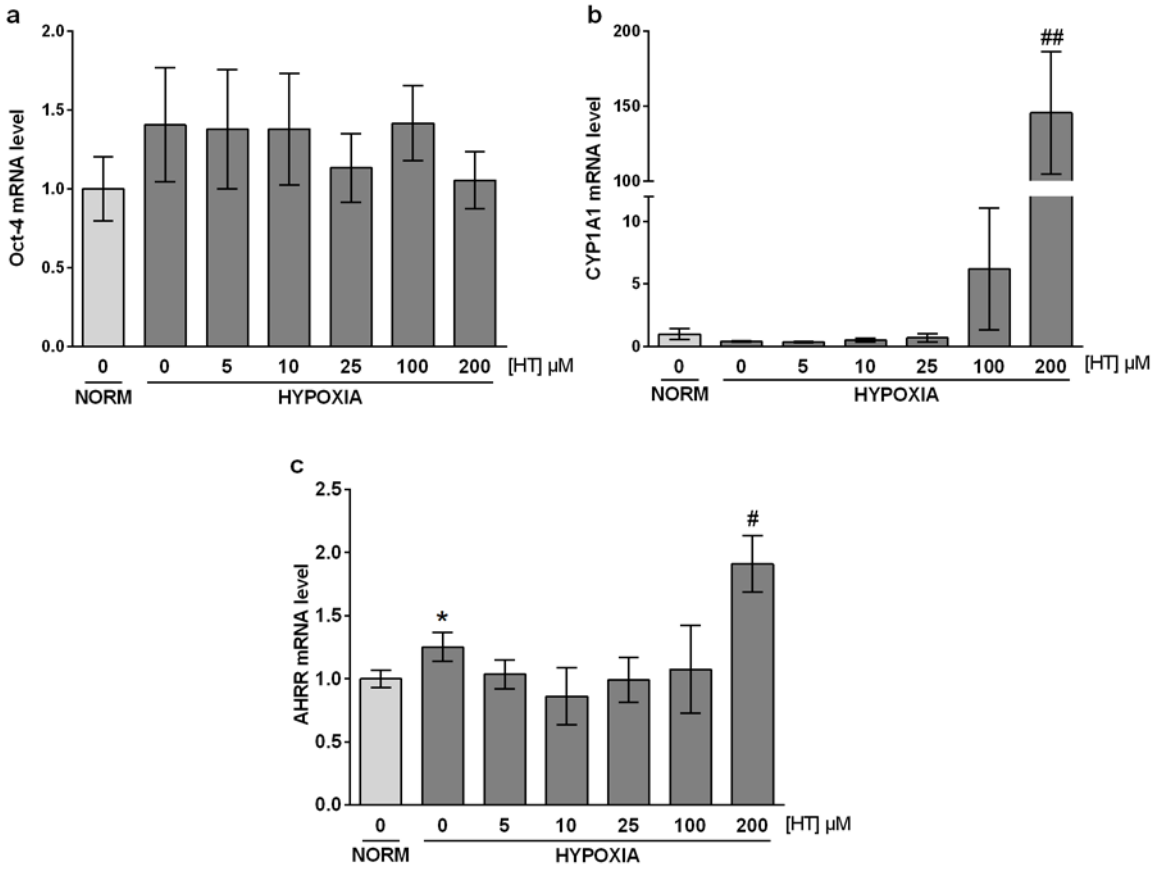

Figure 6. HT does not modulate HIF-2 but activates AHR at high concentrations. mRNA levels of Oct-4 (a), CYP1A1 (b) and AHRR (c). Results are expressed as mRNA expression relative to normoxic non HT-treated cells after normalization against PPIA. Values represent the mean ± SD from three independent experiments. Statistically significant differences with the corresponding non-treated normoxic cells: * $p<0.05$. Statistically significant differences with the corresponding non-treated hypoxic cells: $^{\#}$ $p<0.05$; $^{\#\#}$ $p<0.01$.

***In silico* modelling of HT interaction with AHR**

The large central pocket of the AHR PAS-B domain has been shown to promiscuously bind a number of toxic halogenated aromatic hydrocarbons, polycyclic aromatic hydrocarbons, and other natural, endogenous or synthetic agonists and antagonists[32-34], being 2,3,7,8-tetrachlorodibenzo-p-dioxin (TCDD) the most potent ligand. In order to support our results pointing that HT is an AHR ligand, we performed a docking analysis. As it has been shown that there exist important differences between the *apo* and *holo* structures of the HIF-2α PAS-B domain, used as template for homology modelling of the AHR PAS-B domain[35,36], we obtained a model for our docking analysis using three *holo* structures of the HIF-2α domain[37]. We have used and compared two different docking methodologies, one rigid docking that uses a pre-defined binding cavity and the Autodock Vina program[38], and another one that does not need the binding pocket to be defined, based on deep neural networks, using the web program Bindscope[39]. The first methodology rendered ten possible poses that were scored both with the Autodock Vina scoring function and with 3D-convolutional neural networks, using the web program K_{DEEP}[40]. The two best-scored consensus poses are shown, together with the pose obtained by Bindscope, in Fig. 8. Interestingly, Bindscope, which is not biased by a pre-defined binding site, predicted HT to interact with the same parts of the protein of our defined binding site, although this pose reflects a different orientation as compared to those obtained with Autodock Vina, which showed two poses in which the main difference is which OH group is establishing a hydrogen bond with GLY321. In all cases, the poses predicted

for HT establish interactions with residues which have been proven to form the so-called TCDD binding fingerprint[41] or others proved to be important for binding[42,43] (3,4 and 5 of these residues interacting with HT for the two poses from Autodock Vina and the pose from Bindscope, respectively). The poses obtained with Autodock Vina agreed in exhibiting a previously described crucial π-π interaction between HT and PHE295[41], also obtained in previous docking experiments[44]. Overall these docking results support the findings of HT as ligand of human AHR.

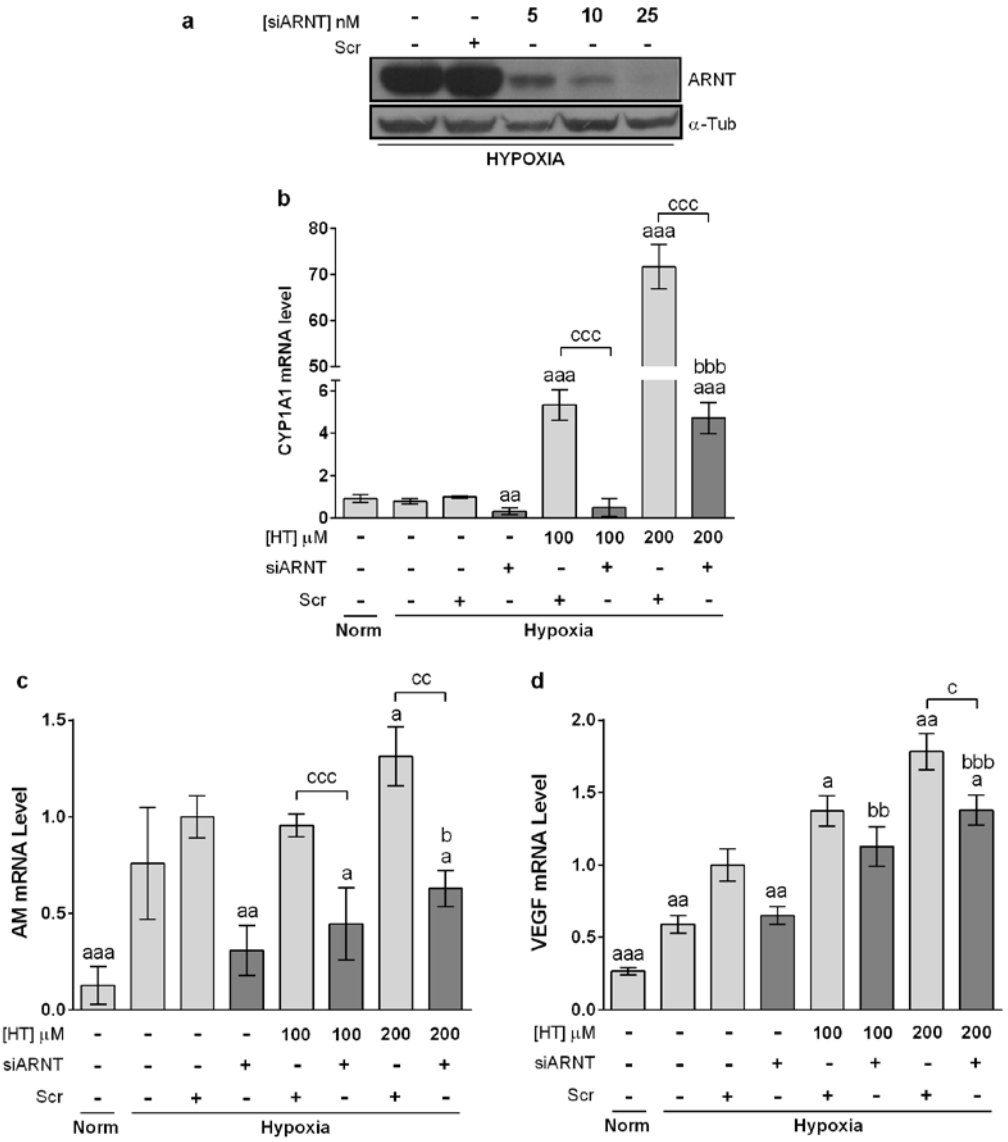

Figure 7. Role of ARNT in HT effect. (a) Immunoblot of ARNT knockdown with siARNT. Effect of ARNT silencing on the transcription level of (b) CYP1A1, (c) AM and (d) VEGF in hypoxic cells after treatment with HT 100 and 200 μM. Results are expressed as mRNA levels relative to Scr hipoxic cells after normalization against PPIA. Values represent the mean ± SD from three independent experiments. Statistically significant differences with the corresponding Scr hypoxic cells: ^{a} $p<0.05$, ^{aa} $p<0.01$, ^{aaa} $p<0.001$. Statistically significant differences with the corresponding ARNT-silenced cells: ^{b} $p<0.05$, ^{bb} $p<0.01$, ^{bbb} $p<0.001$. Statistically significant differences with the corresponding HT treated-non silenced cells: ^{c} $p<0.05$, ^{cc} $p<0.01$, ^{ccc} $p<0.001$.

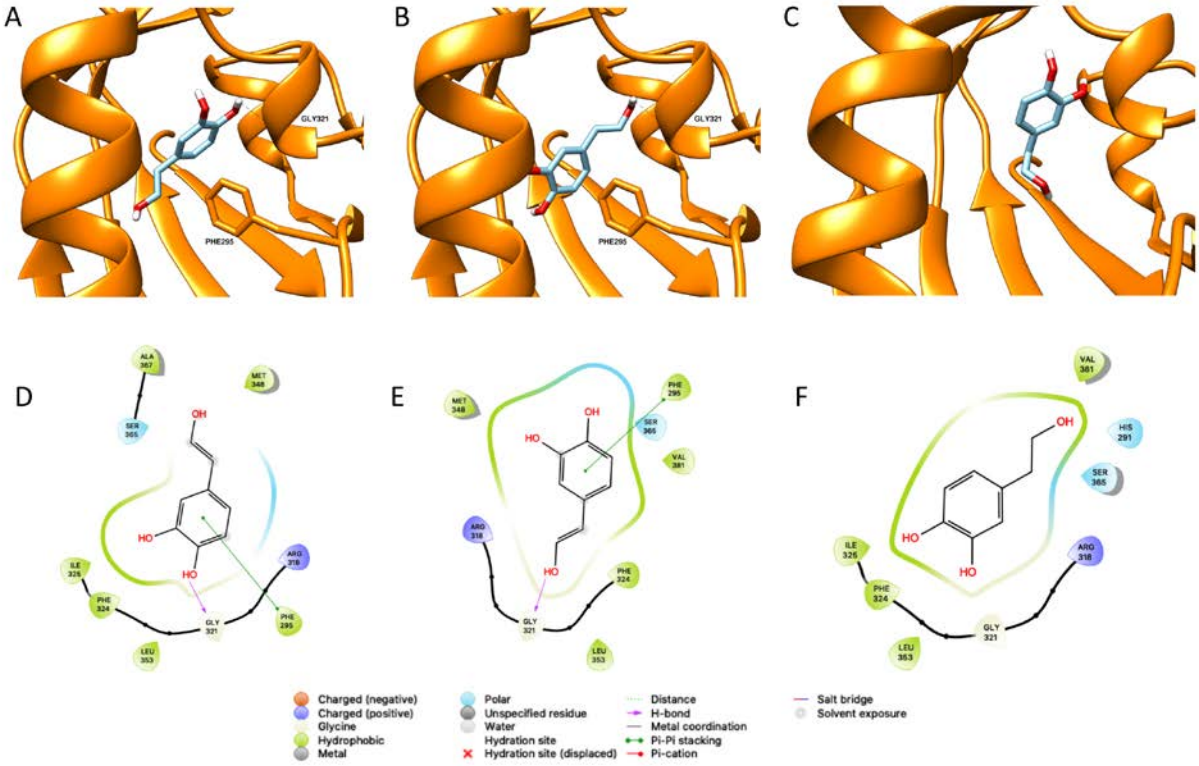

Figure 8. HT docked into human AHR as predicted by Autodock Vina (A, B) or BindScope (C), hydrogens other than those of the OH groups of HT are omitted for clarity. (D-F) 2D representations of the corresponding docked poses highlighting the interactions established between the ligand and the protein.

Discussion

The Mediterranean diet has been linked to a lower incidence of different types of cancer, and particularly of breast cancer[21,24,26,27,45]. In a previous study, we demonstrated that HT, the foremost EVOO phenolic compound in olive oil, modulates the oxidative response to hypoxia of the luminal A breast cancer cell line MCF-7[28]. In the present study, and considering the crucial role of HIF-1 in hypoxia and in cancer prognosis, we have deepened into the modulatory effect that this polyphenol exerts in the response of the HIF-1 pathway.

NO and ROS up-regulates HIF-1α levels by impairing PHDs and pVHL-mediated HIF-1 α degradation [14,46]. The effect of HT on the production of NO has been previously reported in a number of studies. Although some of them show that HT results ineffective in reducing NO production[47], most of them demonstrate that this polyphenol down-regulates NO levels, and point to the inhibition of the iNOS isoform as the plausible mechanism underlying this effect[48,49.] However, these studies were carried out in cells grown in normoxia and the data about the effect that HT exerts in NO production in hypoxic cells are scarce. We reported[50] that in hypoxic non tumoral cells NO levels were decreased by treatment with this polyphenol (100 and 200 μM). Breast cancer cells exhibit NO levels that are particularly high, and decreasing those level would help to counteract several malignancy-related effects including angiogenesis, apoptosis, cell cycle, invasion, and metastasis[51]. In this study we show that HT is unable to exert any effect on NO levels, suggesting that the plausible inhibition of iNOS is overwhelmed in hypoxic MCF-7 cells.

PARP-1 activity is induced by oxidative and nitrosative species and the crucial role of this protein in the response to hypoxia, both in non-tumoral and tumoral cells, has been extensively described by our group [17,52,53]. The inhibition of PARP-1 has proven to decrease the response of HIF-1α and is currently being used to treat breast cancer. Pharmacological inhibition of PARP-1 provides protection from oxidative stress-associated tissue injury, down-regulates the inflammatory response and is also beneficial in cancer treatment by mechanisms such as selective killing of homologous recombination-deficient tumor cells, down regulation of tumor-related gene expression (eg. AP-1 and NF-κB-mediated transcription) and of the apoptotic threshold in the co-treatment with chemo and radiotherapy[54]. There is strong evidence in support of the concept that hypoxia increases both the expression and the activity of PARP-1, contributing to tumor malignancy. Hence, the down-regulation of PARP-1 by HT would potentially be beneficial in cancer patients eg. could counteract the cardiovascular and

musculoskeletal complications associated to anti-cancer therapies. Our results corroborate the up-regulation of PARP-1 expression and activity in hypoxic MCF-7 cells, and demonstrate that HT treatment decreases both. However, these results although positive, cannot be exclusively linked to the antioxidant effect of HT, as they are achieved at high concentrations (≥75 μM) clearly over the antioxidant ones (≥5 μM)[28].

Breast cancer patients exhibit significantly high HIF-1α levels, which correlate with more aggressive cancer characteristics, and particularly with a poor disease free and overall survival[55]. Our results showed that HT (50-200 μM) decreased HIF-1α protein level without modulating its mRNA expression. These data resemble those previously observed by our group in hypoxic non-tumoral renal cells[50] and by others in human colon adenocarcinoma HT-29 cells grown *in vitro* and *in vivo* in a xenograft model[56], however the *in vitro* results were obtained after treatment with much higher concentrations of this polyphenol (400-800 μM)[57]. Although HT induced no changes in NO levels in MCF-7 hypoxic cells, the down-regulation of HIF-1α by HT treatment can be attributed to the antioxidant effect of HT, which reactivates PHD activity. Besides, HIF-1α expression can also be regulated by the PI3K/Akt/mTOR pathway. According to the literature, the effect of HT on this pathway is controversial. Some authors have pointed that HT inhibits Akt phosphorylation in tumoral and non-tumoral cells at 50, 100 and 200 μM[58-60]. However, HT has also been shown to promote Akt phosphorylation[61-63]. The data presented here support the proposition that HT inhibits the activity of this pathway, as lower levels of p-P70 and p-S6 were observed in hypoxic HT-treated cells at the same doses previously described (100 and 200 μM), suggesting that the down-regulation of HIF-1α by HT is not only achieved post-translationally, through ROS down-regulation, but also at a translational level through the inhibition of the PI3K/Akt/mTOR pathway. This modulatory effect of HT would contribute to counteract breast cancer progression as high levels of PI3K, pAKT an p-mTOR are recurrently used as predictors of an adverse outcome in breast cancer patients[64-66].

HIF-1 plays a central role in the adaptive response to hypoxia. It therefore appears crucial to investigate the effect of HT in the expression of some HIF-1 target genes. The induction of angiogenesis and an increased glucose uptake are two key molecular pathways that favor cell survival in a hypoxic environment. Those pathways are induced, among others, by the angiogenic factors VEGF and AM and by the metabolic proteins Glut-1 and LDH. As shown above, the treatment of MCF-7 cells with HT decreases the expression of HIF-1 α. Thus, we expected those genes to follow a similar pattern of response and to be downregulated in HT-treated hypoxic cells. However, our findings showed that HT exerts no effect on the mRNA levels of LDHA but, strikingly, high doses of this polyphenol up-regulated the transcription of AM, VEGF and Glut-1, suggesting that HT does not reduce but induces the transcriptional activity of HIF-1. While this result stands at odds with previous studies showing lower levels of VEGF in different models [56,67,68], they support our previous findings in renal cells[50]. FIH, through its ability to hydroxylate HIF-1α Asn-803, depresses HIF-1 transcriptional activity[3]. Thus, a plausible decrease in this protein could be responsible for the higher transcriptional activity of HIF-1. However, as the expression of FIH seems not to be modulated by HT, we suggested that other regulatory pathways, different to HIF-1, are probably underlying the up-regulation of these genes. In order to corroborate the particular involvement of HIF-1 in the response of AM, VEGF and Glut-1 to HT treatment, we silenced HIF-1α expression by siRNA. The induction of Glut-1 by HT was completely abolished in these cells, suggesting that its up-regulation after HT treatment is highly dependent on HIF-1 transcriptional activity. However, AM and VEGF were only partially down-regulated, corroborating the involvement of other regulatory mechanisms, additional to HIF-1, in the HT-mediated induction of those genes. HIF-2 is another member of the HIF family also involved in the response to hypoxia. The effect of HT in the activity of this transcription factor is largely unknown. Hence, we wonder whether the reported increase in AM and VEGF could be mediated by HIF-2[69]. To test this hypothesis, we assessed the impact of HT in the transcriptional activity of HIF-2. Erythropoietin or angiopoietin 2 are canonical HIF-2 targets but they are very poorly expressed in MCF-7 cells[70,71], therefore we evaluated the mRNA levels of another specific HIF-2α target, Oct-4[72]. HT did not affect Oct-4 transcription so HIF-2 does not seem to be involved in the response of AM and VEGF to HT. AM and VEGF can also be upregulated by the hydrocarbon receptor (AHR)[29,30,73,74]. AHR is a cytoplasmic bHLH-PAS transcription factor that can be activated by diverse chemicals. Upon ligand binding, and similarly to HIF-1α, AHR is translocated to the nucleus where it dimerizes with HIF-β (ARNT) and forms an active transcription factor that regulates the expression of several genes involved in detoxification, angiogenesis, cell proliferation, adhesion and migration, among others processes[75]. CYP1A1 is classically induced in response to AHR activation and, according to our results, the treatment of hypoxic MCF-7 cells with high concentrations of HT dramatically up-regulates the transcription of this protein involved in the metabolism of exogenous chemicals. These data appear to indicate that, at those concentrations, HT acts as an AHR ligand and promotes the expression of AM and VEGF through binding to their AHR-responsive elements. Although a complete view of the role of AHR in breast tumor growth is not currently available, AHR activation has been extensively linked with malignant transformation. In fact, a recent study in a cohort of 439 breast tumors showed that high AHR expression correlated with the up-regulation of genes involved in inflammation, metabolism, invasion and growth factor signaling while high AHRR mRNA levels correlated with good-metastasis free survival[31]. Ligands for AHR are diverse and include not only pharmaceuticals but also dietary compounds such as polyphenols, natural and synthetic flavonoids[76]. The rank of concentrations at which those compounds exert

such effect is highly variable and depends on the chemical structure but also on the biological model used[77]. Our structural modelling of HT binding to AHR supports that this polyphenol can act as an AHR ligand. In fact, the binding poses found show a π-π interaction proved to be crucial for TCDD binding, together with interactions with residues already shown to be important for TCDD binding to AHR[41,44]. Moreover, we also address the importance of concentration in the AHR agonist activity of HT, as only high levels of this polyphenol, clearly over its dietary intake, are able to induce CYP1A1. A deeper *in silico* analysis, going from less computationally intensive methods, like MMGBSA[78], to other requesting much more computational resources such as alchemical free energy calculations[79,80], should be necessary to shed light into the molecular basis of the different expected binding free energy of HT as compared to TCDD. However, the fact that the induction of AM and VEGF by HT is not completely abolished in ARNT-silenced cells suggests the plausible involvement of other mechanisms additional to HIF-1 and AHR. ARNT2 is a homologous to ARNT protein. Its expression is restricted to neural tissues and the kidney, but it is also found in multiple cancer cells. Although both ARNT and ARNT2 bind equally with HIF-α subunits, ARNT is much more efficient that ARNT2 in the AHR-mediated up-regulation of CYP1A1[81]. Therefore, although further experiment should be carried out, it could be hypothesized that the transcriptional effect of HT may be exerted through a combination of the AHR-ARNT and HIF-1α-ARNT/ARNT2 pathways.

In conclusion, our results suggest that HT decreases the PI3K/Akt/mTOR pathway and HIF-1α in hypoxic MCF-7 cells. Moreover, we describe for the first time that high doses of HT, recurrently used in the literature, may act as an AHR agonist favoring the induction of angiogenic genes under hypoxic conditions. Therefore, our results provide new insights into the effect of HT in a hypoxic environment, and point to the importance of concentration in the comprehensive analysis of the biological potential of this compound.

Methods

Chemicals and reagents.
HT (purity ≥98%) was obtained from Extrasynthese. Dulbecco's modified Eagle's medium (DMEM) and sodium pyruvate were from Capricorn Scientific and foetal bovine serum (FBS) was from Sigma. Primary antibodies p-mTOR (2971S), p-P70 S6 kinase (9205S) and p-S6 (2211S) were purchased from Cell signaling Technology, HIF-1α (A300-286A) from Bethyl, PARP-1 (C-2-10) from Calbiochem, α-Tubulin antibody (T5168) from SIGMA and FIH-1 (sc-26219) from Santa Cruz. RNA was isolated using the RNeasyPlus Mini kit (Qiagen). cDNA Synthesis Kit for RT-qPCR and iTaq UniverSYBR for Real-time PCR were from Bio-Rad. Primers were synthesized by Biomedal S.L. (Sevilla, Spain). ARNT siRNA (s1613 and s1615), HIF-1α siRNA (Sigma, forward 5′-CUGAUGACCAGCAACUUGA-3′, reverse 5′-UCAAGUUGCUGGUCAUCAG-3′), scramble siRNA (sc-37007) and the transfection reagent jetPRIME were from Ambion, (casa commercial siHIFalfa), Santa Cruz and Polyplus Transfection, respectively.

Cell culture and treatments.
Human breast cancer MCF-7 cells were grown in 10% foetal bovine serum and 1% sodium pyruvate supplemented DMEM at 37ºC in 5% CO_2 and 21% O_2. Cells were pre-treated or not with different concentrations of HT, prepared in ethanol immediately before use, for 16 h under normoxic conditions (21% O_2), being cultured during the last 4 h either in normoxic or hypoxic conditions (1% O_2). Control cells were treated with an equal ethanol concentration.

Measurement of nitric oxide level.
Nitric oxide (NO) level was indirectly quantified by determining nitrate/nitrite and S-nitroso compounds (NOx), using an ozone chemiluminescence-based method. For this purpose, cells of each experimental condition were collected and lysed by 3 freeze–thaw cycles. After centrifugation at 14000g for 30 min, the supernatants were collected and protein was quantified. Samples were deproteinized in a deproteinization solution (0.8 N NaOH and 16% $ZnSO_4$). The total amount of NOx in the deproteinized samples was determined the purge system of Sievers Instruments, model NOA 280i. NOx concentrations were calculated by comparison with standard solutions of sodium nitrate. Final NOx values were referred to the total protein concentration in the initial extracts.

Western blot.
For western blot analysis, equal amounts of denatured total-protein extracts (20 μg) were loaded and separated on a 7.5% (HIF-1α, p-mTOR and PARP-1), or 10% (p-P70, FIH-1 and p-S6) SDS-polyacrylamide gel. Proteins in the gel were transferred to a PVDF membrane (Amersham Pharmacia Biotech) and then blocked. Monoclonal antibodies to HIF-1α (1/5000), p-mTOR (1/1000), PARP-1 (1/1000), p-P70 (1/5000), FIH-1 (1/7000), p-S6 (1/5000) and to α-tubulin (1/20.000), as a loading control, were used for detection of the respective proteins. Antibody reaction was revealed by means of chemiluminescence detection procedures according to the manufacturer's recommendations (ECL kit, Amersham Corp). Western-blot was quantified by using TotalLab

software.

Quantitative Real-time PCR (qRT-PCR).
Real-time PCR was performed in a CFX384 Touch Real-Time PCR Detection System (Bio-Rad) using iTaq UniverSYBR. The sequences of the primers are below: *HIF-1α*, forward 5′-TGCTTTAACTTTGCTGGCCC-3′, reverse 5′-GTTTCTGTGTCGTTGCTGCC-3′; *AM*, forward 5′-CTCTGAGTCGTGGGAAGAGG-3′, reverse 5′-CCCTGGAAGTTGTTCATGCT-3′; *VEGF*, forward 5′-TTGTACAAGATCCGCAGACG-3′, reverse 5′-TCACATCTGCAAGTACGTTCG-3′; *GLUT-1*, forward 5′-AGGCTTCTCCAACTGGACCT-3′, reverse 5′-CCTCGGGTGTCTTGTCACTT-3′; *LDHA*, forward 5′-AGGCTACACATCCTGGGCTA-3′, reverse 5′-CCCAAAATGCAAGGAACACT-3′; *Oct-4*, forward 5′-GGCTCGAGAAGGATGTGGTC-3′, reverse 5′-CCAGCAGACACCTTAGACGA-3′; *AHRR*, forward 5′-GAAGGAGCAGCAGAGAGAGC-3′, reverse 5′-CTTTGTGGGTCCTGGAGTCT-3′; *CYP1A1*, forward 5′-CAAGGGGCGTTGTGTCTTTG-3′, reverse 5′-GTCGATAGCACCATCAGGGG-3′; *PPIA*, forward 5′-TTCATCTGCACTGCCAAGAC-3′, reverse 5′-TCGAGTTGTCCACAGTCAGC-3′. Experiments were performed in triplicate, and the relative quantities of target genes, corrected with the normalizing gene PPIA, were calculated using the Bio-Rad CFX Manager Software.

HIF-1α and ARNT siRNA transfection.
HIF-1α, ARNT and Scr siRNAs were transfected with transfection reagent according to the manufacturer's instructions. Briefly, MCF-7 cells (11×10^4/well) were plated into 6-well plates, allowed to adhere for 24 h and incubated with the siRNAs for 24 h. Different concentrations of each siRNA were initially tested (20, 40 and 60nM of siHIF-1α; 5, 10 and 25nM of siARNTs). Finally, siHIF-1α 40 nM, siARNTs 25 nM and similar concentrations of Scr-siRNA were used. Two pairs of ARNT siRNAs were used to ensure a maximum silencing. The transfection medium was then replaced with fresh medium for 24 h before further treatment with HT and/or hypoxia. The efficiency of silencing was evaluated by western-blot analysis of HIF-1α and ARNT.

Modelling of HT binding to AHR.
The model of the human AHR PAS-B domain was obtained by homology modelling using as templates three holo structures of the HIF-2α PAS-B domain, with PDB IDs 3F1O[35], 3H7W[36] and 3H82[82]. The Prime module of the Schrödinger Maestro 2017-1 suite was used to obtain an homology model using the Consensus Homology Model, using as query sequence residues 284-390 of human AHR. The model was subsequently loaded into the web program ProteinPrepare[83], which protonates at pH=7 and optimizes the hydrogen bond network. The model for HT was manually drawn and imported into UCSF Chimera[84], where its structure was optimized for 100 steepest-descent followed by 100 conjugate-gradient steps. The HR model, together with the human AHR one, were on the one hand uploaded into Bindscope[39], and on the other one prepared with the DockPrep utility of Chimera to be used in a docking calculation with Autodock Vina[38]. Amber ff14SB[85] charges were used for the protein, whilst AM1-BCC[86,87] charges were assigned to HT. The binding pocket used, which is the same found in other docking experiments, was determined with DeepSite[88]. The cartesian coordinates of the center of the binding pocket found with DeepSite were used to define a search box for Autodock Vina of 10x10x10 $Å^3$, and for other parameters, defaults were used. Figures were rendered with UCSF Chimera and Maestro.

Statistical analysis.
Data are expressed as means ± SD of at least three independent experiments. Statistical comparisons between the different experimental groups and their corresponding controls were made with Student's t-test, accepting $p<0.05$ as the level of significance, using GraphPad Prism 6 software (GraphPad Software Inc.).

Experimental methods guidelines statement.
All experiments were performed in accordance with relevant guidelines and regulations.

Data availability:

The datasets generated during and/or analysed during the current study are available from the corresponding author on reasonable request.

References

1 Alkabban, F. M. & Ferguson, T. Cancer, Breast. *Treasure Island: StatPearls Publishing* (2018).
2 Lundgren, K., Holm, C. & Landberg, G. Hypoxia and breast cancer: prognostic and therapeutic implications. *Cell Mol Life Sci* **64**, 3233-3247, doi:10.1007/s00018-007-7390-6 (2007).
3 Masoud, G. N. & Li, W. HIF-1α pathway: role, regulation and intervention for cancer therapy. *Acta Pharmaceutica Sinica B* **5**, 378-389, doi:10.1016/j.apsb.2015.05.007 (2015).

4 Doktorova, H., Hrabeta, J., Khalil, M. A. & Eckschlager, T. Hypoxia-induced chemoresistance in cancer cells: The role of not only HIF-1. *Biomedical Papers of the Medical Faculty of Palacky University in Olomouc* **159**, doi:10.5507/bp.2015.025 (2015).
5 Harada, H. Hypoxia-inducible factor 1–mediated characteristic features of cancer cells for tumor radioresistance. *Journal of radiation research* **57**, i99-i105, doi:10.1093/jrr/rrw012 (2016).
6 Minet, E. *et al.* HIF1A gene transcription is dependent on a core promoter sequence encompassing activating and inhibiting sequences located upstream from the transcription initiation site and cis elements located within the 5′ UTR. *Biochemical and biophysical research communications* **261**, 534-540, doi:10.1006/bbrc.1999.0995 (1999).
7 BelAiba, R. S. *et al.* Hypoxia up-regulates hypoxia-inducible factor-1α transcription by involving phosphatidylinositol 3-kinase and nuclear factor κB in pulmonary artery smooth muscle cells. *Molecular biology of the cell* **18**, 4691-4697, doi:10.1091/mbc.e07-04-0391 (2007).
8 Sperandio, S. *et al.* The transcription factor Egr1 regulates the HIF-1α gene during hypoxia. *Molecular Carcinogenesis: Published in cooperation with the University of Texas MD Anderson Cancer Center* **48**, 38-44, doi:10.1002/mc.20454 (2009).
9 Agani, F. & Jiang, B.-H. Oxygen-independent regulation of HIF-1: novel involvement of PI3K/AKT/mTOR pathway in cancer. *Current cancer drug targets* **13**, 245-251 (2013).
10 Tafani, M. *et al.* The interplay of reactive oxygen species, hypoxia, inflammation, and sirtuins in cancer initiation and progression. *Oxidative medicine and cellular longevity* **2016**, doi:10.1155/2016/3907147 (2016).
11 Galadari, S., Rahman, A., Pallichankandy, S. & Thayyullathil, F. Reactive oxygen species and cancer paradox: to promote or to suppress? *Free Radical Biology and Medicine* **104**, 144-164, doi:10.1016/j.freeradbiomed.2017.01.004 (2017).
12 Fong, G. & Takeda, K. Role and regulation of prolyl hydroxylase domain proteins. *Cell death and differentiation* **15**, 635, doi:10.1038/cdd.2008.10 (2008).
13 Movafagh, S., Crook, S. & Vo, K. Regulation of hypoxia-inducible factor-1a by reactive oxygen species: new developments in an old debate. *Journal of cellular biochemistry* **116**, 696-703, doi:10.1002/jcb.25074 (2015).
14 Ho, J. D., Man, H. J. & Marsden, P. A. Nitric oxide signaling in hypoxia. *Journal of molecular medicine* **90**, 217-231, doi:10.1016/B978-0-12-800254-4.00007-6 (2012).
15 Lando, D., Gorman, J. J., Whitelaw, M. L. & Peet, D. J. Oxygen-dependent regulation of hypoxia-inducible factors by prolyl and asparaginyl hydroxylation. *European Journal of Biochemistry* **270**, 781-790 (2003).
16 Martin-Oliva, D. *et al.* Inhibition of poly (ADP-ribose) polymerase modulates tumor-related gene expression, including hypoxia-inducible factor-1 activation, during skin carcinogenesis. *Cancer research* **66**, 5744-5756, doi:10.1158/0008-5472.CAN-05-3050 (2006).
17 Martínez-Romero, R. *et al.* Poly (ADP-ribose) polymerase-1 modulation of in vivo response of brain hypoxia-inducible factor-1 to hypoxia/reoxygenation is mediated by nitric oxide and factor inhibiting HIF. *Journal of neurochemistry* **111**, 150-159, doi: 10.1111/j.1471-4159.2009.06307.x (2009).
18 Weaver, A. N. & Yang, E. S. Beyond DNA repair: additional functions of PARP-1 in cancer. *Frontiers in oncology* **3**, 290, doi:10.3389/fonc.2013.00290 (2013).
19 Rodríguez, M. I. *et al.* Deciphering the Insights of Poly (ADP-Ribosylation) in Tumor Progression. *Medicinal research reviews* **35**, 678-697, doi:10.1002/med.21339 (2015).
20 Nagini, S. Breast cancer: Current molecular therapeutic targets and new players. *Anti-Cancer Agents in Medicinal Chemistry (Formerly Current Medicinal Chemistry-Anti-Cancer Agents)* **17**, 152-163, doi:10.2174/1871520616666160502122724 (2017).
21 Toledo, E. *et al.* Mediterranean diet and invasive breast cancer risk among women at high cardiovascular risk in the PREDIMED trial: a randomized clinical trial. *JAMA internal medicine* **175**, 1752-1760, doi:10.1001/jamainternmed.2015.4838 (2015).
22 Echeverría, F., Ortiz, M., Valenzuela, R. & Videla, L. Hydroxytyrosol and cytoprotection: a projection for clinical interventions. *International journal of molecular sciences* **18**, 930, doi:https://doi.org/10.3390/ijms18050930 (2017).
23 Robles-Almazan, M. *et al.* Hydroxytyrosol: Bioavailability, toxicity, and clinical applications. *Food Research International*, doi:10.1016/j.foodres.2017.11.053 (2017).
24 Granados-Principal, S. *et al.* Hydroxytyrosol ameliorates oxidative stress and mitochondrial dysfunction in doxorubicin-induced cardiotoxicity in rats with breast cancer. *Biochemical pharmacology* **90**, 25-33 (2014).
25 Cruz-Lozano, M. *et al.* Hydroxytyrosol inhibits cancer stem cells and the metastatic capacity of triple-negative breast cancer cell lines by the simultaneous targeting of epithelial-to-mesenchymal transition, Wnt/β-catenin and TGFβ signaling pathways. *European journal of nutrition*, 1-13, doi:10.1007/s00394-018-1864-1 (2018).
26 Granados-Principal, S. *et al.* Hydroxytyrosol inhibits growth and cell proliferation and promotes high

expression of sfrp4 in rat mammary tumours. *Molecular nutrition & food research* **55**, S117-S126, doi:10.1002/mnfr.201000220 (2011).
27 Martínez, N. *et al.* A combination of hydroxytyrosol, omega-3 fatty acids and curcumin improves pain and inflammation among early stage breast cancer patients receiving adjuvant hormonal therapy: results of a pilot study. *Clinical and Translational Oncology*, 1-10 (2018).
28 Calahorra, J., Martínez-Lara, E., De Dios, C. & Siles, E. Hypoxia modulates the antioxidant effect of hydroxytyrosol in MCF-7 breast cancer cells. *PloS one* **13**, e0203892, doi:https://doi.org/10.1371/journal.pone.0203892 (2018).
29 Iwano, S., Ichikawa, M., Takizawa, S., Hashimoto, H. & Miyamoto, Y. Identification of AhR-regulated genes involved in PAH-induced immunotoxicity using a highly-sensitive DNA chip, 3D-GeneTM Human Immunity and Metabolic Syndrome 9k. *Toxicology in Vitro* **24**, 85-91, doi:10.1016/j.tiv.2009.08.030 (2010).
30 Chiappini, F. *et al.* Exposure to environmental concentrations of hexachlorobenzene induces alterations associated with endometriosis progression in a rat model. *Food and Chemical Toxicology* **123**, 151-161, doi:10.1016/j.fct.2018.10.056 (2019).
31 Vacher, S. *et al.* High AHR expression in breast tumors correlates with expression of genes from several signaling pathways namely inflammation and endogenous tryptophan metabolism. *PloS one* **13**, e0190619, doi:10.1371/journal.pone.0190619 (2018).
32 Poland, A. & Knutson, J. C. 2,3,7,8-tetrachlorodibenzo-p-dioxin and related halogenated aromatic hydrocarbons: examination of the mechanism of toxicity. *Annu Rev Pharmacol Toxicol* **22**, 517-554, doi:10.1146/annurev.pa.22.040182.002505 (1982).
33 Safe, S. Polychlorinated biphenyls (PCBs), dibenzo-p-dioxins (PCDDs), dibenzofurans (PCDFs), and related compounds: environmental and mechanistic considerations which support the development of toxic equivalency factors (TEFs). *Crit Rev Toxicol* **21**, 51-88, doi:10.3109/10408449009089873 (1990).
34 Denison, M. S. & Nagy, S. R. Activation of the aryl hydrocarbon receptor by structurally diverse exogenous and endogenous chemicals. *Annu Rev Pharmacol Toxicol* **43**, 309-334, doi:10.1146/annurev.pharmtox.43.100901.135828 (2003).
35 Scheuermann, T. H. *et al.* Artificial ligand binding within the HIF2 alpha PAS-B domain of the HIF2 transcription factor. *P Natl Acad Sci USA* **106**, 450-455, doi:10.1073/pnas.0808092106 (2009).
36 Key, J., Scheuermann, T. H., Anderson, P. C., Daggett, V. & Gardner, K. H. Principles of Ligand Binding within a Completely Buried Cavity in HIF2 alpha PAS-B. *J Am Chem Soc* **131**, 17647-17654, doi:10.1021/ja9073062 (2009).
37 Motto, I., Bordogna, A., Soshilov, A. A., Denison, M. S. & Bonati, L. New aryl hydrocarbon receptor homology model targeted to improve docking reliability. *J Chem Inf Model* **51**, 2868-2881, doi:10.1021/ci2001617 (2011).
38 Trott, O. & Olson, A. J. AutoDock Vina: improving the speed and accuracy of docking with a new scoring function, efficient optimization, and multithreading. *J Comput Chem* **31**, 455-461, doi:10.1002/jcc.21334 (2010).
39 Skalic, M., Martinez-Rosell, G., Jimenez, J. & De Fabritiis, G. PlayMolecule BindScope: large scale CNN-based virtual screening on the web. *Bioinformatics* **35**, 1237-1238, doi:10.1093/bioinformatics/bty758 (2019).
40 Jimenez, J., Skalic, M., Martinez-Rosell, G. & De Fabritiis, G. KDEEP: Protein-Ligand Absolute Binding Affinity Prediction via 3D-Convolutional Neural Networks. *J Chem Inf Model* **58**, 287-296, doi:10.1021/acs.jcim.7b00650 (2018).
41 Pandini, A. *et al.* Detection of the TCDD binding-fingerprint within the Ah receptor ligand binding domain by structurally driven mutagenesis and functional analysis. *Biochemistry* **48**, 5972-5983, doi:10.1021/bi900259z (2009).
42 Henry, E. C. & Gasiewicz, T. A. Molecular determinants of species-specific agonist and antagonist activity of a substituted flavone towards the aryl hydrocarbon receptor. *Arch Biochem Biophys* **472**, 77-88, doi:10.1016/j.abb.2008.02.005 (2008).
43 Goryo, K. *et al.* Identification of amino acid residues in the Ah receptor involved in ligand binding. *Biochem Biophys Res Commun* **354**, 396-402, doi:10.1016/j.bbrc.2006.12.227 (2007).
44 Jogalekar, A. S., Reiling, S. & Vaz, R. J. Identification of optimum computational protocols for modeling the aryl hydrocarbon receptor (AHR) and its interaction with ligands. *Bioorganic & medicinal chemistry letters* **20**, 6616-6619, doi:10.1016/j.bmcl.2010.09.019 (2010).
45 García-Segovia, P., Sánchez-Villegas, A., Doreste, J., Santana, F. & Serra-Majem, L. Olive oil consumption and risk of breast cancer in the Canary Islands: a population-based case–control study. *Public health nutrition* **9**, 163-167 (2006).
46 Metzen, E., Zhou, J., Jelkmann, W., Fandrey, J. & Brune, B. Nitric oxide impairs normoxic degradation of HIF-1α by inhibition of prolyl hydroxylases. *Molecular biology of the cell* **14**, 3470-3481, doi:10.1091/mbc.e02-12-0791 (2003).
47 Plastina, P. *et al.* Identification of hydroxytyrosyl oleate, a derivative of hydroxytyrosol with anti-

inflammatory properties, in olive oil by-products. *Food chemistry* **279**, 105-113, doi:10.1016/j.foodchem.2018.12.007 (2019).
48 Deiana, M. *et al.* Inhibition of peroxynitrite dependent DNA base modification and tyrosine nitration by the extra virgin olive oil-derived antioxidant hydroxytyrosol. *Free Radical Biology and Medicine* **26**, 762-769, doi:https://doi.org/10.1016/S0891-5849(98)00231-7 (1999).
49 Zhang, X., Cao, J. & Zhong, L. Hydroxytyrosol inhibits pro-inflammatory cytokines, iNOS, and COX-2 expression in human monocytic cells. *Naunyn-Schmiedeberg's archives of pharmacology* **379**, 581, doi:10.1007/s00210-009-0399-7 (2009).
50 Martínez-Lara, E., Peña, A., Calahorra, J., Cañuelo, A. & Siles, E. Hydroxytyrosol decreases the oxidative and nitrosative stress levels and promotes angiogenesis through HIF-1 independent mechanisms in renal hypoxic cells. *Food & function* **7**, 540-548, doi:10.1039/C5FO00928F (2016).
51 Choudhari, S. K., Chaudhary, M., Bagde, S., Gadbail, A. R. & Joshi, V. Nitric oxide and cancer: a review. *World journal of surgical oncology* **11**, 118, doi:10.1186/1477-7819-11-118 (2013).
52 Rodríguez, M. I. *et al.* PARP-1 regulates metastatic melanoma through modulation of vimentin-induced malignant transformation. *PLoS genetics* **9**, e1003531, doi:10.18632/oncotarget.2993 (2013).
53 Gonzalez-Flores, A. *et al.* Interaction between PARP-1 and HIF-2α in the hypoxic response. *Oncogene* **33**, 891, doi:10.1038/onc.2013.9 (2014).
54 Aguilar-Quesada, R. *et al.* Modulation of transcription by PARP-1: consequences in carcinogenesis and inflammation. *Current medicinal chemistry* **14**, 1179-1187, doi:10.2174/092986707780597998 (2007).
55 Cai, F.-F. *et al.* Prognostic value of plasma levels of HIF-1a and PGC-1a in breast cancer. *Oncotarget* **7**, 77793, doi:10.18632/oncotarget.12796 (2016).
56 Terzuoli, E. *et al.* Inhibition of hypoxia inducible factor-1α by dihydroxyphenylethanol, a product from olive oil, blocks microsomal prostaglandin-E synthase-1/vascular endothelial growth factor expression and reduces tumor angiogenesis. *Clinical Cancer Research* **16**, 4207-4216, doi:10.1158/1078-0432.CCR-10-0156 (2010).
57 Cárdeno, A., Sánchez-Hidalgo, M., Rosillo, M. A. & de la Lastra, C. A. Oleuropein, a secoiridoid derived from olive tree, inhibits the proliferation of human colorectal cancer cell through downregulation of HIF-1α. *Nutrition and cancer* **65**, 147-156, doi:10.1080/01635581.2013.741758 (2013).
58 Zhao, B. *et al.* Hydroxytyrosol, a natural molecule from olive oil, suppresses the growth of human hepatocellular carcinoma cells via inactivating AKT and nuclear factor-kappa B pathways. *Cancer letters* **347**, 79-87, doi:10.1016/j.canlet.2014.01.028 (2014).
59 Wang, W. *et al.* Hydroxytyrosol regulates the autophagy of vascular adventitial fibroblasts through the SIRT1-mediated signaling pathway. *Canadian journal of physiology and pharmacology* **96**, 88-96, doi:10.1139/cjpp-2016-0676 (2017).
60 Zubair, H. *et al.* Hydroxytyrosol induces apoptosis and cell cycle arrest and suppresses multiple oncogenic signaling pathways in prostate cancer cells. *Nutrition and cancer* **69**, 932-942, doi:10.1080/01635581.2017.1339818 (2017).
61 Incani, A. *et al.* Involvement of ERK, Akt and JNK signalling in H2O2-induced cell injury and protection by hydroxytyrosol and its metabolite homovanillic alcohol. *Molecular nutrition & food research* **54**, 788-796, doi:10.1016/j.jnutbio.2011.05.006 (2010).
62 Sun, L., Luo, C. & Liu, J. Hydroxytyrosol induces apoptosis in human colon cancer cells through ROS generation. *Food & function* **5**, 1909-1914, doi:10.1039/c4fo00187g (2014).
63 Zou, X. *et al.* Stimulation of GSH synthesis to prevent oxidative stress-induced apoptosis by hydroxytyrosol in human retinal pigment epithelial cells: activation of Nrf2 and JNK-p62/SQSTM1 pathways. *The Journal of nutritional biochemistry* **23**, 994-1006, doi:10.1016/j.jnutbio.2011.05.006 (2012).
64 Charpin, C. *et al.* Validation of an immunohistochemical signature predictive of 8-year outcome for patients with breast carcinoma. *International journal of cancer* **131**, E236-E243, doi:10.1002/ijc.27371 (2012).
65 Gallardo, A. *et al.* Increased signalling of EGFR and IGF1R, and deregulation of PTEN/PI3K/Akt pathway are related with trastuzumab resistance in HER2 breast carcinomas. *British journal of cancer* **106**, 1367, doi:10.1038/bjc.2012.85 (2012).
66 Yu, B.-H., Li, B.-Z., Zhou, X.-Y., Shi, D.-R. & Yang, W.-T. Cytoplasmic FOXP1 expression is correlated with ER and calpain II expression and predicts a poor outcome in breast cancer. *Diagnostic pathology* **13**, 36, doi:10.1186/s13000-018-0715-y (2018).
67 Lamy, S., Ouanouki, A., Béliveau, R. & Desrosiers, R. R. Olive oil compounds inhibit vascular endothelial growth factor receptor-2 phosphorylation. *Experimental cell research* **322**, 89-98, doi:10.1016/j.yexcr.2013.11.022 (2014).
68 Granner, T., Maloney, S., Antecka, E., Correa, J. A. & Burnier, M. N. 3, 4 dihydroxyphenyl ethanol reduces secretion of angiogenin in human retinal pigment epithelial cells. *British Journal of Ophthalmology* **97**, 371-374, doi:10.1136/bjophthalmol-2012-302002 (2013).
69 Hu, C.-J., Wang, L.-Y., Chodosh, L. A., Keith, B. & Simon, M. C. Differential roles of hypoxia-

inducible factor 1α (HIF-1α) and HIF-2α in hypoxic gene regulation. *Molecular and cellular biology* **23**, 9361-9374, doi:10.1128/MCB.23.24.9361-9374.2003 (2003).
70 Rankin, E. B. *et al.* Hypoxia-inducible factor–2 (HIF-2) regulates hepatic erythropoietin in vivo. *The Journal of clinical investigation* **117**, 1068-1077, doi:10.1172/JCI30117 (2007).
71 Park, Y. S. *et al.* Expression of angiopoietin-1 in hypoxic pericytes: regulation by hypoxia-inducible factor-2α and participation in endothelial cell migration and tube formation. *Biochemical and biophysical research communications* **469**, 263-269, doi:10.1016/j.bbrc.2015.11.108 (2016).
72 Covello, K. L. *et al.* HIF-2α regulates Oct-4: effects of hypoxia on stem cell function, embryonic development, and tumor growth. *Genes & development* **20**, 557-570, doi:10.1101/gad.1399906 (2006).
73 Tsai, M.-J. *et al.* Aryl hydrocarbon receptor agonists upregulate VEGF secretion from bronchial epithelial cells. *Journal of Molecular Medicine* **93**, 1257-1269, doi:10.1007/s00109-015-1304-0 (2015).
74 Portal-Nuñez, S. *et al.* Aryl hydrocarbon receptor-induced adrenomedullin mediates cigarette smoke carcinogenicity in humans and mice. *Cancer research* **72**, 5790-5800, doi:10.1158/0008-5472.CAN-12-0818 (2012).
75 Vorrink, S. U. & Domann, F. E. Regulatory crosstalk and interference between the xenobiotic and hypoxia sensing pathways at the AhR-ARNT-HIF1α signaling node. *Chemico-biological interactions* **218**, 82-88, doi:10.1016/j.cbi.2014.05.001 (2014).
76 Larigot, L., Juricek, L., Dairou, J. & Coumoul, X. AhR signaling pathways and regulatory functions. *Biochimie open*, doi:10.1016/j.biopen.2018.05.001 (2018).
77 Zhang, S., Qin, C. & Safe, S. H. Flavonoids as aryl hydrocarbon receptor agonists/antagonists: effects of structure and cell context. *Environmental health perspectives* **111**, 1877-1882, doi:10.1289/ehp.6322 (2003).
78 Miller, B. R. *et al.* MMPBSA.py: An Efficient Program for End-State Free Energy Calculations. *Journal of Chemical Theory and Computation* **8**, 3314-3321, doi:10.1021/ct300418h (2012).
79 Michel, J., Foloppe, N. & Essex, J. W. Rigorous Free Energy Calculations in Structure-Based Drug Design. *Mol. Inform.* **29**, 570-578, doi:10.1002/minf.201000051 (2010).
80 Granadino-Roldán, J. M. *et al.* Effect of set up protocols on the accuracy of alchemical free energy calculation over a set of ACK1 inhibitors. *PLOS ONE* **14**, e0213217, doi:10.1371/journal.pone.0213217 (2019).
81 Dougherty, E. J. & Pollenz, R. S. Analysis of Ah receptor-ARNT and Ah receptor-ARNT2 complexes in vitro and in cell culture. *Toxicological sciences* **103**, 191-206, doi:10.1093/toxsci/kfm300 (2007).
82 Amezcua, C. A., Harper, S. M., Rutter, J. & Gardner, K. H. Structure and interactions of PAS kinase N-terminal PAS domain: Model for intramolecular kinase regulation. *Structure* **10**, 1349-1361, doi:Pii S0969-2126(02)00857-2
Doi 10.1016/S0969-2126(02)00857-2 (2002).
83 Martinez-Rosell, G., Giorgino, T. & De Fabritiis, G. PlayMolecule ProteinPrepare: A Web Application for Protein Preparation for Molecular Dynamics Simulations. *J Chem Inf Model* **57**, 1511-1516, doi:10.1021/acs.jcim.7b00190 (2017).
84 Pettersen, E. F. *et al.* UCSF Chimera—A visualization system for exploratory research and analysis. *Journal of Computational Chemistry* **25**, 1605-1612, doi:10.1002/jcc.20084 (2004).
85 Maier, J. A. *et al.* ff14SB: Improving the Accuracy of Protein Side Chain and Backbone Parameters from ff99SB. *Journal of Chemical Theory Computation* **11**, 3696-3713, doi:10.1021/acs.jctc.5b00255 (2015).
86 Jakalian, A., Bush, B. L., Jack, D. B. & Bayly, C. I. Fast, efficient generation of high-quality atomic charges. AM1-BCC model: I. Method. *Journal of Computational Chemistry* **21**, 132-146, doi:10.1002/(SICI)1096-987X(20000130)21:2<132::AID-JCC5>3.0.CO;2-P (2000).
87 Jakalian, A., Jack, D. B. & Bayly, C. I. Fast, efficient generation of high-quality atomic charges. AM1-BCC model: II. Parameterization and validation. *Journal of Computational Chemistry* **23**, 1623-1641 (2002).
88 Jiménez, J., Doerr, S., Martínez-Rosell, G., Rose, A. S. & De Fabritiis, G. DeepSite: protein-binding site predictor using 3D-convolutional neural networks. *Bioinformatics* **33**, 3036-3042, doi:10.1093/bioinformatics/btx350 (2017).

Acknowledgements

This work was partially supported by Universidad de Jaén (Acción 1_PIUJA_2017-2018). Technical and human (Ana Jiménez and Ricardo Oya) support provided by CICT of Universidad de Jaén (UJA, MINECO, Junta de Andalucía, FEDER) is gratefully acknowledged.

Author contributions statement

E.S., E.M.L., and F.J.O. conceived the experiments, J.C. and J.M.M. conducted the experiments, J.C, E.S. and E.M.L. analysed the results, J.C. prepared the figures, A.C. and S.B. contributed to discussion and suggestions and performed NO quantification. J.M.G.R. performed the docking analysis, J.C. and E.S. wrote the original draft. All authors reviewed the manuscript.

Additional information

Competing interests: The authors declare no competing interests.

Artículo 3

El hidroxitirosol, uno de los principales fenoles del aceite de oliva, como estrategia terapéutica aguda tras un ictus isquémico

Jesús Calahorra García-Moreno, Justin Shenk, Vera H. Wielenga, Mª Ángeles Peinado Herreros, Eva Siles, Maximilian Wiesmann, Amanda J. Kiliaan

Envío previsto a la revista *Nutrients*

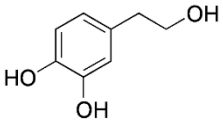

nutrients

MDPI

Article

Hydroxytyrosol, the major phenolic compound of olive oil as acute therapeutic strategy after ischemic stroke

Jesús Calahorra García-Moreno[1], Justin Shenk[2], Vera H. Wielenga[2], Vivienne Verweij[2], Bram Geenen[2], Pieter J. Dederen[2], Mª Ángeles Peinado Herreros, Eva Siles, Maximilian Wiesmann[2]# and Amanda J. Kiliaan[2]#*

[1] Department of Experimental Biology, University of Jaen, Campus Las Lagunillas s/n, Jaen, Spain
[2] Radboud university medical center, Donders Institute for Brain, Cognition & Behaviour, Radboud Alzheimer Center, Department of Anatomy, Preclinical Imaging Centre PRIME, Nijmegen, The Netherlands
* Correspondence: Amanda.kiliaan@radboudumc.nl

 # shared last author

Received: -; Accepted: -; Published: -

Abstract: Stroke is one of the leading causes of adult disability worldwide. After ischemic stroke, damaged tissue surrounding the irreversibly damaged core of the infarct, the penumbra, is still salvageable and therefore a target for acute therapeutic strategies. Mediterranean diet (MD) has been shown to lower stroke risk. MD is characterized by increased intake of extra-virgin olive oil, of which hydroxytyrosol (HT) is the foremost phenolic component. This study investigates the effect of an HT-enriched diet directly after stroke on regain of motor and cognitive functioning, MRI parameters, neuroinflammation and neurogenesis. Stroke mice on HT diet showed increased strength in the forepaws, as well as improved short-term recognition memory probably due to improvement in functional connectivity and increased cerebral blood flow. Moreover, mice on HT diet also showed more doublecortin+ cells in the lesioned hippocampus indicating a novel neurogenic potential of HT. This result was additionally accompanied by an enhanced transcription of the postsynaptic marker Psd-95 and by a decreased IBA-1 level indicative of lower neuroinflamation. These results suggest that a HT-enriched diet could serve as a beneficial therapeutic approach to attenuate ischemic stroke-associated damage.

Keywords: Stroke; Hydroxytyrosol; Dietary treatment; Neuroinflammation; Cerebral Connectivity; Cerebral Blood Flow; MRI; Animal Model

1. Introduction

Stroke is a leading cause of death and long-term disability worldwide. Whereas two-third of stroke deaths occur in less developed countries, it is the second most common cause of death in Europe [1]. Ischemic stroke, caused by obstruction of a blood vessel by for example a thrombus, is the most common type of stroke (80-85%). The neuronal injury after ischemic stroke is caused by the depletion of oxygen and glucose during the ischemic period and, more importantly, by oxidative stress and increase in inflammation along the reperfusion period [2]. Consequently, neurodegeneration especially in the core of the infarct takes place, giving rise to a gradual and continuous deterioration of behavioral and cognitive functions [3,4]. The penumbra, the ischemic boundary zone around the irreversibly injured core, is a potentially salvageable tissue and may be the objective of restorative interventions [5].

Endovascular interventions and intravenous thrombolysis restore brain perfusion and limit the acute effects of stroke. However, no further stroke treatments are available, except for some rehabilitative therapies such as training, progressive task-related practice of skills, and neurostimulation [6]. The decrease of the oxidative stress level, the reduction of the inflammatory processes or the stimulation of neuro- and synaptogenesis are some of the strategies that, particularly when combined, could help to reduce the impact of stroke in the potentially salvageable tissue. A dietary approach could play an essential role in this field. In fact, several studies prove its significance [7]. Our group has already demonstrated that a multinutrient intervention (Fortasyn) containing long chain poly unsaturated fatty acids (LCPUFAS), extra vitamins and antioxidants improve sensorimotor integration, brain integrity and neurogenesis after ischemic stroke induction [8,9]. The PREDIMED trial, which studies the effect of Mediterranean diets in health, has highlighted the positive association between extra virgin olive oil (EVOO) consumption and the risk of stroke in humans [10,11]. This beneficial effect of EVOO has also been shown to be protective in terms of redox homeostatic balance, lipid and protein damage, activation of NO synthase (NOS) in penumbra and reduction of apoptosis level in chronic ischemic models [12-14].

EVOO, obtained by mechanical processes under cold temperatures, is constituted by two fractions: the major saponificable fraction (98%) composed by fatty acids such as oleic acid, and the minor unsaponificable fraction (2%) formed by more than 230 components, among which are the phenolic alcohols [15]. Hydroxytyrosol (HT), together with tyrosol and oleuropein, are the most abundant phenolic alcohols in EVOO [16]. A number of studies have demonstrated that many of the beneficial properties of EVOO are strongly related with HT. This polyphenol has shown numerous biological effects, among others such as antioxidant and anti-inflammatory capacity, antitumour properties and neuroprotective effects [17]. Until now, all studies concerning the neuroprotective effect of HT under ischemic conditions have been carried out ex vivo, using thick brain sections [18-22]. These sections were incubated with different concentrations of HT or extracted from previously treated animals. The results obtained from these experiments, indicate that HT exerts a neuroprotective effect associated with lower release of lactic dehydrogenase, decreased levels of nitrosative and oxidative stress and decrease in inflammation. The neuroprotective effect of this compound in ischemic processes has also been studied in diabetic rats, indicating that its neuroprotective action is not exclusively linked to its antioxidant action.

With this background, the objective of the present study is to longitudinally evaluate till one-month post-stroke, *in vivo* the effect of an HT-enriched diet both on motor and cognitive skills as well as structural and functional MRI outcomes like cerebral blood flow (CBF) and grey and white matter integrity at day 7 and day 35 post-stroke. In addition, metabolic, neurogenic and inflammatory markers were evaluated as well as oxidative levels in serum, in a well-known and broadly used mouse transient middle cerebral artery occlusion (tMCAo) model in order to investigate the potential of HT as acute therapeutic strategy after stroke.

2. Materials and Methods

2.1. Animals

The present study was double-blinded randomized and performed at the Preclinical Imaging Center (PRIME) of the Radboud university medical center (Radboudumc, Nijmegen, The Netherlands) using 28 male 2-3 months old C57BL/6JRj mice (Harlan Laboratories Inc., Horst, the Netherlands). Before tMCAO, the mice had *ad libitum* access to standard food pellets (Ssniff rm/h V1534-000, Bio Services, Uden, the Netherlands) and autoclaved water. The room where the animals were kept had artificial 12h light-dark cycle (lights on at 7 a.m.), humidity and temperature controlled at 21 ± 1℃ and background music playing during the light cycle. All experiments were performed in

accordance with the Dutch federal law for animal experimentation ("Wet op de Dierproeven", 1996) and the regulations of the European Union Directive of 22 September 2010 (2010/63/EU). All experiments were approved by the Animal Ethics Committee of the RadboudUMC (protocol number: RU-DEC 2017-0021) and performed according to the ARRIVE guidelines.

2.2. Transient middle cerebral artery occlusion (tMCAo)

At ~3 months of age, mice underwent transient (30min) occlusion of the right middle cerebral artery (tMCAo), as previously described [9]. Mice were anesthetized with 1.5% isoflurane in a 2:1 (air:oxygen) mixture and were kept under anaesthesia for the duration of the surgery. Just prior to the occlusion procedure, a Laser Doppler probe (moorVMS-LDF2, Moor Instruments, UK) was placed on the skull of the mice to monitor cerebral blood flow (CBF) as an assessment of the efficacy of the occlusion (≥80% loss of CBF). A 7-0 monofilament (190-200µm, coating length 2-3mm, 70SPRePK5, Doccol Corp., Sharon, MA, USA) was inserted in the right carotid cerebral artery (CCA) and pushed upwards to the proximal part of the middle cerebral artery (MCA). The filament occluded the MCA for 30min, after which it was retracted to allow reperfusion. As a control, part of the mice underwent sham surgery instead of tMCAo. In these mice, the filament was immediately retracted after touching the circle of Willis. After surgery, all mice were carefully assessed for pain and other discomforts, weighed every day for 7 days, and food intake was monitored. Exclusion criteria were decreased motor activity (< 50% of the baseline measurements combined from the baseline values of each behavioural test) or extreme weight loss (> 20% within three consecutive days). Using a T2-weighted RARE sequence to measure lesion size and ratio between stroke (right) and unaffected (left) hemispheres, all stroke animals showed a comparable lesion size at 7 days post-stroke and no dietary effect on lesion size (data not shown). Notably, both dietary groups demonstrated atrophy over time visible in a decrease in left-to-right ratio (D7: 0.97±0.03; D35: 0.85±0.08; $F(1,12)=31.3$, $p<0.006$). The time line of the experimental design is illustrated in **Figure 1.**

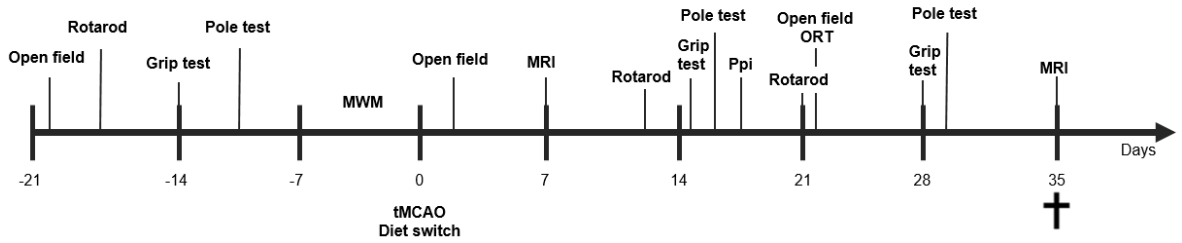

Figure 1. **Study design.** After a transient occlusion of the middle cerebral artery (tMCAo) for 30 min, mice were divided into two dietary groups (Control or HT-enriched). At 7 and 35 days post tMCAo all mice underwent MRI. In between, all mice were tested on motor and cognitive impairments via several behavioral tests, like the Open field, Rotarod, Pole test, Prepulse inhibition (Ppi), grip strength test, and novel object recognition test (ORT). After MRI at day 35, animals were sacrificed, serum samples were recollected and all brains were processed for immunohistochemical stainings and qPCR analysis.

2.3. Group allocation and diet

After stroke, mice were randomly allocated, using a random sequence generator, to one of two diets: an HT-enriched diet (n=13; stroke (n=6), sham (n=7)) or an isocaloric control diet (n=15; stroke (n=8), sham (n=7)). Group sizes were calculated according to effect sizes (p=0.05, statistical power: 0.80), exclusion and mortality rates previously determined by a similar study of our group [9]. Both diets contained 24.0% kcal protein, 15.0% kcal fat, and 61.0% kcal carbohydrates (Research Diet Services B.V., Wijk bij Duurstede, The Netherlands), based on a previous study from another group

[23-25]. The HT-enriched diet was supplied with 0.03g% HT (Seprox Biotech, Spain). Food intake and body weight was measured before and during the weeks after surgery.

2.4. Open Field

Mice were placed in a square open field (45 x 45 x 30cm) for 10 min to assess locomotion and explorative behaviour. The open field test was performed three times: once prior to surgery, at 3 days and at 21 days postsurgery. Locomotion was automatically recorded, using EthoVision XT 10.1 (Noldus, Wageningen, The Netherlands). In EthoVision, the floor of the open field arena was divided in zones to distinguish the periphery, corners and center. The frequency of entered these zones was automatically recorded. Additionally, manual scoring of exploratory behaviours (sitting, walking, grooming, wall-leaning, rearing, jumping) was performed, as previously described [26]. No mice were excluded from statistical analysis.

2.5. Grip test

Grip strength of the mice was measured with a grip strength meter (Grip Strength Meter, 47200, Ugo Basile, Italy) at three time points: pre-stroke, and day 15 and day 29 (post-stroke). Mice were held by their tail so they could grab a trapeze or grid (connected to the grip strength meter) to measure, respectively, muscle strength in the fore limbs (trapeze) or strength in all four limbs collectively (grid). Trials in which mice grabbed the trapeze with only one forepaw or the grid with less than four paws, were excluded. Additionally, trials in which the mouse grabbed the side of the trapeze were also excluded. The maximum value of peak force (in gram per force (gf)) was averaged per experimental group for both trapeze and grid. No animals were excluded from statistical analysis.

2.6. Pole test

The pole test is a measure for motor dysfunction. It was performed pre-stroke, and post stroke at day 14 and day 28. The mouse was placed vertically on a pole with its head pointed upwards and had to turn 180 degrees to walk down the pole. The time needed to fully turn 180 degrees (turning time) and the turning direction were manually recorded. Additionally, video recordings of each trial were automatically analysed with EthoVision XT 10.1 (Noldus, Wageningen, The Netherlands) to calculate the velocity (cm/s) with which the mouse walked down the pole. Trials that were excluded from statistical analysis consisted of: every first trial of a mouse (acclimatization), trials in which the mouse was already turning when placed on the pole, and trials in which the mouse showed no motivation and was assisted by the researcher to go down. In total three stroke mice (HT, n=1; Control, n=2) were excluded from statistical analysis due to technical issues.

2.7. Rotarod

Rotarod was performed as a measure of balance, coordination, physical condition and motor planning presurgery, and at day 10 and day 21 postsurgery. The mice were placed on the Rotarod (ITC LifeScience INC., Woodland Hills, CA, USA) and left to acclimatize for 10-30 sec. Then the Rotarod was turned on to accelerate for 300 sec from 4 to 40 rpm. The latency time to fall was recorded. One mouse (Stroke-control diet group) was excluded from statistical analysis due to technical issues. No significant effects (data not shown) were found.

2.8. Prepulse inhibition (Ppi)

The prepulse inhibition (Ppi) test was performed 16 days post-stroke to examine the sensorimotor gating integration of the mice, as previously described [27]. To measure the startle

reactivity, the mouse was placed in a restrainer in the chamber of the SR-LAB startle response system (San Diego Instruments, San Diego, CA, USA) and exposed to blocks of startle pulses. Prepulse inhibition was calculated during the second blok of startle pulses as 100 - reponse to starte pulse after prepulse/response to startle pulse x 100%. Additionally, habituation to startle pulses was investigated by comparing the startle response to the first startle pulse block to the startle response in the third (last) startle pulse block. One sham-HT mouse and one stroke-control mouse was excluded from statistical analysis.

2.9. Morris water maze (MWM)

The Morris water maze (MWM) was used to test spatial learning and memory in rodents. In short, before surgery all mice were placed in a circular pool, filled with opaque water, and were trained to find a submerged platform in the northeast (NE) quadrant of the pool by using distant visual cues. At the end of the fourth day, mice performed additionally a single probe trial, in which the platform was removed from the swimming pool. Mice were allowed to swim for 120 s and the time spent swimming and searching in the NE quadrant (where the platform had been located) was recorded. The MWM is used to analyze spatial learning and memory before surgery (data not shown). All mice learned to find the hidden platform revealed by a decrease in latency time from acquisition day 1 to day 4 (-16.33s±5.68s; $F(3,81)=3.8$, $p<0.013$).

2.10. Novel object recognition test (ORT)

Short-term memory of the mice was measured with the novel object recognition test (ORT), as previously described [9]. This test spanned over 3 days. On the first day, mice were acclimatized to the open field box by letting them explore freely for 10min. On the second and third day, mice underwent object recognition trials. First, mice performed a familiarization trial. In this trial two identical objects (eggs, tea light holders, yellow plastic ice cream cones, or bottles filled with sand) (F1 and F2) were placed in the open field, equidistant from the center, and the mouse was then placed in the open field to freely explore the objects for 4 minutes. After a certain delay (30 min on day 2 and 60 min on day 3) the trial was repeated, with one of the familiar objects (F3) and one object replaced for a novel object (N1). Exploratory behaviour of the mice was measured using EthoVision XT 10.1 (Noldus, Wageningen, The Netherlands) as direct contact with the object, or movement within a 2cm diameter around the object.

To measure object recognition, several indexes were calculated in both the familiarization and the test phase. In the test phase, discrimination between objects was calculated with the discrimination index (DI), as the time spend around N1 minus F3, divided by the time spend around both objects (DI = (N1-F3)/(N1+F3)). From this index, a number between +1 and -1 is obtained, where closer to +1 shows more time spend around N1, closer to -1 more time spend around F3, and 0 shows no difference in time spend at either object. To measure recognition memory, the recognition index (RI) was calculated as the time spend around N1 as a fraction of the time spend around both objects (RI = N1/(N1+F3)). The preference for either object was calculated with the preference index (PI), as time the mouse spend around N1 (or F3) as a percentage of the time spend around both objects (PI = 100 x ([N1 or F3]/(N1+F3)). If N1 is the numerator, closer to 100% indicates preference for N1, 50% indicates no preference, and below 50% preference for F3 (vice versa if F3 is the numerator) [28]. One sham-control mouse and one stroke-HT mouse were excluded from statistical analysis.

2.11. In vivo magnetic resonance imaging (MRI)

MRI measurements were performed 7 and 35 days after surgery with an 11.7T BioSpec Avance III small animal MR system (Bruker BioSpin, Ettlingen, Germany) operating on Paravision 6.0.1. software (Bruker, Karlsruhe, Germany) under full isoflurane anaesthesia (3.5% for induction and

1.8% for maintenance; in a 2:1 (medical air:oxygen) mixture). Body temperature was monitored with a rectal probe, and maintained at 37°C using hot air flow. A pneumatic cushion respiratory monitoring system (Small Animal Instruments Inc, NY, USA) was used to measure the respiration rate of the mouse. Mice with scans that showed motion and/or echo planar imaging artifacts were excluded from MRI analysis.

2.12. Arterial spin labelling (ASL)

To assess cerebral blood flow (CBF), perfusion imaging was performed using a flow sensitive alternating inversion recovery arterial (FAIR) technique as previously described [5,9]. Hippocampus, cerebral cortex and thalamus, according to the Paxinos and Franklin atlas [30], were analysed as regions of interest (ROI) by a researcher blinded to the surgery and treatment groups. For each ROI, CBF was analysed in the affected (ipsilateral/right) and unaffected (contralateral/left) hemisphere separately for each group. One sham-HT, one stroke-control and two stroke-HT mice were excluded from statistical analysis due to EPI/movement artefacts.

2.13. Diffusion tensor imaging (DTI)

Diffusion of water was imaged as described previously [31-33]. In short, 22 axial slices covering the whole brain were acquired with a four-shot SE-EPI protocol. B0 shift compensation, navigator echoes and an automatic correction algorithm to limit the occurrence of ghosts and artefacts were implemented. Encoding b-factors of 0 s/mm^2 (b0 images; 5×) and 1000 s/mm^2 were used and diffusion-sensitizing gradients were applied along 30 non-collinear directions in three-dimensional space. The diffusion tensor was estimated for every voxel using the PATCH algorithm [34]; mean water diffusivity (MD) and fractional anisotropy (FA) were derived from the tensor estimation following a protocol as described elsewhere [33]. MD and FA values were measured in several white matter (WM) and grey matter (GM) areas, manually selected based on an anatomical atlas [35].

2.14. Resting state functional MRI (rs-fMRI)

Subsequently after the acquisition of the anatomical reference images, resting state fMRI (rsfMRI) datasets were acquired using a single-shot spin-echo sequence with echo-planar readout (SE-EPI) sequence. Six hundred repetitions with a repetition time (TR) of 1.8 s and echo time of 16.9 ms were recorded for a total acquisition time of 18 min. The rsfMRI datasets were first realigned using a least-squares method and rigid-body transformation with Statistical Parametric Mapping (SPM) mouse toolbox (SPM5, University College London; http://www.fil.ion.ucl.ac.uk/spm/; Sawiak *et al.*, 2009). Mean and maximum displacement across the six degrees of freedom (along the x-, y-, and z-axes and on three rotation parameters pitch, roll, and yaw) were measured in each mouse. The mean SE-EPI images for each mouse were then used to generate a study-specific template through linear affine and nonlinear diffeomorphic transformation (ANTs. v1.9; http://picsl.upenn.edu/ANTS/). Visual inspection of the normalised dataset was performed to screen for possible normalization biases. On the template, 12 areas were selected in left and right hemisphere. The selected regions were based on previous work concerning functional connectivity in mice [36], and included: left and right dorsal hippocampus, left and right ventral hippocampus, left and right auditory cortex, left and right motor cortex, left and right somatosensory cortex, and left and right visual cortex. All cortical ROIs were selected 1–2 voxels away from the edge of the cortex, to minimise the impact of susceptibility artefacts, which are more prominent in areas close to tissue interfaces (e.g., near the skull or near the ear canals). In-plane spatial smoothing (0.4 × 0.4 mm), linear detrending, and temporal high-pass filtering (cut-off at 0.01 Hz) were applied to compensate for small across-mouse misregistration and temporal low-frequency noise. Functional connectivity (FC) group comparison between ROIs were calculated from the BOLD time series using total and partial correlation analyses

implemented in FSLNets (FSLNets v0.3; www.fmrib.ox.ac.uk/fsl). Pearson's correlation values were Fisher transformed to Z-scores for group comparisons and statistical analysis. Statistical results for both total and partial correlations can be found in the supplementary material.

2.15. qPCR

RNA was isolated from frontal parts (divided in to left and right) of the brain (Bregma: −0.10 to 4.28 using TRIzol method (Thermo Scientific, Waltham, USA). The samples were treated with RNase-free DNase I (RQ1, Promega, Fitchburg, USA) to eliminate any genomic DNA. cDNA was synthesized using the iScript kit (Bio-Rad, Hercules, USA). qPCR was done in 96-well plates (Thermo Scientific) using a StepOnePlus system (Thermo Scientific). Gene expression of postsynaptic density protein 95 (Psd-95) and brain derived neurotrophic factor (Bdnf) were quantitatively assessed by using hypoxanthine guanine phosphoribosyl transferase (Hprt) and beta-2 microglobulin (B2m) as the normalizing genes. The sequences of primers are shown in Table 1.

2.16. (Immuno)histochemistry

After the last scanning session, the mice were sacrificed by transcardial perfusion using 0.1M phosphate-buffered saline (PBS) followed by 4% paraformaldehyde in 0.1M PBS. The brains were harvested and stored separately. The brains were postfixed overnight in 4% paraformaldehyde at 4°C and transferred to 0.1M PBS containing 0.01% sodium azide the next day. One part of the brain (Bregma: -0.1-4.36) was cut in 30 μm frontal sections using a sliding microtome (Microm HC 440, Walldorf, Germany) equipped with an object table for freeze-sectioning at -60°C. 24 Hours before cutting, the brains were transferred in 30% sucrose in 0.1M phosphate buffer. 8 Series were cut and stored in 0.1M PBS with 0.01% sodium azide so multiple immunohistochemical stainings could be performed.

All sections were stained in one session to minimize differences in staining intensity. In total two stainings were performed for activated microglia via ionized calcium-binding adapter molecule 1 (IBA-1) as indicator for neuroinflammation, and for immature neurons (measure for neurogenesis) with antibodies against doublecortin (DCX) on free-floating brain sections on shaker tables at room temperature. Immunohistochemistry was performed using standard free-floating labelling procedures, using previously described protocols [37]. For IBA-1, as primary antibody against IBA-1 polyclonal goat anti-IBA-1 (1:3000; Abcam) and for DCX, polyclonal goat anti-DCX (1:8000; Santa Cruz Biotechnology Inc., Santa Cruz, CA, USA) was used as a primary antibody to assess neurogenesis. For both as secondary antibody donkey anti-goat biotin (1:1500; Jackson ImmunoResearch, West Grove, PA, USA) was used. From a more frontal part of the brain tissue (Bregma: -0.10 to 0.98) was fixed in 4% paraformaldehyde in 0.1 M phosphate buffer (pH 7.4) and embedded in paraffin according to a standard protocol.

2.17. Quantification (IBA-1, and DCX)

Brain sections (Bregma: -1.46 to -2.30) were preselected for quantification accordingly to the atlas of Franklin and Paxinos [30]. Quantification was done on images at a 5x objective using an Axio Imager A2 (Zeiss Germany). ImageJ (National Institute of Health, Bethesda, MD, USA) was used to analyze the regions of interest (IBA-1: Cortex, Caudate Putamen and Corpus Callosum; DCX: Hippocampus).

2.18. Determination of Serum NO Level

Nitric oxide production was indirectly quantified by determining nitrate/nitrite and S-nitroso compounds (NOx), using an ozone chemiluminescence-based assay adapted to serum samples [38,39]. In brief, serum samples were deproteinized with 0.8 N NaOH and 16% ZnSO4 solutions (1/0.5/0.5). After centrifugation at 10,000g for 5 minutes, the resulting supernatants were removed for chemiluminescence analysis [40] in an NO analyzer (NOA 280i; Sievers Instrumments, Boulder, CO). NOx concentration was calculated by comparison with standard solutions of sodium nitrate. Final NOx values were expressed as μM.

2.19. Determination of Serum Oxidative Stress Level

Thiobarbituric acid reactive substances (TBARS), a major indicator of oxidative stress, was determined using an adaptation of the method described by Buege and Aust [41]. Specifically, 8% sodium dodecyl sulfate was added (1:1) to each serum sample. Samples were vortexed and mixed (1:6) with a reagent containing 15% trichloroacetic acid, 0.38% thiobarbituric acid, and 2% HCl and then heated for 30 minutes at 96°C, cooled, and centrifuged (3000g for 5 minutes). The supernatants were collected, and the absorbance was measured at 532 nm. The concentration of TBARS was determined by extrapolation from a malondialdehyde standard curve. Results were expressed as μM.

2.20. Statistical Analyses

A random and blinded selection procedure was maintained throughout the study. Group means were compared using univariate analysis of variance (ANOVA) with Bonferroni correction for multiple testing with a statistical program, SPSS 24 (IBM SPSS Statistics 24, IBM Corporation, Armonk, NY, USA). Parameter correlation tests were performed using Pearson correlations. Nonparametric tests were used when assumptions of normality and homogeneity of variance were not met. p-values lower than 0.05 were considered significant. Data are presented as mean ± SEM.

3. Results

3.1. Food intake and body weight

Body weight (**Figure 2A)** of sham mice did not decrease over time comparing presurgery and the first week after surgery ($F(1,12)=3.3$, $p<.095$), while body weight of both dietary stroke groups decreased post-stroke versus pre-stroke ($F(1,12)=18.2$, $p<.002$). Food intake **(Figure 2B)** of both stroke and sham mice decreased over time comparing presurgery and the first week after surgery (Stroke: $F(1,12)=19.8$, $p<.001$; Sham: $F(1,12)=40.5$, $p<.001$).

Investigating the development over time of body weight and food intake, these parameters were weekly analyzed after the surgery. Sham mice showed a significant time interaction in body weight ($F(1,48)=14.5$, $p<.001$) and also in food intake ($F(1,48)=16.5$, $p<.001$). In detail, sham mice lost body weight comparing week 1 with week 2 ($p<.001$), while this effect was not present in the upcoming weeks comparing week 2 with week 3, week 3 with week 4, and week 4 with week 5. Sham mice had a lowered food intake comparing week 1 to week 2 ($p<.006$) and also week 3 to week 4 ($p<.009$). Notably, sham mice on HT diet had a higher food intake during all postsurgery weeks than sham mice on control diet ($F(1,12)=5.3$, $p<.041$). Stroke mice demonstrated a time interaction in food intake ($F(1,48)=10.2$, $p<.001$). After deeper statistical analysis, stroke mice ate less comparing week 1 with week 2 ($p<.025$) and started to eat more comparing week 2 with 3 ($p<.008$).

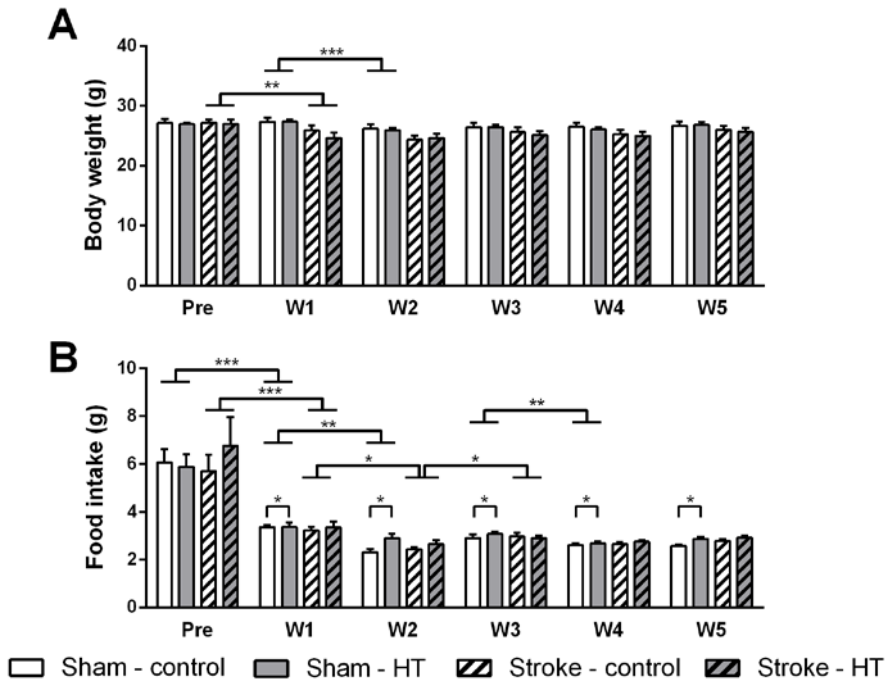

Figure 2. **Effect of HT-diet on body weight and food intake**. (A) Body weight of both dietary stroke groups decreased post-stroke versus pre-stroke (p<.002). Sham mice lost body weight comparing week 1 with week 2 (p<.001), with no effect in the upcoming weeks. (B) Food intake of both stroke and sham mice decreased over time comparing presurgery and the first week after surgery (Sham: p<.001; Stroke: p<.001). Sham mice had a lower food intake comparing week 1 to week 2 (p<.006) and also week 3 to week 4 (p<.009). Sham mice on HT diet had a higher food intake during all postsurgery weeks than sham mice on control diet (p<.041). Stroke mice ate less comparing week 1 with week 2 (p<.025) and started to eat more comparing week 2 with 3 (p<.008). Only sham mice showed a significant time interaction in body weight (p<.001) and in food intake (p<.001). Values represent mean ± SEM. *p<0.05, **p<0.01, ***p<0.001.

3.2. Behaviour, cognition and motor tasks

3.2.1. Open field

At 3 days postsurgery, all sham and all stroke mice moved a shorter distance (Sham: $F(1,12)=137.1$, $p<0.001$; Stroke: $F(1,12)=116.2$, $p<0.001$) **(Figure 3A)** and with a lower velocity (Sham: $F(1,12)=99.4$, $p<0.001$; Stroke: $F(1,12)=116.5$, $p<0.001$) in the arena **(Figure 3B)**, compared to baseline. At 21 days post-surgery, sham animals walked more in the open field compared to 3 days post-surgery ($F(1,12)=17.1$, $p<0.002$), however stroke animals did not **(Figure 3A)**. No diet effects were observed in distance moved and velocity in the open field.

Anxiety and exploration were assessed by tracking the position of the mice in the open field (center, corners, periphery). Compared to baseline, stroke mice visited the center ($F(1,12)=60.7$, $p<0.001$), periphery ($F(1,12)=230.2$, $p<0.001$) and corners ($F(1,12)=85.5$, $p<0.001$) less frequently at 3 days post-stroke **(Figure 3C)**, but showed no change in time spent at all locations **(Figure 3D)**. Sham animals also visited the periphery ($F(1,12)=73.4$, $p<0.001$) and corners ($F(1,12)=172.0$, $p<0.001$) less frequently at 3 days post-stroke compared to baseline **(Figure 3C)**, however they spent less time in the corners ($F(1,12)=6.7$, $p<0.024$) at 3 days **(Figure 3D)**. No diets effects were observed in these parameters.

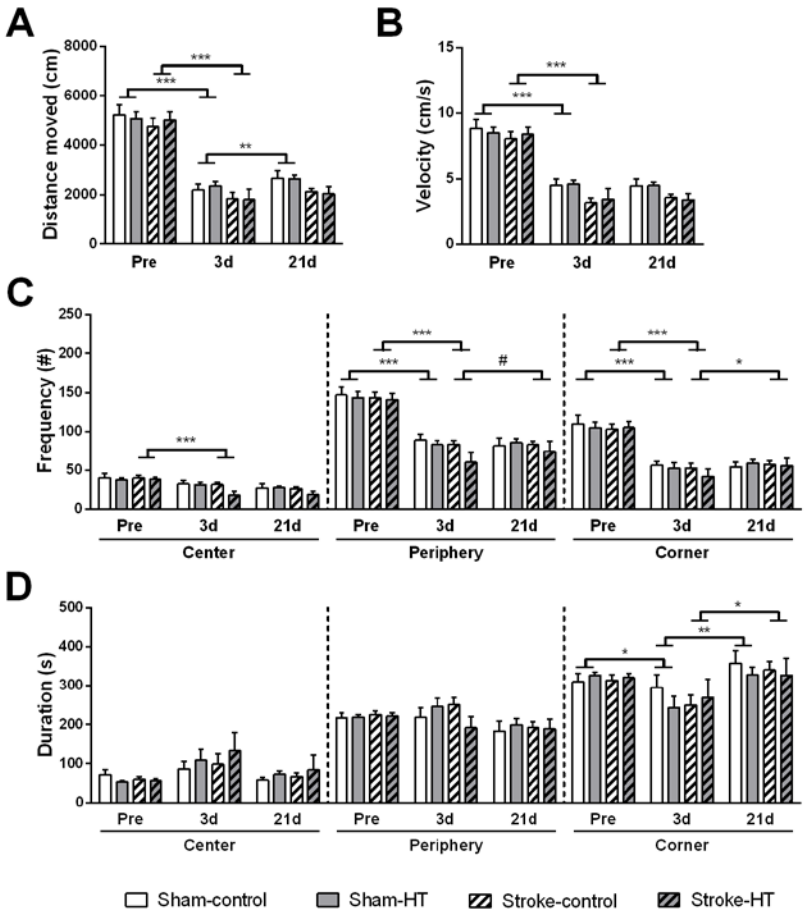

Figure 3. Activity, anxiety and explorative behavior measured in open field prior to stroke, and at 3 and 21 days post-stroke. Locomotion was assessed by evaluating (A) the distance moved and (B) the velocity. Anxiety and exploration were evaluated by tracking (C) the frequency and (D) the time spent in the different zones in the arena (center, periphery and corner). (A,B) At 3 days postsurgery, all sham and all stroke mice moved a shorter distance (Sham: $p<0.001$; Stroke: $p<0.001$) with lower velocity (Sham: $p<0.001$; Stroke: $p<0.001$) compared to baseline. At 21 days post-stroke, sham animals walked more in the open field compared to 3 days post-stroke animals ($p<0.002$). (C-D) Stroke mice visited the center ($p<0.001$), periphery ($p<0.001$) and corners ($p<0.001$) less frequently at 3 days post-stroke. Sham animals also visited the periphery ($p<0.001$) and corners ($p<0.001$) less frequently at 3 days post-stroke compared to baseline, however they spent less time in the corners ($p<0.024$) at 3 days. Values represent mean ± SEM. # $0.05<p<0.08$, *$p<0.05$, **$p<0.01$, ***$p<0.001$.

The frequency with which the mice engaged in different types of exploratory behavior was manually scored **(Figure 4)**. Compared to baseline, all mice showed decreased frequency of wall leaning (Sham: $F(1,12)=64.5$, $p<0.001$; Stroke: $F(1,12)=258.1$, $p<0.001$) and walking (Sham: $F(1,12)=26.7$, $p<0.001$; Stroke: $F(1,12)=157.3$, $p<0.001$) and also spent less time performing these behaviors (*Wall leaning*: Sham: $F(1,12)=123.0$, $p<0.001$; Stroke: $F(1,12)=78.1$, $p<0.001$; *Walking*: Sham: $F(1,12)=84.2$, $p<0.001$; Stroke: $F(1,12)=40.3$, $p<0.001$) at 3 days post-stroke, while they spent more time sitting (Sham: $F(1,12)=172.4$, $p<0.001$; Stroke: $F(1,12)=62.3$) and grooming (Sham: $F(1,12)=6.2$, $p<0.028$). At baseline and 3 days post-stroke, sham-HT mice groomed less frequently than sham-control mice ($F(1,12)=5.6$, $p<0.036$; *not shown in graph*). Additionally, stroke mice also reared less frequently at 3 days compared to pre-stroke ($F(1,12)=8.6$, $p<0.012$). At 21 days post-stroke, walking frequency ($F(1,12)=6.4$, $p<0.026$) was even further decreased in sham mice, whereas stroke mice showed no change in walking frequency or duration, but did show increased rearing frequency ($F(1,12)=8.6$, $p<0.012$) and wall leaning frequency ($F(1,12)=7.2$, $p<0.020$). Sham mice groomed more frequently at 21 days compared

to 3 days post-stroke ($F(1,12)=12.3$, $p<0.004$). No additional diet effects were found in these parameters **(Figure 4)**.

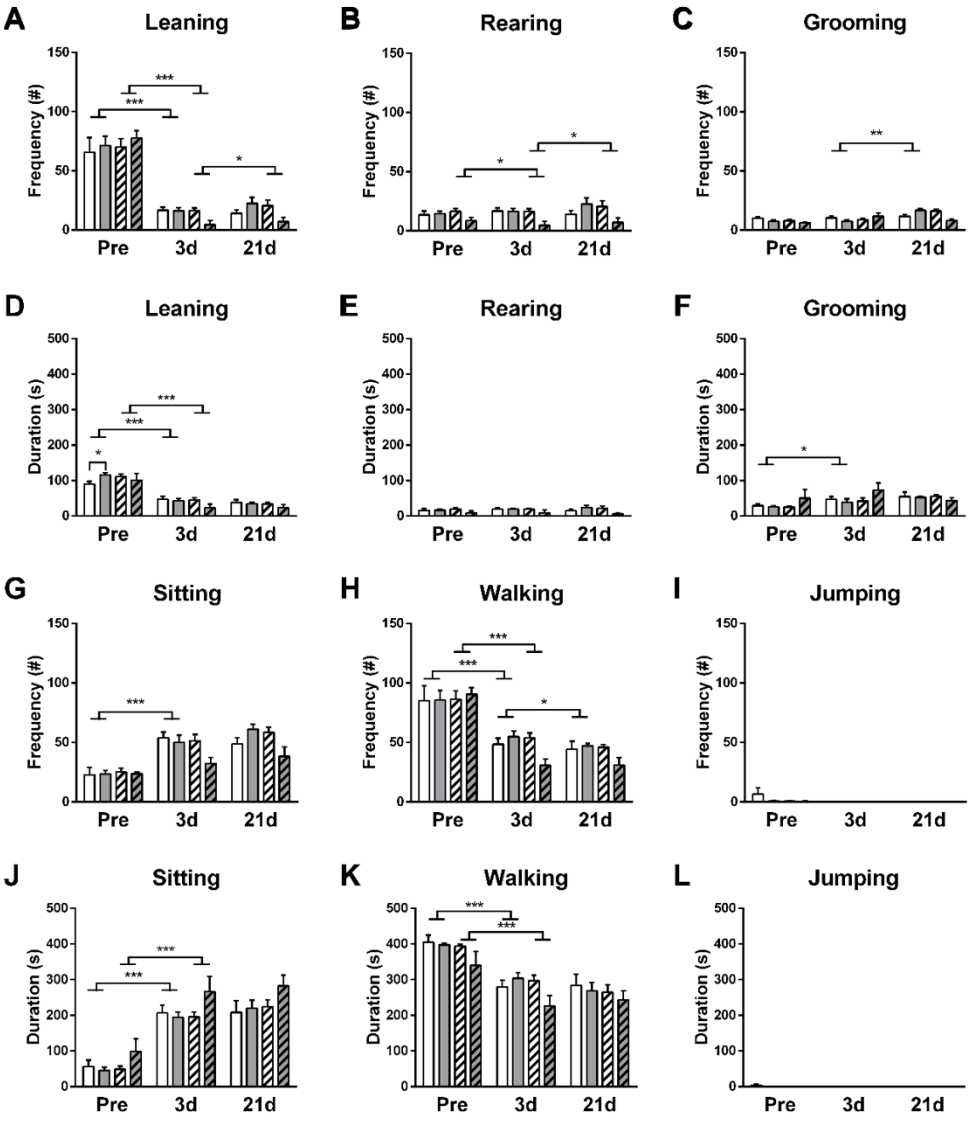

Figure 4. Behaviors in the open field. The behaviors of the mice in the arena during the open field were manually scored as another measure of locomotion, activity and explorative behavior. (A-C, G-I) Frequency and (D-F, J-L) duration of leaning, rearing, grooming, sitting, walking and jumping were quantified presurgery and 3 and 21 days after surgery. (A,H) All mice showed decreased frequency of wall leaning (Sham: $p<0.001$; Stroke: $p<0.001$) and walking (Sham: $p<0.001$; Stroke: $p<0.001$) and (D,K) also spent less time performing these behaviors (Wall leaning: Sham: $p<0.001$; Stroke: $p<0.001$; Walking: Sham: $p<0.001$; Stroke: $p<0.001$) at 3 days post-stroke, (J,F) while they spent more time sitting (Sham: $p<0.001$) and grooming (Sham: $p<0.028$). (C) At baseline and 3 days post-stroke, sham-HT mice groomed less frequently than sham-control mice ($p<0.036$; not shown in graph). (B) Stroke mice also reared less frequently at 3 days compared to pre-stroke ($p<0.012$). (H,D) At 21 days post-stroke, walking frequency ($p<0.026$) was even further decreased in sham mice, (A,B) whereas stroke show increased rearing frequency ($p<0.012$) and wall leaning frequency ($p<0.020$). (C,F) Sham mice groomed more frequently at 21 days compared to 3 days post-stroke ($p<0.004$). Values represent mean ± SEM. # $0.05<p<0.08$, *$p<0.05$, **$p<0.01$, ***$p<0.001$.

3.2.2. Grip test

Forelimb strength of the mice was quantified with the grip test, by letting the mice grip a small trapeze connected to a grip strength meter. Fore- and hind limb strength was determined in a similar fashion, using a grid instead of a trapeze. At week 2, only sham mice showed a lower grip strength on the grid compared to pre-surgery ($F(1,12)=13.0$, $p<0.004$) **(Figure 5A)**. Stroke mice showed no significant decreased grip strength on either the trapeze or grid 2 weeks after stroke compared to baseline. A surgery effect was observed at week 2, shown by weaker grip strength in forelimbs in stroke-control mice compared to sham-control mice ($F(1,9)=17.3$, $p<0.002$) **(Figure 5A)**. At 4 weeks postsurgery, sham mice show a decreased forelimb grip strength compared to 2 weeks postsurgery ($F(1,10)=26.0$, $p<0.001$) **(Figure 5A).** Interestingly, HT-fed stroke mice demonstrated a higher grip strength on the trapeze at week 2 and 4 compared to stroke control diet-mice ($F(1,12)=497.0$, $p<0.018$). No diet effects were observed on the grid **(Figure 5B)**.

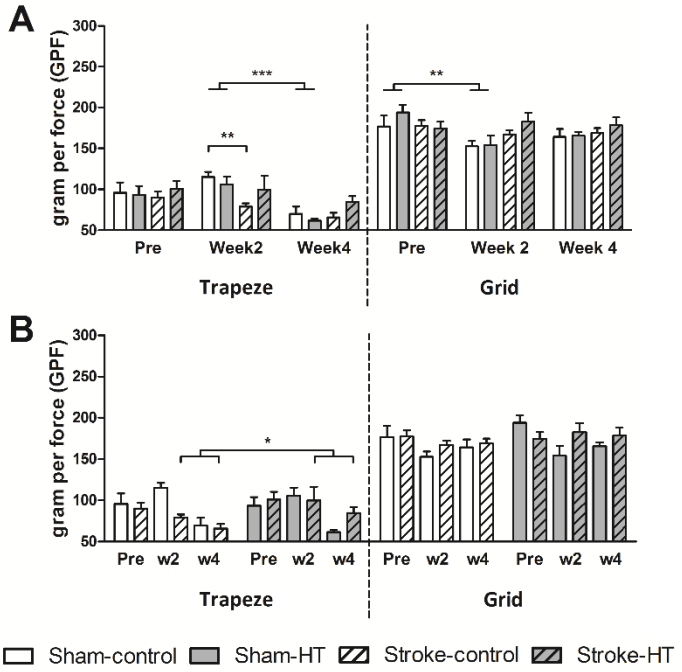

Figure 5. Strength in the forelimbs (trapeze) and in all four paws (grid) before (pre) and after (week 2 and 4) stroke. (A) Time effects and (B) diet effects on maximum grip strength are shown. (A) At week 2, sham mice showed a lower grip strength on the grid compared to pre-surgery ($p<0.004$). A surgery effect was observed at week 2, shown by weaker grip strength in forelimbs in stroke-control mice compared to sham-control mice ($p<0.002$). At 4 weeks postsurgery, sham mice showed a decreased forelimb grip strength compared to 2 weeks postsurgery ($p<0.001$). (B) HT-fed stroke mice demonstrated a higher grip strength on the trapeze at week 2 and 4 compared to stroke control diet-mice ($p<0.018$). Values represent mean ± SEM. *$p<0.05$, **$p<0.01$, ***$p<0.001$.

3.2.3. Pole test

The pole test was performed to assess motor dysfunction. The time needed to make a full 180 degree turn on the pole and the turning direction was manually scored, and the velocity with which the mice walked down the pole was calculated. There was no change in velocity between baseline measurement and the first measurement after surgery (at 14 days). At 28 days postsurgery, sham mice ($F(1,12)=21.4$, $p<0.001$) and stroke mice ($F(1,9)=5.2$, $p<0.049$) walked down the pole with a lower velocity compared to 14 days postsurgery **(Figure 6)**. Neither time nor diet effects on turning side preference or turning time were observed.

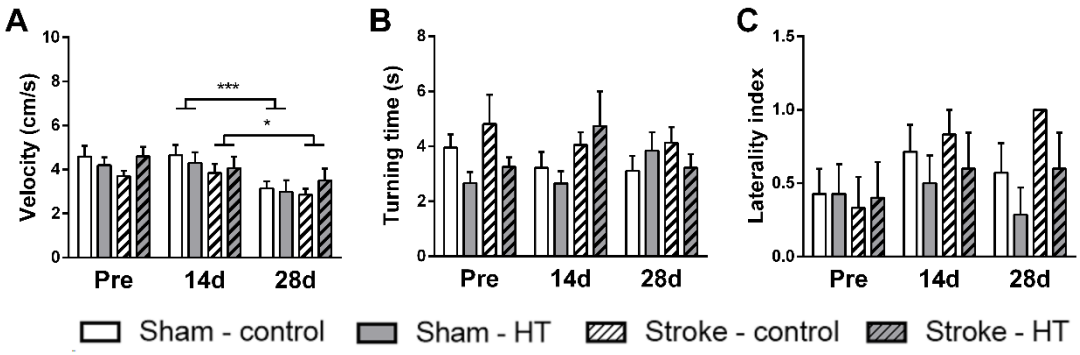

Figure 6. Motor coordination assessed pre-stroke and 14 days and 28 days post-stroke by the pole test. (A) Downwards walking velocity. (B) Time to turn around on the pole (turning time) and (C) tendency to turn right vs left (laterally index). (A) At 28 days postsurgery, sham mice ($p<0.001$) and stroke mice ($p<0.049$) walked down the pole with a lower velocity compared to 14 days postsurgery. Values represent mean ± SEM. Values represent mean ± SEM. # $0.05<p<0.08$, *$p<0.05$, ***$p<0.001$.

3.2.4. Prepulse inhibition (Ppi)

The pre-pulse inhibition test was performed to assess sensorimotor gating after stroke. In both surgery and diet groups, no effects could be detected on PPI. No habituation effects were observed, however an overall diet effect was detected. HT-mice showed a higher startle amplitude to the basal and final startle stimulus of 120dB than control-mice ($F(1,22)=8.3$, $p<0.009$) **(Figure 7)**.

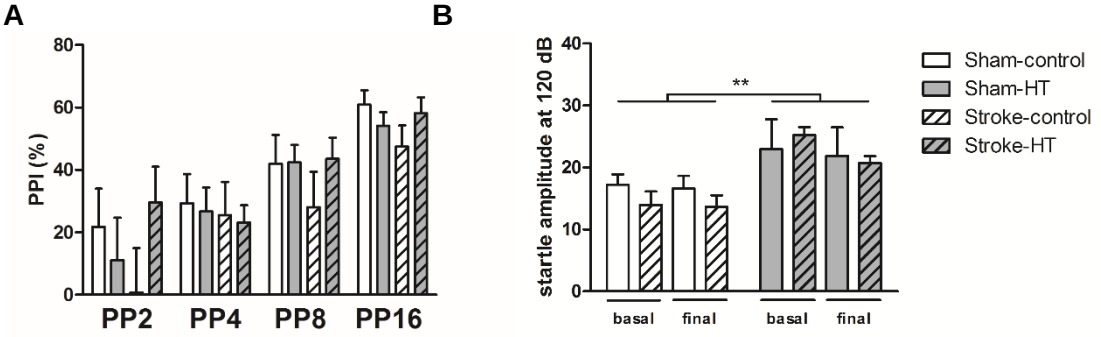

Figure 7. **Sensorimotor integration measured before and after (16 days) stroke induction by the prepulse inhibition test (PPI).** (A) PPI data shown as percentage. (B) Habituation to startle pulse. HT-mice showed a higher startle amplitude to the basal and final startle stimulus of 120dB than control-mice ($p<0.009$). Values represent mean ± SEM. **$p<0.01$.

3.2.5. Novel object recognition test (ORT)

The object recognition task (ORT) was performed once after stroke to measure short-term memory of the mice. In the 30min trials of the familiarization phase, all discrimination index (DI), recognition index (RI) and preference index (PI) all showed that stroke animals have a preference for object 2 and sham animals a preference for object 1, as they visited it more frequently ($F(1,22)=5.7$, $p<0.026$). However, in stroke animals this effect was largely caused by mice on control diet, as they only showed as PI above 50% **(Figure 8)**. In the 30min trials of the test phase, HT-fed animals showed a preference for the novel object and visited it more frequently than control diet-animals ($F(1,22)=6.4$, $p<0.019$), as shown by all indexes (DI, RI and PI) **(Figure 9)**.

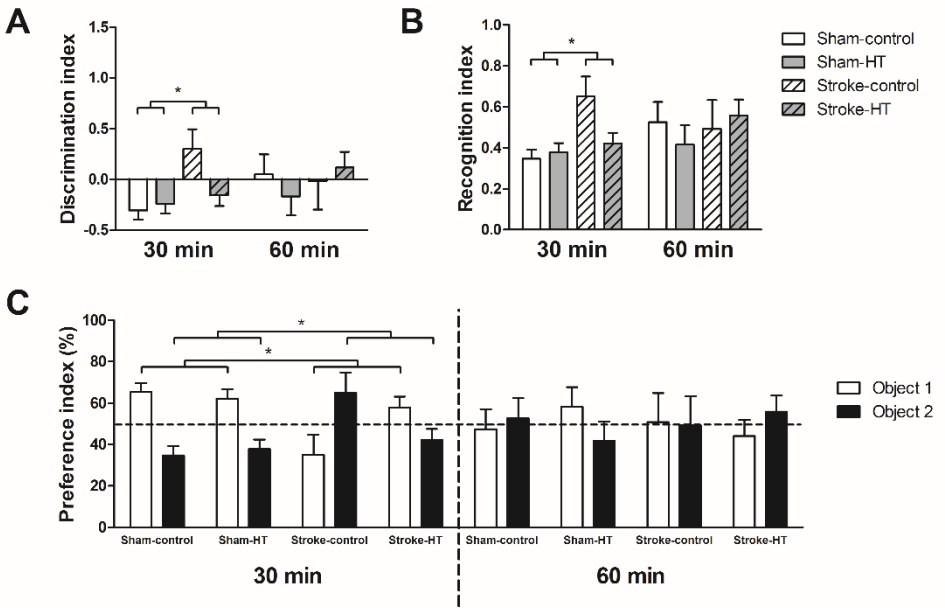

Figure 8. Familiarization phase ORT. Short-term memory of sham and stroke mice assessed by the novel object recognition test (ORT). (A) Discrimination index (B) Recognition index and (C) preference index. (A,B,C) Stroke animals had a preference for object 2 and sham animals a preference for object 1 ($p<0.026$). Values represent mean ± SEM. *$p<0.05$.

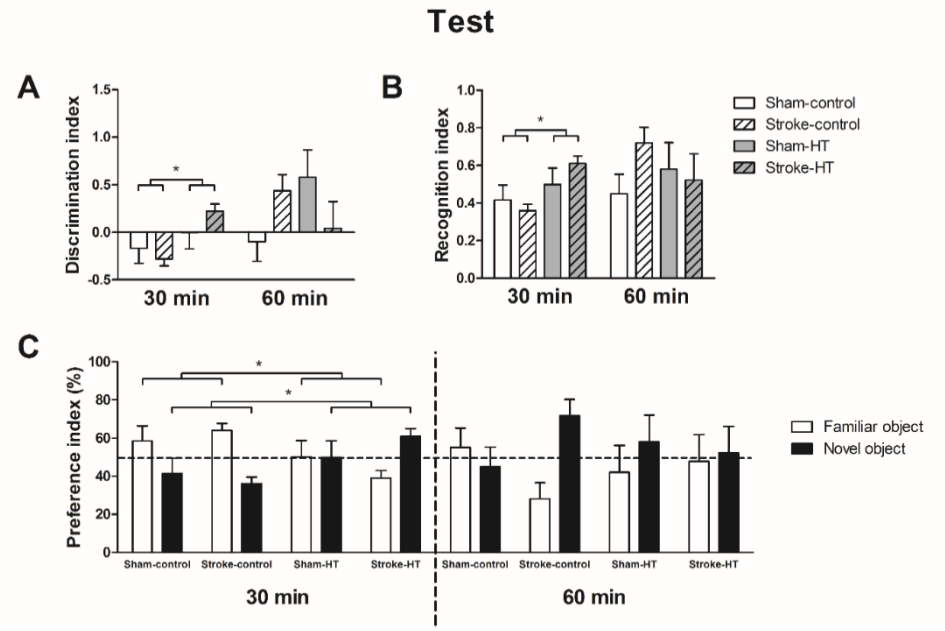

Figure 9. Test phase ORT. Short-term memory of sham and stroke mice assessed by the novel object recognition test (ORT). (A) Discrimination index (B) Recognition index and (C) preference index. (A,B,C) HT-fed animals showed a preference for the novel object and visited it more frequently than control diet-animals ($p<0.019$). Values represent mean ± SEM. *$p<0.05$.

3.3. In vivo magnetic resonance imaging (MRI)

3.3.1. Cerebral Blood Flow (CBF)

Using an ASL-FAIR technique, CBF was assessed in the lesioned and unlesioned hemisphere at 7 and 35 days post-stroke in the hippocampus, thalamus and cortex **(Figure 10)**. At 7 days post-stroke, CBF was lower in all groups in the right cortex (Sham-control: $F(1,6)=24.9$, $p<0.002$; Sham-HT: $F(1,5)=24.5$, $p<0.004$; Stroke-control: $F(1,6)=16.1$, $p<0.007$; Stroke-HT: $F(1,4)=12.6$, $p<0.024$), right hippocampus (Sham-control: $F(1,6)=24.2$, $p<0.003$; Sham-HT: $F(1,5)=50.5$, $p<0.001$; Stroke-control: $F(1,6)=70.1$, $p<0.001$; Stroke-HT: $F(1,4)=16.3$, $p<0.016$), and right thalamus (Sham-control: $F(1,6)=28.5$, $p<0.002$; Sham-HT: $F(1,5)=262.5$, $p<0.001$; Stroke-control: $F(1,6)=21.2$, $p<0.004$; Stroke-HT: $F(1,3)=10.3$, $p<0.049$) than in the corresponding ROI in the left hemisphere (not shown in figure).

At 35 days post-stroke, all groups still displayed a lower CBF in the right cortex (Sham-control: $F(1,6)=14.0$, $p<0.10$; Sham-HT: $F(1,6)=10.8$, $p<0.017$; Stroke-control: $F(1,6)=12.7$, $p<0.012$, Stroke-HT: $F(1,5)=18.9$, $p<0.007$) and right hippocampus (Sham-control: $F(1,6)=19.5$, $p<0.004$; Sham-HT: $F(1,6)=43.0$, $p<0.001$; Stroke-control: $F(1,6)=5.9$, $p<0.051$, Stroke-HT: $F(1,5)=33.5$, $p<0.002$) compared to respectively the left cortex and left hippocampus. In the right thalamus, a lower CBF was also observed in sham animals at 35 days, compared to the left thalamus (Sham-control: $F(1,6)=25.2$, $p<0.002$; Sham-HT: $F(1,6)=38.8$, $p<0.001$). Interestingly, reperfusion was observed in stroke animals in the right thalamus, as demonstrated by the lack of significant difference in CBF between the left and right thalamus at 35 days (not shown in figure).

An overall diet effect was observed in the right hippocampus at 7 and 35 days post-stroke, as shown by an increased CBF in HT-fed mice of both surgery groups (Sham-HT: $F(1,11)=5.0$, $p<0.046$; Stroke-HT: $F(1,10)=4.8$, $p<0.054$). Additionally, an increased CBF was also observed in the left cortex of stroke-HT mice compared to stroke-control mice at 7 and 35 days post-stroke ($F(1,10)=5.4$, $p<0.043$) **(Figure 10).**

Both sham-control and sham-HT mice showed a decreased CBF in the left hippocampus at 35 days compared to 7 days post-stroke ($F(1,11)=4.8$, $p<0.051$). All stroke animals showed a significantly increased CBF at 35 days post-stroke in the right hippocampus and compared to 7 days post-stroke ($F(1,10)=8.6$, $p<0.015$). In the left hippocampus, stroke-control mice showed a decrease of CBF over time (35 days vs. 7 days) ($F(1,6)=5.5$ $p<0.058$), whereas HT-fed stroke mice maintained an increased CBF at 35 days compared to control diet-fed mice ($F(1,10)=5.1$, $p<0.048$) **(Figure 10)**. In the left thalamus, a decreased CBF was observed at 35 days compared to 7 days post-stroke in stroke-control ($F(1,6)=5.1$, $p<0.065$) and in stroke-HT mice ($F(1,3)=13.1$, $p<0.036$). Conversely, an increase of CBF was observed in the right thalamus in stroke-control mice at 35 days post-stroke, compared to 7 days post-stroke ($F(1,6)=23.4$, $p<0.003$).

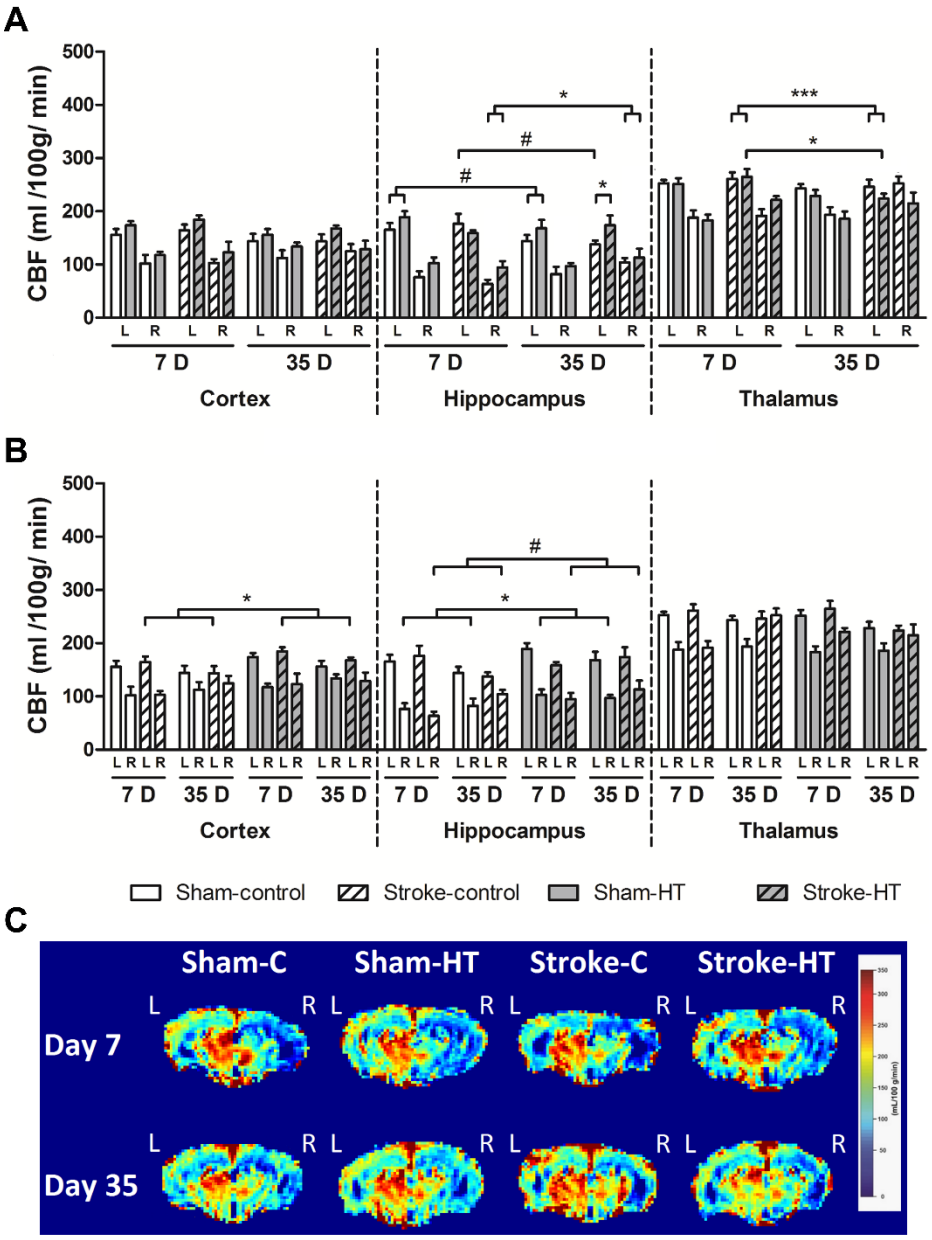

Figure 10. CBF was assessed in the lesioned and unlesioned hemisphere at 7 and 35 days post-stroke in the hippocampus, thalamus and cortex. At 7 days post-stroke, CBF was lower in all groups in the right cortex (Sham-control: $p<0.002$; Sham-HT: $p<0.004$; Stroke-control: $p<0.007$; Stroke-HT: $p<0.024$), right hippocampus (Sham-control: $p<0.003$; Sham-HT: $p<0.001$; Stroke-control: $p<0.001$; Stroke-HT: $p<0.016$), and right thalamus (Sham-control: $p<0.002$; Sham-HT: $p<0.001$; Stroke-control: $p<0.004$; Stroke-HT: $p<0.049$) than in the corresponding ROI in the left hemisphere (not shown in figure). At 35 days post-stroke, all groups still displayed a lower CBF in the right cortex (Sham-control: $p<0.10$; Sham-HT: $p<0.017$; Stroke-control: $p<0.012$, Stroke-HT: $p<0.007$) and right hippocampus (Sham-control: $p<0.004$; Sham-HT: $p<0.001$; Stroke-control: $p<0.051$, Stroke-HT: $p<0.002$) compared to the left cortex and left hippocampus, respectively (not shown in figure). In the right thalamus, a lower CBF was also observed in sham animals at 35 days, compared to the left thalamus (Sham-control: $p<0.002$; Sham-HT: $p<0.001$) (not shown in figure). CBF was also increased in the left cortex of stroke-HT mice compared to stroke-control mice at 7 and 35 days post-stroke (B, $p<0.043$). Both sham-control and sham-HT mice showed a decreased CBF in the left hippocampus at 35 days compared to 7 days post-surgery ($p<0.051$). All stroke animals showed a significantly increased CBF at 35 days post-stroke in the right hippocampus and compared to 7 days post-stroke (A, $p<0.015$). Notably, CBF in the right hippocampus was increased in HT-fed mice of both surgery groups at both 7 and 35 days post-surgery (B, Sham-HT: $p<0.046$; Stroke-HT: $p<0.054$). In the left hippocampus, stroke-control mice showed a

decrease of CBF over time (35 days vs. 7 days) ($p<0.058$), whereas HT-fed stroke mice maintained an increased CBF at 35 days compared to control diet-fed mice ($p<0.048$). In the left thalamus, a decreased CBF was observed at 35 days compared to 7 days post-stroke in stroke-control ($p<0.065$) and in stroke-HT mice ($p<0.036$). Conversely, an increase of CBF was observed in the right thalamus in stroke-control mice at 35 days post-stroke, compared to 7 days post-stroke ($p<0.003$). (C) Representative high-resolution voxel-wise analyzed CBF images at 7 and 35 poststroke. Values represent mean ± SEM. Sham-control: n=7, sham-HT: n=6, stroke-control: n=7, stroke-HT: n=4. # $0.05<p<0.08$, *$p<0.05$, ***$p<0.001$.

3.3.2. DTI

3.3.2.1. Fractional anisotropy (FA)

In sham-control and sham-HT mice, the right hippocampus showed a lower FA than the left hippocampus at 7 days (Sham-control: $F(1,6)=32.1$, $p<0.001$; Sham-HT: $F(1,5)=11.4$, $p<0.020$) and 35 days (Sham-control: $F(1,6)=13.1$, $p<0.011$; Sham-HT: $F(1,5)=49.7$, $p<0.001$) after surgery. In stroke mice, only the control group at 7 days post-stroke showed that FA was lower in the right hippocampus than its contralateral counterpart ($F(1,6)=9.3$, $p<0.022$). In the left hippocampus, FA was higher at 35 days after surgery compared to 7 days after surgery in all sham mice ($F(1,11)=4.2$, $p<0.064$). Additionally, FA in the right hippocampus also increased between 7 days and 35 days after surgery in sham-control mice ($F(1,6)=7.4$, $p<0.035$). In the motor cortex, a decreased FA in the right compared to left hemisphere was only observed at 35 days in sham-control ($F(1,6)=4.8$, $p<0.070$) and stroke-control ($F(1,6)=7.6$, $p<0.033$) mice. In the motor cortex, stroke mice showed an FA increase in the left hemisphere at 35 days post-stroke compared to 7 days post-stroke ($F(1,11)=11.6$, $p<0.006$). However, sham animals showed a decrease of FA in both the left ($F(1,11)=13.7$, $p<0.003$) and right ($F(1,11)=12.8$, $p<0.004$) motor cortex over time (35 days vs. 7 days) **(Figure 11A)**.

3.3.2.2. Mean diffusivity (MD)

In the hippocampus, MD was higher in the lesioned (right) hemisphere than in the unaffected (left) hemisphere at 7 days postsurgery in all groups (Sham-control: $F(1,6)=12.0$, $p<0.013$; Sham-HT: $F(1,5)=25.8$, $p<0.004$; Stroke-control: $F(1,6)=17.4$, $p<0.006$; Stroke-HT: $F(1,5)=6.6$, $p<0.050$), and at 35 days only in sham mice (Sham-control: $F(1,6)=61.6$, $p<0.001$; Sham-HT: $F(1,5)=34.9$, $p<0.002$). In the motor cortex, a higher MD in the right motor cortex than the left motor cortex was only observed at 7 days postsurgery in stroke-control mice ($F(1,6)=4.6$, $p<0.075$).

Sham-HT mice showed an increase in MD of the corpus callosum at 35 days compared to 7 days postsurgery ($F(1,5)=8.5$, $p<0.033$). All stroke mice also showed a higher MD in the corpus callosum 35 days compared to 7 days postsurgery ($F(1,11)=10.7$, $p<0.008$) (**Figure 11B)**.

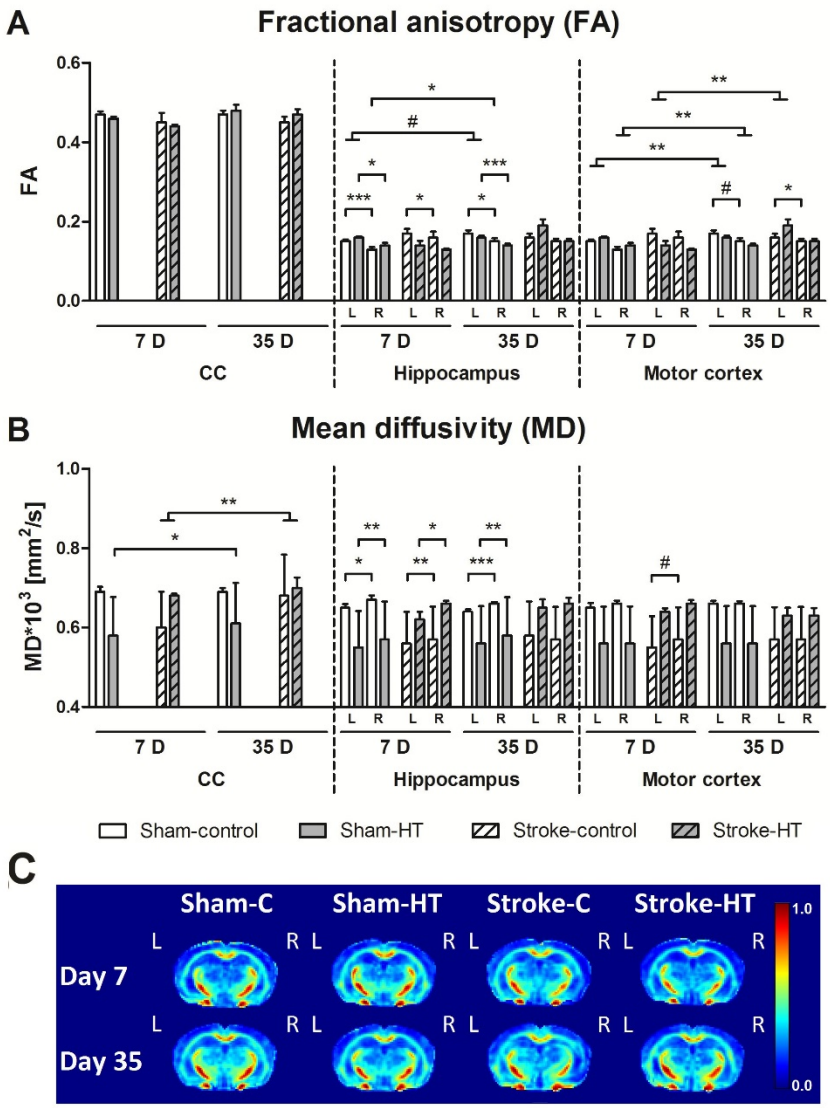

Figure 11. White matter (WM) and gray matter (GM) integrity as measured by quantitatively assessed diffusion tensor-derived indices at 7 + 35 days poststroke in mice fed HT or Control diet. Fractional anisotropy (FA) (A) and mean diffusivity (MD) (B) were measured for ROI drawn in white (Corpus Callosum, CC) and gray matter (Hippocampus, motor cortex) regions. (A) In sham-control (7D, $p<0.001$; 35D, $p<0.011$) and sham-HT mice (7D, $p<0.020$; 35D, $p<0.001$), FA in the right hippocampus was lower than in the left hippocampus at 7 days and 35 days after surgery. Only in stroke-control mice at 7 days post-stroke FA was decreased in the right hippocampus compared to its contralateral counterpart ($p<0.022$). In the left hippocampus, in all sham mice FA was higher at 35 days after surgery compared to 7 days after surgery ($p<0.064$). Additionally, FA in the right hippocampus also increased between 7 days and 35 days after surgery in sham-control mice ($p<0.035$). A lowered FA in the right the motor cortex compared to left motor cortex was only found at 35 days in sham-control ($p<0.070$) and stroke-control ($p<0.033$) mice. In the left motor cortex, stroke mice had an FA increase in the hemisphere at 35 days post-stroke compared to 7 days post-stroke ($p<0.006$). Sham animals showed a decrease of FA in both the left ($p<0.003$) and right ($p<0.004$) motor cortex over time (35 days vs. 7 days). (B) MD was higher in the right hippocampus than in the left hippocampus at 7 days postsurgery in all groups (Sham-control: $p<0.013$; Sham-HT: $p<0.004$; Stroke-control: $p<0.006$; Stroke-HT: $p<0.050$), while at 35 days only in sham mice (Sham-control: $p<0.001$; Sham-HT: $Fp<0.002$). Only in stroke-control mice at 7 days postsurgery, a higher MD in the right motor cortex than the left motor cortex was detected ($p<0.075$). Sham-HT mice had a heightened MD of the corpus callosum at 35 days compared to 7 days postsurgery ($p<0.033$). All stroke mice also showed a higher

MD in the corpus callosum 35 days compared to 7 days postsurgery ($p<0.008$). (C) Representative high-resolution set of FA images for each dietary group at 7 and 35 days poststroke.

3.3.3 rsfMRI

Only in stroke mice, HT diet improved FC from day 7 to day 35 after stroke between several cerebral regions: left dorsal hippocampus (DHL) to right dorsal hippocampus (DHR, $F(1,8)=4.5$, $p<.068$); DHL to left motor cortex (MCL, $F(1,8)=4.5$, $p<.069$); DHR to MCL ($F(1,8)=8.1$, $p<.022$); DHR to right motor cortex (MCR, $F(1,8)=6.1$, $p<.040$); left ventral hippocampus (VHL) to MCL ($F(1,8)=4.5$, $p<.067$); MCL to left visual cortex (VCL, $F(1,8)=4.4$, $p<.071$); MCL to right visual cortex (VCR, $F(1,8)=9.4$, $p<.014$); VCR to MCR ($F(1,8)=5.5$, $p<.048$) (**Figure 12A)**.

At 7 days after surgery sham animals FC from DHR to MCR ($F(1,10)=4.4$, $p<.063$) was non-significantly lower in HT than control mice, while in stroke animals HT mice tended to have a decreased FC between VCR and MCL compared to control mice ($F(1,9)=4.3$, $p<.069$). No diets effect were found 35 days after surgery.

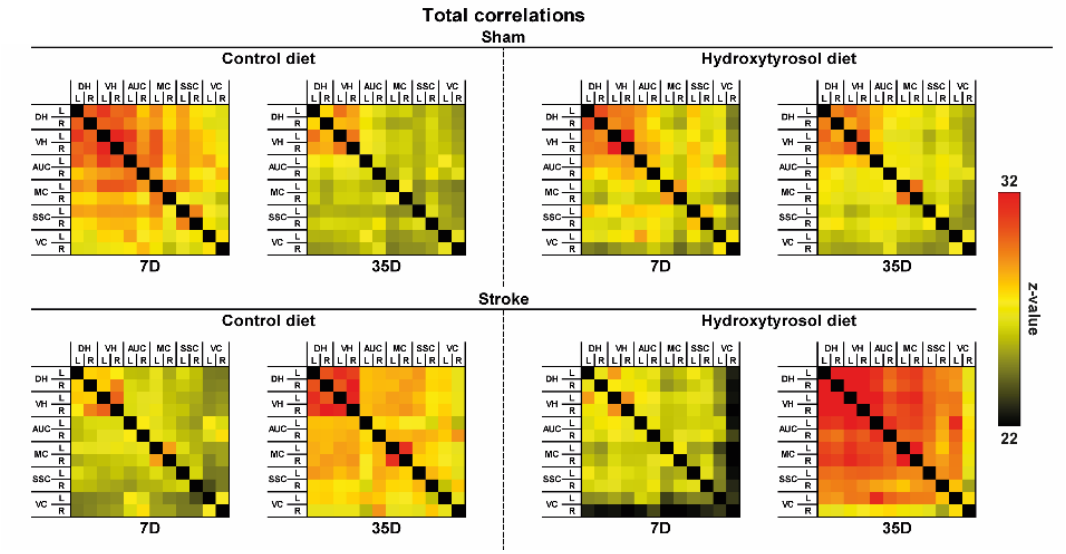

Figure 12. Resting-state functional connectivity (FC) based on total in the brains of mice fed HT or Control diet 7 and 35 days poststroke. FC was measured between 12 ROI: dorsal hippocampus (DH), ventral hippocampus (VH), auditory cortex (AU), motor cortex (M1), somatosensory cortex (S1), and visual cortex (V1). (A) Total correlations revealed that HT diet improved FC in stroke mice between several ROI, i.e. right DH to left MC ($p<.022$); right DH to right M1 ($p<.040$).

3.4 (Immuno)histochemistry and Biochemical analysis

3.4.1. DCX Staining

To visualize immature neurons, we used an anti-DCX antibody as a neurogenesis marker. DCX+ cells were quantified in hippocampus. We found an increased number of DCX+ cells/mm^2 in all stroke mice compared to sham mice ($F(1,23)=8.4$, $p<0.008$). In HT mice *versus* Control mice, both in stroke and sham condition ($F(1,23)=3.5$, $p<0.076$) in the hippocampus **(Figure 13A)** more DCX+ cells/mm^2 were detected. The hippocampus size was reduced significantly in stroke mice without a diet effect ($F(1,23)=7.0$, $p<0.015$) (**Figure 13B)**.

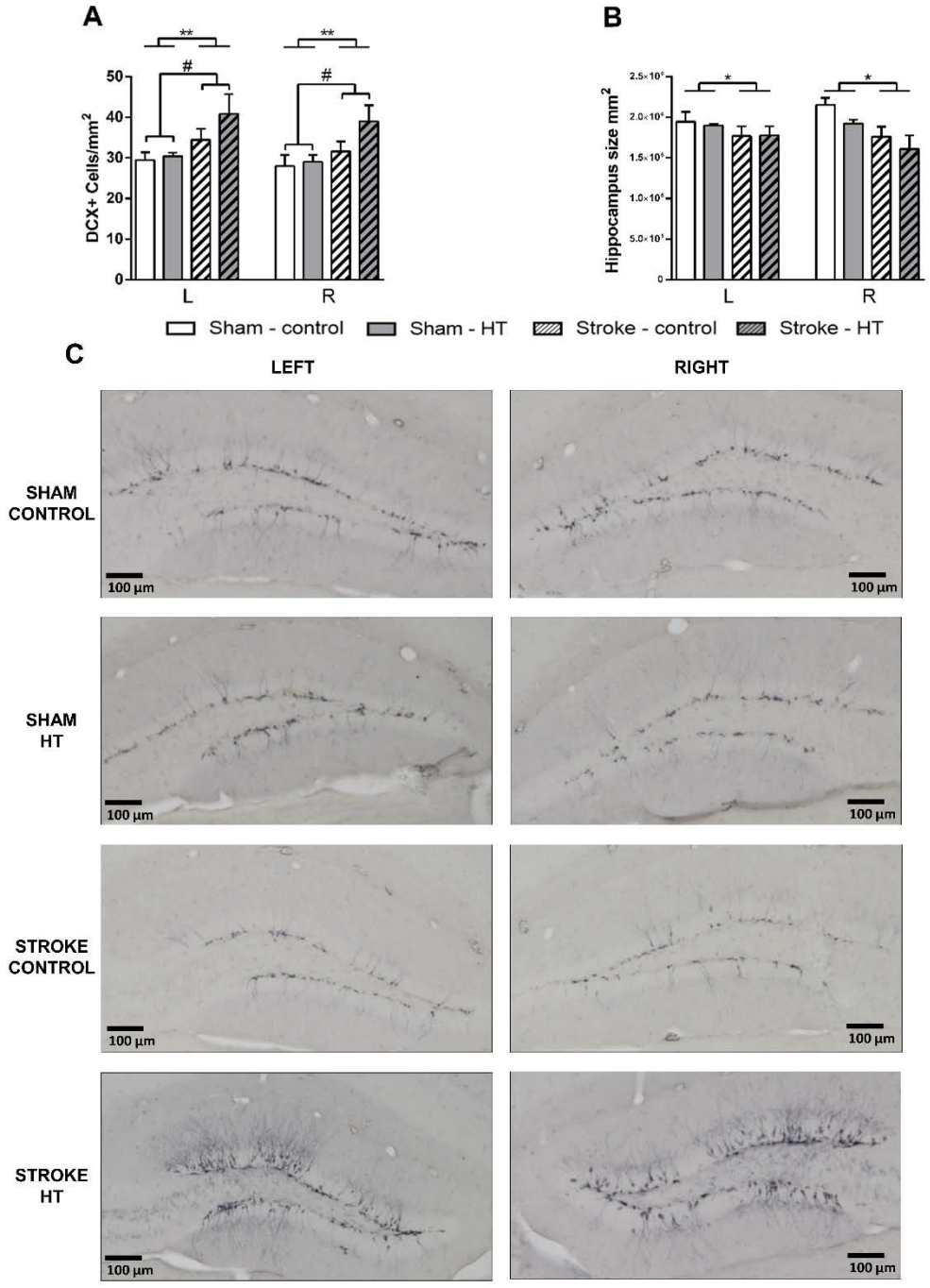

Figure 13. Immnunohistological stainings for doublecortin (DCX) in hippocampus of the brains of HT and control fed mice 35 days after surgery. (A) All stroke mice showed an increased number of DCX+ cells/mm2 compared to sham mice ($p<0.008$). In HT mice versus Control mice, both in stroke and sham condition ($p<0.076$) more DCX+ cells/mm2 were detected. (B) The hippocampus size was reduced significantly in stroke mice without a diet effect ($p<0.015$). Values represent mean ± SEM.

3.4.2. IBA-1 Staining

All stroke mice showed an higher IBA1+-area **(Figure 14)** than sham mice in the cortex at bregma -1.94 ($F(1,21)=4.5$, $p<0.046$), hippocampus ($F(1,19)=6.6$, $p<0.019$), in both left ($F(1,23)=10.9$, $p<0.002$) and right ($F(1,23)=11.6$, $p<0.002$) thalamus, cortex at bregma 0.62 ($F(1,21)=5.6$, $p<0.027$), and in both left ($F(1,23)=5.0$, $p<0.037$) and right ($F(1,23)=35.8$, $p<0.001$) caudate putamen. Notably, in the corpus callosum only in stroke-control mice a heightened IBA1+-area was found compared to sham-control mice ($F(1,13)=8.9$, $p<0.011$). Moreover, only in stroke mice in the right thalamus ($F(1,12)=11.7$, $p<0.006$) and in the right caudate putamen ($F(1,12)=34.6$, $p<0.001$) IBA1+-area was increased compared to their

corresponding left hemispheric part. In the cortex at bregma 0.62 HT-diet lowered IBA1+-area compared to control diet in both sham and stroke mice ($F(1,21)=4.9$, $p<0.039$). While in the corpus callosum IBA1+-area was decreased by HT-diet only in stroke mice ($F(1,12)=6.9$, $p<0.022$).

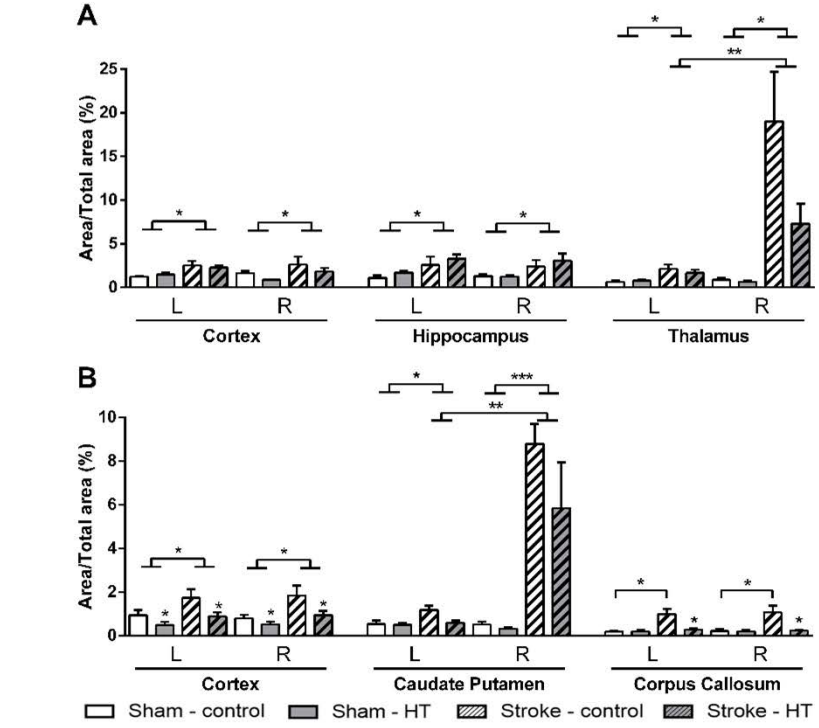

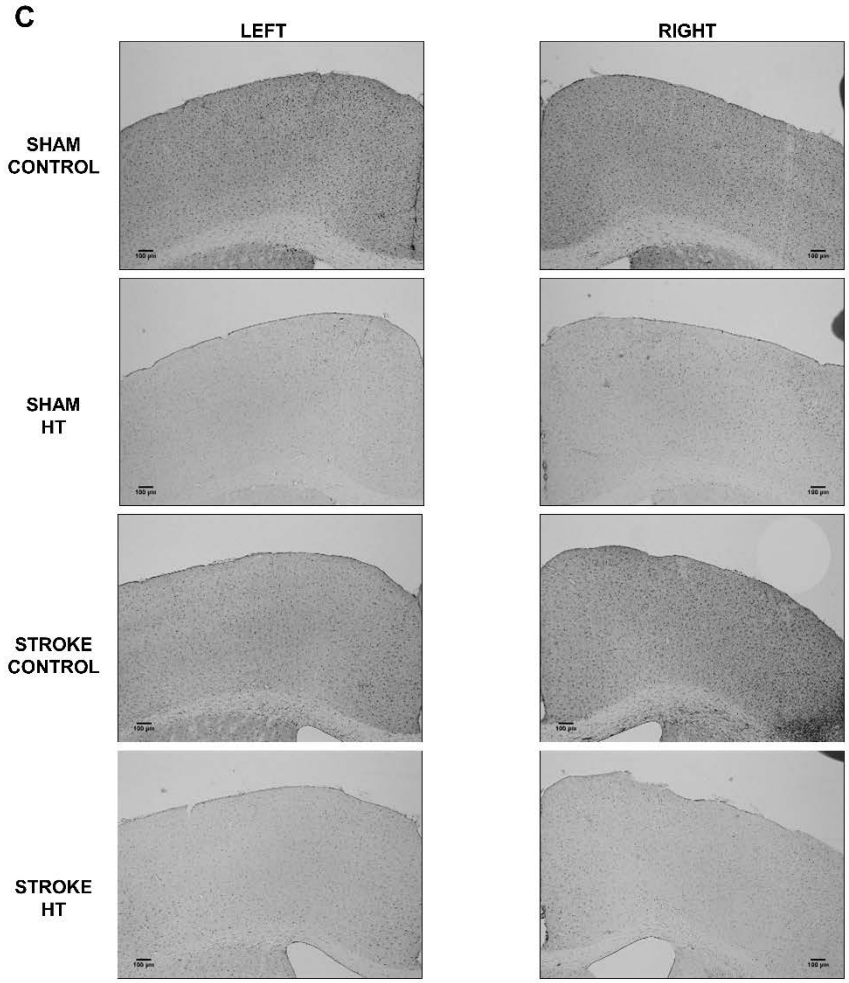

Figure 14. Immnunohistological stainings for ionized calcium-binding adapter molecule-1 (IBA-1) in brains of HT and control fed mice 35 days after surgery. All stroke mice showed a higher IBA1+-area than sham mice in (A) the cortex at bregma -1.94 ($p<0.046$), hippocampus ($p<0.019$), in both left ($p<0.002$) and right ($p<0.002$) thalamus, (B) cortex at bregma 0.62 ($p<0.027$), and in both left ($p<0.037$) and right ($p<0.001$) caudate putamen. (B) Notably, in the corpus callosum only in stroke-control mice a heightened IBA1+-area was found compared to sham-control mice ($p<0.011$). Moreover, only in stroke mice in the right thalamus ($p<0.006$) and in the right caudate putamen ($p<0.001$) IBA1+-area was increased compared to their corresponding left hemispheric part. In the cortex at bregma 0.62 HT-diet lowered IBA1+-area compared to control diet in both sham and stroke mice ($p<0.039$). While in the corpus callosum IBA1+-area was decreased by HT-diet only in stroke mice ($p<0.022$). (C) Representative images of IBA-1 staining in cortex (bregma 0.62). Values represent mean ± SEM.

3.4.3. NO and reactive oxygen species (ROS) levels

NO and ROS levels were determined in serum samples obtained before sacrifice **(Figure 15)**. NO production was quantified indirectly by the determination of nitrates/nitrites using an ozone chemiluminescence-based assay. A reduction in NO levels was detected in stroke animals with no evident diet effect ($p=0.02$). ROS levels were also indirectly quantified by analyzing the level of lipid peroxidation. No changes were detected.

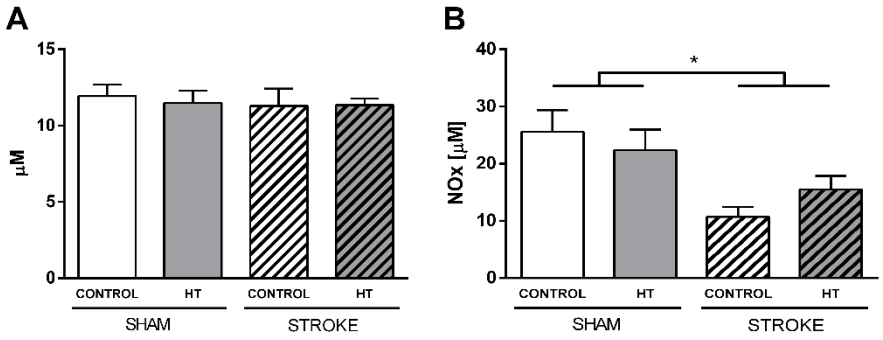

Figure 15. **ROS and NO levels in serum samples obtained 35 days after surgery.** (A) ROS level evaluated by analyzing TBARS (B) NO production quantified by using an ozone chemiluminiscence-based assay. A reduction of NO levels was detected in stroke animals ($p<0.02$). Values represent mean ± SEM.

3.4.4. Psd95 and BDNF mRNA expression

The expression of Bdnf, as a regulator of neurogenesis, and Psd-95, as postsynaptic marker, were determined by qPCR (**Figure 16)**. All HT-mice showed an up-regulation in Psd-95 expression without differences between hemispheres ($F(1,21)=6.3$, $p<0.021$). In addition, BDNF was higher expressed in stroke HT-mice ($F(1,9)=8.4$, $p<0.018$) than in stroke control mice. In contrast, only in sham mice Bdnf was down-regulated in HT-mice in comparison with control-mice ($F(1,11)=4.7$, $p<0.053$).

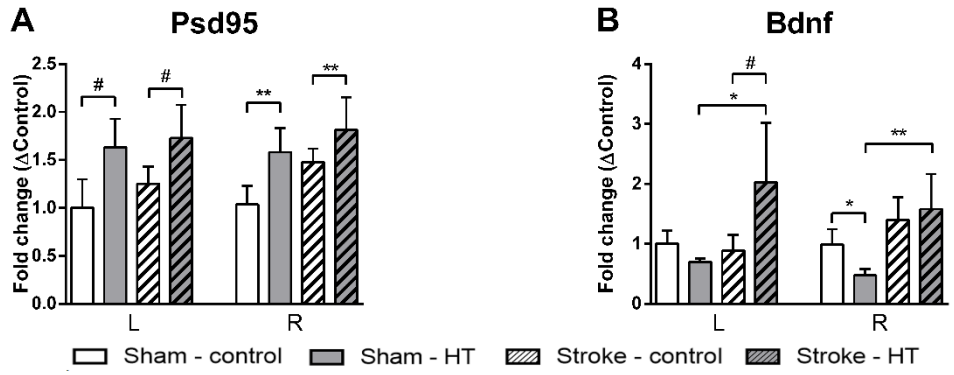

Figure 16. mRNA expression of (A) Psd95, (B) Bdnf in frontal parts of the brain 35 days after surgery. (A) All HT-mice showed an up-regulation in Psd-95 expression without differences between hemispheres ($p<0.021$). (B) BDNF was higher expressed in stroke HT-mice ($p<0.018$) than in stroke control mice. Only in sham mice Bdnf was down-regulated in HT-mice in comparison with control-mice ($p<0.053$). Values represent mean ± SEM.

4. Discussion

Although ischemic stroke is one of the main causes of death and disability worldwide, the only medical treatment for this disease is to favor reperfusion by using recombinant tissue plasminogen activator or by endovascular thrombectomy with medical devices. However, the risk of hemorrhage, the narrow therapeutic window and the need of neurointerventional expertise makes it urgent to find other treatment options focused not only on reperfusion but on neuroprotection as well. In this sense, it has been previously described that olive oil and an olive leaf extract exert a neuroprotective effect in ischemic rats [12,42]. Oleuropein, another polyphenol from olive oil and a precursor of HT, has also demonstrated to be neuroprotective in a mouse model of focal cerebral ischemia [43]. However, a comprehensive analysis of the effect of HT as a therapeutic approach in an *in vivo* stroke model is lacking. The present study shows that an HT-diet could be used as a therapeutic approach in stroke recovery by improving: i) learning, short term memory and grip strength, ii) CBF and FC, and iii) different parameters related to neurogenesis and neuroinflammation.

Motor functions, behavior and cognition are severely affected after focal ischemia and decisive in the quality of life of stroke patients [44,45]. In our previous study, we described that a multicomponent diet, Fortasyn, improved grip strength in male mice [9]. In the current study, we show that HT improved grip strength on the trapeze, highlighting the potential restorative effect of this single compound on motor network connections. Exploring the HT effects on behavior and motor skills, no diet effects were detected neither in the open field, DVC nor the pole test. Short-term memory of mice was also evaluated with the novel object recognition test (ORT). Here, mice on HT-diet visited the novel object more frequently than mice on control-diet. Similarly, in the PPI test, HT-fed mice showed a higher startle amplitude to the basal and final startle stimulus of 120dB control-mice. Altogether, ORT and PPI results suggest that HT improves short-term memory and promotes non-associative learning processes such as habituation, being a promising approach to reduce stroke-associated cognitive deficits.

After ischemic stroke, rsfMRI demonstrated alterations in neuronal functional architecture, both in animal models and in humans [46]. In a human study, it was demonstrated that the alteration of sensorimotor function after a stroke correlated with a loss of interhemispheric connectivity between sensory-motor regions, and that this disruption normalized partially weeks after the infarction [47]. Thus, in patients with stroke, changes in neuronal activity are closely associated with functional recovery. The increase in rsfMRI activity in the supplementary motor cortex, the lateral premotor cortex and the superior parietal cortex in the first 14 days after infarction correlates with an improvement in motor function of the upper extremities during this period [48]. In the present study we also investigated brain diffusivity with DTI as an imaging biomarker for white and gray matter (GM) integrity. Here, we revealed only impaired GM microstructure in the stroke mice on control

diet measured by a decreased FA accompanied by an increased MD at seven days poststroke in the right hippocampus and right motor cortex compared to their corresponding left counterpart. This effect was not visible in stroke mice on HT diet. Therefore, the HT-diet improved functional and also structural connectivity between several cerebral regions in the stroke animals. We suggest that these improvements in connectivity could be related to the increase in the grip strength of HT-fed mice as well as with their higher habituation and improved short-term memory described above and on the up-regulation of different neurogenic markers that will be mentioned later.

CBF alterations are also clinically associated with cognitive and motor dysfunction, especially after stroke [49]. In fact, we already described that a post-stroke diet intervention can improve CBF [9,50]. Other phenolic compounds such as resveratrol have shown to increase CBF in the frontal cortex of healthy humans after a task performance [51]. Moreover, in a rat ischemic model, resveratrol increased hippocampal CBF [52]. Our results show that an acute therapeutic approach with a HT-diet was able to significantly increase CBF in the right hippocampus of all mice on HT-diet, and to mitigate the decreased CBF in the left hippocampus stroke-control mice. Additionally, in the left cortex, HT-diet also increased CBF after stroke. The positive effect of HT on this parameter probably also underlies the improvement in short-term memory and learning processes described above.

CBF is linked to a balanced production of NO. The particular effect of NO varies depending on the stage of evolution along the ischemic process and on the cellular source of NO [53,54]. Of the three NOS isoforms responsible for NO production, the activity of neuronal NOS and inducible NOS results detrimental while endothelial NOS activation is related with neuroprotective effects. We have previously shown in stroke patients that an initial elevation of NO favors neurological recovery while a latter elevation predicts growth of the infarct volume [55]. In the present study we have observed a significant decrease in serum NO concentration in stroke animals. This decrease has also been reported by ours and other research groups, and may be attributed to the low profile of L-arginine, the NO precursor, in stroke patients [55-57]. The HT-diet was unable to significantly up-regulate those decreased levels, suggesting a lack of effect of this diet on the NO system. Nevertheless, this result should be corroborated in a future study with more animals.

A burst in ROS follows after a stroke insult damaging cellular macromolecules and leading to cell death and tissue loss [58]. HT has been consistently described as an antioxidant compound in several models [59]. Therefore, we evaluated if the HT-diet was able to modulate the oxidative level in serum samples obtained from mice after sacrifice. The fact that no changes were detected in any experimental group, not even between sham and stroke animals, seems to indicate that 35 days after surgery may be too late to detect changes in serum ROS levels. In fact, in a previous study with hypoxic mice we observed that ROS brain levels begin to normalize two hours after the insult [60]. As previously mentioned, further analysis with more animals should be carried out, both in serum and in brain samples, and at time-points closer to surgery to re-evaluate the temporal profile of NO production and the particular isoenzymes of NOS modulated by HT and to analyze the antioxidant capacity of HT-diet after stroke.

HT has shown its anti-inflammatory capacity in different models [61-63] and although its particular effect on microglia-mediated neuroinflammation remained unexplored other phenolic compounds such as oleuropein have been shown to attenuate microglia activation [64]. The decreased level of IBA-1 immunoreactivity 35 days after stroke in the cortex and corpus callosum of mice on the HT-diet corroborates that HT can also reduce the inflammatory environment after stroke. This effect is probably involved in the improved impairments of stroke mice on a HT-diet and points to the interest of carrying out future experiments to deepen into the activity of HT on neuroinflammation.

Neurogenesis is an important process in stroke recovery and a number of therapeutic strategies to promote this process after ischemic events have been investigated with poor outcomes [65]. DCX, a microtubule-associated protein expressed in neural progenitor cells and immature neurons, is an excellent marker for adult neurogenesis [66]. The increased number of DCX+ cells in the hippocampus of HT-fed mice is indicative of the neurogenic potential of HT, and could explain the positive effect of this polyphenol on the short-term memory and learning processes described above.

Stroke insult also involves synaptic degradation which dampens the activity of the CNS. Bdnf is a neurotrophin that regulates synaptic connections, synapse structure, neurotransmitter release and synaptic plasticity [67]. Moreover, Bdnf is required for the induction of neurogenesis and lack of this protein can lead to a lack of neurogenic response in a heterozygous knockout mice model [68] Additionally, the postsynaptic protein Psd95 is also involved in the regulation of synaptic plasticity and synaptogenesis. Previous studies demonstrate that the administration of olive leaf or oil polyphenol extracts increases Bdnf levels in the olfactory lobes and hippocampus [69,70]. The synaptogenic potential of HT has been also reported in prenatally stressed rats in which HT prevented the stress-induced downregulation of Bdnf [71]. In accordance, in our study the expression of Psd95 was significantly induced in all HT-fed mice. However, the HT-diet only induced Bdnf in the non-infarcted hemisphere of stroke HT-mice, and even decreased it in the right hemisphere of sham-HT mice, suggesting a difference in the response between Bdnf and DCX [72]. Although further analyses at the protein level are necessary, it is remarkable that HT, a single compound, exhibits these promising effects.

5. Conclusions

The data presented here indicate that a post-stroke intervention with a HT-enriched diet improve the recovery after ischemic stroke by ameliorating stroke-associated learning and motor impairments. This effect, probably linked to an increase in CBF, functional and structural connectivity and to its anti-inflammatory and neurogenic potential, makes HT an interesting and safety compound to be further tested in ischemic stroke treatment.

References

1. Nichols, M.; Townsend, N.; Luengo-Fernandez, R.; Leal, J.; Gray, A.; Scarborough, P.; Rayner, M. European cardiovascular disease statistics 2012. **2012**.
2. Di Domenico, F.; Casalena, G.; Jia, J.; Sultana, R.; Barone, E.; Cai, J.; Pierce, W.M.; Cini, C.; Mancuso, C.; Perluigi, M. Sex differences in brain proteomes of neuron-specific STAT3-null mice after cerebral ischemia/reperfusion. *Journal of neurochemistry* **2012**, *121*, 680-692, doi:10.1111/j.1471-4159.2012.07721.x.
3. Jokinen, H.; Melkas, S.; Ylikoski, R.; Pohjasvaara, T.; Kaste, M.; Erkinjuntti, T.; Hietanen, M. Post-stroke cognitive impairment is common even after successful clinical recovery. *European Journal of Neurology* **2015**, *22*, 1288-1294, doi:10.1111/ene.12743.
4. Auriel, E.; Bornstein, N. Neuroprotection in acute ischemic stroke–current status. *Journal of cellular and molecular medicine* **2010**, *14*, 2200-2202, doi:10.1111/j.1582-4934.2010.01135.x.
5. Zerbi, V.; Jansen, D.; Wiesmann, M.; Fang, X.; Broersen, L.M.; Veltien, A.; Heerschap, A.; Kiliaan, A.J. Multinutrient diets improve cerebral perfusion and neuroprotection in a murine model of Alzheimer's disease. *Neurobiology of aging* **2014**, *35*, 600-613, doi:10.1016/j.neurobiolaging.2013.09.038.
6. Dobkin, B.H.; Dorsch, A. New evidence for therapies in stroke rehabilitation. *Current atherosclerosis reports* **2013**, *15*, 331, doi:10.1007/s11883-013-0331-y.
7. Ayuso, M.I.; Gonzalo-Gobernado, R.; Montaner, J. Neuroprotective diets for stroke. *Neurochemistry international* **2017**, *107*, 4-10, doi:10.1016/j.neuint.2017.01.013.
8. Wiesmann, M.; Timmer, N.M.; Zinnhardt, B.; Reinhard, D.; Eligehausen, S.; Königs, A.; Ben Jeddi, H.; Dederen, P.J.; Jacobs, A.H.; Kiliaan, A.J. Effect of a multinutrient intervention after ischemic stroke in female C57Bl/6 mice. *Journal of neurochemistry* **2018**, *144*, 549-564, doi:10.1111/jnc.14213.
9. Wiesmann, M.; Zinnhardt, B.; Reinhardt, D.; Eligehausen, S.; Wachsmuth, L.; Hermann, S.; Dederen, P.J.; Hellwich, M.; Kuhlmann, M.T.; Broersen, L.M. A specific dietary intervention to restore brain structure and function after ischemic stroke. *Theranostics* **2017**, *7*, 493, doi:10.7150/thno.17559.
10. Martínez-González, M.A.; Dominguez, L.J.; Delgado-Rodríguez, M. Olive oil consumption and risk of CHD and/or stroke: a meta-analysis of case–control, cohort and intervention studies. *British Journal of Nutrition* **2014**, *112*, 248-259, doi:10.1017/S0007114514000713.
11. Estruch, R.; Ros, E.; Salas-Salvadó, J.; Covas, M.-I.; Corella, D.; Arós, F.; Gómez-Gracia, E.; Ruiz-Gutiérrez, V.; Fiol, M.; Lapetra, J. Primary prevention of cardiovascular disease with a mediterranean diet supplemented with extra-virgin olive oil or nuts. *New England Journal of Medicine* **2018**, 10.1056/NEJMoa1800389, doi:10.1056/NEJMoa1800389.
12. Mohagheghi, F.; Bigdeli, M.R.; Rasoulian, B.; Zeinanloo, A.A.; Khoshbaten, A. Dietary virgin olive oil reduces blood brain barrier permeability, brain edema, and brain injury in rats subjected to ischemia-reperfusion. *The Scientific World Journal* **2010**, *10*, 1180-1191, doi:10.1100/tsw.2010.128.
13. Rabiei, Z.; Bigdeli, M.R.; Rasoulian, B. Neuroprotection of dietary virgin olive oil on brain lipidomics during stroke. *Current neurovascular research* **2013**, *10*, 231-237.
14. Lausada, N.; Arnal, N.; Astiz, M.; Marín, M.C.; Lofeudo, J.M.; Stringa, P.; de Alaniz, M.J.T.; de Gómez Dumm, N.T.; de Catalfo, G.H.; de Piñero, N.C. Dietary fats significantly influence the survival of penumbral neurons in a rat model of chronic ischemic by modifying lipid mediators, inflammatory biomarkers, NOS production, and redox-dependent apoptotic signals. *Nutrition* **2015**, *31*, 1430-1442, doi:10.1016/j.nut.2015.05.023.

15. Granados-Principal, S.; Quiles, J.L.; Ramirez-Tortosa, C.L.; Sanchez-Rovira, P.; Ramirez-Tortosa, M.C. Hydroxytyrosol: from laboratory investigations to future clinical trials. *Nutrition reviews* **2010**, *68*, 191-206, doi:10.1111/j.1753-4887.2010.00278.x.
16. De la Torre-Carbot, K.; Jauregui, O.; Gimeno, E.; Castellote, A.I.; Lamuela-Raventós, R.M.; López-Sabater, M.C. Characterization and quantification of phenolic compounds in olive oils by solid-phase extraction, HPLC-DAD, and HPLC-MS/MS. *Journal of agricultural and food chemistry* **2005**, *53*, 4331-4340, doi:10.1021/jf0501948.
17. Robles-Almazan, M.; Pulido-Moran, M.; Moreno-Fernandez, J.; Ramirez-Tortosa, C.; Rodriguez-Garcia, C.; Quiles, J.L.; Ramirez-Tortosa, M. Hydroxytyrosol: Bioavailability, toxicity, and clinical applications. *Food Research International* **2017**, 10.1016/j.foodres.2017.11.053, doi:10.1016/j.foodres.2017.11.053.
18. González-Correa, J.A.; Navas, M.D.; Lopez-Villodres, J.A.; Trujillo, M.; Espartero, J.L.; De La Cruz, J.P. Neuroprotective effect of hydroxytyrosol and hydroxytyrosol acetate in rat brain slices subjected to hypoxia–reoxygenation. *Neuroscience letters* **2008**, *446*, 143-146, doi:10.1016/j.neulet.2008.09.022.
19. Cabrerizo, S.; De La Cruz, J.P.; López-Villodres, J.A.; Muñoz-Marín, J.; Guerrero, A.; Reyes, J.J.; Labajos, M.T.; González-Correa, J.A. Role of the inhibition of oxidative stress and inflammatory mediators in the neuroprotective effects of hydroxytyrosol in rat brain slices subjected to hypoxia reoxygenation. *The Journal of nutritional biochemistry* **2013**, *24*, 2152-2157, doi:10.1016/j.jnutbio.2013.08.007.
20. De La Cruz, J.; Ruiz-Moreno, M.; Guerrero, A.; López-Villodres, J.; Reyes, J.; Espartero, J.; Labajos, M.; González-Correa, J. Role of the catechol group in the antioxidant and neuroprotective effects of virgin olive oil components in rat brain. *The Journal of nutritional biochemistry* **2015**, *26*, 549-555, doi:10.1016/j.jnutbio.2014.12.013.
21. De La Cruz, J.P.; Ruiz-Moreno, M.I.; Guerrero, A.; Reyes, J.J.; Benitez-Guerrero, A.; Espartero, J.L.; González-Correa, J.A. Differences in the neuroprotective effect of orally administered virgin olive oil (Olea europaea) polyphenols tyrosol and hydroxytyrosol in rats. *Journal of agricultural and food chemistry* **2015**, *63*, 5957-5963, doi:10.1021/acs.jafc.5b00627.
22. Reyes, J.J.; Villanueva, B.; López-Villodres, J.A.; De La Cruz, J.P.; Romero, L.; Rodríguez-Pérez, M.a.D.; Rodriguez-Gutierrez, G.; Fernández-Bolaños, J.; González-Correa, J.A. Neuroprotective effect of hydroxytyrosol in experimental diabetes mellitus. *Journal of agricultural and food chemistry* **2017**, *65*, 4378-4383, doi:10.1021/acs.jafc.6b02945.
23. Tomé-Carneiro, J.; Crespo, M.C.; García-Calvo, E.; Luque-García, J.L.; Dávalos, A.; Visioli, F. Proteomic evaluation of mouse adipose tissue and liver following hydroxytyrosol supplementation. *Food and Chemical Toxicology* **2017**, *107*, 329-338, doi:10.1016/j.fct.2017.07.009.
24. Giordano, E.; Dávalos, A.; Visioli, F. Chronic hydroxytyrosol feeding modulates glutathione-mediated oxido-reduction pathways in adipose tissue: A nutrigenomic study. *Nutrition, Metabolism and Cardiovascular Diseases* **2014**, *24*, 1144-1150, doi:10.1016/j.numecd.2014.05.003.
25. Tomé-Carneiro, J.; Crespo, M.C.; Iglesias-Gutierrez, E.; Martín, R.; Gil-Zamorano, J.; Tomas-Zapico, C.; Burgos-Ramos, E.; Correa, C.; Gómez-Coronado, D.; Lasunción, M.A. Hydroxytyrosol supplementation modulates the expression of miRNAs in rodents and in humans. *The Journal of nutritional biochemistry* **2016**, *34*, 146-155, doi:10.1016/j.jnutbio.2016.05.009.
26. Streijger, F.; Oerlemans, F.; Ellenbroek, B.A.; Jost, C.R.; Wieringa, B.; Van der Zee, C.E. Structural and behavioural consequences of double deficiency for creatine kinases BCK and UbCKmit. *Behavioural brain research* **2005**, *157*, 219-234, doi:10.1016/j.bbr.2004.07.002.
27. Janssen, C.I.; Zerbi, V.; Mutsaers, M.P.; de Jong, B.S.; Wiesmann, M.; Arnoldussen, I.A.; Geenen, B.; Heerschap, A.; Muskiet, F.A.; Jouni, Z.E. Impact of dietary n-3 polyunsaturated fatty acids on cognition, motor skills and

hippocampal neurogenesis in developing C57BL/6J mice. *The Journal of nutritional biochemistry* **2015**, *26*, 24-35, doi:10.1016/j.jnutbio.2014.08.002.

28. Antunes, M.; Biala, G. The novel object recognition memory: neurobiology, test procedure, and its modifications. *Cognitive processing* **2012**, *13*, 93-110, doi:10.1007/s10339-011-0430-z.
29. Giles, J.M.; Whitaker, J.W.; Moy, S.S.; Fletcher, C.A. Effect of Environmental Enrichment on Aggression in BALB/cJ and BALB/cByJ Mice Monitored by Using an Automated System. *Journal of the American Association for Laboratory Animal Science* **2018**, *57*, 236-243, doi:10.30802/AALAS-JAALAS-17-000122.
30. Paxinos, G.; Franklin, K.B. *The mouse brain in stereotaxic coordinates*; Gulf professional publishing: 2004.
31. Harsan, L.A.; Paul, D.; Schnell, S.; Kreher, B.W.; Hennig, J.; Staiger, J.F.; von Elverfeldt, D. In vivo diffusion tensor magnetic resonance imaging and fiber tracking of the mouse brain. *NMR Biomed* **2010**, *23*, 884-896, doi:10.1002/nbm.1496.
32. Jansen, D.; Zerbi, V.; Arnoldussen, I.A.C.; Wiesmann, M.; Rijpma, A.; Fang, X.T.; Dederen, P.J.; Mutsaers, M.P.C.; Broersen, L.M.; Lütjohann, D., et al. Effects of Specific Multi-Nutrient Enriched Diets on Cerebral Metabolism, Cognition and Neuropathology in AβPPswe-PS1dE9 Mice. *PLoS ONE* **2013**, *8*, e75393, doi:10.1371/journal.pone.0075393.
33. Jansen, D.; Zerbi, V.; Janssen, C.F.; van Rooij, D.; Zinnhardt, B.; Dederen, P.; Wright, A.; Broersen, L.; Lütjohann, D.; Heerschap, A., et al. Impact of a multi-nutrient diet on cognition, brain metabolism, hemodynamics, and plasticity in apoE4 carrier and apoE knockout mice. *Brain Struct Funct* **2014**, *219*, 1841-1868, doi:10.1007/s00429-013-0606-7.
34. Zwiers, M.P. Patching cardiac and head motion artefacts in diffusion-weighted images. *Neuroimage* **2010**, *53*, 565-575, doi:10.1016/j.neuroimage.2010.06.014.
35. Paxinos, G.; Franklin, K.B. *The mouse brain in stereotaxic coordinates / George Paxinos, Keith Franklin*; Academic: London :, 2004.
36. Jonckers, E.; Van Audekerke, J.; De Visscher, G.; Van der Linden, A.; Verhoye, M. Functional connectivity fMRI of the rodent brain: comparison of functional connectivity networks in rat and mouse. *PloS one* **2011**, *6*, e18876, doi:10.1371/journal.pone.0018876.
37. Janssen, C.I.; Jansen, D.; Mutsaers, M.P.; Dederen, P.J.; Geenen, B.; Mulder, M.T.; Kiliaan, A.J. The effect of a high-fat diet on brain plasticity, inflammation and cognition in female ApoE4-knockin and ApoE-knockout mice. *PLoS One* **2016**, *11*, e0155307, doi:10.1016/j.jnutbio.2016.05.009.
38. Lopez-Ramos, J.; Martinez-Romero, R.; Molina, F.; Cañuelo, A.; Martínez-Lara, E.; Siles, E.; Peinado, M. Evidence of a decrease in nitric oxide-storage molecules following acute hypoxia and/or hypobaria, by means of chemiluminescence analysis. *Nitric Oxide* **2005**, *13*, 62-67, doi:10.1016/j.niox.2005.05.003.
39. Peinado, M.; Lopez-Ramos, J.; Camacho, M.; Molina, F.; Martínez-Romero, R.; Hernández, R.; Siles, E.; Martínez-Lara, E.; Del Moral, M.; Pedrosa, J. Age and sex-related serum changes in nitric oxide: correlations with serological markers. *International journal of cardiology* **2007**, *121*, 88-90, doi:10.1016/j.ijcard.2006.08.032.
40. Braman, R.S.; Hendrix, S.A. Nanogram nitrite and nitrate determination in environmental and biological materials by vanadium (III) reduction with chemiluminescence detection. *Analytical Chemistry* **1989**, *61*, 2715-2718.
41. Buege, J.A.; Aust, S.D. [30] Microsomal lipid peroxidation. In *Methods in enzymology*, Elsevier: 1978; Vol. 52, pp. 302-310.
42. Mohagheghi, F.; Bigdeli, M.R.; Rasoulian, B.; Hashemi, P.; Pour, M.R. The neuroprotective effect of olive leaf extract is related to improved blood–brain barrier permeability and brain edema in rat with experimental focal cerebral ischemia. *Phytomedicine* **2011**, *18*, 170-175, doi:10.1016/j.phymed.2010.06.007.

43. Yu, H.; Liu, P.; Tang, H.; Jing, J.; Lv, X.; Chen, L.; Jiang, L.; Xu, J.; Li, J. Oleuropein, a natural extract from plants, offers neuroprotection in focal cerebral ischemia/reperfusion injury in mice. *European journal of pharmacology* **2016**, *775*, 113-119, doi:10.1016/j.ejphar.2016.02.027.
44. Balkaya, M.; Kröber, J.M.; Rex, A.; Endres, M. Assessing post-stroke behavior in mouse models of focal ischemia. *Journal of Cerebral Blood Flow & Metabolism* **2013**, *33*, 330-338, doi:10.1038/jcbfm.2012.185.
45. Schaapsmeerders, P.; Maaijwee, N.A.; van Dijk, E.J.; Rutten-Jacobs, L.C.; Arntz, R.M.; Schoonderwaldt, H.C.; Dorresteijn, L.D.; Kessels, R.P.; de Leeuw, F.-E. Long-term cognitive impairment after first-ever ischemic stroke in young adults. *Stroke* **2013**, *44*, 1621-1628, doi:10.1161/STROKEAHA.111.000792.
46. Kroll, H.; Zaharchuk, G.; Christen, T.; Heit, J.; Iv, M. Resting State BOLD MRI for Perfusion and Ischemia. *Topics in magnetic resonance imaging: TMRI* **2017**, *26*, 91, doi:10.1097/RMR.0000000000000119.
47. Carter, A.R.; Astafiev, S.V.; Lang, C.E.; Connor, L.T.; Rengachary, J.; Strube, M.J.; Pope, D.L.; Shulman, G.L.; Corbetta, M. Resting interhemispheric functional magnetic resonance imaging connectivity predicts performance after stroke. *Annals of neurology* **2010**, *67*, 365-375, doi:10.1002/ana.21905.
48. Rehme, A.K.; Fink, G.R.; von Cramon, D.Y.; Grefkes, C. The role of the contralesional motor cortex for motor recovery in the early days after stroke assessed with longitudinal FMRI. *Cerebral cortex* **2010**, *21*, 756-768, doi:10.1093/cercor/bhq140.
49. Ogoh, S. Relationship between cognitive function and regulation of cerebral blood flow. *The Journal of Physiological Sciences* **2017**, *67*, 345-351, doi:10.1007/s12576-017-0525-0.
50. Wiesmann, M.; Zerbi, V.; Jansen, D.; Haast, R.; Lütjohann, D.; Broersen, L.M.; Heerschap, A.; Kiliaan, A.J. A dietary treatment improves cerebral blood flow and brain connectivity in aging apoE4 mice. *Neural plasticity* **2016**, *2016*, doi:10.1155/2016/6846721.
51. Kennedy, D.O.; Wightman, E.L.; Reay, J.L.; Lietz, G.; Okello, E.J.; Wilde, A.; Haskell, C.F. Effects of resveratrol on cerebral blood flow variables and cognitive performance in humans: a double-blind, placebo-controlled, crossover investigation. *The American journal of clinical nutrition* **2010**, *91*, 1590-1597, doi:10.3945/ajcn.2009.28641.
52. Lu, K.T.; Chiou, R.Y.; Chen, L.G.; Chen, M.H.; Tseng, W.T.; Hsieh, H.T.; Yang, Y.L. Neuroprotective effects of resveratrol on cerebral ischemia-induced neuron loss mediated by free radical scavenging and cerebral blood flow elevation. *Journal of agricultural and food chemistry* **2006**, *54*, 3126-3131, doi:10.1021/jf053011q.
53. Rodrigo, J.; Fernandez, A.; Serrano, J.; Peinado, M.; Martinez, A. The role of free radicals in cerebral hypoxia and ischemia. *Free Radical Biology and Medicine* **2005**, *39*, 26-50, doi:10.1016/j.freeradbiomed.2005.02.010.
54. Martinez-Lara, E.; Canuelo, A.; Siles, E.; Hernandez, R.; Del Moral, M.; Blanco, S.; Pedrosa, J.; Rodrigo, J.; Peinado, M. Constitutive nitric oxide synthases are responsible for the nitric oxide production in the ischemic aged cerebral cortex. *Brain research* **2005**, *1054*, 88-94, doi:10.1016/j.brainres.2005.06.060.
55. Serrano-Ponz, M.; Rodrigo-Gasqué, C.; Siles, E.; Martínez-Lara, E.; Ochoa-Callejero, L.; Martínez, A. Temporal profiles of blood pressure, circulating nitric oxide, and adrenomedullin as predictors of clinical outcome in acute ischemic stroke patients. *Molecular medicine reports* **2016**, *13*, 3724-3734, doi:10.3892/mmr.2016.5001.
56. Rashid, P.A.; Whitehurst, A.; Lawson, N.; Bath, P.M. Plasma nitric oxide (nitrate/nitrite) levels in acute stroke and their relationship with severity and outcome. *Journal of Stroke and Cerebrovascular Diseases* **2003**, *12*, 82-87, doi:10.1053/jscd.2003.9.
57. Abdullah, A.; Ssefer, V.; Ertugrul, U.; Osman, E.; Esref, A.; Ugur, C.M.; Adalet, A.; Yavuz, Y.; Faysal, E.; Nebahat, T. Evaluation of serum oxidant/antioxidant balance in patients with acute stroke. *J Pak Med Assoc* **2013**, *63*, 590-593.
58. Rodrigo, R.; Fernández-Gajardo, R.; Gutiérrez, R.; Manuel Matamala, J.; Carrasco, R.; Miranda-Merchak, A.; Feuerhake, W. Oxidative stress and pathophysiology of ischemic stroke: novel therapeutic opportunities. *CNS &*

Neurological Disorders-Drug Targets (Formerly Current Drug Targets-CNS & Neurological Disorders) **2013**, *12*, 698-714, doi:10.2174/1871527311312050015.

59. Echeverría, F.; Ortiz, M.; Valenzuela, R.; Videla, L. Hydroxytyrosol and cytoprotection: a projection for clinical interventions. *International journal of molecular sciences* **2017**, *18*, 930, doi:https://doi.org/10.3390/ijms18050930.
60. Martínez-Romero, R.; Cañuelo, A.; Martínez-Lara, E.; Javier Oliver, F.; Cárdenas, S.; Siles, E. Poly (ADP-ribose) polymerase-1 modulation of in vivo response of brain hypoxia-inducible factor-1 to hypoxia/reoxygenation is mediated by nitric oxide and factor inhibiting HIF. *Journal of neurochemistry* **2009**, *111*, 150-159, doi: 10.1111/j.1471-4159.2009.06307.x.
61. Richard, N.; Arnold, S.; Hoeller, U.; Kilpert, C.; Wertz, K.; Schwager, J. Hydroxytyrosol is the major anti-inflammatory compound in aqueous olive extracts and impairs cytokine and chemokine production in macrophages. *Planta medica* **2011**, *77*, 1890-1897, doi:10.1055/s-0031-1280022.
62. Pirozzi, C.; Lama, A.; Simeoli, R.; Paciello, O.; Pagano, T.B.; Mollica, M.P.; Di Guida, F.; Russo, R.; Magliocca, S.; Canani, R.B. Hydroxytyrosol prevents metabolic impairment reducing hepatic inflammation and restoring duodenal integrity in a rat model of NAFLD. *The Journal of nutritional biochemistry* **2016**, *30*, 108-115, doi:10.1016/j.jnutbio.2015.12.004.
63. Lopez, S.; Montserrat-de la Paz, S.; Lucas, R.; Bermudez, B.; Abia, R.; Morales, J.C.; Muriana, F.J. Effect of metabolites of hydroxytyrosol on protection against oxidative stress and inflammation in human endothelial cells. *Journal of functional foods* **2017**, *29*, 238-247, doi:10.1016/j.jff.2016.12.033.
64. Hornedo-Ortega, R.; Cerezo, A.B.; de Pablos, R.M.; Krisa, S.; Richard, T.; García-Parrilla, M.C.; Troncoso, A.M. Phenolic compounds characteristic of the Mediterranean diet in mitigating microglia-mediated neuroinflammation. *Frontiers in cellular neuroscience* **2018**, *12*, doi:10.3389/fncel.2018.00373.
65. Koh, S.-H.; Park, H.-H. Neurogenesis in stroke recovery. *Translational stroke research* **2017**, *8*, 3-13, doi:10.1007/s12975-016-0460-z.
66. Brown, J.P.; Couillard-Després, S.; Cooper-Kuhn, C.M.; Winkler, J.; Aigner, L.; Kuhn, H.G. Transient expression of doublecortin during adult neurogenesis. *Journal of Comparative Neurology* **2003**, *467*, 1-10, doi:10.1002/cne.10874.
67. Song, M.; Martinowich, K.; Lee, F.S. BDNF at the synapse: why location matters. *Molecular psychiatry* **2017**, *22*, 1370, doi:10.1038/mp.2017.144.
68. Rossi, C.; Angelucci, A.; Costantin, L.; Braschi, C.; Mazzantini, M.; Babbini, F.; Fabbri, M.E.; Tessarollo, L.; Maffei, L.; Berardi, N. Brain-derived neurotrophic factor (BDNF) is required for the enhancement of hippocampal neurogenesis following environmental enrichment. *European Journal of Neuroscience* **2006**, *24*, 1850-1856, doi:10.1111/j.1460-9568.2006.05059.x.
69. Carito, V.; Venditti, A.; Bianco, A.; Ceccanti, M.; Serrilli, A.M.; Chaldakov, G.; Tarani, L.; De Nicolò, S.; Fiore, M. Effects of olive leaf polyphenols on male mouse brain NGF, BDNF and their receptors TrkA, TrkB and p75. *Natural product research* **2014**, *28*, 1970-1984, doi:10.1080/14786419.2014.918977.
70. De Nicoló, S.; Tarani, L.; Ceccanti, M.; Maldini, M.; Natella, F.; Vania, A.; Chaldakov, G.N.; Fiore, M. Effects of olive polyphenols administration on nerve growth factor and brain-derived neurotrophic factor in the mouse brain. *Nutrition* **2013**, *29*, 681-687, doi:10.1016/j.nut.2012.11.007.
71. Zheng, A.; Li, H.; Cao, K.; Xu, J.; Zou, X.; Li, Y.; Chen, C.; Liu, J.; Feng, Z. Maternal hydroxytyrosol administration improves neurogenesis and cognitive function in prenatally stressed offspring. *The Journal of nutritional biochemistry* **2015**, *26*, 190-199, doi:10.1016/j.jnutbio.2014.10.006.

72. Gualtieri, F.; Brégère, C.; Laws, G.C.; Armstrong, E.A.; Wylie, N.J.; Moxham, T.T.; Guzman, R.; Boswell, T.; Smulders, T.V. Effects of environmental enrichment on doublecortin and BDNF expression along the dorso-ventral axis of the dentate gyrus. *Frontiers in neuroscience* **2017**, *11*, 488, doi:10.3389/fnins.2017.00488.

Artículo 4

El tirosol, fenol simple del AOVE, modula múltiples mecanismos patogénicos relacionados con la neurodegeneración en modelos de *C. elegans* de la enfermedad de Parkinson

Jesús Calahorra, Montserrat Porta de la Riva, Esther Martínez-Lara, Eva Siles, Ana Cañuelo

*Neurobiology of ag*ing. 2019; j.neurobiolaging.2019.07.003

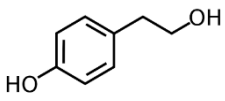

Accepted Manuscript

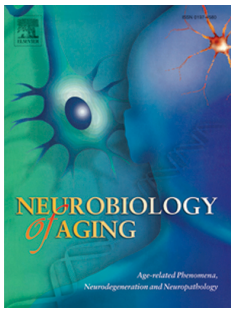

Tyrosol, a simple phenol from EVOO, targets multiple pathogenic mechanisms of neurodegeneration in a *C. elegans* model of Parkinson´s Disease

Jesús Calahorra García-Moreno, Montserrat Porta de la Riva, Esther Martínez-Lara, Eva Siles, Ana Cañuelo

PII: S0197-4580(19)30205-2

DOI: https://doi.org/10.1016/j.neurobiolaging.2019.07.003

Reference: NBA 10612

To appear in: *Neurobiology of Aging*

Received Date: 16 January 2019

Revised Date: 13 May 2019

Accepted Date: 4 July 2019

Please cite this article as: García-Moreno, J.C., Porta de la Riva, M., Martínez-Lara, E., Siles, E., Cañuelo, A., Tyrosol, a simple phenol from EVOO, targets multiple pathogenic mechanisms of neurodegeneration in a *C. elegans* model of Parkinson´s Disease, *Neurobiology of Aging* (2019), doi: https://doi.org/10.1016/j.neurobiolaging.2019.07.003.

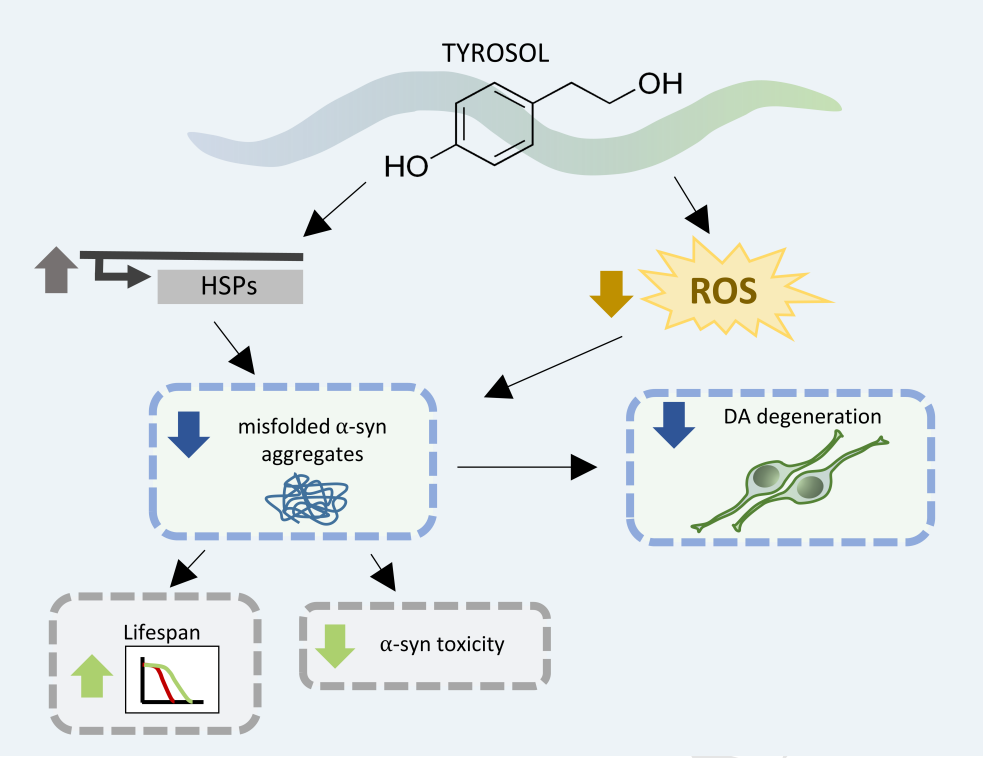

Tyrosol, a simple phenol from EVOO, targets multiple pathogenic mechanisms of neurodegeneration in a *C. elegans* model of Parkinson´s Disease

Jesús Calahorra García-Moreno[a], Montserrat Porta de la Riva[b], Esther Martínez-Lara[a], Eva Siles[a], Ana Cañuelo [a*]

[a]Biochemistry and Molecular Biology Section, Department of Experimental Biology, University of Jaen, Jaen, Spain.

[b]Cancer and Human Molecular Genetics, *C. elegans* Core Facility, Bellvitge Biomedical Research Institute-IDIBELL, L'Hospitalet de Llobregat, Barcelona, Spain.

***Corresponding author:**

Ana Cañuelo Navarro, PhD.

Biochemistry and Molecular Biology Section, Department of Experimental Biology

University of Jaén

Campus Las Lagunillas

23071 Jaén, Spain

Tel.: +34953212767

Fax: +34953211875

E-mail: acanuelo@ujaen.es

Abstract

Parkinson's Disease (PD) is a common neurodegenerative disorder involving α-synuclein (α-syn) aggregation, oxidative stress, dysregulation of redox metal homeostasis and neurotoxicity. Different phenolic compounds with known antioxidant or anti-chelating properties have been shown to also interfere with aggregation of amyloid proteins and modulate intracellular signaling pathways. The present study aims to investigate for the first time the effect of tyrosol (TYR), a simple phenol present in Extra Virgin Olive Oil (EVOO), on α-syn aggregation in a *C. elegans* model of PD and evaluate its potential to prevent α-syn toxicity, neurodegeneration and oxidative stress in this model organism. Our results show that TYR is effective in reducing α-syn inclusions, resulting in a lower toxicity and extended lifespan of treated nematodes. Moreover, TYR delayed α-syn-dependent degeneration of dopaminergic neurons *in vivo*. TYR treatment also reduced ROS level and promoted the expression of specific chaperones and antioxidant enzymes. Overall, our study puts into perspective TYR potential to be considered as nutraceutical that targets pivotal causal factors in PD.

Key words: Tyrosol; α-synuclein; *C. elegans*; Parkinson´s Disease; Chaperones; Reactive Oxygen species.

Abbreviations:

TYR: tyrosol

ROS: Reactive oxygen species

EVOO: Extra virgin olive oil

NGM: nematode growth media

FUDR: fluorodeoxyuridine

CEP: cephalic

ADE: anterior deirid

2',7'-Dichlorodihydrofluorescein diacetate: DCFH-DA

1. Introduction

Aggregation of the presynaptic protein α-synuclein (α-syn) in dopaminergic neurons of the *substantia nigra pars compacta* is one of the main toxic mechanisms in the pathogenesis of Parkinson's disease (PD). Under physiological conditions, α-syn is found in its free disordered cytosolic native form, but under cellular stress, α-syn can also appear as an α-helix-rich form with a high propensity to aggregate (Burré et al., 2013; Fauvet et al., 2012). Progressive accumulation of this protein in form of oligomers and subsequent fibrils results in the formation of cytoplasmatic inclusions known as Lewy bodies, also including proteins such as ubiquitin and chaperone Hsp70, among others (Sharma and Priya, 2017; Wakabayashi et al., 2007). Recently, studies have pointed to α-syn oligomers and protofibrils as the true toxic species that trigger neurodegeneration and suggest that the formation of Lewy bodies could constitute a cytoprotective mechanism in PD (Ingelsson, 2016; Winner et al., 2011).

Reactive oxygen species (ROS) in dopaminergic neurons (DA) have been strongly associated to the development of PD (Dias et al., 2013). In contrast to other brain regions, the *substantia nigra* is especially susceptible to attack by ROS, considering its additional oxidative stress burden due to dopamine metabolism, a lower antioxidant level, a high composition in fatty acids prone to peroxidation and its high iron concentration which enhance ROS generation through Fenton reaction (Reeve et al., 2014; Reynolds et al., 2007; Zhao et al., 2017). In addition, elevated ROS levels in neurons is known to affect α-syn aggregation into toxic oligomers, leading to pathological events such as synaptic dysfunction, mitochondrial inhibition and interruption of correct chaperone function (Dias et al., 2013). Altogether, these factors finally converge in neurodegeneration and cell death (Schildknecht et al., 2013). The use of antioxidant therapies has been shown to promote either protection or slowdown of cell death progression in PD (Filograna et al., 2016; Liu et al., 2007; Wang et al., 2006).

The invertebrate model *C. elegans* provides several appealing advantages to investigate the connection between oxidative stress, α-syn aggregation and toxicity. In this sense, transgenic strains that reproduce distinct aspects of PD upon human α-syn expression in muscle cells or in dopaminergic neurons have been developed in the last decade (Harrington et al., 2012; Van Ham et al., 2008). Moreover, its transparent body enables *in vivo* visualization of dopaminergic neurodegeneration and α-syn inclusions in

body wall cells, making it a simple but useful system to investigate both, cell loss and α-syn aggregation in PD (Chakraborty et al., 2013).

In the last decades, several phenolic compounds present in olive leaf and fruit have shown important beneficial effects against different pathologies including neurodegenerative disorders, although the mechanisms involved in the latter are not clearly defined yet (Coccia et al., 2016; Grossi et al., 2013; Luccarini et al., 2014; Rosillo et al., 2014; Santangelo et al., 2016; Vauzour et al., 2010). In previous studies, our group has reported a pro-longevity effect of tyrosol (TYR), one of the main polyphenols in olive leaf and fruit, also present in extra virgin olive oil (EVOO), using *wild type* strains of *C. elegans* (Cañuelo et al., 2015a; Cañuelo et al., 2012; Cañuelo and Peragón, 2013). Although we have described interesting biological effects of this phenol in delaying aging and protecting from thermal and oxidative stress, its therapeutic potential in a neurodegeneration context has not been examined before in this model organism.

In this study, we have analyzed the effect of TYR on α-syn aggregation using a transgenic strain of *C. elegans* which constitutively overexpresses this human protein in body wall cells thus exhibiting a progressive paralysis phenotype. We have also evaluated the effect of TYR on neurodegeneration *in vivo* using a *C. elegans* strain that expresses α-syn exclusively in dopaminergic neurons, which show accelerated degeneration over time. Finally, we have measured TYR effect on both, lifespan and ROS level, and determined the expression of specific chaperones and antioxidant enzymes in this experimental model in order to assess its potential protective role in PD pathogenesis.

2. Materials and Methods

2.1. Strains and growth conditions

The *C. elegans* strains N2, NL5901 (pkIs2386; unc-54p:: α-syn::YFP + unc-119(+)) and UA44 (bal11;Pdat-1::α-syn, Pdat-1::gfp) used in this study were obtained from the CGC (Caenorhabditis Genetics Center). The strain NL5901 overexpresses α-syn::YFP within worm body wall muscle cells and also exhibits age-dependent mobility defects associated with α-syn::YFP aggregation, which can be easily monitored. The strain UA44 expresses α-syn::GFP under the control of the dopamine transporter *dat-1* promoter, causing an age-dependent neurodegeneration of DA. Worms were propagated at 21°C either on

solid Nematode Growth Media (NGM) seeded with the *E. coli* strain OP50 (Brenner, 1974) or in liquid media (S-complete medium) as described by Solis & Petrascheck (Solis and Petrascheck, 2011).

2.2. Treatment with TYR

For all the analysis, TYR (2-(4-hydroxyphenyl) ethylalcohol); (Extrasynthese, France) was dissolved in DMSO and added to its final concentrations to NGM previously autoclaved and cooled to 50ºC. The media was immediately dispensed into Petri dishes that were kept protected from light and stored at 4ºC until use. For liquid media experiments, TYR dissolved in DMSO was added directly to S-complete medium. A final DMSO concentration of 0.1% (v/v) was maintained in all experimental groups. All the experiments involving TYR were always carried out in parallel with a control group that contained only DMSO.

2.3. Lifespan assays

The screening procedure was carried out as previously described (Solis and Petrascheck, 2011). Briefly, L1 synchronized adult worms were grown in S-complete medium containing 5 mg/ml *E. coli* OP50 and a mixture of penicillin-streptomycin 1% (v/v). An aliquot of the worm suspension was transferred to each well of a 96-well plate, mixed for 2 min and incubated for 45 h at 20 °C until the animals reached the L4 stage. The animals were sterilized by adding 30 µl of a stock solution of 0.6 mM fluorodeoxyuridine (FUDR) to each well. After 24 h, on day 1 of adulthood, TYR was added at 4 different concentrations ranging from 50 µM to 1 mM, the plates were sealed and incubated at 20 °C. Every 7 days, 5 µl of the *E. coli* OP50 (100 mg/ml) were added to each well. The number of surviving animals was monitored daily until death. Nematodes were considered to be dead when they did not respond to a mechanical stimulus with a platinum wire or no pharyngeal pumping was observed. An average of 120 nematodes were used per experimental condition.

2.4. Quantification of aggregates

TYR was added to the NGM media of synchronized L4 worms and maintained during the whole assay. At the 6th day of adulthood, worms (n=60/treatment) were mounted in a 5µl drop of 10 mM levamisole (Sigma) on a 3% agarose pad, covered with a 24x24 mm coverslip and observed under confocal microscopy to visualize fluorescent α-syn inclusions in the head region. Confocal microphotographs were obtained with Leica TCS SP5 II and equal adjustment of brightness and contrast on control and matched

experimental images was done using confocal software LAS-AF. For a more accurate quantification of individual inclusions, z-stack overlay images were analyzed using Image J software. An average of 20 worms per experimental condition were analyzed.

2.5. Paralysis assay in liquid culture

Synchronized populations were obtained using hypochlorite extraction. Worms were grown on solid media up to day 1 of adulthood. FUDR 0.12 mM was added when worms reached the L4 stage. At adult day 1, N2 or NL5901 worms per well were transferred to S-medium with OP50 *E. coli* (optical density 0.5) in a flat-bottom 96-well plate at 20ºC. TYR 1 mM was added and locomotion under control and treatment conditions was assessed for 90 minutes after 3, 7, 9 and 11 days using WMicrotracker (Phylumtech, Santa Fe, Argentina). A total of 180 worms were used per experimental condition.

2.6. Preparation of Worm Protein Extracts and Western Blotting

For protein extraction, 20 worms per condition were manually collected at the 6th day of adulthood and pooled in 15 µl of Laemmli buffer. After freezing in liquid nitrogen, the mix was heated at 95ºC for 10 minutes. Proteins were separated by SDS-PAGE in a 4-20% gradient polyacrylamide gel (BioRad) and transferred to Immobilon P PVDF membranes (Millipore). For α-syn::YFP detection, blots were probed with anti α-syn monoclonal antibody (Invitrogen, Camarillo, CA) at a 1:1000 dilution. An anti-rabbit secondary antibody at a 1:5000 dilution was used (Sigma-Aldrich). Actin was used as loading control. ECL Prime kit (GE Healthcare Life Sciences) was used for signal detection, following manufacturer´s instructions.

2.7. DA neurons degeneration assay

For neurodegeneration assay, the *C. elegans* transgenic strain UA44 (bal11;Pdat-1::α-syn, Pdat-1::gfp) was used. TYR was added to the NGM media of synchronized L4 worms and maintained during the whole assay. Worms were transferred to fresh treatment plates with OP50 every 2-3 days. On the 14th day of adulthood, nematodes were placed on glass slides with 10 µl of levamisole and GFP was visualized with a CX 31 (Olympus) fluorescence microscope fitted with a camera (C-7070 Wide Zoom, Olympus). The integrity of the six anterior DA neurons, four cephalic (CEP) and two anterior deirid (ADE), was evaluated for neurodegeneration according to previously described criteria (Berkowitz et al., 2008). Briefly, animals with complete GFP fluorescence in all 4 CEP and 2 ADE neurons were scored as *wild-*

177 *type*, whereas individual animals exhibiting loss of DA neurons or signs of degeneration such as axonal
178 blebbing were scored as non-*wild-type* or *degenerating*. An average of 40 worms per experimental
179 condition were analyzed.

180

181 **2.8. Measurement of ROS**

182 The 2',7'-Dichlorodihydrofluorescein diacetate (DCFH-DA) assay have been adapted from a previously
183 described protocol (Wang and Joseph, 1999). Briefly, L1 synchronized worms were grown in S-complete
184 medium (10–15 worms per 20 µl) containing 5 mg/ml *E. coli* OP50. In L4 stage, worms were sterilized
185 by adding 0.6 mM FUDR and after 24 h, on day 1 of adulthood, TYR was added. On adult day 6, ten
186 worms per well were transferred to a 96 wells plate with 75 µL of PBS per well. Subsequently 25 µL of
187 DCF-DA 150 µM dissolved in PBS buffer was added and immediately fluorescence was measured for
188 125 min at 10 min intervals, using excitation and emission λ at 485 nm and 535 nm, respectively
189 (Synergy HT, BioTek). An average of 60 worms per experimental condition were analyzed.

190 **2.9. RNA isolation**

191 Synchronized nematodes were collected at the 6th day of adulthood, washed 3 times in M9 buffer and
192 pelleted by centrifugation for RNA isolation. After centrifugation, worms were resuspended in 350 µl of
193 TRIzol Reagent (Invitrogen, Carlsbad, CA, USA), flash frozen in liquid nitrogen and thawed at 37 °C
194 three times for disruption and total RNA was purified using the RNeasy Mini kit (Qiagen, Venlo,
195 Netherlands) following the manufacturer recommended protocol. Final volume of isolated RNA was 50
196 µl per biological sample.

197 **2.10. Real time qPCR**

198 Briefly, cDNA was synthesized from 1 µg of total RNA using the Maxima First Strand cDNA Synthesis
199 Kit for real-time qPCR (Thermo Scientific, Waltham, MA, USA). qPCR was performed in a CFX384
200 Touch Real-Time PCR Detection System (Bio-Rad) using Kapa SYBR FAST qPCR kit (Kapa
201 Biosystems, Wilmington, MA, USA) with 1 µl cDNA in a 10 µl reaction volume using the following
202 gene-specific oligonucleotide primers: *hsp-70* (NM_060084.2),
203 CGTTTCGAAGAGCTCTGTGCTGATCTTTTCCGC (F) and

TTAATCAACTTCCTCTACAGTAGGTCCTTGTGG (R); *hsp-4* (NM_063135), GCAACCAAGATGCCTCTACTG (F) and CCTCCCGCCGAGTAAAGTTT (R); *hsp-12.6* (NM_069267.1), ATGATGAGCGTTCCAGTGATGGCTGACG (F) and TTAATGCATTTTTCTTGCTTCAATGTGAAGAATTCC (R); *hsp-16.1* (NM_072953.3), GTCACTTTACCACTATTTCCGTCCAGCTCAACGTTC (F) and CAACGGGCGCTTGCTGAATTGGAATAGATCTTCC (R); *gst-4* (NM_069447.5), TTTTCTATGGAAGTGACGCTGA (F) and TTTTCTATGGAAGTGACGCTGA (R); *sod-3* (NM_078363.5) CAAACCAGGATCCTTTGGAA (F) and TGGCAAATCTCTCGCTGATA (R); *sod-1* (NM_001026785.2), TGGATCACACAGAAGTCCGA (F) and GGAATCCATGAAGACCGGGA (R); *gpx-1* (NM_060197.1), CAAAGAATTGCTCGATGTGTACA (F) and TGCATCGAACATGAATCCACC (R); *gpx-2* (NM_001306618.1), GGAGCTCCTCGATGTGTACA (F) and ACCACCGAATTGATTGCACG (R); *ctl-1* (NM_064578.4), TCCATTTCAAGCCTGCTCAAG (F) and AATGGCATTGAACAGGTCGC (R); *ctl-2* (NM_001027302.5), GCTGAGGTTGAACAATCCGC (F) and AAGGCGGTGGAAATGAGTGT (R); *ama-1* (NM_068122.6), AAGCTATAGCCCTTCGTCGC (F) and CGAGGATGGAGTGTACGTCG (R). All samples were run in triplicate. Cycle thresholds of amplification, expression levels of the target genes normalized to the housekeeping gene *ama-1* and relative FC for transcripts were calculated using the CFX Manager (Bio-Rad).

2.11. Statistical analysis

Data are expressed as mean values ± SEM of at least three independent experiments. Statistical comparisons between the different experimental groups and their corresponding controls were made with Student's *t*-test or Log-Rank test, accepting $p<0.05$ as the level of significance, using GraphPad Prism 6 software (GraphPad Software Inc.).

3. Results

3.1. TYR extends lifespan in a *C. elegans* model of PD

In a previous study by our group, we described that TYR was able to induce a significant lifespan extension in a *wild type C. elegans* strain (Cañuelo et al., 2012). In the present study, we have used the transgenic strain NL5901 as a *C. elegans* model of PD. Overexpression of α-syn in body-wall cells of this

strain has been reported to induce significant toxicity and reduced lifespan, as well as impaired motility and pharyngeal pumping as compared to the *wild type* N2 strain (Bodhicharla et al., 2012). Thus, we decided to start our study by analyzing if TYR was also capable of stimulating longevity in this transgenic strain. With this aim, we performed lifespan assays adding four different TYR doses to the NGM. As shown in Figure 1, TYR at 1 mM concentration exerted a significant lifespan increase in worms compared to control group (Mean survival days: Control 18.67±0.33 vs. TYR 1 mM 21.33±0.66; *t*-test **p*=0.0232), supporting our previously reported TYR effects on *C. elegans* longevity. However, lower TYR doses did not induce significant increases in survival.

3.2. TYR decreases the amount of α-syn inclusions without affecting its expression

The transgenic *C. elegans* strain NL5901 used in this study, constitutively expresses YFP-fused human α-syn protein in body wall cells, allowing *in vivo* quantification of fluorescent inclusions of this protein. Thus, we also chose this strain to study the effect of TYR treatment on α-syn aggregation. As shown in Figure 2A-B, by adult day 6, a pronounced decrease of α-syn inclusions was observed in the 1 mM TYR group as compared to non-treated control nematodes (nº aggregates/animal: Control 58.72±3.47 vs. TYR 1 mM 22.63±5.17; *t*-test ***p* =0.0044). Nevertheless, no changes in total α-syn::YFP levels were observed (Figure 2C). These results suggest that TYR supplementation protects against the aggregation of α-syn, a critical process in PD development in humans.

3.3. Motility impairment in NL5901 strain is ameliorated in response to TYR

α-syn toxicity in NL5901 strain is associated with its aggregation in body wall cells causing age-dependent mobility defects which can be monitored (van Ham et al., 2010). As shown in figure 5, NL5901 strain exhibits a premature and progressive decline in body movement compared to the wild type strain N2 (Figure 5-A). This decline becomes more evident by adult day 7 in both, control and TYR treated NL5901 nematodes. However, by adult day 9, 1 mM TYR treated nematodes exhibited a significantly faster body movement as compared to untreated controls (nº of activity counts per 30 min: Control 7,7±1.81 vs. TYR 1mM 20,9±5.62; *t*-test **p*=0.0364) (Figure 3-B). By adult day 11, both groups showed a similar level of body movements, close to 100% paralysis. These results may be related to the lower amount of α-syn inclusions shown earlier in treated worms, supporting the notion that TYR

treatment could prevent α-syn toxic effects by interfering with its cytoplasmic aggregation process in this model organism.

3.4. TYR delays dopaminergic neurodegeneration in a *C. elegans* model of PD

DA are the main neuronal type affected in PD (Spillantini et al., 1998). In order to investigate if the observed effect of TYR on α-syn aggregation could be also extrapolated to a *C. elegans* model of DA neurodegeneration induced by α-syn, we used the transgenic strain UA44 (bal11;Pdat-1::α-syn, Pdat-1::GFP). The expression of human α-syn under the control of the dopamine transporter *dat-1* promoter in this strain causes an age-dependent neurodegeneration of DA, allowing the easy identification of these neurons by the simultaneous expression of GFP (Ray et al., 2015). Under our culture conditions, we established that degenerative changes were more evident in non-treated worms at adult days 12-14, when approximately 40% of nematodes have their 6 anterior DA intact. Treatment with 1mM TYR induced a significant increase in the percentage of nematodes with intact neurons at 14^{th} day of adulthood as compared with controls (% wild type animals: Control 45.33±3.52 vs. TYR 1 mM 80±2.30; *t*-test ***p* =0.0012) (Figure 4). Thus, our data shows that TYR is also protective against α-syn dependent neurodegeneration *in vivo*.

3.5. TYR decreases ROS level in a *C. elegans* model of PD

Oxidative stress is thought to be an underlying mechanism for the pathology of PD in both, sporadic and familial forms. In line with this, increases in the oxidized lipids, proteins and DNA were observed in the brain of PD patients (Hwang, 2013). In a previous study, we showed that TYR treatment was able to promote oxidative stress resistance induced by paraquat in *wild type C. elegans* strains (Cañuelo et al., 2012). Herbicides and pesticides such as rotenone, paraquat, and maneb are commonly used as PD models that result in increased ROS production and altered mitochondrial energetics (Blesa et al., 2012). In a recent study, Dewapriya et al. reported a protective effect of TYR treatment against MPP+ induced cytotoxicity in mouse brain-derived catecholaminergic neuron cells (CATH) by supressing the oxidative and nitrosative stress in these cells (Dewapriya et al., 2013). Thus, we decided to assess whether TYR could lower the intracellular ROS level in NL5901 nematodes by using CM-H2DCFDA, a fluorescent probe that reacts with ROS. As expected, paraquat treatment used as positive control, induced a marked increase in intraworm ROS levels compared to control group (Fluorescence AU: Control 124.5±3.5 vs. Control + PQ 250±16.17; *t*-test **p*=0.0132) (Figures 5-A and 5-B). However, pretreatment with TYR

significantly reduced ROS accumulation compared to control (Control 124.5±3.5 vs. TYR 1 mM 82±12.06; *t*-test *p=0.0347) and to paraquat treated worms, confirming that this phenol has an effective antioxidant effect in this *C. elegans* strain.

3.6. The reduction of α-syn accumulation by TYR is accompanied by the up-regulation of specific chaperone and antioxidant enzymes

In *C. elegans*, coordinated induction of genes involved in antioxidant/heat-shock response and detoxification results in a longer lifespan and an improved proteostasis (Honda and Honda, 1999; Johnson et al., 2002). In order to investigate the molecular mechanism for TYR protective effect in an α-syn-overexpression scenario, we performed qPCR analysis of several known oxidative/heat stress response genes in NL5901 transgenic nematodes.

Worms were cultured with 0 or 1mM TYR from L1 stage. On day 5 of adulthood, the mRNA level of target genes was analyzed using qPCR. We detected a significant increase in the chaperone genes *hsp-70* (Relative mRNA levels: Control 1±0.30 vs. TYR 1 mM 4.2±0.85; t-test ***p*=0.0037) , *hsp-12.6* (Control 1±0.05 vs. TYR 1 mM 2.038±0.36; t-test **p*=0.047) and *hsp-16.2* (Control 1±0.15 vs. TYR 1 mM 1.934±0.32; t-test **p*=0.011) in response to TYR as compared to controls (Figure 6). In addition, the antioxidant gene *gst-4* (Control 1±0.056 vs. TYR 1 mM 1.64±0.15; *t*-test **p*=0.017) was also significantly up-regulated in response to TYR treatment. However, TYR did not affect the expression of other genes analyzed (*hsp-4, sod-3, sod-1, ctl-1, ctl-2, gpx-1 and gpx-2).*

4. Discussion

In previous studies, we had shown that TYR supplementation was able to induce lifespan increases and promote stress resistance in the model organism *C. elegans* (Cañuelo et al., 2012). Thus, we next sought to assess the effect of this simple phenol in transgenic *C. elegans* strains that express human α-syn and recapitulate key pathogenic processes in PD.

In order to determine the most effective TYR concentration in the *C. elegans* strain NL5901, we first performed lifespan assays in parallel adding TYR at different doses ranging from 50 µM to 1 mM. We observed a moderate increase in lifespan at the higher dose of TYR (1 mM). Recently, different phytochemicals have been also shown to promote longevity in this strain (Govindan et al., 2018; Jadiya et

al., 2011; Ji et al., 2016) indicating a clear connection between lifespan and α-syn expression in these nematodes. Although significant, the observed lifespan increase promoted by TYR in this strain was less prominent compared to the one previously described in *wild type* nematodes and this effect was achieved at a higher TYR dose (1 mM instead of 250 µM)(Cañuelo et al., 2012); these differences suggest that TYR may act through additional cellular mechanisms in the context of α-syn expression that could influence its effect on longevity in this specific strain.

One of the main findings in this study is that TYR treatment is able to substantially reduce the amount or formation of α-syn inclusions in a well-studied *C. elegans* model of PD. This effect was accompanied by a delay in the onset of motility dysfunction induced by α-syn in this model. These results, together with the increased survival observed in this PD strain, supports a positive effect of TYR supplementation in reducing α-syn-associated toxicity *in vivo*. In recent studies, different plant extracts have been shown to also reduce α-syn aggregation in the *C. elegans* strain NL5901 (Chalorak et al., 2018; Jadiya et al., 2011; Ji et al., 2016). Although the precise mechanisms underlying their effect remain to be clarified, it has been suggested that it may involve binding to α-syn monomers and oligomers via hydrophobic interaction with β-structures, which leads to delay of the nucleation process and further assembly of toxic oligomers (Ji et al., 2016). During the last decade, much investigation has focused on small natural molecules, rich in aromatic groups (like polyphenols) as amyloid inhibitors with very variable results. In this sense, different natural polyphenols like apigenin, curcumin, Epigallocatechin-3-gallate among others have been proven effective inhibiting α-syn misfolding and aggregation *in vitro* (Dhouafli et al., 2018). Nevertheless, their capacity to prevent DA degeneration *in vivo* has not been evaluated in depth. Regarding TYR, although there have been a few studies suggesting protective effects of this phenol in PD (Dewapriya et al., 2013; Vauzour et al., 2010), none of them have assessed the direct effect of this phenol in DA expressing α-syn *in vivo*. In this sense, our study using the *C. elegans* strain UA44 provides another relevant result, showing for the first time that TYR treatment is able to induce a significant delay in dopaminergic neurodegeneration associated to α-syn expression in a model organism. This effect on neurodegeneration is probably related to the observed decrease in α-syn aggregation also induced by TYR in *C. elegans*, suggesting the potential of this simple phenol to reduce the toxicity of α-syn in a dopaminergic environment.

Fibrils of α-syn in Lewy bodies and the formation of aggregates have been associated with an increased oxidative stress (Dias et al., 2013). In this sense, it has been suggested that oxidative conjugation of

dopamine with α-syn protein inhibits its transition from protofibrils to mature fibrils, leading to the potential accumulation of cytotoxic soluble protofibrils in DA. Moreover, the addition of antioxidants has the ability to reverse the formation of these adducts, suggesting that catechol oxidation can contribute to the accumulation of α-syn protofibrils (Conway et al., 2001; Chinta and Andersen, 2008). Experiments both *in vivo* and using cultured cells suggest that ROS are able to induce α-syn aggregation, which in turn increases ROS, creating a vicious cycle leading to neurodegeneration (Nieto et al., 2006; Tabrizi et al., 2000). In this sense, our results showing an effective decrease of intraworm ROS accumulation following TYR treatment, suggest that the reported reduction of α-syn inclusions may also be related to the ability of TYR to act as a ROS scavenger. Thus, TYR could ameliorate the cellular oxidative environment that contributes to the formation of toxic α-syn species.

It has been reported that, when overexpressed *in vivo* and *in vitro*, the molecular chaperone *hsp-70* is able to reduce the amount of misfolded, aggregated α-syn protein, also protecting from its toxicity (Klucken et al., 2004). Hence, the reduction in α-syn inclusions observed in TYR-treated nematodes could be related to the detected increase in this chaperone expression. On the other hand, *hsp-16.2* and *hsp-12.6* are members of the 16kDa and 12 kDa families of small heat shock proteins (smHSPs) known to function as molecular chaperones in *C. elegans*, preventing the aggregation of denatured proteins and guiding misfolded proteins to refold to their native state (Horwitz, 1992; Leroux et al., 1997). In particular *hsp-16.2* is likely to function as a passive ligand temporarily preventing unfolded proteins from aggregating and it has been shown to interact with intracellular human beta amyloid peptide, a primary component of the extracellular plaques found in Alzheimer's disease (Fonte et al., 2008). The expression of smHSPs is activated by transcription factors HSF-1 and DAF-16 in response to stress, in turn promoting *C. elegans* longevity (Hsu et al., 2003). Interestingly, we have previously reported that TYR supplementation is able to induce specific smHSP expression both, at the mRNA and protein level in *C. elegans*, and this effect was associated to an increased lifespan and stress resistance in *wild type* strains (Cañuelo et al., 2015b; Cañuelo et al., 2012; Cañuelo and Peragón, 2013). Moreover, we described that this effect was partially dependent on HSF-1. GST-4 (glutathione transferase-4) is involved in the phase II oxidative stress response and several studies have reported that specific GSTs are able to modulate the response to oxidative stress in *C. elegans* as mediated by SKN-1 (Park et al., 2009). Thus, overexpression of this gene increased resistance to oxidative stress in this animal model (Ayyadevara et al., 2005; Leiers et al., 2003).

The fact that TYR induces the expression of this antioxidant gene in α-syn expressing nematodes, may explain the lower ROS level observed as well in TYR-treated animals.

In summary, although further analyses should be conducted in order to narrow down the molecular mechanisms involved, our study reveals important and novel biological activities of TYR, a simple phenol naturally present in the typical Mediterranean Diet, that would act in a synergic manner to prevent or delay the main pathogenic causal factors in PD (Figure 7). Moreover, our results provide an interesting source for molecular docking analyses using TYR structure as a model molecule in drug design aimed to discover new PD neuroprotective therapies.

5. Conclusions

The present study reports for the first time that dietary supplementation with TYR is able to significantly reduce the amount of α-syn aggregates in a *C. elegans* model of PD and, more importantly, delay the onset of dopaminergic neurodegeneration *in vivo*. In parallel, TYR ameliorated the toxic effects of α-syn aggregation on nematode mobility, also promoting a significant lifespan increase. Moreover, our results show that TYR treatment induces an effective decrease of cellular ROS level in the *C. elegans* strain used, supporting a protective effect of this phenol against oxidative stress *in vivo*. These results were concomitant to the up-regulation of the antioxidant gene *gst-4* as well as chaperones *hsp-70*, *hsp-12.6* and *hsp-16.2*. In conclusion, although we cannot rule out the involvement of other mechanisms in the observed TYR effects in this PD model, it seems quite feasible that TYR neuroprotective effects may result from combining direct inhibition of α-syn aggregation, chaperone modulation and ROS scavenging, making it a suitable candidate as nutraceutical compound in PD.

Conflict of interest

On behalf of all authors, the corresponding author states that there is no conflict of interests.

Acknowledgements

NL5901 and UA44 strains were provided by the CGC, which is funded by NIH Office of Research Infrastructure Programs (P40 OD010440). We gratefully acknowledge Antonio Miranda Vizuete for his valuable guidance and technical advice. This work was supported by Grants from Universidad de Jaen (UJA2013/08/08), (R3/2-3/2014), (R3/8/2016 and Instituto de Estudios Giennenses (IEG2012).

403
404
405
406
407
408
409
410
411
412

References

414 Ayyadevara, S., Dandapat, A., Singh, S.P., Beneš, H., Zimniak, L., Reis, R.J.S., Zimniak, P., 2005.
415 Lifespan extension in hypomorphic daf-2 mutants of Caenorhabditis elegans is partially mediated by
416 glutathione transferase CeGSTP2-2. Aging cell 4(6), 299-307.

417 Berkowitz, L.A., Hamamichi, S., Knight, A.L., Harrington, A.J., Caldwell, G.A., Caldwell, K.A., 2008.
418 Application of a C. elegans dopamine neuron degeneration assay for the validation of potential
419 Parkinson's disease genes. Journal of visualized experiments: JoVE(17).

420 Blesa, J., Phani, S., Jackson-Lewis, V., Przedborski, S., 2012. Classic and new animal models of
421 Parkinson's disease. BioMed Research International 2012.

422 Bodhicharla, R., Nagarajan, A., Winter, J., Adenle, A., Nazir, A., Brady, D., Vere, K., Richens, J.,
423 O'Shea, P., R Bell, D., 2012. Effects of α-synuclein overexpression in transgenic Caenorhabditis elegans
424 strains. CNS & Neurological Disorders-Drug Targets (Formerly Current Drug Targets-CNS &
425 Neurological Disorders) 11(8), 965-975.

426 Brenner, S., 1974. The genetics of Caenorhabditis elegans. Genetics 77(1), 71-94.

427 Burré, J., Vivona, S., Diao, J., Sharma, M., Brunger, A.T., Südhof, T.C., 2013. Properties of native brain
428 α-synuclein. Nature 498(7453), E4.

429 Cañuelo, A., Esteban, F.J., Peragón, J., 2015a. Gene expression profiling to investigate tyrosol-induced
430 lifespan extension in Caenorhabditis elegans. European journal of nutrition, 1-12.

431 Cañuelo, A., Esteban, F.J., Peragón, J., 2015b. Gene expression profiling to investigate tyrosol-induced
432 lifespan extension in Caenorhabditis elegans. European Journal of Nutrition 55(2), 639-650.

433 Cañuelo, A., Gilbert-López, B., Pacheco-Liñán, P., Martínez-Lara, E., Siles, E., Miranda-Vizuete, A.,
434 2012. Tyrosol, a main phenol present in extra virgin olive oil, increases lifespan and stress resistance in
435 Caenorhabditis elegans. Mechanisms of ageing and development 133(8), 563-574.
436 Cañuelo, A., Peragón, J., 2013. Proteomics analysis in Caenorhabditis elegans to elucidate the response
437 induced by tyrosol, an olive phenol that stimulates longevity and stress resistance. Proteomics 13(20),
438 3064-3075.
439 Coccia, A., Mosca, L., Puca, R., Mangino, G., Rossi, A., Lendaro, E., 2016. Extra-virgin olive oil phenols
440 block cell cycle progression and modulate chemotherapeutic toxicity in bladder cancer cells. Oncology
441 reports 36(6), 3095-3104.
442 Conway, K.A., Rochet, J.-C., Bieganski, R.M., Lansbury, P.T., 2001. Kinetic stabilization of the α-
443 synuclein protofibril by a dopamine-α-synuclein adduct. Science 294(5545), 1346-1349.
444 Chakraborty, S., Bornhorst, J., Nguyen, T.T., Aschner, M., 2013. Oxidative stress mechanisms underlying
445 Parkinson's disease-associated neurodegeneration in C. elegans. International journal of molecular
446 sciences 14(11), 23103-23128.
447 Chalorak, P., Jattujan, P., Nobsathian, S., Poomtong, T., Sobhon, P., Meemon, K., 2018. Holothuria
448 scabra extracts exhibit anti-Parkinson potential in C. elegans: A model for anti-Parkinson testing.
449 Nutritional neuroscience 21(6), 427-438.
450 Chinta, S.J., Andersen, J.K., 2008. Redox imbalance in Parkinson's disease. Biochimica et Biophysica
451 Acta (BBA)-General Subjects 1780(11), 1362-1367.
452 Dewapriya, P., Himaya, S., Li, Y.-X., Kim, S.-K., 2013. Tyrosol exerts a protective effect against
453 dopaminergic neuronal cell death in in vitro model of Parkinson's disease. Food chemistry 141(2), 1147-
454 1157.
455 Dhouafli, Z., Cuanalo-Contreras, K., Hayouni, E.A., Mays, C.E., Soto, C., Moreno-Gonzalez, I., 2018.
456 Inhibition of protein misfolding and aggregation by natural phenolic compounds. Cellular and Molecular
457 Life Sciences, 1-18.
458 Dias, V., Junn, E., Mouradian, M.M., 2013. The role of oxidative stress in Parkinson's disease. Journal of
459 Parkinson's disease 3(4), 461-491.
460 Fauvet, B., Kamdem, M.M., Fares, M.-B., Desobry, C., Michael, S., Ardah, M.T., Tsika, E., Coune, P.,
461 Prudent, M., Lion, N., 2012. Alpha-synuclein in the central nervous system and from erythrocytes,

462 mammalian cells and E. coli exists predominantly as a disordered monomer. Journal of Biological
463 Chemistry, jbc. M111. 318949.
464 Filograna, R., Godena, V.K., Sanchez-Martinez, A., Ferrari, E., Casella, L., Beltramini, M., Bubacco, L.,
465 Whitworth, A.J., Bisaglia, M., 2016. SOD-mimetic M40403 is protective in cell and fly models of
466 paraquat toxicity: Implications for Parkinson disease. Journal of Biological Chemistry, jbc. M115.
467 708057.
468 Fonte, V., Kipp, D.R., Yerg, J., Merin, D., Forrestal, M., Wagner, E., Roberts, C.M., Link, C.D., 2008.
469 Suppression of in vivo β-amyloid peptide toxicity by overexpression of the HSP-16.2 small chaperone
470 protein. Journal of Biological Chemistry 283(2), 784-791.
471 Govindan, S., Amirthalingam, M., Duraisamy, K., Govindhan, T., Sundararaj, N., Palanisamy, S., 2018.
472 Phytochemicals-induced hormesis protects Caenorhabditis elegans against α-synuclein protein
473 aggregation and stress through modulating HSF-1 and SKN-1/Nrf2 signaling pathways. Biomedicine &
474 Pharmacotherapy 102, 812-822.
475 Grossi, C., Rigacci, S., Ambrosini, S., Dami, T.E., Luccarini, I., Traini, C., Failli, P., Berti, A.,
476 Casamenti, F., Stefani, M., 2013. The polyphenol oleuropein aglycone protects TgCRND8 mice against
477 Aß plaque pathology. PLoS One 8(8), 1-13.
478 Harrington, A.J., Yacoubian, T.A., Slone, S.R., Caldwell, K.A., Caldwell, G.A., 2012. Functional
479 analysis of VPS41-mediated neuroprotection in Caenorhabditis elegans and mammalian models of
480 Parkinson's disease. Journal of Neuroscience 32(6), 2142-2153.
481 Honda, Y., Honda, S., 1999. The daf-2 gene network for longevity regulates oxidative stress resistance
482 and Mn-superoxide dismutase gene expression in Caenorhabditis elegans. The FASEB journal 13(11),
483 1385-1393.
484 Horwitz, J., 1992. Alpha-crystallin can function as a molecular chaperone. Proceedings of the National
485 Academy of Sciences 89(21), 10449-10453.
486 Hsu, A.-L., Murphy, C.T., Kenyon, C., 2003. Regulation of aging and age-related disease by DAF-16 and
487 heat-shock factor. Science 300(5622), 1142-1145.
488 Hwang, O., 2013. Role of oxidative stress in Parkinson's disease. Experimental neurobiology 22(1), 11-
489 17.
490 Ingelsson, M., 2016. Alpha-Synuclein Oligomers—Neurotoxic Molecules in Parkinson's Disease and
491 Other Lewy Body Disorders. Frontiers in neuroscience 10, 408.

492 Jadiya, P., Khan, A., Sammi, S.R., Kaur, S., Mir, S.S., Nazir, A., 2011. Anti-Parkinsonian effects of
493 Bacopa monnieri: insights from transgenic and pharmacological Caenorhabditis elegans models of
494 Parkinson's disease. Biochemical and biophysical research communications 413(4), 605-610.
495 Ji, K., Zhao, Y., Yu, T., Wang, Z., Gong, H., Yang, X., Liu, Y., Huang, K., 2016. Inhibition effects of
496 tanshinone on the aggregation of α-synuclein. Food & function 7(1), 409-416.
497 Johnson, T., Henderson, S., Murakami, S., De Castro, E., de Castro, S.H., Cypser, J., Rikke, B., Tedesco,
498 P., Link, C., 2002. Longevity genes in the nematode Caenorhabditis elegans also mediate increased
499 resistance to stress and prevent disease. Journal of inherited metabolic disease 25(3), 197-206.
500 Klucken, J., Shin, Y., Masliah, E., Hyman, B.T., McLean, P.J., 2004. Hsp70 reduces α-synuclein
501 aggregation and toxicity. Journal of Biological Chemistry 279(24), 25497-25502.
502 Leiers, B., Kampkötter, A., Grevelding, C.G., Link, C.D., Johnson, T.E., Henkle-Dührsen, K., 2003. A
503 stress-responsive glutathione S-transferase confers resistance to oxidative stress in Caenorhabditis
504 elegans. Free Radical Biology and Medicine 34(11), 1405-1415.
505 Leroux, M.R., Melki, R., Gordon, B., Batelier, G., Candido, E.P.M., 1997. Structure-function studies on
506 small heat shock protein oligomeric assembly and interaction with unfolded polypeptides. Journal of
507 Biological Chemistry 272(39), 24646-24656.
508 Liu, Q., Xie, F., Rolston, R., Moreira, P.I., Nunomura, A., Zhu, X., Smith, M.A., Perry, G., 2007.
509 Prevention and treatment of Alzheimer disease and aging: antioxidants. Mini reviews in medicinal
510 chemistry 7(2), 171-180.
511 Luccarini, I., Dami, T.E., Grossi, C., Rigacci, S., Stefani, M., Casamenti, F., 2014. Oleuropein aglycone
512 counteracts Aβ42 toxicity in the rat brain. Neuroscience letters 558, 67-72.
513 Nieto, M., Gil-Bea, F.J., Dalfó, E., Cuadrado, M., Cabodevilla, F., Sánchez, B., Catena, S., Sesma, T.,
514 Ribé, E., Ferrer, I., 2006. Increased sensitivity to MPTP in human α-synuclein A30P transgenic mice.
515 Neurobiology of aging 27(6), 848-856.
516 Park, S.K., Tedesco, P.M., Johnson, T.E., 2009. Oxidative stress and longevity in Caenorhabditis elegans
517 as mediated by SKN-1. Aging cell 8(3), 258-269.
518 Ray, A., Martinez, B., Berkowitz, L., Caldwell, G., Caldwell, K., 2015. Mitochondrial dysfunction,
519 oxidative stress, and neurodegeneration elicited by a bacterial metabolite in a C. elegans Parkinson's
520 model. Cell death & disease 5(1), e984.

521 Reeve, A., Simcox, E., Turnbull, D., 2014. Ageing and Parkinson's disease: why is advancing age the
522 biggest risk factor? Ageing research reviews 14, 19-30.
523 Reynolds, A., Laurie, C., Mosley, R.L., Gendelman, H.E., 2007. Oxidative stress and the pathogenesis of
524 neurodegenerative disorders. International review of neurobiology 82, 297-325.
525 Rosillo, M.Á., Alcaraz, M.J., Sánchez-Hidalgo, M., Fernández-Bolaños, J.G., Alarcón-de-la-Lastra, C.,
526 Ferrándiz, M.L., 2014. Anti-inflammatory and joint protective effects of extra-virgin olive-oil polyphenol
527 extract in experimental arthritis. The Journal of nutritional biochemistry 25(12), 1275-1281.
528 Santangelo, C., Filesi, C., Varì, R., Scazzocchio, B., Filardi, T., Fogliano, V., D'Archivio, M.,
529 Giovannini, C., Lenzi, A., Morano, S., 2016. Consumption of extra-virgin olive oil rich in phenolic
530 compounds improves metabolic control in patients with type 2 diabetes mellitus: a possible involvement
531 of reduced levels of circulating visfatin. Journal of endocrinological investigation 39(11), 1295-1301.
532 Schildknecht, S., Gerding, H.R., Karreman, C., Drescher, M., Lashuel, H.A., Outeiro, T.F., Di Monte,
533 D.A., Leist, M., 2013. Oxidative and nitrative alpha-synuclein modifications and proteostatic stress:
534 implications for disease mechanisms and interventions in synucleinopathies. Journal of neurochemistry
535 125(4), 491-511.
536 Sharma, S.K., Priya, S., 2017. Expanding role of molecular chaperones in regulating α-synuclein
537 misfolding; implications in Parkinson's disease. Cellular and molecular life sciences 74(4), 617-629.
538 Solis, G.M., Petrascheck, M., 2011. Measuring Caenorhabditis elegans life span in 96 well microtiter
539 plates. Journal of visualized experiments: JoVE(49).
540 Spillantini, M.G., Crowther, R.A., Jakes, R., Hasegawa, M., Goedert, M., 1998. α-Synuclein in
541 filamentous inclusions of Lewy bodies from Parkinson's disease and dementia with Lewy bodies.
542 Proceedings of the National Academy of Sciences 95(11), 6469-6473.
543 Tabrizi, S.J., Orth, M., Wilkinson, J.M., Taanman, J.-W., Warner, T.T., Cooper, J.M., Schapira, A.H.,
544 2000. Expression of mutant α-synuclein causes increased susceptibility to dopamine toxicity. Human
545 molecular genetics 9(18), 2683-2689.
546 van Ham, T.J., Holmberg, M.A., van der Goot, A.T., Teuling, E., Garcia-Arencibia, M., Kim, H.-e., Du,
547 D., Thijssen, K.L., Wiersma, M., Burggraaff, R., 2010. Identification of MOAG-4/SERF as a regulator of
548 age-related proteotoxicity. Cell 142(4), 601-612.
549 Van Ham, T.J., Thijssen, K.L., Breitling, R., Hofstra, R.M., Plasterk, R.H., Nollen, E.A., 2008. C. elegans
550 model identifies genetic modifiers of α-synuclein inclusion formation during aging.

551 Vauzour, D., Corona, G., Spencer, J.P., 2010. Caffeic acid, tyrosol and p-coumaric acid are potent
552 inhibitors of 5-S-cysteinyl-dopamine induced neurotoxicity. Archives of Biochemistry and Biophysics
553 501(1), 106-111.
554 Wakabayashi, K., Tanji, K., Mori, F., Takahashi, H., 2007. The Lewy body in Parkinson's disease:
555 Molecules implicated in the formation and degradation of α-synuclein aggregates. Neuropathology 27(5),
556 494-506.
557 Wang, D., Qian, L., Xiong, H., Liu, J., Neckameyer, W.S., Oldham, S., Xia, K., Wang, J., Bodmer, R.,
558 Zhang, Z., 2006. Antioxidants protect PINK1-dependent dopaminergic neurons in Drosophila.
559 Proceedings of the National Academy of Sciences 103(36), 13520-13525.
560 Wang, H., Joseph, J.A., 1999. Quantifying cellular oxidative stress by dichlorofluorescein assay using
561 microplate reader1. Free Radical Biology and Medicine 27(5-6), 612-616.
562 Winner, B., Jappelli, R., Maji, S.K., Desplats, P.A., Boyer, L., Aigner, S., Hetzer, C., Loher, T., Vilar, M.,
563 Campioni, S., 2011. In vivo demonstration that α-synuclein oligomers are toxic. Proceedings of the
564 National Academy of Sciences 108(10), 4194-4199.
565 Zhao, J., Yu, S., Zheng, Y., Yang, H., Zhang, J., 2017. Oxidative modification and its implications for the
566 neurodegeneration of Parkinson’s disease. Molecular neurobiology 54(2), 1404-1418.

Figure legends

Figure 1. ***(A)*** Representative graph of a lifespan assay at different TYR doses on NL5901 nematodes cultured in 96 well plates at 22 °C. Nematodes were treated with TYR from adult day 1 until death and monitored for survival. The median survival for 0 μM, 50 μM, 250 μM, 500 μM and 1 mM tyrosol were (days): 19, 18, 20, 20 and 22, respectively. 1 mM TYR dose exerted a significant increase in lifespan as compared to vehicle-treated nematodes (Median survival days: Control 19 vs. TYR 1mM 22; ****p*<0.0005; Log-Rank test). (B) Mean survival values from three independent experiments showing that 1mM TYR significantly extends the lifespan of NL5901 strain (Control 18.67±0.33 vs. TYR 1 mM 21.33±0.66; *t*-test **p*=0.0232).

Figure 2. (A) Confocal microscopy images showing α-syn::YFP aggregates in muscle cells of the head region of 6-day adult NL5901 worms grown in presence of 0 μM or 1 mM TYR (Scale bar 20 μm). (B) Quantification of α- syn::YFP aggregates (size above 6 μm^2) per worm in each experimental condition (Control 58.72±3.47 vs. TYR 1 mM 22.63±5.17; *t*-test ***p* value=0.0044). (C) Western blot densitometry showing α-syn::YFP levels in TYR treated worms at the same experimental conditions as in (A-B). All lanes were loaded with equal protein extract from synchronized 6-day adult NL5901 worms. Actin was used as loading control. No significant differences in the total amount of α-syn::YFP were found.

Figure 3. Effect of TYR treatment on worm locomotion quantified as number of activity counts in 30 minutes. 1 mM TYR was added on day 1 of adulthood and locomotion under control and treatment conditions was assessed after 3, 7, 9 and 11 days. (A) In N2 (*wild-type*) strain no significant differences

were observed in locomotion after TYR treatment and paralysis started between days 9 and 11 of the assay. (B) In NL5901 strain, paralysis started earlier than in the *wild-type* strain (between days 3 and 7). TYR treatment delayed worm paralysis compared to non- treated worms. This difference was more evident by day 9 (Control 7,7±1.81 vs. TYR 1mM 20,9±5.62; *t*-test **p*=0.0364).

Figure 4. (A-B): GFP expression pattern in DA of transgenic *C. elegans* (UA44) at adult day 14. A: Untreated control; B: TYR treated nematode (1 mM). Scale bar, 50 μm. (C) Percentage of UA44 worms that had the six anterior DA (CEP and ADE) intact, expressed as *wild-type* animals, at day 14. The graph represents the average of three independent assays (Control 45.33±3.52 vs. TYR 1 mM 80±2.30; *t*-test ***p* value=0.0012).

Figure 5. (A) Effect of 1 mM TYR on ROS level in NL5901 *C. elegans* strain measured by DCF fluorescence. Paraquat was used as a control of oxidative stress. TYR treatment induces a lower accumulation of intraworm ROS levels as revealed by DCFH-DA fluorescence over time. (B) Mean fluorescence at the end point of three DCF assays showing a significant decrease in ROS level in TYR treated nematodes compared to controls (Control 124.5±3.5 vs. TYR 1 mM 82±12.06; *t*-test **p*=0.0347).

Figure 6. Effect of TYR on the mRNA expression of *hsp-70*, *hsp-4*, *hsp-16.6*, *hsp-12.2*, *sod-3*, *sod-1*, *ctl-1*, *ctl-2*, *gpx-1*, *gpx-2* and *gst-4*. Results are expressed as normalized mRNA expression relative to control worms using *ama-1* as housekeeping gene. *hsp-70* (Control 1±0.30 vs. TYR 1 mM 4.2±0.85; *t*-test ***p*=0.0037), *hsp-12.6* (Control 1±0.05 vs. TYR 1 mM 2.038±0.36; *t*-test **p*=0.047), *hsp-16.2* (Control 1±0.15 vs. TYR 1 mM 1.934±0.32; *t*-test **p*=0.011), *gst-4* (Control 1±0.056 vs. TYR 1 mM 1.64±0.15; *t*-test **p*=0.017).

Graphical abstract. TYR exerts synergical protective effects in PD pathogenesis. TYR reduces α-syn inclusions and toxicity by both, promoting chaperone expression and neutralizing ROS, although direct inhibition of α-syn aggregation cannot be ruled out. Moreover, and probably related to the previous result, TYR also shows effectiveness in delaying α-syn-dependent degeneration of DA in *C. elegans*.

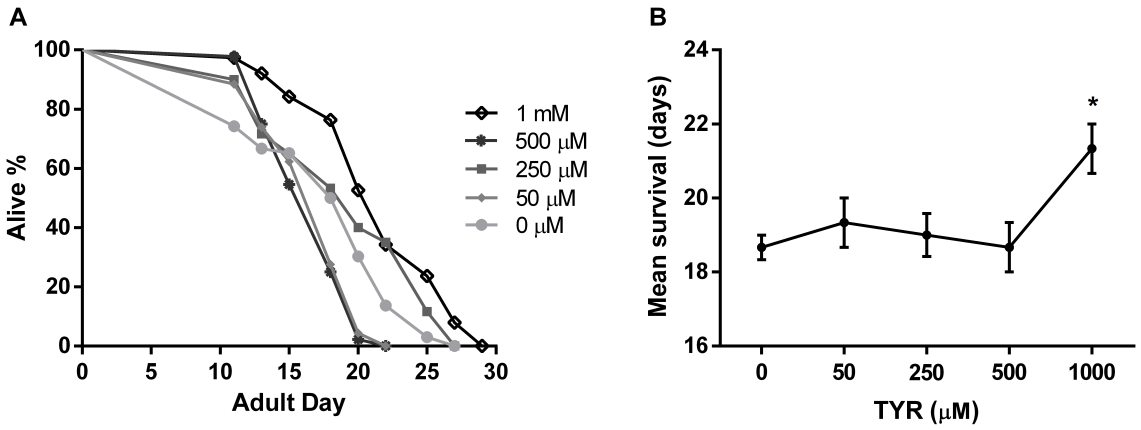

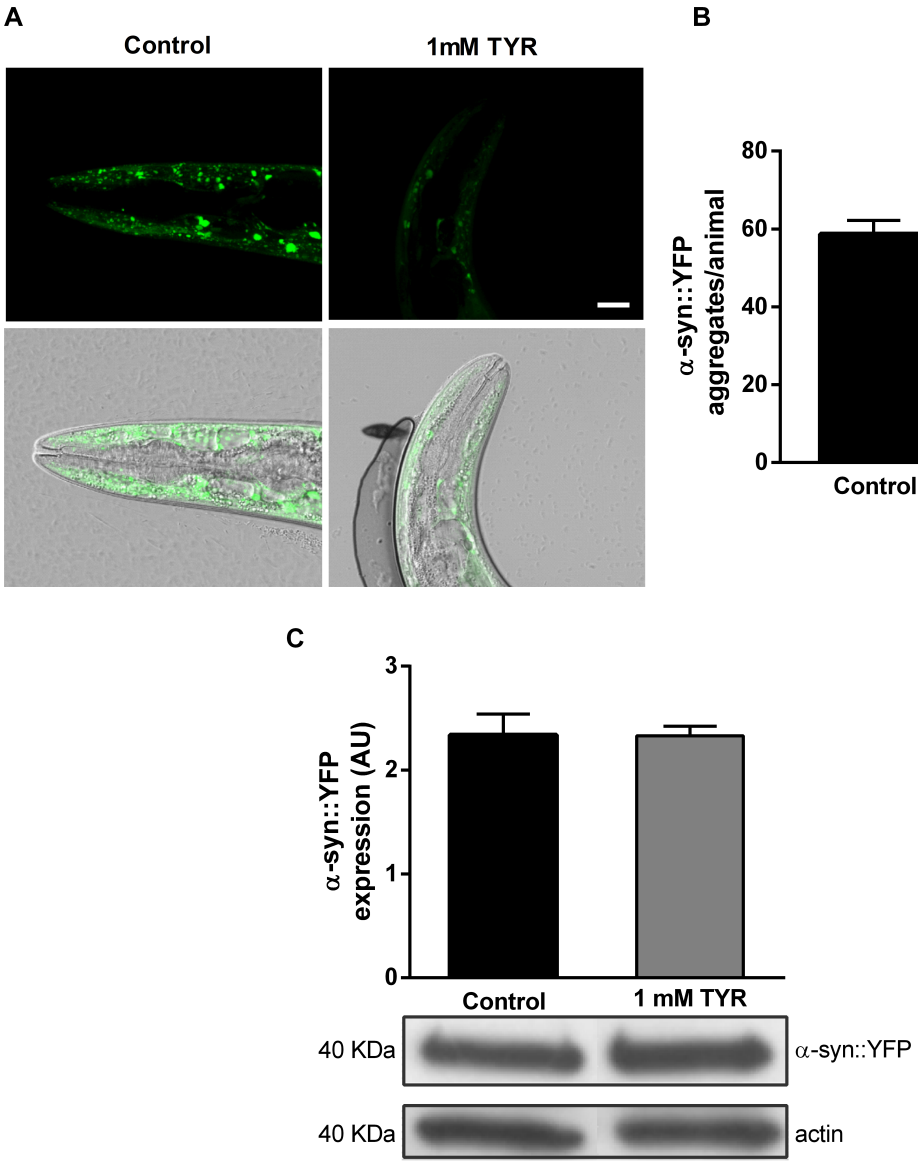
A
Control
1mM TYR
B
α-syn::YFP aggregates/animal
80
60
40
20
0
**
Control
1 mM TYR
C
α-syn::YFP expression (AU)
3
2
1
0
Control
1 mM TYR
40 KDa
α-syn::YFP
40 KDa
actin

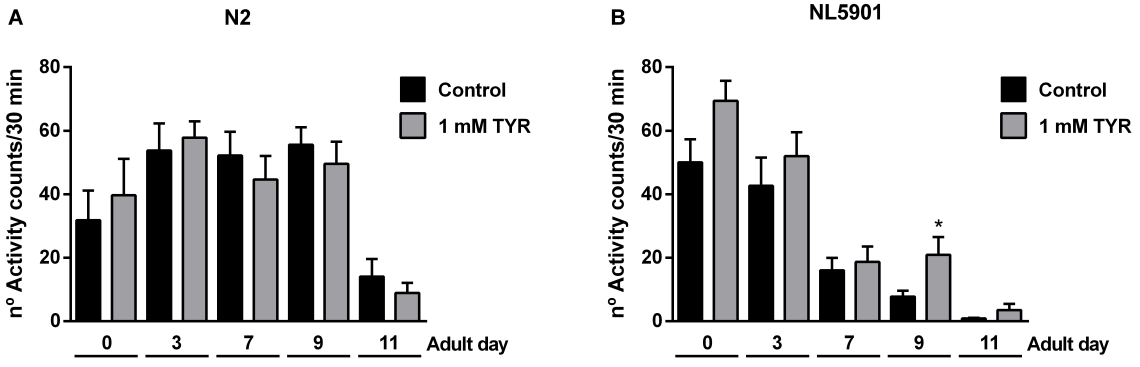

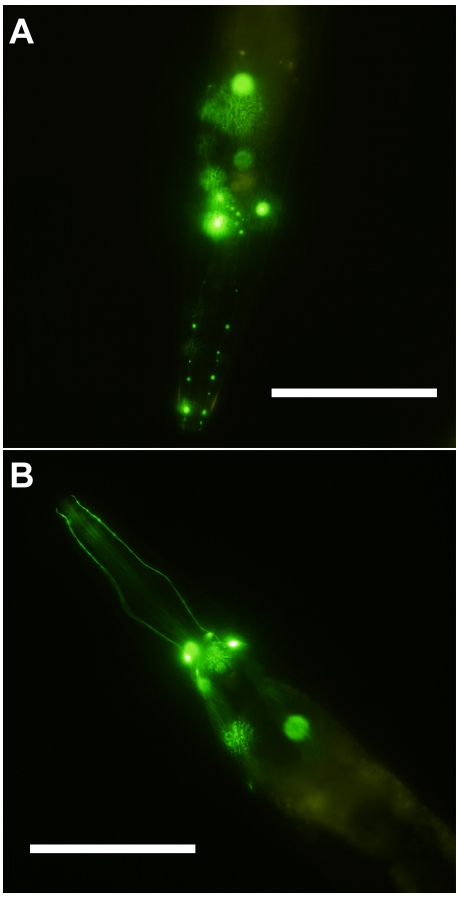

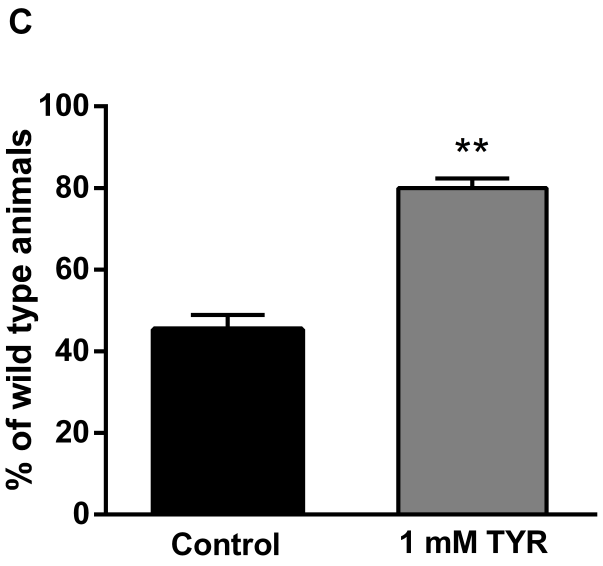

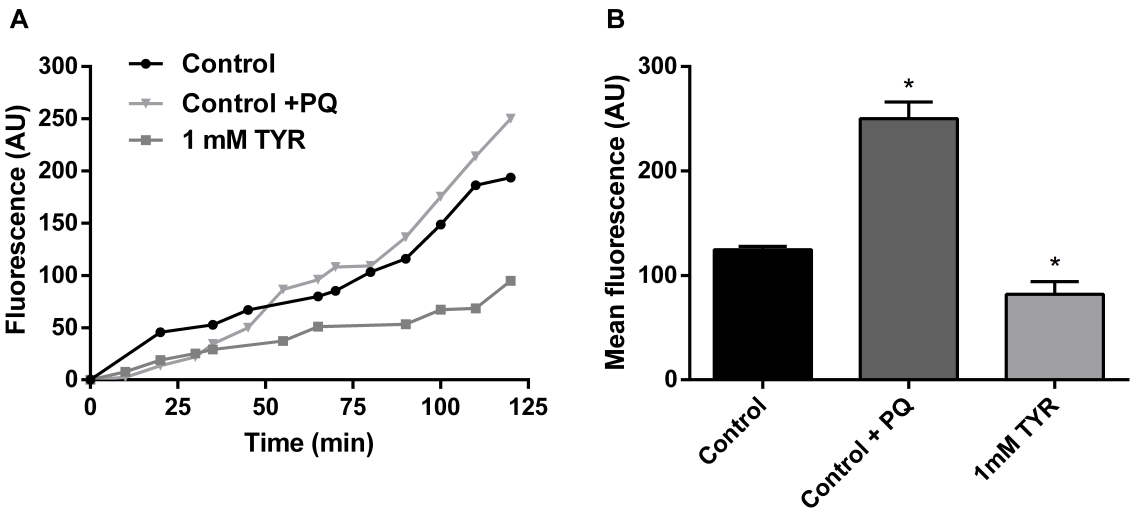

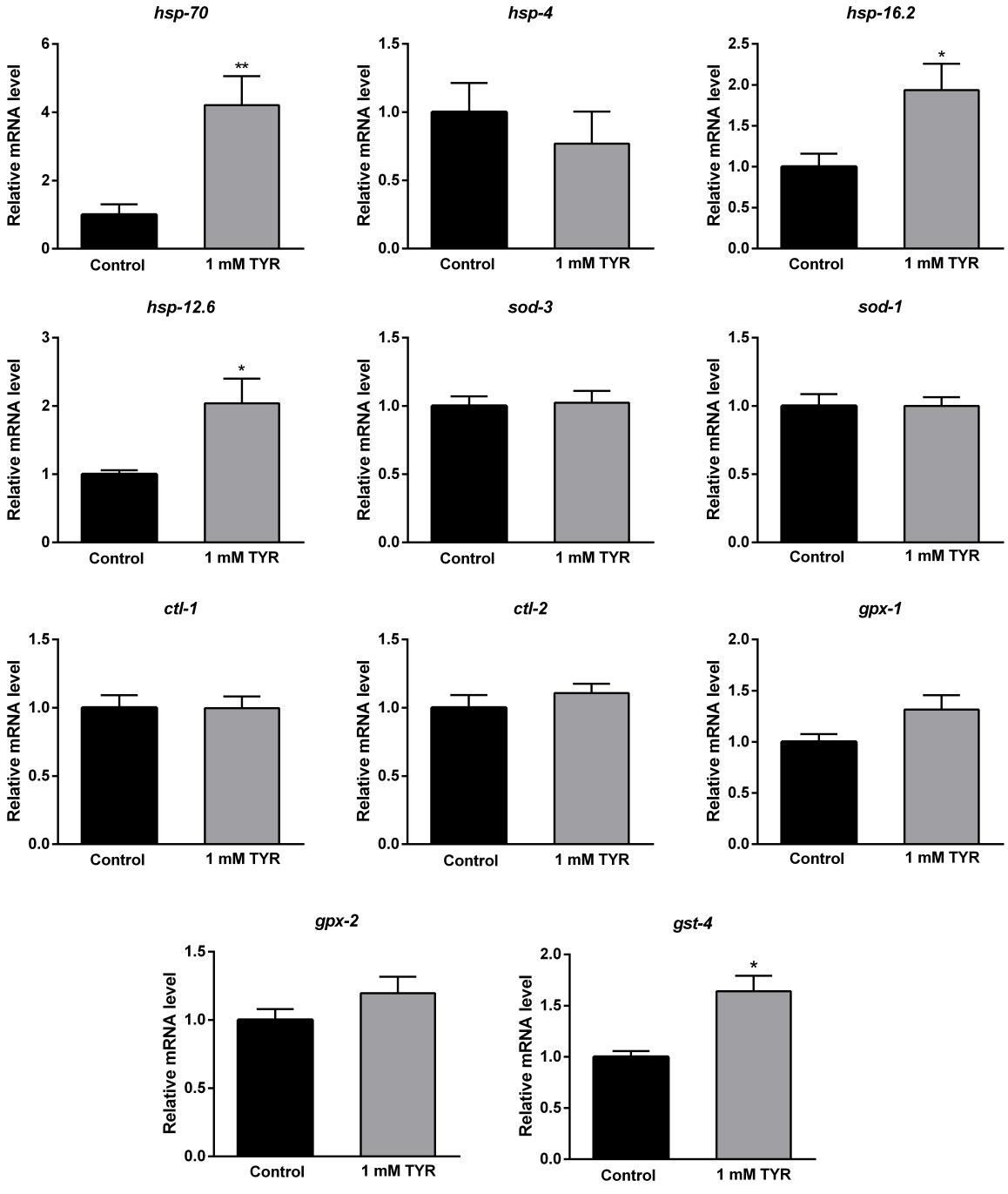

- Tyrosol, a phenolic compound present in Extra Virgin Olive Oil, delays neurodegeneration in a *C. elegans* model of Parkinson´s Disease.
- *In vivo* aggregation of α-synuclein decreased after treating *C. elegans* with Tyrosol.
- Tyrosol reduced oxidative stress and induced the expression of different protective genes in a model of Parkinsonism.

Discusión

Tal y como se ha mencionado en la introducción, la DM, rica en componentes bioactivos como los compuestos fenólicos del AOVE, se ha asociado con una menor incidencia de diversas patologías. Las propiedades beneficiosas de los compuestos fenólicos se habían atribuido principalmente a su carácter antioxidante. Sin embargo, durante los últimos años diferentes autores han demostrado que su acción no se restringe únicamente a su potencial antioxidante. En los artículos que se presentan en esta memoria se ha analizado el efecto de dos fenoles del olivo, el HT y el TIR, en diversas situaciones patológicas muy ligadas al estrés oxidativo analizando la capacidad antioxidante directa e indirecta de estos compuestos, así como su efecto sobre diferentes rutas y mecanismos de interés para cada patología. Concretamente, el HT se ha estudiado en cáncer de mama y en ictus isquémico, dos patologías asociadas a la hipoxia, y el TIR en la EP. Aunque se dispone de resultados preliminares sobre la acción del TIR en la respuesta a la hipoxia y del HT en el modelo de EP, han sido insuficientes para permitir la redacción de un artículo por lo que estos estudios no se han incluido finalmente en esta memoria de tesis doctoral.

Capacidad antioxidante del HT y su efecto sobre la respuesta a la hipoxia en células MCF-7

A lo largo de los dos primeros trabajos se ha estudiado el efecto del HT sobre la línea celular de cáncer de mama hormonodependiente MCF-7 valorando, entre otros parámetros, la capacidad antioxidante del compuesto y su acción sobre rutas como la regulada por Nrf-2, así como su efecto sobre el mecanismo de respuesta a la hipoxia mediado por HIF-1.

El HT es un potente antioxidante que ha demostrado su capacidad en multitud de modelos y patologías[1]. Su acción citotóxica en células de cáncer de mama es muy escasa[2-4] y, a pesar de la importancia de la hipoxia en la malignidad tumoral, no se ha analizado de forma detallada su influencia en el efecto antioxidante de este fenol. Nuestros resultados indican que el tratamiento con HT disminuye los niveles de ERO de forma dependiente en células sometidas a un estrés hipóxico, sin observarse este efecto en condiciones de normoxia. Estudios anteriores ya habían señalado que este potencial antioxidante es predominante en situaciones donde existe una sobreproducción de ERO[2]. La hipoxia aguda que aparece en los tumores como consecuencia de una obstrucción temporal o discontinua del flujo sanguíneo, involucra períodos de reperfusión durante los cuales tienen lugar picos de producción de ERO adicionales al incremento de estrés oxidativo propio de la hipoxia[5]. El estrés oxidativo subletal acelera la progresión tumoral e incrementa el riesgo de metástasis al aumentar, entre otros procesos, la tasa de mutación, el crecimiento celular y la respuesta angiogénica[6]. De hecho, estudios recientes señalan cómo la disminución del estrés oxidativo en pacientes con cáncer de mama con tratamiento quimioterápico se correlaciona con mayores tasas de supervivencia[7]. Aunque sin lugar a dudas, el empleo de antioxidantes en el tratamiento del cáncer es un tema controvertido, multitud de estudios demuestran como el empleo de compuestos como la vitamina C y E, el GSH, la melatonina e incluso polifenoles del té como la epigalocatequina galato, reducen la toxicidad de la quimioterapia en tejidos sanos sin afectar a su eficacia, llegando incluso en algunos casos a aumentarla[8]. Además, recientemente se ha descrito que el tratamiento conjunto del quimioterápico paclitaxel con HT disminuye el estrés oxidativo sin contrarrestar el efecto de la quimioterapia[4]. En consecuencia, nuestros resultados respaldan que el HT podría ser beneficioso para minimizar el incremento de ERO asociado a la hipoxia tumoral y ponen de manifiesto la necesidad de tener en cuenta el ambiente hipóxico a la hora de estudiar los efectos del HT en modelos *in vivo*.

Al igual que ocurre con el nivel de ERO, las pacientes con cáncer de mama presentan niveles particularmente altos de NO en sangre. De hecho, en tumores de mama invasivos la actividad eNOS e iNOS es superior a la del tejido mamario sano, lo que sugiere una correlación positiva entre la biosíntesis de NO y el grado de malignidad tumoral[9]. Por tanto, la disminución de los niveles de NO también podría ayudar a contrarrestar varios efectos relacionados con la malignidad, incluida la angiogénesis, la apoptosis, el ciclo celular, la invasión y la metástasis[10]. La acción del HT en la producción de NO se ha descrito previamente en varios estudios. Aunque en alguno de ellos el HT no ejerció ningún efecto sobre los niveles de NO a bajas concentraciones (0.5-5μM)[11], la mayoría de ellos demuestran que reduce sus niveles, y apuntan a la

inhibición de la isoforma iNOS como principal mecanismo responsable[12,13]. Sin embargo, estos trabajos solo consideran la acción del compuesto en células cultivadas en normoxia. En nuestro grupo ya describimos como el HT reduce los niveles de NO en células no tumorales sometidas a la misma situación de hipoxia utilizada en esta tesis[14]. Sin embargo, no hemos observado este efecto en la línea celular MCF-7, lo que podría indicar que en un contexto tumoral la capacidad del HT para inhibir la actividad de la iNOS es insuficiente. El anión $O_2^{\cdot-}$ y el NO reaccionan rápidamente para originar peroxinitrito ($ONOO^-$), altamente reactivo y con importantes implicaciones en la iniciación y progresión del cáncer[10]. Por tanto, aunque el HT no modifica los niveles de NO, si analizamos de forma conjunta este resultado con su acción sobre el nivel de ERO es posible que el HT esté contribuyendo a minimizar la producción de esta ERN y el daño producido por la misma. Una de las formas de valorar indirectamente el daño por estrés oxidativo/nitrosativo es analizar alguna de las muchas proteínas que se activan en respuesta al mismo. En este sentido, nuestro grupo tenía experiencia previa en el estudio de PARP-1 en un contexto hipóxico. Así, hemos descrito que la supresión de PARP-1 disminuye la respuesta a la hipoxia y, como a su vez, la hipoxia aumenta tanto la expresión como la actividad de PARP-1, contribuyendo a la malignidad tumoral[15-17]. De igual forma, se sabe que la inhibición farmacológica de PARP-1 proporciona protección frente al daño celular asociado a las ERO, reduciendo la respuesta inflamatoria, inhibiendo la expresión de genes como AP-1 y NF-κB, y potenciando la apoptosis en cotratamiento con quimio- y radioterapia[18]. Por todo ello, el que el tratamiento con HT disminuya tanto el nivel como la actividad de PARP-1 en células hipóxicas sería *a priori* un resultado positivo que podría conllevar una menor malignidad tumoral. Sin embargo, no podemos dejar de señalar que la acción antioxidante del HT y la menor actividad/expresión de PARP-1 no parecen estar directamente relacionadas ya que su efecto sobre las ERO es patente a concentraciones mucho más bajas (≥5 µM), apuntando a que el HT estaría regulando la estabilidad de PARP-1 a través de mecanismos adicionales.

La mitocondria es una de las principales fuentes de producción de ERO en la célula, desempeñando además un papel central en el metabolismo[19]. PGC-1α es un coactivador transcripcional que regula la biogénesis mitocondrial al interactúar y potenciar la actividad de diversos factores de transcripción (PPARs, Nrf1 y Nrf2, YY1 y ERR). Variaciones en su expresión y actividad afectan directamente a la adaptación metabólica de los tumores[20]. De hecho, en cáncer de mama se ha descrito como su expresión está aumentada en células que metastatizan a hueso y pulmón[21]. El vínculo entre la expresión de PCG-1α y el HT ha sido poco analizado en la bibliografía y aún menos en modelos de cáncer o bajo condiciones hipóxicas, en las que se sabe que se induce[22]. En adipocitos y en ratas sometidas a un ejercicio excesivo, se ha descrito que la suplementación con HT aumenta el nivel y la actividad de PGC-1α, así como la expresión de complejos de la cadena transportadora de electrones[23,24]. Del mismo modo, Signorile et al.[25] describieron que la represión de PCG-1α y de la fosforilación oxidativa mitocondrial en fibroblastos deprivados de suero se revirtió mediante el tratamiento con HT. Sin embargo, estos autores sólo analizaron el efecto del HT a nivel de proteína. Al evaluar la acción del HT sobre PGC-1α tanto a nivel de ARNm como de proteína, y en condiciones de hipoxia y de normoxia, observamos que el efecto no es paralelo. Así, independientemente de la presión parcial de oxígeno el HT disminuye la transcripción de este gen. Sin embargo, cuando nos centramos en el efecto sobre la proteína, la hipoxia anula la inducción de PGC-1α asociada al tratamiento con HT en normoxia. Para profundizar en el efecto del HT sobre PGC-1α, consideramos de interés centrarnos en dos de los factores de transcripción coactivados por esta proteína, ERRα y Nrf-2. ERRα es un receptor nuclear huérfano cuyo aumento de actividad se ha relacionado, a través de una análisis genómico de más de 800 tumores mamarios, con una menor supervivencia libre de la enfermedad[26,27]. También se ha descrito que la inhibición ERRα en células MCF-7 ralentiza la proliferación celular y disminuye el crecimiento de xenoinjertos[27,28]. En definitiva, la disminución de la actividad del eje PGC-1α/ERRα inducida por el tratamiento con HT resultaría positiva para el control tumoral. Sin embargo, nuestros resultados no nos permiten afirmar que el HT ejerza esta acción, independientemente de que las células se sometan o no a una situación de hipoxia. Así, la expresión de ERRα y de SIRT3, una desacetilasa mitocondrial inducida por PGC-1α/ERRα y relacionada con un mal pronóstico en cáncer de mama[29], solo aumenta a nivel de ARNm a la mayor concentración ensayada (200 µM) sin que haya un efecto similar a nivel de proteína. Las discrepancias observadas entre los niveles de

ARNm y proteína pueden ser debidas al papel modulador del HT sobre la expresión de ARN no codificantes y proteínas de unión al ARN[30,31]. Además, ante una situación de hipoxia, la traducción proteica es uno de los principales procesos que se inhiben con el objetivo de redirigir la energía disponible a funciones esenciales como el mantenimiento de la homeostasis iónica y osmótica[32]. El mecanismo molecular implicado en esta adaptación a la hipoxia implica la activación de PERK y la inhibición de mTOR, dos moduladores principales de la maquinaria de traducción[33]**.** Más adelante describiremos como el HT podría afectar a estos mecanismos la actividad de mTOR en hipoxia.

Diferentes estudios apuntan a que la acción antioxidante del HT no puede ser mediada únicamente por su acción directa como neutralizador de ERO. Con el objetivo de seguir profundizando en los mecanismos subyacentes al efecto antioxidante del HT, se evaluó su efecto sobre el factor de transcripción Nrf2, otro de los factores de transcripción coactivados por PGC-1α. Como se ha mencionado previamente, la ruta Nrf2/Keap1 actúa como mecanismo de protección frente al estrés ambiental y oxidativo. En las células MCF-7, el HT a concentración 200 µM induce un aumento de Nrf2 a nivel de ARNm, acompañado por un aumento paralelo en los niveles de proteína, tanto en condiciones de hipoxia como de normoxia. Estudios previos, han analizado el efecto del HT sobre la transcripción de Nrf2 después de 48 h de tratamiento (0-50 µM) y, sorprendentemente, observaron un aumento en los niveles de ARNm solo a la concentración 1 µM[24]. La transcripción de Nfe2l2, gen de Nrf2, está regulada por varios factores de transcripción, entre ellos, el receptor de hidrocarburos arilo (AHR). Tal y como detallaremos posteriormente, proponemos que el HT a altas concentraciones (200µM) puede actuar como ligando de AHR y, por tanto, este mecanismo podría ser el principal responsable del aumento transcripcional de Nrf2[34]. Por otro lado, el incremento del nivel de proteína Nrf2 podría estar relacionado no solo con la propia sobreexpresión del gen sino con otros mecanismos post-traduccionales que aumentarían su estabilidad. Así, se ha descrito como el HT podría mediar la fosforilación de Nrf2 a través de las quinasas ERK y Akt[35] o reducir al residuo de cisteína involucrado en la unión de Nrf2 a Keap1[36]. Ambas modificaciones postraduccionales permitirían la disociación de Nrf2 de Keap-1, aumentando los niveles de Nrf2 libre, que se translocaria al núcleo donde se unirá a los ARE de diversos genes. GSTA2 y HO-1 son algunas de las proteínas antioxidantes reguladas por Nrf2. GSTA2 es una enzima que posee actividad glutatión peroxidasa y que participa en la detoxificación de compuestos electrofílicos. HO-1 es la isoforma inducible de HO en mamíferos, y cataliza la degradación del grupo hemo en monóxido de carbono y biliverdina/bilirrubina con la liberación paralela de hierro. El tratamiento con HT 200 µM aumenta la transcripción de ambos genes diana, corroborando que el HT induce no solo la expresión sino también la actividad de Nrf2. Sin embargo, este aumento en los niveles de ARNm no se correlaciona con un aumento en los niveles de estas proteínas, con la única excepción de HO-1, cuya expresión se incrementó en normoxia. Estos resultados sugieren que el efecto del HT sobre esta ruta se minimiza en una situación de hipoxia y, por lo tanto, el efecto antioxidante del HT en estas condiciones apenas puede ser atribuido a esta ruta de regulación. Para corroborar que el efecto que el HT ejerce sobre la transcripción de GSTA2 y HO-1 es mediado a través de Nrf2, se silenció su expresión mediante siRNA. Al silenciar Nrf2 se demostró que, aunque la expresión de GSTA2 depende exclusivamente de Nrf2, otros mecanismos parecen participar en la transcripción de HO-1. La expresión de HO-1 independiente de Nrf2 ya se ha descrito en la bibliografía. Así, se sabe que el compuesto natural gartanina induce la expresión de HO-1 independiente de Nrf2[37] y se ha descrito que el ácido nitro-linoleico promueve la expresión de la HO-1 en células deficientes de Nrf2 a través de la respuesta a AMPc, AP-1 e interacciones con elementos de respuesta E-box[38]. Además, en la atrofia muscular, el aumento de HO-1 es dependiente de FOXO1 pero no de Nrf2[39]. Por lo tanto, nuestros resultados evidencian que el HT estaría actuando mediante diferentes mecanismos independientes de Nrf2 para inducir la expresión de enzimas antioxidantes como HO-1.

Como se mencionó en la introducción, la función protectora de Nrf2 en la prevención de la carcinogénesis inducida por sustancias químicas o por diferentes tipos de radiación ha sido detallada en multitud de estudios mediante el empleo de ratones $Nrf2^{-/-}$. Nrf2 previene la carcinogénesis asegurando, a través de sus genes diana, una rápida respuesta enzimática que inicia la detoxificación de carcinógenos químicos, regula el

estrés oxidativo y repara el daño originado por el mismo. Sin embargo, durante la última década, muchos estudios han descrito que la activación de Nrf2 en células tumorales promueve la progresión del cáncer y la metástasis, confiriendo resistencia a la quimio- y la radioterapia[40]. Por lo tanto, el papel de Nrf2 depende de la etapa concreta en la que se encuentre el cáncer, e influyen en el abordaje terapéutico empleado de cara a su activación o inhibición. Así, la activación controlada de Nrf2 en células normales a través de su mecanismo canónico previene la tumorigénesis y resulta prometedora como estrategia preventiva. Sin embargo, su activación descontrolada participa en la promoción, la progresión y la metástasis, siendo en este caso su inhibición la estrategia terapéutica más adecuada. Por lo tanto, aunque el efecto del HT sobre los niveles de Nrf2 tiene lugar a concentraciones muy altas y no sería positivo en células MCF-7, sería de interés investigar si en células de mama sanas el HT ejerce este mismo efecto.

La hipoxia intratumoral tiene implicaciones negativas para la supervivencia de las pacientes con cáncer de mama. Así, los tumores que muestran altos niveles de HIF-1α se asocian con un fenotipo más agresivo, un mayor riesgo de metástasis, una mayor resistencia a la radio- y la quimioterapia, y una supresión de la respuesta inmune[41]. Hemos descrito que el HT (50-200 μM) disminuye el nivel de proteína HIF-1α en células MCF-7, sin afectar a los niveles de su ARNm. Las ERO y las ERN favorecen la estabilidad de HIF-1α al oxidar el centro catalítico de las PHDs e impedir mediante nitrosilaciones su interacción con pVHL, facilitando la respuesta a la hipoxia[42]. Por tanto, el tratamiento con HT podría estar protegiendo a las PHDs de su oxidación, favoreciendo así la degradación de HIF-1α. No obstante, valorar la actividad de las PHDs[43] sería clave para demostrar este posible mecanismo. En cualquier caso, estos resultados se asemejan a los observados previamente por nuestro grupo en células renales no tumorales sometidas a hipoxia[14] y a los obtenidos por otros grupos en células HT-29 de adenocarcinoma de colon, a concentraciones mucho más altas (400-800 μM), e *in vivo* en un modelo de xenoinjerto[44,45]. Por otro lado, los niveles de proteína HIF-1α también pueden ser regulados a través de la ruta PI3K/Akt/mTOR. Según la bibliografía, el efecto del HT sobre esta ruta es controvertido. Algunos autores han señalado que el HT inhibe la fosforilación de Akt en células tumorales y no tumorales a concentraciones de 50, 100 y 200 μM[46-48]. Sin embargo, también se ha demostrado que el HT puede promover la fosforilación de Akt[49-51]. Nuestros resultados apoyan que el HT inhibe la actividad de esta vía ya que reduce los niveles p-P70 y p-S6, dianas de mTOR, así como la propia mTOR fosforilada, lo que sugiere que la disminución de HIF-1α observada tras el tratamiento con HT podría estar mediada también a nivel traduccional mediante la inhibición de la ruta PI3K/Akt/mTOR. En definitiva, el efecto observado del HT podría contribuir a contrarrestar los efectos negativos asociados a la hipoxia en pacientes con cáncer de mama.

El dímero HIF-1 juega un papel central en la respuesta adaptativa a la hipoxia. Por lo tanto, ya que el HT disminuye los niveles de HIF-1α, resulta crucial investigar su efecto sobre la expresión de algunos genes diana HIF-1. Dado el efecto del HT sobre HIF-1α, era de esperar que la transcripción de genes dianas de HIF-1 como los factores angiogénicos VEGF y AM y las proteínas implicadas en el metabolismo de la glucosa Glut-1 y LDHA, estuviera inhibida. Sin embargo, el HT no ejerce ningún efecto sobre los niveles de ARNm de LDHA y, sorprendentemente, concentraciones altas del mismo incrementan la transcripción de AM, VEGF y Glut-1, lo que sugiere que el HT no reduce, sino que induce la actividad transcripcional de HIF-1. Si bien, este resultado es contradictorio con estudios anteriores que muestran como el HT disminuye los niveles de VEGF en diferentes modelos[44,52,53], a su vez respaldan nuestros resultados previos en células renales[14]. FIH, a través de su capacidad para hidroxilar la Asn-803 de HIF 1α, suprime la actividad transcripcional de HIF-1[46]. Por lo tanto, una disminución en esta proteína podría ser responsable de la mayor actividad transcripcional de HIF-1. La expresión de FIH no parece estar modulada por el HT, lo que indica que deben de existir otros mecanismos independientes de HIF-1 sobre los cuales el HT estaría ejerciendo este efecto. Para corroborar la participación particular de HIF-1 en la respuesta de AM, VEGF y Glut-1 tras el tratamiento con HT, se silenció la expresión de HIF-1α mediante siRNA. La inducción de Glut-1 por el tratamiento con el HT fue completamente suprimida en estas células en ausencia de HIF-1α, lo que sugiere que su sobreexpresión después del tratamiento con HT depende en gran medida de la actividad transcripcional de HIF-1. Sin

embargo, AM y VEGF solo disminuyeron su expresión parcialmente, lo que corroboró la participación de otros mecanismos reguladores adicionales al de HIF-1. HIF-2 es otro miembro de la familia HIF que también participa en la respuesta a la hipoxia. El efecto del HT en la actividad de este factor de transcripción es en gran parte desconocido. Por lo tanto, nos preguntamos si el aumento observado en AM y VEGF podría estar mediado por HIF-2 [54]. Para probar esta hipótesis, evaluamos la acción del HT en la actividad transcripcional de HIF-2. La eritropoyetina o la angiopoyetina-2 son algunas de las dianas canónicas de HIF-2. Sin embargo, su expresión es muy reducida en células MCF-7[55], por lo que evaluamos los niveles de ARNm de Oct-4, gen regulado también específicamente por HIF-2α y que se encuentra implicado en el mantenimiento de la pluripotencialidad de células madre[56]. Nuestros resultados muestran que el HT no afecta a la transcripción de Oct-4, por lo que HIF-2 no parece estar involucrado en la respuesta de AM y VEGF al HT. Aun así, debería analizarse el efecto del HT sobre los niveles de HIF-2α, así como silenciar simultáneamente ambas subunidades α, la 1 y la 2, para descartar de forma concluyente su implicación en el efecto observado del HT sobre estos genes. AM y VEGF también pueden ser regulados por otros factores de transcripción, como AHR[57-60]. AHR es un receptor citoplásmico, que presenta el motivo de unión al ADN bHLH-PAS y que puede ser activado por diversos químicos. Tras la unión de cualquiera de sus diversos ligandos, y de manera similar a HIF-1α, AHR se transloca al núcleo donde dimeriza con HIF-β (ARNT) y forma un factor de transcripción activo que regula la expresión de genes involucrados en la detoxificación, la angiogénesis, la proliferación, la adhesión y la migración celular, entre otros procesos[61]. CYP1A1 es el gen que se induce clásicamente en respuesta a la activación de AHR. De acuerdo con nuestros resultados, el tratamiento de células MCF-7 hipóxicas con altas concentraciones de HT regula drásticamente la transcripción de CYP1A1, proteína involucrada en el metabolismo de xenobioticos. Como se ha descrito anteriormente el HT también induce el nivel de Nrf2, otra de las dianas de AHR. Estos datos parecen indicar que, a altas concentraciones, el HT actúa como ligando de AHR y podría ser responsable de la sobreexpresión de AM y VEGF en respuesta al HT. Aunque no se dispone actualmente de una visión completa de la función de AHR en el cáncer de mama, la activación de AHR se ha relacionado en gran medida con la transformación maligna. De hecho, un estudio reciente en una cohorte de 439 tumores de mama demostró que altos niveles de AHR se correlacionan con la sobreexpresión de genes relacionados con la inflamación, la invasión y la señalización de factores de crecimiento, mientras que, niveles altos de su represor AHRR, se han correlacionado con aumentos en la supervivencia libre de metástasis[62]. Los ligandos de AHR son muy diversos e incluyen polifenoles y flavonoides naturales y sintéticos[63]. El rango de concentraciones en el que estos compuestos interactúan con AHR es muy variable y depende de su estructura química, pero también del modelo biológico utilizado[64]. El modelo estructural de unión del HT a AHR que hemos elaborado demuestra que este fenol puede actuar como ligando de AHR. De hecho, las diferentes posturas de unión encontradas muestran un tipo de interacción π-π entre el HT y AHR, así como interacciones con residuos que ya han demostrado ser importantes para la unión del ligando clásico TCDD a AHR[65,66]. Además, es importante recalcar el HT puede actuar como agonista de AHR solo a concentraciones que sobrepasan claramente las alcanzables tras la ingesta de cualquier AOVE. Sería necesario un análisis más profundo,[67-69] que permitiera evaluar la energía libre de unión esperada del HT en comparación con la del TCDD[77,78]. Sin embargo, el hecho de que la inducción de AM y VEGF por el HT no se elimine completamente en células ARNT silenciadas sugiere la participación plausible de otros mecanismos adicionales a HIF-1 y AHR. ARNT2 es un homólogo a la proteína ARNT. Su expresión está restringida a los tejidos neurales y al riñón, pero también se encuentra presente en múltiples células tumorales. Aunque tanto ARNT como ARNT2 se unen por igual a las subunidades HIF-α, ARNT es mucho más eficiente que ARNT2 en la regulación positiva mediada por AHR de CYP1A1[70]. Por lo tanto, aunque se deberían realizar experimentos adicionales, podría plantearse la hipótesis de que el efecto transcripcional del HT puede ejercerse a través de una combinación de las vías AHR-ARNT y HIF-1α ARNT/ARNT2.

Empleo del HT como estrategia terapéutica después de una isquemia cerebral

Como se ha descrito, el HT regula el nivel de estrés oxidativo y la respuesta a la hipoxia de la línea celular de cáncer de mama MCF-7. La hipoxia es clave en la patogenia de otras afecciones como el ictus isquémico, en las que el HT podría ejercer un efecto beneficioso. Durante un episodio isquémico la adaptación del cerebro a la deprivación de oxígeno y glucosa resulta clave para mitigar el daño asociado al ictus y mantener la homeostasis[71]. Diferentes estudios describen el efecto neuroprotector del aceite de oliva, de extractos de hoja de olivo e incluso de la OL en diferentes modelos murinos de isquemia cerebral[72-74]. Sin embargo, no existen trabajos sobre el efecto del HT *in vivo,* y aún menos utilizado como terapia tras un ictus isquémico. Por lo tanto, mediante un modelo de tMCAo en ratones, se valoró el efecto de este compuesto sobre procesos y parámetros alterados en esta patología tales como el aprendizaje, la memoria a corto plazo, la fuerza, el FSC, así como sobre la neurogénesis y la neuroinflamación.

La calidad de vida de los pacientes que sufren un ictus depende del grado de afectación y de recuperación de sus funciones motoras y cognitivas, por lo que resulta crucial encontrar nuevos enfoques terapéuticos que mitiguen el daño y ayuden durante la recuperación[86,87]. En estudios anteriores realizados por el grupo de la Doctora Kiliaan con un diseño experimental similar al empleado en esta tesis, se describió que la dieta Fortasyn mejoraba la fuerza de agarre en ratones machos sin efecto en hembras[75,76]. Esta dieta contenía una combinación específica de múltiples nutrientes entre los que se encontraban uridina, ácidos grasos poliinsaturados omega-3, colina, vitaminas B, fosfolípidos y antioxidantes. En nuestro estudio con machos, la suplementación solo con HT mejoró la fuerza de agarre en el trapecio (*grip test)*, poniendo de manifiesto la acción beneficiosa de este compuesto sobre el estado físico de los animales. Sin embargo, no se observó ningún efecto sobre el comportamiento ni sobre diferentes habilidades motoras (*open field* o el *pole test)*. Aunque no se encontraron efectos positivos, estos resultados también son indicativos de la ausencia de conductas adversas como ansiedad, perdida de coordinación motora o estereotipias.

El deterioro neurológico del hipocampo tras un ictus isquémico, puede conllevar la pérdida de memoria y de otras funciones cognitivas como el aprendizaje. Para valorar si el HT ejercía alguna acción sobre estos procesos, evaluamos su efecto sobre la memoria a corto plazo mediante la prueba de reconocimiento de objetos (ORT) y la prueba de inhibición prepulso (PPI). En primer lugar, durante el test ORT, se realizó una prueba de familiarización en la que los animales podían interactuar dos objetos idénticos. Después de un cierto tiempo (30 min en el día 1 y 60 min en el día 2), se repitió el ensayo reemplazando uno de los objetos familiares por otro nuevo. Las pruebas de 30 minutos indicaron que los ratones alimentados con dieta HT mostraban preferencia por el nuevo objeto, visitándolo con más frecuencia que los ratones control. La prueba de PPI, realizada para evaluar la integración sensitivomotora de los animales, también indicó que los ratones alimentados con HT se sobresaltaban menos frente a un estímulo provocado. Este resultado, es indicativo de una mayor habituación en los animales alimentados con HT, lo que se traduce en una mejor modulación de la respuesta sesitivomotora y de adaptación al entorno[77]. En conjunto, los resultados del ORT y PPI sugieren que el HT mejora la memoria a corto plazo y promueve procesos de aprendizaje no asociativo, como la habituación, siendo un compuesto prometedor para reducir los déficits cognitivos asociados con el ictus.

Para profundizar en los mecanismos involucrados en los efectos del HT descritos hasta ahora se emplearon diferentes técnicas de neuroimagen. La resonancia magnética funcional en estado de reposo (rsfMRI), mide los cambios dependientes del nivel de oxigenación sanguínea (contraste BOLD) debidos a la actividad cerebral en una situación de inactividad. Esta técnica puede utilizarse para examinar la anatomía funcional del cerebro y para determinar la conectividad entre zonas que no están en contacto directo[78]. En los estudios con rsfMRI en pacientes que han sufrido un ictus isquémico se han identificado alteraciones en la arquitectura funcional, tanto en modelos animales como en humanos[79]. En un estudio en humanos se

demostró que la alteración de la función sensitivomotora tras un ictus se correlacionaba con una pérdida de conectividad interhemisférica entre regiones sensitivomotoras, y que esta disrupción comienza a normalizarse parcialmente semanas después del infarto[80]. Así, en pacientes con un accidente cerebrovascular, los cambios en la actividad neuronal están estrechamente asociados con la recuperación funcional. Concretamente, el aumento de la actividad rsfMRI en la corteza motora suplementaria, la corteza premotora lateral y la corteza parietal superior en los primeros 14 días después del infarto se correlaciona con una mejoría de la función motora de las extremidades superiores durante este período[81]. Por otra parte, la resonancia magnética con tensor de difusión (DTI) evalúa la integridad de la sustancia blanca y gris y también resulta muy útil para predecir la capacidad de recuperación de la función motora de los pacientes que han sufrido un ictus[82]. Por último, la alteración del FSC, analizada mediante ASL (*arterial spin labelling*), se asocia clínicamente con disfunción cognitiva y motora, resultando especialmente grave después de un ictus[83]. Los estudios anteriores realizados con Fortasyn describieron cómo esta dieta mejoraba el FSC[76,84,85]. Además, compuestos fenólicos como el resveratrol también han demostrado aumentar el FSC en la corteza frontal de personas sanas y en el hipocampo de ratas isquémicas[86,87]. Nuestros resultados señalan que una dieta suplementada con HT: mejora la conectividad funcional entre varias regiones cerebrales en los animales infartados; atenua la alteración de la de la microestructura de la sustancia gris asociada al ictus, tanto en hipocampo como corteza motora derecha en comparación con su correspondiente contraparte izquierda; y aumenta significativamente el FSC en el hipocampo derecho de todos los animales, en la corteza izquierda de los infartados y mitiga la disminución del FSC asociada al ictus en el hipocampo izquierdo. Estas mejoras en la conectividad funcional y estructural junto a los efectos sobre la irrigación de diferentes regiones cerebrales podrían estar relacionadas con el aumento en la fuerza de agarre, así como con la mejora de la memoria a corto plazo y procesos de aprendizaje en ratones alimentados con HT.

El FSC está vinculado con la producción de NO debido a su papel como molécula vasodilatadora. El efecto del NO varía según la etapa del proceso isquémico y su fuente celular[88,89]. Así, de las tres isoformas de la NOS responsables de la producción de NO, la actividad de la nNOS y la iNOS son negativas para la recuperación tras el ictus, mientras que la activación de la eNOS se ha asociado con efectos neuroprotectores. Trabajos previos del grupo han demostrado que una elevación inicial de NO en pacientes que han sufrido un accidente cerebrovascular favorece la recuperación neurológica, mientras que su elevación posterior estaría asociada a incrementos del volumen del infarto[90]. Coincidiendo con estudios previos[91,92], hemos observado una disminución significativa en la concentración de NO en el suero de los animales infartados, sin efecto evidente de la dieta. Esta disminución podría ser debida al bajo nivel de L-arginina, precursor del NO, en pacientes de ictus isquémico[90]. Sin embargo, y considerando el mayor FSC de los animales infartados alimentados con HT, sería de interés realizar estudios adicionales a tiempos más próximos a la intervención de tMCAo, no solo en suero sino también en muestras de cerebro, para analizar el perfil temporal de producción de NO y las isoenzimas específicas de NOS que podrían estar moduladas por el HT. Por otro lado, durante la etapa de reperfusión tiene lugar un incremento en los niveles de ERO que puede dar lugar a la muerte celular y a la consiguiente pérdida de tejido[93]. Por lo tanto, considerando los resultados previos, evaluamos si el compuesto era capaz de modular el nivel de estrés oxidativo en muestras de suero obtenidas tras el sacrificio de los animales (35 días después del ictus). El hecho de que no se detectaran cambios en los niveles de ERO en ningún grupo experimental, ni siquiera entre animales infartados y sanos, parece indicar que la obtención de las muestras podría ser demasiado tardía para detectar un posible efecto en los niveles séricos de ERO. De hecho, en un estudio previo con ratones sometidos a hipoxia, se observó que los niveles de ERO en el cerebro, comienzan a normalizarse dos horas después del accidente[15]. Como se mencionó anteriormente en el caso del NO, sería conveniente llevar a cabo análisis adicionales, en momentos más próximos a la cirugía, para reevaluar la capacidad antioxidante de la dieta HT después del accidente cerebrovascular.

En respuesta al daño provocado por el ictus la microglía se activa. A grandes rasgos, el fenotipo M1 de la microglia produce mediadores proinflamatorios, como altos niveles de ERO y NO, mientras que el fenotipo M2 muestra un efecto antiinflamatorio. La dinámica del estado de polarización de la microglía es compleja. Se ha propuesto que la microglía activada de forma persistente después del accidente cerebrovascular presenta predominantemente un fenotipo M1 que contribuye al daño tisular[94]. La capacidad antiinflamatoria del HT se ha demostrado en diferentes modelos[95-97] y, aunque su efecto particular en la neuroinflamación mediada por la microglia no se ha explorado, otros compuestos fenólicos como su precursor la OL atenúan la activación de la microglia[98]. La disminución de los niveles del marcador de microglía IBA-1, 35 días después del ictus en la corteza y el cuerpo calloso de los ratones alimentados con HT, corrobora que este fenol también puede reducir el entorno inflamatorio después de un ictus isquémico. Este resultado probablemente esté involucrado en los efectos beneficiosos descritos previamente y nuevamente apunta al interés de realizar experimentos futuros para profundizar en la actividad neuroinflamatoria del HT a lo largo del tiempo, desde el momento de la cirugía hasta el sacrificio de los animales. El empleo de la técnica PET con diferentes marcadores específicos de neuroinflamación serían muy útiles para profundizar en la dinámica de acción antiinflamatoria del compuesto.

La neurogénesis es crucial para la recuperación tras el ictus isquémico. Aunque se han abordado diferentes estrategias terapéuticas para promoverla, los resultados hasta el momento han sido poco relevantes[99]. DCX, proteína asociada a los microtúbulos y que se expresa en células progenitoras neurales y neuronas inmaduras, es un excelente marcador para la neurogénesis en adultos[100]. En nuestro trabajo, se observó un aumento en el número de células DCX positivas en el hipocampo de ratones alimentados con HT, lo que es indicativo del potencial neurogénico del compuesto. Este efecto podría explicar la acción positiva de este fenol en la memoria a corto plazo y sobre los procesos de aprendizaje descritos anteriormente. El ictus isquémico también implica un deterioro en las sinapsis que daña gravemente la actividad del SNC. Bdnf es una neurotrofina que, además de participar en la inducción de la neurogenesis[101], regula las conexiones sinápticas, la estructura y plasticidad sináptica y la liberación de neurotransmisores[102]. La proteína postsináptica Psd95 también participa en la regulación de la plasticidad sináptica y la sinaptogénesis. Estudios anteriores demuestran que la administración de extractos de hoja de olivo o de polifenoles del aceite aumentan los niveles de Bdnf en los lóbulos olfativos y el hipocampo de ratones[103,104]. El potencial sinaptogénico del HT también se ha descrito en ratas con estrés prenatal en las que el HT evitó la inhibición de Bdnf[105]. Nuestros resultados reflejan que la expresión de Psd95 se induce significativamente en todos los ratones alimentados con HT. Sin embargo, la dieta HT solo aumentó la expresión de Bdnf en el hemisferio no infartado (izquierdo), e incluso la disminuye en el derecho de ratones no sometidos a tMCAO. Por tanto, se puede concluir que el HT afecta de forma diferencial a Bdnf, Psd95 y DCX. Aunque son necesarios análisis adicionales a nivel de proteína, es notable que la administración de un único compuesto simple como el HT muestre efectos tan prometedores, incluso mejores que los observados con la dieta Fortasyn en la que se combinan multiples nutrientes[76].

Los datos presentados a lo largo de este estudio indican que la intervención con una dieta suplementada con HT tras un ictus isquémico, favorece la recuperación al mejorar el aprendizaje pre-asociativo y las capacidades motoras. Este efecto, probablemente vinculado a una mejor conectividad funcional y estructural, al aumento del FSC y a su potencial antiinflamatorio y neurogénico, hace que el HT sea un compuesto prometedor que podría mejorar el estado clínico de los pacientes tras un ictus. De hecho, el conjunto de resultados positivos descritos en este trabajo nos anima a plantear nuevos estudios en los que, además de profundizar en los mecanismos moleculares responsables de los mismos por ejemplo mediante un análisis proteómico que proporcione una visión global de los cambios inducidos por el HT, se analice también su acción preventiva e incluso el posible efecto aditivo de la administración combinada de esta dieta de forma preventiva y terapéutica.

Efecto del TIR sobre mecanismos patogénicos de la EP en modelos de *C.elegans*

En el último trabajo de esta tesis doctoral, se ha estudiado el efecto del TIR en modelos de *C. elegans* de la EP. En este estudio, se ha evaluado desde el efecto del compuesto sobre la longevidad de los animales hasta su acción sobre la expresión de genes directamente relacionados con la enfermedad. El empleo de este organismo modelo permitió la evaluación *in vivo* de diferentes parámetros que mediante otros modelos habría resultado sumamente complicado o inabordable. Las estirpes transgénicas empleadas en este estudio fueron la NL5901 y la UA44. La estirpe NL5901, sobreexpresa la α-syn humana fusionada a YFP en sus células musculares, y fue empleada como modelo de agregación y parálisis progresiva. La estirpe UA44, que sobreexpresa la α-syn marcada específicamente en las 8 neuronas dopaminérgicas, 6 anteriores y 2 posteriores de los animales, se empleó como modelo de neurodegeneración.

En estudios anteriores del grupo, se demostró que el TIR aumenta la vida media y promueve la resistencia a distintos tipos de estrés en estirpes silvestres de *C. elegans*[106]. En base a estos resultados, se evaluó el efecto de este compuesto a diferentes dosis entre sobre la vida media de la estirpe NL5901 para investigar la concentración de TIR más efectiva en esta estirpe. Los resultados obtenidos muestran un aumento moderado de la longevidad en animales tratados con la dosis más alta de TIR (1 mM). Recientemente, también se ha demostrado que diferentes fitoquímicos aumentan la vida media en la misma estirpe[107-109]. Aunque significativo, el aumento en la vida media observado tras el tratamiento con TIR fue menos prominente y a concentraciones más altas, que con el descrito anteriormente en nematodos silvestres[106] (1 mM en lugar de 250 µM). Estas diferencias sugieren que el TIR podría actuar a través de mecanismos celulares adicionales bajo el contexto de la expresión de α-syn, lo que podría influir en su efecto sobre la longevidad de esta estirpe específica. Así, tanto la propia toxicidad que desencadena la sobreexpresión de la α-syn en el modelo, como las posibles limitaciones en cuanto a la captación del compuesto originada por la parálisis progresiva de estos animales, podrían ser la razón por la cual, en la estirpe NL5901, sólo concentraciones de 1 mM resultan eficaces de cara a aumentar la esperanza de vida de estos animales. En este sentido, sería interesante cuantificar la cantidad total de TIR asimilado por los animales teniendo en cuenta las diferencias observadas entre estirpes silvestres y transgénicas. Para ello, sería necesario cuantificar la concentración de TIR libre mediante espectrometría de masas, previa homogenización y obtención de extractos celulares de los nematodos tratados con el compuesto. Esta técnica permitiría además analizar los metabolitos secundarios originados a partir del TIR tras su asimilación por los nematodos.

Tal y como se detalló en la introducción, multitud de estudios apuntan a que la nucleación y formación de protofibrillas y fibras maduras a partir de monómeros de α-syn hasta dar lugar a los cuerpos de Lewy, es el principal mecanismo patológico subyacente a la EP. En este sentido, uno de los principales hallazgos de nuestro estudio fue que el tratamiento con TIR es capaz de reducir sustancialmente la cantidad y/o formación de inclusiones de α-syn en nematodos que sobreexpresan en sus células esta proteína transgénica. Además, este efecto estuvo acompañado por un retraso leve, aunque significativo en el inicio de la disfunción motora inducida por la α-syn en este modelo. Estos resultados, junto con el aumento de la longevidad observado en la misma estirpe, confirman un efecto beneficioso del TIR a la hora de reducir la toxicidad asociada a la sobreexpresión de α-syn *in vivo*. Estudios recientes, han demostrado que diferentes extractos vegetales reducen la agregación de la α-syn en la estirpe NL5901[108-110]. Aunque los mecanismos precisos que subyacen a su efecto aún no se han esclarecido, se ha sugerido que éste puede estar relacionado con la unión de estos compuestos a monómeros y oligómeros de α-syn a través de interacciones hidrofóbicas con estructuras en lámina β, lo que conduciría a un retraso en el proceso de nucleación y a un mayor ensamblaje de los oligómeros tóxicos hacia derivados más estables [109]. Durante la última década, muchos grupos de investigación se han centrado en el estudio de pequeñas moléculas naturales, ricas en grupos aromáticos, como inhibidores de la agregación amiloide con resultados muy variables. En este

sentido, diferentes compuestos fenólicos naturales como la apigenina, la curcumina, la epigalocatequina-3-galato, entre otros, han demostrado ser eficaces para inhibir el mal plegamiento de la α-syn, así como, su agregación *in vitro*[111]. Sin embargo, su capacidad para prevenir la degeneración de neuronas dopaminérgicas *in vivo* no se ha evaluado en profundidad. Respecto al TIR, aunque algunos estudios sugieren efectos protectores de este fenol en la EP[112,113], ninguno de ellos ha evaluado su efecto directo sobre neuronas dopaminérgicas que expresen la α-syn en organismos vivos. En este sentido, nuestros resultados demuestran que el tratamiento de la estirpe UA44 con TIR, da lugar a un retraso significativo en la neurodegeneración dopaminérgica asociada a la expresión de α-syn en este modelo. Este efecto en la neurodegeneración probablemente esté relacionado con la disminución observada en la agregación α-syn también inducida por TIR, lo que demostraría el potencial de este fenol simple para reducir la toxicidad dependiente de α-syn en un entorno dopaminérgico. De hecho, multitud de estudios señalan a los polifenoles como los fitoquimicos mas potentes para inhibir la agregación amiloide de la α-syn [114]. Estos efectos podrían ser extensivos a otras enfermedades de origen amiloide ya que, por ejemplo, otros polifenoles del olivo como la OL han demostrado su capacidad para reducir los depósitos de placas amiloides y la formación de oligómeros, con disminución de la parálisis y aumento de la esperanza de vida en una estirpe de *C. elegans* que expresa constitutivamente Aβ3–42[115]. En este sentido, sería interesante complementar estos resultados mediante el empleo de técnicas *in vitro* que permitan comparar los efectos de diferentes concentraciones del compuesto sobre la cinética de fibrilación de la α-syn. Los ensayos de fibrilación *in vitro* requieren de técnicas eficaces para detectar la formación de fibrillas y monitorizar la cinética de fibrilación en tiempo real. Para ello se utilizan dos colorantes histológicos comunes, la tioflavina T (ThT) y el rojo Congo. El mecanismo de interacción entre estos colorantes y las fibrillas amiloides es poco conocido; sin embargo, ambos compuestos parecen interactuar con las láminas β, experimentando cambios en su fluorescencia. El ThT es un colorante de benzotiazol que emite fluorescencia al unirse a fibrillas amiloides y es la principal técnica utilizada para monitorizar la cinética de fibrilación *in vitro*. En presencia de fibrillas, el ThT presenta un máximo de excitación a 450 nm y emite fluorescencia a 482 nm, mientras que el ThT libre no es fluorescente a estas longitudes de onda[116]. El empleo de esta técnica, sería de utilidad para ahondar en los mecanismos mediante los cuales el TIR actúa en la cascada de agregación de la α-syn. De hecho, ya se ha investigado el efecto del HT sobre la fibrilación *in vitro* de la α-syn, mediante el empleo de la técnica ThT y otras como microscopía electrónica y electroforesis, demostrando que el HT puede inhibir hasta en un 80% la formación de fibras de α-syn, además de desestabilizar fibras preformadas[117].

Como se detalla en la introducción, la formación de fibrillas y agregados de α-syn en los cuerpos de Lewy se ha asociado con un aumento de los niveles de estrés oxidativo[118]. En este sentido, se ha sugerido que la conjugación oxidativa de dopamina con α-syn inhibe la transición de protofibrillas a fibrillas maduras, dando lugar a la acumulación de protofibrillas solubles citotóxicas en las neuronas dopaminergicas[119,120]. Además, experimentos tanto *in vivo* como *in vitro* en cultivos celulares sugieren que las ERO inducen la agregación de la α-syn, lo que, a su vez, aumenta aún más los niveles de ERO, creando un círculo vicioso que conduce a la neurodegeneración[121,122]. De hecho, se ha demostrado que el empleo de antioxidantes tiene la capacidad de revertir la formación de oligómeros tóxicos de esta proteína[123,124]. En este sentido, nuestros resultados muestran una disminución en los niveles de ERO de la estirpe NL5901 tras el tratamiento con TIR, lo que sugiere que la menor acumulación de agregados de α-syn en respuesta al TIR en esta misma estirpe podría estar relacionada con la capacidad del TIR para actuar como neutralizador de ERO. Así, la presencia de TIR podría mejorar el ambiente oxidativo celular que contribuye a la formación de especies tóxicas de α-syn. Por otro lado, como se detalló en el primer trabajo, el HT es capaz de inducir la expresión y actividad de Nrf2. Este factor de transcripción, encargado de la inducción de enzimas de fase II, se encuentra altamente conservado a lo largo de la evolución y presenta su ortólogo, denominado SKN-1, en *C. elegans.* En base al efecto del HT en células MCF-7 y a otros trabajos que demuestran cómo distintos compuestos naturales inducen SKN-1, sería interesante evaluar el efecto de esta ruta en la estirpe NL5901, ya que también podría jugar un papel importante en la disminución de los niveles de ERO tras el tratamiento con el TIR[125].

Las chaperonas son cruciales para el correcto plegamiento y mantenimiento de muchas proteínas celulares, ya que están implicadas tanto en el replegamiento de las mismas como en su degradación por el proteasoma. La familia de proteínas de choque térmico (HSPs), y en particular *hsp-70*, juega un papel clave en estos procesos, estando ampliamente descrito su papel en el mantenimiento de la proteostasis en multitud de enfermedades[126]. En la EP, diferentes estudios han mostrado que, cuando se sobreexpresa *in vivo* e *in vitro*, la chaperona molecular *hsp-70* es capaz de reducir la cantidad de proteína α-syn agregada y mal plegada, protegiendo así frente a su toxicidad[127]. En este sentido, nuestros resultados muestran que el tratamiento con TIR induce la expresión de esta chaperona en la estirpe NL5901, lo que podría relacionarse también con la menor agregación de α-syn observada en respuesta a la misma dosis de TIR en esta estirpe. Por otro lado, *hsp-16.2* y *hsp-12.6* son miembros de las familias de proteínas de choque térmico pequeñas (smHSPs) de 16 kDa y 12 kDa que se sabe que funcionan como chaperonas moleculares específicas en *C. elegans*, evitando la agregación de proteínas desnaturalizadas y guiando proteínas mal plegadas para replegarse a su estado nativo[128,129]. En particular, *hsp-16.2* podría actuar como ligando pasivo evitando temporalmente la agregación de proteínas desplegadas. De hecho, se ha demostrado que esta chaperona es capaz de interactuar con el péptido beta amiloide humano[130]. En *C. elegans*, la expresión de las smHSPs, así como de otras chaperonas, se activa por los factores de transcripción HSF-1 y DAF-16 en respuesta al estrés, lo que a su vez promueve la longevidad en este nematodo[131]. Curiosamente, estudios previos de nuestro grupo demuestran que la suplementación con TIR es capaz de inducir la expresión específica de smHSPs tanto a nivel de mRNA como de proteína en *C. elegans*, asociando este efecto a una mayor vida media y resistencia al estrés en estirpes silvestres[106,132,133]. Además, describimos que este efecto dependía parcialmente de HSF-1. De forma paralela a estos resultados, en este trabajo hemos descrito cómo el TIR también aumenta la expresión tanto de *hsp-70* como de *hsp-16.2* y *hsp-12.6* en la estirpe NL5901. En cuanto a las enzimas antioxidantes estudiadas en nuestro modelo, la GST-4, es capaz junto al resto de GSTs, de mediar la respuesta detoxificante de proteínas de fase II regulada a través del factor de transcripción SKN-1 en respuesta al estrés oxidativo en *C. elegans*[134]. El hecho de que el TIR induzca la expresión de este gen antioxidante podría estar relacionado con la disminución en los niveles de ERO observada en animales tratados con TIR y apoyaría la teoría de que este compuesto ejerce su efecto a través del ortólogo de Nrf-2, SKN-1 en este modelo[135,136]. En la EP, la inducción de Nrf2 ha demostrado mitigar de forma eficaz los efectos neurotóxicos de agentes parkinsonianos como MPP^+, rotenona y H_2O_2 *in vitro* e *in vivo*. Además, la variabilidad genética en vías dependientes de Nrf2 puede promover la susceptibilidad neuronal a agentes exógenos y correlacionarse con el inicio de la EP en ciertas poblaciones[137].

En resumen, aunque son necesarios estudios adicionales para esclarecer los mecanismos moleculares involucrados, en este trabajo se describe cómo el TIR modula diferentes procesos y mecanismos relevantes en la EP. Los resultados de nuestro estudio añaden nuevas actividades biológicas a las ya descritas previamente para el TIR, reforzando su importancia como potencial compuesto nutracéutico. Además, este trabajo puede servir de base para el empleo del TIR o sus derivados en estudios de modelización molecular encaminados al diseño de fármacos con capacidad neuroprotectora en la EP.

Referencias bibliográficas

1 Echeverría, F., Ortiz, M., Valenzuela, R. & Videla, L. Hydroxytyrosol and cytoprotection: a projection for clinical interventions. *International journal of molecular sciences* **18**, 930, doi:https://doi.org/10.3390/ijms18050930 (2017).

2 Warleta, F. *et al.* Hydroxytyrosol protects against oxidative DNA damage in human breast cells. *Nutrients* **3**, 839-857, doi:10.3390/nu3100839 (2011).

3 Han, J., Talorete, T. P., Yamada, P. & Isoda, H. Anti-proliferative and apoptotic effects of oleuropein and hydroxytyrosol on human breast cancer MCF-7 cells. *Cytotechnology* **59**, 45-53, doi:10.1007/s10616-009-9191-2 (2009).

4 El-azem, N. *et al.* Modulation by hydroxytyrosol of oxidative stress and antitumor activities of paclitaxel in breast cancer. *European journal of nutrition*, 1-9, doi:10.1007/s00394-018-1638-9 (2018).

5 Almendros, I. & Gozal, D. Intermittent hypoxia and cancer: Undesirable bed partners? *Respiratory physiology & neurobiology* **256**, 79-86, doi:10.1016/j.resp.2017.08.008 (2018).

6 Moloney, J. N. & Cotter, T. G. in *Seminars in cell & developmental biology.* 50-64 (Elsevier).

7 Vera-Ramirez, L. *et al.* Oxidative stress status in metastatic breast cancer patients receiving palliative chemotherapy and its impact on survival rates. *Free radical research* **46**, 2-10, doi:10.3109/10715762.2011.635658 (2012).

8 Galadari, S., Rahman, A., Pallichankandy, S. & Thayyullathil, F. Reactive oxygen species and cancer paradox: to promote or to suppress? *Free Radical Biology and Medicine* **104**, 144-164, doi:10.1016/j.freeradbiomed.2017.01.004 (2017).

9 Ehrenfeld, P., Cordova, F., Duran, W. N. & Sanchez, F. A. S-nitrosylation and its role in breast cancer angiogenesis and metastasis. *Nitric Oxide*, doi:10.1016/j.niox.2019.03.002 (2019).

10 Choudhari, S. K., Chaudhary, M., Bagde, S., Gadbail, A. R. & Joshi, V. Nitric oxide and cancer: a review. *World journal of surgical oncology* **11**, 118, doi:10.1186/1477-7819-11-118 (2013).

11 Plastina, P. *et al.* Identification of hydroxytyrosyl oleate, a derivative of hydroxytyrosol with anti-inflammatory properties, in olive oil by-products. *Food chemistry* **279**, 105-113, doi:10.1016/j.foodchem.2018.12.007 (2019).

12 Deiana, M. *et al.* Inhibition of peroxynitrite dependent DNA base modification and tyrosine nitration by the extra virgin olive oil-derived antioxidant hydroxytyrosol. *Free Radical Biology and Medicine* **26**, 762-769, doi:https://doi.org/10.1016/S0891-5849(98)00231-7 (1999).

13 Zhang, X., Cao, J. & Zhong, L. Hydroxytyrosol inhibits pro-inflammatory cytokines, iNOS, and COX-2 expression in human monocytic cells. *Naunyn-Schmiedeberg's archives of pharmacology* **379**, 581, doi:10.1007/s00210-009-0399-7 (2009).

14 Martínez-Lara, E., Peña, A., Calahorra, J., Cañuelo, A. & Siles, E. Hydroxytyrosol decreases the oxidative and nitrosative stress levels and promotes angiogenesis through HIF-1 independent mechanisms in renal hypoxic cells. *Food & function* **7**, 540-548, doi:10.1039/C5FO00928F (2016).

15 Martínez-Romero, R. *et al.* Poly (ADP-ribose) polymerase-1 modulation of in vivo response of brain hypoxia-inducible factor-1 to hypoxia/reoxygenation is mediated by nitric oxide and factor inhibiting HIF. *Journal of neurochemistry* **111**, 150-159, doi: 10.1111/j.1471-4159.2009.06307.x (2009).

16 Rodríguez, M. I. *et al.* PARP-1 regulates metastatic melanoma through modulation of vimentin-induced malignant transformation. *PLoS genetics* **9**, e1003531, doi:10.18632/oncotarget.2993 (2013).

17 Gonzalez-Flores, A. *et al.* Interaction between PARP-1 and HIF-2α in the hypoxic response. *Oncogene* **33**, 891, doi:10.1038/onc.2013.9 (2014).

18 Aguilar-Quesada, R. *et al.* Modulation of transcription by PARP-1: consequences in carcinogenesis and inflammation. *Current medicinal chemistry* **14**, 1179-1187, doi:10.2174/092986707780597998 (2007).

19 Carew, J. S. & Huang, P. Mitochondrial defects in cancer. *Molecular cancer* **1**, 9, doi:10.1186/1476-4598-1-9 (2002).

20 Luo, C., Widlund, H. R. & Puigserver, P. PGC-1 coactivators: shepherding the mitochondrial biogenesis of tumors. *Trends in cancer* **2**, 619-631, doi:10.1016/j.trecan.2016.09.006 (2016).

21 Andrzejewski, S. *et al.* PGC-1α promotes breast cancer metastasis and confers bioenergetic flexibility against metabolic drugs. *Cell metabolism* **26**, 778-787. e775, doi:10.1016/j.cmet.2017.09.006 (2017).

22 Shoag, J. & Arany, Z. Regulation of hypoxia-inducible genes by PGC-1α. *Arteriosclerosis, thrombosis, and vascular biology* **30**, 662-666, doi:10.1161/ATVBAHA.108.181636 (2010).

23 Feng, Z. *et al.* Mitochondrial dynamic remodeling in strenuous exercise-induced muscle and mitochondrial dysfunction: regulatory effects of hydroxytyrosol. *Free Radical Biology and Medicine* **50**, 1437-1446, doi:10.1016/j.freeradbiomed.2011.03.001 (2011).

24 Hao, J. *et al.* Hydroxytyrosol promotes mitochondrial biogenesis and mitochondrial function in 3T3-L1 adipocytes. *The Journal of nutritional biochemistry* **21**, 634-644, doi:10.1016/j.jnutbio.2009.03.012 (2010).

25 Signorile, A. *et al.* Regulation of the biogenesis of OXPHOS complexes in cell transition from replicating to quiescent state: involvement of PKA and effect of hydroxytyrosol. *Biochimica et Biophysica Acta (BBA)-Molecular Cell Research* **1843**, 675-684, doi:10.1016/j.bbamcr.2013.12.017 (2014).

26 Ranhotra, H. S. The estrogen-related receptors in metabolism and cancer: Newer insights. *Journal of Receptors and Signal Transduction* **38**, 95-100, doi:10.1080/10799893.2018.1456552 (2018).

27 Chang, C.-y. & McDonnell, D. P. Molecular pathways: the metabolic regulator estrogen-related receptor α as a therapeutic target in cancer. *Clinical Cancer Research* **18**, 6089-6095, doi:10.1158/1078-0432.CCR-11-3221 (2012).

28 Chisamore, M. J., Cunningham, M. E., Flores, O., Wilkinson, H. A. & Chen, J. D. Characterization of a novel small molecule subtype specific estrogen-related receptor α antagonist in MCF-7 breast cancer cells. *PloS one* **4**, e5624, doi:10.1371/journal.pone.0005624 (2009).

29 Yu, F.-Y., Xu, Q., Wu, D.-D., Lau, A. T. & Xu, Y.-M. The prognostic and clinicopathological roles of sirtuin-3 in various cancers. *PLoS one* **11**, e0159801, doi:10.1371/journal.pone.0159801 (2016).

30 Tomé-Carneiro, J. *et al.* Proteomic evaluation of mouse adipose tissue and liver following hydroxytyrosol supplementation. *Food and Chemical Toxicology* **107**, 329-338, doi:10.1016/j.fct.2017.07.009 (2017).

31 Tomé-Carneiro, J. *et al.* Hydroxytyrosol supplementation modulates the expression of miRNAs in rodents and in humans. *The Journal of nutritional biochemistry* **34**, 146-155, doi:10.1016/j.jnutbio.2016.05.009 (2016).

32 Cavadas, M. A., Cheong, A. & Taylor, C. T. The regulation of transcriptional repression in hypoxia. *Experimental cell research* **356**, 173-181, doi:10.1016/j.yexcr.2017.02.024 (2017).

33 Rocha, S. Gene regulation under low oxygen: holding your breath for transcription. *Trends in biochemical sciences* **32**, 389-397, doi:10.1016/j.tibs.2007.06.005 (2007).

34 Tonelli, C., Chio, I. I. C. & Tuveson, D. A. Transcriptional regulation by Nrf2. *Antioxidants & redox signaling* **29**, 1727-1745, doi:10.1089/ars.2017.7342 (2018).

35 Martín, M. A. *et al.* Hydroxytyrosol induces antioxidant/detoxificant enzymes and Nrf2 translocation via extracellular regulated kinases and phosphatidylinositol-3-kinase/protein kinase B pathways in HepG2 cells. *Molecular nutrition & food research* **54**, 956-966, doi:10.1002/mnfr.200900159 (2010).

36 Peng, S., Zhang, B., Yao, J., Duan, D. & Fang, J. Dual protection of hydroxytyrosol, an olive oil polyphenol, against oxidative damage in PC12 cells. *Food & function* **6**, 2091-2100, doi:10.1039/C5FO00097A (2015).

37 Gao, X.-y. *et al.* Gartanin protects neurons against glutamate-induced cell death in HT22 cells: independence of Nrf-2 but involvement of HO-1 and AMPK. *Neurochemical research* **41**, 2267-2277, doi:10.1007/s11064-016-1941-x (2016).

38 Wright, M. M., Junghyun, K., LEITINGER, N., FREEMAN, B. A. & AGARWAL, A. Human haem oxygenase-1 induction by nitro-linoleic acid is mediated by cAMP, AP-1 and E-box response element interactions. *Biochemical Journal* **422**, 353-361, doi:10.1042/BJ20090339 (2009).

39 Kang, J. *et al.* A FoxO1-dependent, but NRF2-independent induction of heme oxygenase-1 during muscle atrophy. *FEBS letters* **588**, 79-85, doi:10.1016/j.febslet.2013.11.009 (2014).

40 de la Vega, M. R., Chapman, E. & Zhang, D. D. NRF2 and the hallmarks of cancer. *Cancer cell* **34**, 21-43, doi:10.1016/j.ccell.2018.03.022 (2018).

41 Liu, Z.-j., Semenza, G. L. & Zhang, H.-f. Hypoxia-inducible factor 1 and breast cancer metastasis. *Journal of Zhejiang University-SCIENCE B* **16**, 32-43, doi:10.1631/jzus.B1400221 (2015).

42 Gorres, K. L. & Raines, R. T. Direct and continuous assay for prolyl 4-hydroxylase. *Analytical biochemistry* **386**, 181-185, doi:10.1016/j.ab.2008.11.046 (2009).

43 Strowitzki, M. J., Cummins, E. P. & Taylor, C. T. Protein Hydroxylation by Hypoxia-Inducible Factor (HIF) Hydroxylases: Unique or Ubiquitous? *Cells* **8**, 384, doi:10.3390/cells8050384 (2019).

44 Terzuoli, E. *et al.* Inhibition of hypoxia inducible factor-1α by dihydroxyphenylethanol, a product from olive oil, blocks microsomal prostaglandin-E synthase-1/vascular endothelial growth factor expression and reduces tumor angiogenesis. *Clinical Cancer Research* **16**, 4207-4216, doi:10.1158/1078-0432.CCR-10-0156 (2010).

45 Cárdeno, A., Sánchez-Hidalgo, M., Rosillo, M. A. & de la Lastra, C. A. Oleuropein, a secoiridoid derived from olive tree, inhibits the proliferation of human colorectal cancer cell through downregulation of HIF-1α. *Nutrition and cancer* **65**, 147-156, doi:10.1080/01635581.2013.741758 (2013).

46 Zhao, B. *et al.* Hydroxytyrosol, a natural molecule from olive oil, suppresses the growth of human hepatocellular carcinoma cells via inactivating AKT and nuclear factor-kappa B pathways. *Cancer letters* **347**, 79-87, doi:10.1016/j.canlet.2014.01.028 (2014).

47 Wang, W. *et al.* Hydroxytyrosol regulates the autophagy of vascular adventitial fibroblasts through the SIRT1-mediated signaling pathway. *Canadian journal of physiology and pharmacology* **96**, 88-96, doi:10.1139/cjpp-2016-0676 (2017).

48 Zubair, H. *et al.* Hydroxytyrosol induces apoptosis and cell cycle arrest and suppresses multiple oncogenic signaling pathways in prostate cancer cells. *Nutrition and cancer* **69**, 932-942, doi:10.1080/01635581.2017.1339818 (2017).

49 Incani, A. *et al.* Involvement of ERK, Akt and JNK signalling in H2O2-induced cell injury and protection by hydroxytyrosol and its metabolite homovanillic alcohol. *Molecular nutrition & food research* **54**, 788-796, doi:10.1016/j.jnutbio.2011.05.006 (2010).

50 Zou, X. *et al.* Stimulation of GSH synthesis to prevent oxidative stress-induced apoptosis by hydroxytyrosol in human retinal pigment epithelial cells: activation of Nrf2 and JNK-p62/SQSTM1 pathways. *The Journal of nutritional biochemistry* **23**, 994-1006, doi:10.1016/j.jnutbio.2011.05.006 (2012).

51 Sun, L., Luo, C. & Liu, J. Hydroxytyrosol induces apoptosis in human colon cancer cells through ROS generation. *Food & function* **5**, 1909-1914, doi:10.1039/c4fo00187g (2014).

52 Lamy, S., Ouanouki, A., Béliveau, R. & Desrosiers, R. R. Olive oil compounds inhibit vascular endothelial growth factor receptor-2 phosphorylation. *Experimental cell research* **322**, 89-98, doi:10.1016/j.yexcr.2013.11.022 (2014).

53 Granner, T., Maloney, S., Antecka, E., Correa, J. A. & Burnier, M. N. 3, 4 dihydroxyphenyl ethanol reduces secretion of angiogenin in human retinal pigment epithelial cells. *British Journal of Ophthalmology* **97**, 371-374, doi:10.1136/bjophthalmol-2012-302002 (2013).

54 Hu, C.-J., Wang, L.-Y., Chodosh, L. A., Keith, B. & Simon, M. C. Differential roles of hypoxia-inducible factor 1α (HIF-1α) and HIF-2α in hypoxic gene regulation. *Molecular and cellular biology* **23**, 9361-9374, doi:10.1128/MCB.23.24.9361-9374.2003 (2003).

55 Rankin, E. B. *et al.* Hypoxia-inducible factor–2 (HIF-2) regulates hepatic erythropoietin in vivo. *The Journal of clinical investigation* **117**, 1068-1077, doi:10.1172/JCI30117 (2007).

56 Covello, K. L. *et al.* HIF-2α regulates Oct-4: effects of hypoxia on stem cell function, embryonic development, and tumor growth. *Genes & development* **20**, 557-570, doi:10.1101/gad.1399906 (2006).

57 Iwano, S., Ichikawa, M., Takizawa, S., Hashimoto, H. & Miyamoto, Y. Identification of AhR-regulated genes involved in PAH-induced immunotoxicity using a highly-sensitive DNA chip, 3D-GeneTM Human Immunity and Metabolic Syndrome 9k. *Toxicology in Vitro* **24**, 85-91, doi:10.1016/j.tiv.2009.08.030 (2010).

58 Chiappini, F. *et al.* Exposure to environmental concentrations of hexachlorobenzene induces alterations associated with endometriosis progression in a rat model. *Food and Chemical Toxicology* **123**, 151-161, doi:10.1016/j.fct.2018.10.056 (2019).

59 Tsai, M.-J. *et al.* Aryl hydrocarbon receptor agonists upregulate VEGF secretion from bronchial epithelial cells. *Journal of Molecular Medicine* **93**, 1257-1269, doi:10.1007/s00109-015-1304-0 (2015).

60 Portal-Nuñez, S. *et al.* Aryl hydrocarbon receptor-induced adrenomedullin mediates cigarette smoke carcinogenicity in humans and mice. *Cancer research* **72**, 5790-5800, doi:10.1158/0008-5472.CAN-12-0818 (2012).

61 Vorrink, S. U. & Domann, F. E. Regulatory crosstalk and interference between the xenobiotic and hypoxia sensing pathways at the AhR-ARNT-HIF1α signaling node. *Chemico-biological interactions* **218**, 82-88, doi:10.1016/j.cbi.2014.05.001 (2014).

62 Vacher, S. *et al.* High AHR expression in breast tumors correlates with expression of genes from several signaling pathways namely inflammation and endogenous tryptophan metabolism. *PloS one* **13**, e0190619, doi:10.1371/journal.pone.0190619 (2018).

63 Larigot, L., Juricek, L., Dairou, J. & Coumoul, X. AhR signaling pathways and regulatory functions. *Biochimie open*, doi:10.1016/j.biopen.2018.05.001 (2018).

64 Zhang, S., Qin, C. & Safe, S. H. Flavonoids as aryl hydrocarbon receptor agonists/antagonists: effects of structure and cell context. *Environmental health perspectives* **111**, 1877-1882, doi:10.1289/ehp.6322 (2003).

65 Pandini, A. *et al.* Detection of the TCDD binding-fingerprint within the Ah receptor ligand binding domain by structurally driven mutagenesis and functional analysis. *Biochemistry* **48**, 5972-5983, doi:10.1021/bi900259z (2009).

66 Jogalekar, A. S., Reiling, S. & Vaz, R. J. Identification of optimum computational protocols for modeling the aryl hydrocarbon receptor (AHR) and its interaction with ligands. *Bioorganic & medicinal chemistry letters* **20**, 6616-6619, doi:10.1016/j.bmcl.2010.09.019 (2010).

67 Miller III, B. R. *et al.* MMPBSA. py: an efficient program for end-state free energy calculations. *Journal of chemical theory and computation* **8**, 3314-3321, doi:10.1021/ct300418h (2012).

68 Michel, J., Foloppe, N. & Essex, J. W. Rigorous free energy calculations in structure-based drug design. *Molecular informatics* **29**, 570-578, doi:10.1002/minf.201000051 (2010).

69 Granadino-Roldan, J. M. *et al.* Effect of set up protocols on the accuracy of alchemical free energy calculation over a set of ACK1 inhibitors. *PloS one* **14**, e0213217, doi:10.1371/journal.pone.0213217 (2019).

70 Dougherty, E. J. & Pollenz, R. S. Analysis of Ah receptor-ARNT and Ah receptor-ARNT2 complexes in vitro and in cell culture. *Toxicological sciences* **103**, 191-206, doi:10.1093/toxsci/kfm300 (2007).

71 Li, S. *et al.* Preconditioning in neuroprotection: from hypoxia to ischemia. *Progress in neurobiology* **157**, 79-91, doi:10.1016/j.pneurobio.2017.01.001 (2017).

72 Mohagheghi, F., Bigdeli, M. R., Rasoulian, B., Hashemi, P. & Pour, M. R. The neuroprotective effect of olive leaf extract is related to improved blood–brain barrier permeability and brain edema in rat with experimental focal cerebral ischemia. *Phytomedicine* **18**, 170-175, doi:10.1016/j.phymed.2010.06.007 (2011).

73 Mohagheghi, F., Bigdeli, M. R., Rasoulian, B., Zeinanloo, A. A. & Khoshbaten, A. Dietary virgin olive oil reduces blood brain barrier permeability, brain edema, and brain injury in rats subjected to ischemia-reperfusion. *The Scientific World Journal* **10**, 1180-1191, doi:10.1100/tsw.2010.128 (2010).

74 Yu, H. *et al.* Oleuropein, a natural extract from plants, offers neuroprotection in focal cerebral ischemia/reperfusion injury in mice. *European journal of pharmacology* **775**, 113-119, doi:10.1016/j.ejphar.2016.02.027 (2016).

75 Wiesmann, M. *et al.* Effect of a multinutrient intervention after ischemic stroke in female C57Bl/6 mice. *Journal of neurochemistry* **144**, 549-564, doi:10.1111/jnc.14213 (2018).

76 Wiesmann, M. *et al.* A specific dietary intervention to restore brain structure and function after ischemic stroke. *Theranostics* **7**, 493, doi:10.7150/thno.17559 (2017).

77 García-Sánchez, F., Martínez-Gras, I., Rodríguez-Jiménez, R. & Rubio, G. Inhibición prepulso del reflejo de la respuesta de sobresalto en los trastornos neuropsiquiátricos. *Revista de Neurología* **53**, 422-432 (2011).

78 Proal, E., Álvarez-Segura, M., de la Iglesia-Vayá, M., Martí-Bonmatí, L. & Castellanos, F. X. Actividad funcional cerebral en estado de reposo: redes en conexión. *Revista de neurologia* **52**, S3 (2011).

79 Kroll, H., Zaharchuk, G., Christen, T., Heit, J. & Iv, M. Resting State BOLD MRI for Perfusion and Ischemia. *Topics in magnetic resonance imaging: TMRI* **26**, 91, doi:10.1097/RMR.0000000000000119 (2017).

80 Carter, A. R. *et al.* Resting interhemispheric functional magnetic resonance imaging connectivity predicts performance after stroke. *Annals of neurology* **67**, 365-375, doi:10.1002/ana.21905 (2010).

81 Rehme, A. K., Fink, G. R., von Cramon, D. Y. & Grefkes, C. The role of the contralesional motor cortex for motor recovery in the early days after stroke assessed with longitudinal FMRI. *Cerebral cortex* **21**, 756-768, doi:10.1093/cercor/bhq140 (2010).

82 Moura, L. M. *et al.* Diffusion tensor imaging biomarkers to predict motor outcomes in stroke: A narrative review. *Frontiers in neurology* **10**, 445, doi:10.3389/fneur.2019.00445 (2019).

83 Ogoh, S. Relationship between cognitive function and regulation of cerebral blood flow. *The Journal of Physiological Sciences* **67**, 345-351, doi:10.1007/s12576-017-0525-0 (2017).

84 Zerbi, V. *et al.* Multinutrient diets improve cerebral perfusion and neuroprotection in a murine model of Alzheimer's disease. *Neurobiology of aging* **35**, 600-613, doi:10.7150/thno.17559 (2014).

85 Wiesmann, M. *et al.* A dietary treatment improves cerebral blood flow and brain connectivity in aging apoE4 mice. *Neural plasticity* **2016**, doi:10.1155/2016/6846721 (2016).

86 Kennedy, D. O. *et al.* Effects of resveratrol on cerebral blood flow variables and cognitive performance in humans: a double-blind, placebo-controlled, crossover investigation. *The American journal of clinical nutrition* **91**, 1590-1597, doi:10.3945/ajcn.2009.28641 (2010).

87 Lu, K. T. *et al.* Neuroprotective effects of resveratrol on cerebral ischemia-induced neuron loss mediated by free radical scavenging and cerebral blood flow elevation. *Journal of agricultural and food chemistry* **54**, 3126-3131, doi:10.1021/jf053011q (2006).

88 Rodrigo, J., Fernandez, A., Serrano, J., Peinado, M. & Martinez, A. The role of free radicals in cerebral hypoxia and ischemia. *Free Radical Biology and Medicine* **39**, 26-50, doi:10.1016/j.freeradbiomed.2005.02.010 (2005).

89 Martinez-Lara, E. *et al.* Constitutive nitric oxide synthases are responsible for the nitric oxide production in the ischemic aged cerebral cortex. *Brain research* **1054**, 88-94, doi:10.1016/j.brainres.2005.06.060 (2005).

90 Serrano-Ponz, M. *et al.* Temporal profiles of blood pressure, circulating nitric oxide, and adrenomedullin as predictors of clinical outcome in acute ischemic stroke patients. *Molecular medicine reports* **13**, 3724-3734, doi:10.3892/mmr.2016.5001 (2016).

91 Rashid, P. A., Whitehurst, A., Lawson, N. & Bath, P. M. Plasma nitric oxide (nitrate/nitrite) levels in acute stroke and their relationship with severity and outcome. *Journal of Stroke and Cerebrovascular Diseases* **12**, 82-87, doi:10.1053/jscd.2003.9 (2003).

92 Abdullah, A. *et al.* Evaluation of serum oxidant/antioxidant balance in patients with acute stroke. *J Pak Med Assoc* **63**, 590-593 (2013).

93 Rodrigo, R. *et al.* Oxidative stress and pathophysiology of ischemic stroke: novel therapeutic opportunities. *CNS & Neurological Disorders-Drug Targets (Formerly Current Drug Targets-CNS & Neurological Disorders)* **12**, 698-714, doi:10.2174/1871527311312050015 (2013).

94 Xiong, X.-Y., Liu, L. & Yang, Q.-W. Functions and mechanisms of microglia/macrophages in neuroinflammation and neurogenesis after stroke. *Progress in neurobiology* **142**, 23-44, doi:10.1016/j.pneurobio.2016.05.001 (2016).

95 Richard, N. *et al.* Hydroxytyrosol is the major anti-inflammatory compound in aqueous olive extracts and impairs cytokine and chemokine production in macrophages. *Planta medica* **77**, 1890-1897, doi:10.1055/s-0031-1280022 (2011).

96 Pirozzi, C. *et al.* Hydroxytyrosol prevents metabolic impairment reducing hepatic inflammation and restoring duodenal integrity in a rat model of NAFLD. *The Journal of nutritional biochemistry* **30**, 108-115, doi:10.1016/j.jnutbio.2015.12.004 (2016).

97 Lopez, S. *et al.* Effect of metabolites of hydroxytyrosol on protection against oxidative stress and inflammation in human endothelial cells. *Journal of functional foods* **29**, 238-247, doi:10.1016/j.jff.2016.12.033 (2017).

98 Hornedo-Ortega, R. *et al.* Phenolic compounds characteristic of the Mediterranean diet in mitigating microglia-mediated neuroinflammation. *Frontiers in cellular neuroscience* **12**, doi:10.3389/fncel.2018.00373 (2018).

99 Koh, S.-H. & Park, H.-H. Neurogenesis in stroke recovery. *Translational stroke research* **8**, 3-13, doi:10.1007/s12975-016-0460-z (2017).

100 Brown, J. P. *et al.* Transient expression of doublecortin during adult neurogenesis. *Journal of Comparative Neurology* **467**, 1-10, doi:10.1002/cne.10874 (2003).

101 Rossi, C. *et al.* Brain-derived neurotrophic factor (BDNF) is required for the enhancement of hippocampal neurogenesis following environmental enrichment. *European Journal of Neuroscience* **24**, 1850-1856, doi:10.1111/j.1460-9568.2006.05059.x (2006).

102 Song, M., Martinowich, K. & Lee, F. S. BDNF at the synapse: why location matters. *Molecular psychiatry* **22**, 1370, doi:10.1038/mp.2017.144 (2017).

103 Carito, V. *et al.* Effects of olive leaf polyphenols on male mouse brain NGF, BDNF and their receptors TrkA, TrkB and p75. *Natural product research* **28**, 1970-1984, doi:10.1080/14786419.2014.918977 (2014).

104 De Nicoló, S. *et al.* Effects of olive polyphenols administration on nerve growth factor and brain-derived neurotrophic factor in the mouse brain. *Nutrition* **29**, 681-687, doi:10.1016/j.nut.2012.11.007 (2013).

105 Zheng, A. *et al.* Maternal hydroxytyrosol administration improves neurogenesis and cognitive function in prenatally stressed offspring. *The Journal of nutritional biochemistry* **26**, 190-199, doi:10.1016/j.jnutbio.2014.10.006 (2015).

106 Cañuelo, A. *et al.* Tyrosol, a main phenol present in extra virgin olive oil, increases lifespan and stress resistance in Caenorhabditis elegans. *Mechanisms of ageing and development* **133**, 563-574, doi:10.1016/j.mad.2012.07.004 (2012).

107 Govindan, S. *et al.* Phytochemicals-induced hormesis protects Caenorhabditis elegans against α-synuclein protein aggregation and stress through modulating HSF-1 and SKN-1/Nrf2 signaling pathways. *Biomedicine & Pharmacotherapy* **102**, 812-822 (2018).

108 Jadiya, P. *et al.* Anti-Parkinsonian effects of Bacopa monnieri: insights from transgenic and pharmacological Caenorhabditis elegans models of Parkinson's disease. *Biochemical and biophysical research communications* **413**, 605-610, doi:10.1016/j.bbrc.2011.09.010 (2011).

109 Ji, K. *et al.* Inhibition effects of tanshinone on the aggregation of α-synuclein. *Food & function* **7**, 409-416, doi: 10.1039/C5FO00664C (2016).

110 Chalorak, P. *et al.* Holothuria scabra extracts exhibit anti-Parkinson potential in C. elegans: A model for anti-Parkinson testing. *Nutritional neuroscience* **21**, 427-438, doi:10.1080/1028415X.2017.1299437 (2018).

111 Dhouafli, Z. *et al.* Inhibition of protein misfolding and aggregation by natural phenolic compounds. *Cellular and molecular life sciences* **75**, 3521-3538, doi:10.1007/s00018-018-2872-2 (2018).

112 Dewapriya, P., Himaya, S., Li, Y.-X. & Kim, S.-K. Tyrosol exerts a protective effect against dopaminergic neuronal cell death in in vitro model of Parkinson's disease. *Food chemistry* **141**, 1147-1157, doi:10.1016/j.foodchem.2013.04.004 (2013).

113 Vauzour, D., Corona, G. & Spencer, J. P. Caffeic acid, tyrosol and p-coumaric acid are potent inhibitors of 5-S-cysteinyl-dopamine induced neurotoxicity. *Archives of Biochemistry and Biophysics* **501**, 106-111, doi:10.1016/j.abb.2010.03.016 (2010).

114 Javed, H. *et al.* Plant Extracts and Phytochemicals Targeting α-Synuclein Aggregation in Parkinson's Disease Models. *Frontiers in Pharmacology* **9**, doi:10.3389/fphar.2018.01555 (2018).

115 Diomede, L., Rigacci, S., Romeo, M., Stefani, M. & Salmona, M. Oleuropein aglycone protects transgenic C. elegans strains expressing Aβ42 by reducing plaque load and motor deficit. *PLoS one* **8**, e58893, doi:10.1371/journal.pone.0058893 (2013).

116 Narkiewicz, J., Giachin, G. & Legname, G. In vitro aggregation assays for the characterization of α-synuclein prion-like properties. *Prion* **8**, 19-32, doi:10.4161/pri.28125 (2014).

117 Gallardo-Fernández, M., Hornedo-Ortega, R., Cerezo, A. B., Troncoso, A. M. & Garcia-Parrilla, M. C. Simultaneous Occurrence of Bioactive Compounds (Melatonin, Protocatechuic Acid and Hydroxytyrosol) Increases Their Neuroprotective Effects Against Alpha-Synuclein-Induced Proteotoxicity. doi:10.20944/preprints201811.0142.v1 (2018).

118 Dias, V., Junn, E. & Mouradian, M. M. The role of oxidative stress in Parkinson's disease. *Journal of Parkinson's disease* **3**, 461-491, doi:10.3233/JPD-130230 (2013).

119 Butler, B., Sambo, D. & Khoshbouei, H. Alpha-synuclein modulates dopamine neurotransmission. *Journal of chemical neuroanatomy* **83**, 41-49, doi:10.1016/j.jchemneu.2016.06.001 (2017).

120 Chen, L. *et al.* Unregulated cytosolic dopamine causes neurodegeneration associated with oxidative stress in mice. *Journal of Neuroscience* **28**, 425-433, doi:10.1523/JNEUROSCI.3602-07.2008 (2008).

121 Nieto, M. *et al.* Increased sensitivity to MPTP in human α-synuclein A30P transgenic mice. *Neurobiology of aging* **27**, 848-856, doi:10.1016/j.neurobiolaging.2005.04.010 (2006).

122 Tabrizi, S. J. *et al.* Expression of mutant α-synuclein causes increased susceptibility to dopamine toxicity. *Human molecular genetics* **9**, 2683-2689, doi:10.1093/hmg/9.18.2683 (2000).

123 Chinta, S. J. & Andersen, J. K. Redox imbalance in Parkinson's disease. *Biochimica et Biophysica Acta (BBA)-General Subjects* **1780**, 1362-1367, doi:10.1016/j.bbagen.2008.02.005 (2008).

124 Conway, K. A., Rochet, J.-C., Bieganski, R. M. & Lansbury, P. T. Kinetic stabilization of the α-synuclein protofibril by a dopamine-α-synuclein adduct. *Science* **294**, 1346-1349, doi:10.1126/science.1063522 (2001).

125 Lin, C. *et al.* Rosmarinic acid improved antioxidant properties and healthspan via the IIS and MAPK pathways in Caenorhabditis elegans. *BioFactors*, doi:10.1002/biof.1536 (2019).

126 Lackie, R. E. *et al.* The Hsp70/Hsp90 chaperone machinery in neurodegenerative diseases. *Frontiers in neuroscience* **11**, 254, doi:10.3389/fnins.2017.00254 (2017).

127 Klucken, J., Shin, Y., Masliah, E., Hyman, B. T. & McLean, P. J. Hsp70 reduces α-synuclein aggregation and toxicity. *Journal of Biological Chemistry* **279**, 25497-25502, doi:10.1074/jbc.M400255200 (2004).

128 Mendenhall, A. R. *et al.* Expression of a single-copy hsp-16.2 reporter predicts life span. *Journals of Gerontology Series A: Biomedical Sciences and Medical Sciences* **67**, 726-733, doi:10.1093/gerona/glr225 (2012).

129 Leroux, M. R., Melki, R., Gordon, B., Batelier, G. & Candido, E. P. M. Structure-function studies on small heat shock protein oligomeric assembly and interaction with unfolded polypeptides. *Journal of Biological Chemistry* **272**, 24646-24656, doi:10.1074/jbc.272.39.24646 (1997).

130 Fonte, V. *et al.* Suppression of in vivo β-amyloid peptide toxicity by overexpression of the HSP-16.2 small chaperone protein. *Journal of Biological Chemistry* **283**, 784-791, doi:10.1074/jbc.M703339200 (2008).

131 Hsu, A.-L., Murphy, C. T. & Kenyon, C. Regulation of aging and age-related disease by DAF-16 and heat-shock factor. *Science* **300**, 1142-1145, doi:10.1126/science.1083701 (2003).

132 Cañuelo, A., Esteban, F. J. & Peragón, J. Gene expression profiling to investigate tyrosol-induced lifespan extension in caenorhabditis elegans. *European journal of nutrition* **55**, 639-650, doi:10.1007/s00394-015-0884-3 (2016).

133 Cañuelo, A. & Peragón, J. Proteomics analysis in Caenorhabditis elegans to elucidate the response induced by tyrosol, an olive phenol that stimulates longevity and stress resistance. *Proteomics* **13**, 3064-3075, doi:10.1002/pmic.201200579 (2013).

134 Park, S. K., Tedesco, P. M. & Johnson, T. E. Oxidative stress and longevity in Caenorhabditis elegans as mediated by SKN-1. *Aging cell* **8**, 258-269, doi:10.1111/j.1474-9726.2009.00473.x (2009).

135 Ayyadevara, S. *et al.* Lifespan extension in hypomorphic daf-2 mutants of Caenorhabditis elegans is partially mediated by glutathione transferase CeGSTP2-2. *Aging cell* **4**, 299-307, doi:10.1111/j.1474-9726.2005.00172.x (2005).

136 Leiers, B. *et al.* A stress-responsive glutathione S-transferase confers resistance to oxidative stress in Caenorhabditis elegans. *Free Radical Biology and Medicine* **34**, 1405-1415, doi:10.1016/S0891-5849(03)00102-3 (2003).

137 Todorovic, M., Wood, S. A. & Mellick, G. D. Nrf2: a modulator of Parkinson's disease? *Journal of Neural Transmission* **123**, 611-619, doi:10.1007/s00702-016-1563-0 (2016).

Conclusiones/Conclusions

CONCLUSIONES

1. El efecto antioxidante del tratamiento con HT sobre la línea celular de cáncer de mama MCF-7 está condicionado por el ambiente hipóxico y parece ejercerse principalmente por una acción directa.

2. En las células MCF-7, el tratamiento con HT puede modular la respuesta de las rutas PGC-1α/ERRα y PGC-1α/Nrf2 a nivel transcripcional y traduccional. No obstante, la hipoxia atenúa su efecto sobre la traducción.

3. El HT es capaz de regular la respuesta a la hipoxia de células MCF-7 al disminuir la acumulación de HIF-1α mediante mecanismos probablemente relacionados con su acción antioxidante y con la inhibición de la ruta PI3K/Akt/mTOR.

4. A concentraciones altas, en la línea MCF-7, el HT regula la expresión de AM, VEGF y HO-1 mediante mecanismos independientes de HIF-1 y Nrf2, poniendo de manifiesto su capacidad para interactuar con diversas rutas moleculares.

5. Tras un ictus isquémico el consumo de una dieta rica en HT podría ser una buena estrategia terapéutica al mejorar el estado físico y cognitivo. Este efecto parece estar ligado al aumento del FSC, la conectividad funcional, la neurogénesis y a la reducción de la inflamación.

6. El tratamiento con TIR reduce la toxicidad y la neurodegeneración asociadas a la agregación de la α-syn en modelos de la EP en *C. elegans*. Estos efectos podrían estar relacionados con su capacidad antioxidante y con la inducción de diferentes chaperonas moleculares.

CONCLUSIONS

1. The antioxidant effect of HT is particularly effective in hypoxic conditions and appears to be mainly exerted by a direct action of this compound.

2. In MCF-7 cells, HT treatment can modulate the response of the PGC-1α/ERRα and PGC-1α/Nrf2 pathways at both, transcriptional and translational level. However, hypoxia attenuates its effect on translation.

3. HT regulates the response to hypoxia of MCF-7 cells by decreasing the accumulation of HIF-1α. This downregulation is probably achieved by its antioxidant action and by inhibition of the PI3K/Akt/mTOR pathway.

4. In MCF-7 cells, high concentrations of HT modulate the expression of AM, VEGF and HO-1 through HIF-1 and Nrf2-independent mechanisms, highlighting the pleiotropic effect of this phenol.

5. After an ischemic stroke, a HT-enriched diet could be a good therapeutic strategy as it improves physical and cognitive status. This effect seems to be linked to the increase in CBF, functional connectivity, neurogenesis and to the reduction of inflammation.

6. Treatment with TYR reduces the toxicity and neurodegeneration associated with α-syn aggregation in *C. elegans* PD models. These effects could be related to its antioxidant action and to the modulation of different molecular chaperones.